Doctoral Dissertation
Doctoral Program in Architectural and Landscape Heritage (34th Cycle)

Monitoring of architectural heritage with machine learning methods

By

Giorgia Coletta

******

Supervisor:
Prof. Rosario Ceravolo

Doctoral Examination Committee:
Prof. Raimondo Betti, Columbia University
Prof. Andrea Micheletti, Università di Roma Tor Vergata

Politecnico di Torino
2022

Declaration

I hereby declare that, the contents and organization of this dissertation constitute my own original work and does not compromise in any way the rights of third parties, including those relating to the security of personal data.

Giorgia Coletta

2022

To G., S., F. and F.

Abstract

The Architectural Heritage (AH) represents one of the pillars of a country's social and cultural identity, as well as one of its greatest assets. Its protection is a commitment and a responsibility of all generations to come. Like anything else on our planet, assets undergo an evolution over time. Processes of a different nature, chemical, physical, biological triggered by man or completely spontaneous, affect those materials that have been wisely combined over the years to model extraordinary architectures. From a structural perspective, the effects of these phenomena can progress slowly and be perceived only after generations or dramatically fast if triggered by singular events such as earthquakes. Taking measures to mitigate and prevent this damage should be a duty of every developed country.

In the last twenty years of the 20th century, the discipline of Structural Health Monitoring (SHM) was formed and continued to expand across various engineering sectors. It deals with all the processes of implementing a damage detection strategy, which involve observing a structure over time through periodically spaced dynamic response measurements, the extraction of damage-sensitive characteristics and their statistical analysis aimed at determining the current structural state. Its growth was encouraged by the recent technological progress, which has led to the development of increasingly high-performance sensors and instrumentation, capable of automatically acquiring accurate high-frequency measurements at low cost and with the possibility of instantly transmitting online the data they acquire continuously, without needing manual interventions. From the need to extract and synthesize the information enclosed in these large datasets, SHM has naturally moved towards innovative techniques of *Machine Learning* (ML), a branch of *Artificial Intelligence* (AI), which emulates the learning ability of human preserving the advantages of computers, such as computational capacity, speed, automaticity, objectivity, transferability, etc.

Although SHM potentially leads to various advantages over traditional diagnostic techniques, with which it shares the objectives, its approach to Cultural Heritage (CH) has only occurred in recent years. In fact, while other sectors have benefited from the very beginning of the application of SHM, when trying to integrate this procedure into the AH conservation process, some problems arise, related to the complexity of the object involved. This thesis aims to identify and explore the critical aspects of SHM implementation on CH buildings by presenting proposals to address them. It is structured as follows:

Chapter 1: The role of SHM for AH is made explicit and the motivations that lead to turn to this type of approach are explored for different scenarios. The real objectives and limitations are clarified in the definition of what SHM aims to detect and the relationship between structural safety and monitoring systems is probed.

Chapter 2: Vibration-based methods are presented and their application on very different architectural assets is shown, enhancing their peculiarities. Critical aspects are introduced in this chapter and an interesting analogy is outlined. Here, also an overview of the case study of the thesis, the *Sanctuary of Vicoforte* (CN, Italy) is reported.

Chapter 3: Data recorded on the Sanctuary by the static and dynamic monitoring systems, for over ten and three years respectively, are systematically analysed and their correlation with environmental factors is made explicit. Both dependencies already found for other assets and unexpected outcomes emerge from this research.

Chapter 4: Having ascertained the dependence of the diagnostic parameters on the external environment in the previous chapter, here a strategy is proposed to remove it. It is based on cointegration, a technique that comes from econometrics, and ML regression algorithms.

Chapter 5: The issue of the lack of labelled data related to different structural conditions is addressed using a strategy based on Transfer Learning. Virtual data produced with the Finite Element Model (FEM) are exploited to train ML algorithms and support the interpretation of the real measures.

Chapter 6: The design of an experimental test is developed on the FEM of the Sanctuary. The experiment, not yet carried out in practice, aims to obtain data from a like-damaged structural condition. Considerations emerge on the sensitivity of dynamic behavior under certain load conditions, as well as on that of accelerometers and on the trend of historical dynamic data.

Chapter 7: A source of continuous information about the foundation soil of the Sanctuary is identified in remote sensing data. Two geophysical parameters related to the thermal and humidity conditions of the surface, made available by the European Space Agency (ESA), are examined and crossed with those of on-site monitoring.

Contents

List of Figures

List of Tables

Chapter 1

The role of structural health monitoring in the conservation of architectural heritage

1.1 Introduction

The term *monitoring* comes from the Latin verb *monĭtor -oris* and means "to warn", "to inform" (*monitorare* in Vocabulary - Treccani). This practice consists in the control and supervision of the trend over time of some parameters considered interesting for the intended purpose. It is usually set up to observe the evolution of chemical, physical and biological quantities in various scientific and social fields including medicine, ecology, economics, and many others.

The historical structures belonging to our Architectural Heritage (AH), like anything else on our planet, undergo an evolution over time. Chemical or physical, natural or artificial processes progress over the years and change the shape, texture and colour of each element of the work and at different scales and level of intensity, involving frescoes, stuccos, decorations, structural and non-structural elements. From a structural perspective, these changes can be very slow and almost imperceptible processes, relatively rapid, or even sudden if triggered by singular events such as earthquakes. Monitoring structural changes makes it possible to detect worrying phenomena and predict catastrophic mechanisms. These, in a few

simple words, constitutes the main objectives in the sphere of AH of that science that goes by the name of Structural Health Monitoring (SHM).

Until recently, the only way to check the evolution of the structural health of AH was through visual inspections. Qualified personnel physically went to the structure and with limited means at their disposal evaluated the progress of any cracks or deformations already present and tried to find out if new mechanisms could have formed since the previous inspection. These procedures, understandably, are plagued by many limitations as, for example, the inconstancy of inspections, the subjective nature of the diagnosis, the unavoidable superficiality or spatial limitation of some tests, the high costs of inspection, rental, transport and installation of instruments, and so on.

Today, technological progress has led to the development of increasingly high-performance sensors and instrumentation, capable of automatically acquiring accurate high-frequency measurements at low cost and with the possibility of instantly transmitting online the data they acquire continuously on the monitored structure, without needing manual interventions. On the one hand this led to the availability of structural data practically in real time and to the possibility to observe the trend of diagnostic parameters of a structure in any place with an internet access; on the other hand, large amounts of data accumulates, heavy to manage, organize and examine and which often contained redundant information. For this reason, from the need to extract and synthesize the information present in these enormous amounts of data, innovative techniques of *Machine Learning* (ML), a branch of *Artificial Intelligence* (AI), have also spread in the field of structural engineering, especially in the diagnostics sector. ML techniques are currently the most advanced methodologies for analysing large amounts of data and information, even affected by noise. Their application, combined with the density of data, makes it possible to implement a diagnostic path based directly on the acquired data, without the need to define physical models and parameters which in the case of historical constructions could be very complex.

In many cases, conceiving a reliable behavioral model of Cultural Heritage (CH) buildings could be complicated and / or expensive compared to standard and new buildings, as they are characterized by greater uncertainty in the properties of the materials, in the contribution of construction details / architectural elements (even posthumous), in the geometries, in the interaction with the soil and so on. Moreover, keeping a structure monitored allows for always up-to-date information,

a considerable advantage for structures that could be several centuries old, which suffered trauma over years such as earthquakes and have not been conceived according to current safety standards, issues that would make them, in general, more fragile compared to modern buildings.

Despite the potential benefits, certainly even diagnoses driven just by data present issues. Not relying on known physical concepts leads to not having direct control over what is extracted from the monitoring data and this could lead to results that are far from reality if the algorithms for data analysis are not wisely set up. Furthermore, since what guide the procedure and calibrate the algorithms are essentially the data, their availability should be guaranteed, not only in relation to "normal" conditions but also to particular environmental / operational / geophysical conditions to reduce the risk of false diagnoses, as well as examples of the reaction of the structure to damage. The latter, as will be discussed later, are by no means easy to obtain. Issues like these have much less literature available, as data-driven procedure supported by AI algorithms are much newer than traditional diagnostic approaches, especially regarding their application to structural diagnosis of AH.

This should not be seen as a limitation. In fact, the relatively recent development of this field of research, together with the benefits it would bring to the conservation of CH buildings, makes this topic even more attractive and stimulating; new paths and creative solutions can be proposed and evaluated in a research field still little explored, and this is what this thesis has aimed at.

1.2 Structural health monitoring for architectural heritage

The AH represents one of the pillars of a country's social and cultural identity, as well as one of its greatest assets. Its protection is a commitment and a responsibility of all generations to come. Not surprisingly, conservation and rehabilitation interventions aimed to keep assets in the best possible condition currently constitute a large slice of the market in developed countries. Despite this, the AH inevitably tends to deteriorate and accumulate damage, due to the natural process of degradation of the materials and exceptional traumatic events such as earthquakes.

Over the past 30 years, the SHM discipline has seen a growth in research interest worldwide, which in some fields has quickly translated into real-world applications. More recently, it has also caught on in the AH sector, stimulating many studies and applications, although in most cases still at the research level. For

Italy, this is certainly a matter of great interest as it hosts about 5% of the cultural sites recognized by UNESCO on an area characterized by high seismicity.

Damage of a structural nature is very fearsome as it may result into the loss parts of the structure as well as what is contained in it, including people, whose life is seriously at risk. A monitoring system is meant to record the variations of some significant parameters, also called diagnostic, such as crack openings, overturning, deformations, modal features, etc. in order to offer a picture of structural health at relatively short intervals of time.

The Directive PCM (Recommendations PCM, 2011), the most advanced Italian seismic regulations for CH structures, includes this practice as the last step in the path of knowledge of a structure, following identification of the structure, functional characterization, geometric survey, historical analysis, material survey and state of conservation, mechanical characterization of materials and geotechnical aspects. It is defined as the primary tool for knowledge regarding preservation, allowing the planning of maintenance operations and the timely enacting of reparation interventions in case of structural damage, and consolidation for the sake of prevention only when it is really necessary. Three types of monitoring are implicitly distinguished in the standard: visual inspection, static monitoring and dynamic monitoring.

The first is intended as the periodic, not automatic control of the onset of cracking, phenomena of decay, transformations in the structure and in the surrounding environment; it represent, in a certain sense, the ancestor of monitoring as it is conceived to date.

The static monitoring systems aim at acquiring through specific instruments certain parameters which are retained significant for defining the structural condition, e.g. movement of the lesions, absolute shifting or relative to construction points, rotation of walls or other elements). They may be controlled continuously and by radio control. It is attested that in cases where the deterioration is well understood and it is possible to define reliable safety thresholds, monitoring represents an alternative to intervention for the benefit of conservation.

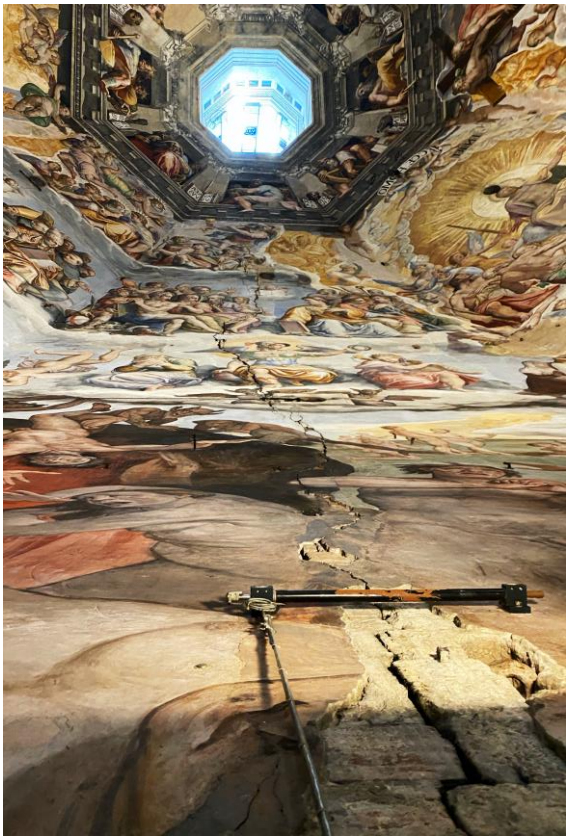

Figure 1. 1: monitored lesion on the Cathedral of Santa Maria del Fiore (Florence, Italy)

Lastly, dynamic monitoring is mentioned. It is based on the observation of the modal parameters of a structure, which are generally extracted from acceleration signals recorded in some interesting points of the construction. A kind of hesitation in dealing with this topic is perceived reading the code. In fact, despite dynamic features such as frequencies and modal shapes are considered significant parameters, which alter as the structural conditions change, the identification of damage from them is considered quite complex. Problems are mentioned, e.g. the non-linearity of the behavior of the masonry structures, while admitting that in some cases the monitoring of these parameters can represent one of the possible elements to identify the changes manifested in the construction.

From the first draft of the directive until today, the practice of dynamic monitoring has begun to spread and more assets have been involved, even if, as anticipated, most of the applications are at the purely scientific research level. In parallel, new experimental procedures have been developed in order to refine the interpretation of the diagnostic information contained in the recorded signals. These

studies, not only related to CH buildings, are part of the SHM discipline, which Farrar and Worden (Farrar & Worden, 2012) have defined as follows:

> *"The term structural health monitoring (SHM) usually refers to the process of implementing a damage detection strategy for aerospace, civil or mechanical engineering infrastructure. This process involves the observation of a structure or mechanical system over time using periodically spaced dynamic response measurements, the extraction of damage-sensitive features from these measurements and the statistical analysis of these features to determine the current state of system health. For long-term SHM, the output of this process is periodically updated information regarding the ability of the structure to continue to perform its intended function in light of the inevitable ageing and degradation resulting from the operational environments. Under an extreme event, such as an earthquake or unanticipated blast loading, SHM could be used for rapid condition screening, to provide, in near real time, reliable information about the performance of the system during the event and about the subsequent integrity of the system."*

SHM is a combination of words that has emerged around the late 1980s, but its idea may date back to the origins of structural engineering (Boller, 2009). It is analogous to what we are used to in the classic medical and healthcare sector, but consider another type of patient, CH buildings in this case. Although it is based on innovative measures, analyses, algorithms and communication techniques, SHM shares the same objectives as traditional approaches. Indeed, SHM can be seen as an extension of established investigative practices as it seeks to overcome the limitations of traditional visual inspections. Two main differences could be highlighted: the type of test and parameters on which the diagnosis is based and the frequency with which the measurements are collected. SHM mainly involves dynamic parameters, which, as will be discussed further on, contain different information compared to the tests traditionally carried out during inspections; moreover, the measurements in a SHM procedure are collected, in certain cases, several times a day: it is a repeatability that could never be achieved by inspections. Reasons related to these differences lead to prefer an automatic monitoring system,

which work in real time or near real time rather than the investigations performed periodically. The next paragraphs explore this and other benefits of SHM.

1.3 Motivations

One of the questions, the answer seems to have been taken for granted so far, is: why has interest in monitoring only now grown, given the potential of SHM for construction? Frangopol in (Frangopol & Messervey, 2008) effectively responded with two main arguments.

1- Because only now we can. We have only recently developed technological means, power generation, more efficient batteries, more powerful computing platforms and wireless capabilities that are making it possible to obtain site-specific response data at low cost. Indeed, although many of these technologies and the ideas have been around for a long time, above all in the aviation industry, they typically have demanded a controlled environment, wired cables and immense effort to obtain data. Even if reasonable for the design and testing of new aircraft, application for the evaluation of constructions in the field it was unfeasible.
2- Because it is necessary. Many traumatic episodes have squandered heritage structures: collapses and damages, which probably could have been avoided or limited with the right prevention.

The protection of CH is the responsibility of an evolved society. Monitoring practice plays a crucial role in the conservation process, providing first-hand data for decision making. The continuous and global structural knowledge, as well as the widespread and accurate information about the structural performance and integrity that only a monitoring procedure can achieve, favors the implementation of preventive conservation and the realization of ready and targeted interventions, limiting cost, invasiveness and reducing the risk of incurring irreparable damage.

Visual inspections require highly qualified personnel, who, in the best cases, return to the structure with a periodic recurrence that may be too distant in time. This could defeat its goal of predicting structural damage. It should also be highlighted that inspections of this type have a strong subjective component, that is, they strictly depend on the judgment of the operator who inspects. The operator is practically given full responsibility for deciding whether or not to act. In case of human error, premature or superfluous structural intervention would occur in the best situation; at worst, damage may be overlooked or underestimated, putting the

building at risk and virtually defeating the purpose of inspections. Tests conducted manually have the limitation of the accessibility of the areas in which they must be carried out: often hard-to-reach areas remain unexplored, in the hope that significant damage will not occur right there. The timing between inspections should be defined by the conditions of the building but very often, other factors such as the economic one, are predominant in the definition of a program. Sometimes expensive test equipment or special means for lifting are necessary and require complete closure or, at least, partial limitations of the usability of the work to carry out inspections (Roach, 2008).

Unlike traditional structural inspections and tests, monitoring systems allow information to be obtained with minimal invasiveness, the sensors are in most cases practically undetectable, and acquire automatically in the normal operating condition of the building. Accessibility limits, complex geometries, depth of hidden damage are overcome by the installation of a network of sensors. In a sense, a transition into "smart structure" takes place. Moreover, a monitoring procedure minimize human factors with automated sensor deployment and data analysis. Against an initial investment that includes hardware, software, installation and procedure design, monitoring is a practice leading in the long term to economic savings obtained on inspections, extent of interventions and possible devastating collapses as it supports the adoption of structural condition-based maintenance. Collapses, in addition to producing priceless artistic, cultural, historical losses, seriously endanger the lives of the people inside and around the structure. For AH, the economic convenience also lies in the fact that they do not have a limited life-cycle to accomplish their function, differently from ordinary structures, so it is reasonable to lean towards an investment that leads to long-term savings, which may also have a significant decrease in the coming years (Abruzzese et al., 2020).

In the literature, also the benefits have been pointed out of a well-designed monitoring system for CH, discussing how they lead to greater resilience of these structures in the occurrence of a destructive event, defined disturbance, e.g. (D'alessandro et al., 2019; Limongelli et al., 2019). This event outlines three phases in the evolution of the structural functionality of the CH building: *before*, *during* and *after* the event (Figure 1. 2). In this context, undertaking monitoring could bring benefits in each of the three phases.

In the pre-event phase, it would help to understand, without any invasive testing, the actual structural state, discern temporary and physiological effects from

pathological ones, and would allow the transition from a *time-based* to a *condition-based* maintenance program. It would also provide an early warning on a possible dangerous event, thus allowing the adoption of emergency measures (e.g. evacuation, closure of critical structures) that reduce exposure to the dangerous event and thus reducing the risk. The benefits of this phase alone, which could be the only one in the event that a disturbance does not occur, would be sufficient to justify the initial investment; but in the unfortunate event that a traumatic event actually occurs, such as earthquakes, landslides, impacts, tornadoes, lightning strikes, etc. the benefits would be even greater.

In a disturbance phase, a more efficient management of emergencies (e.g. building evacuation, traffic limitation, prioritization of interventions) could be achieved, which is particularly important to reduce exposure on CH structures with an important tourist flow or to reduce downtime for buildings hosting strategic functions that require business continuity (e.g. hospitals or government institutions). Not to mention that measuring the response of structures subjected to traumatic events is, in a certain sense, like performing an invasive test (certainly not wanted, but inevitable) and allows the extraction of information that otherwise would be difficult to obtain, since it is unthinkable to submit these buildings to tests that jeopardize their safety. Just to name a few, measuring the response to such events would lead to a more accurate assessment of structural behavior, evolution of failure mechanisms, behavior of materials, etc. In some way it could be possible to take advantage from unfortunate events extracting this information, in order to improve legislation (e.g. building regulations) and to reduce the uncertainty related to the future risk assessment of the same or similar structures, thus favoring the increase of technical skills capacity for possible future events.

Following the traumatic event, in the "post-event" phase, the monitoring would give knowledge of the actual structural condition. After the disturbance, it provides support for decisions relating to various interventions (if any), to optimize recovery plans. This allows for an increase in both organization and economic capabilities. Knowledge of the structural state is the basis for deciding whether a structural intervention should be undertaken or not, even if there is no visible damage. If interventions should be performed, SHM would give the possibility to verify their effectiveness in real time whereas could give an updated estimate also of any previous interventions and their current functionality. Feedback on the effectiveness of a structural intervention is particularly important as it allows for an improvement in technical capacity through the increase of knowledge in structures on which laboratory tests are not always a viable option. Monitoring is even useful

during the delicate intervention phase, when the stability of temporary configurations of the structural elements must be checked so as not to risk accidents. The dissemination of monitoring systems would have an impact not only on the individual work, whose conservation process would have information to be optimized, but also an important influence on the management of the funds to be dedicated to the interventions on different assets, providing objective parameters, as far as possible on structures so different, that they define the urgency to intervene.

Figure 1. 2 show the three phases on the church of *Anime Sante*, in L'Aquila, a symbol of the 2009 Italian earthquake (Boscato et al., 2012; Russo, 2013).

Figure 1. 2: *pre, during* and *post* phases on the *Anime Sante* church (L'Aquila, Italy) damaged by the 2009 earthquake

However, despite the undeniable advantages, to date the practical applications of SHM on heritage structures are still very limited. Probably the challenges that characterize such complex structures, already known for any other approach to their diagnosis, together with the recent approach of SHM techniques to the field of AH, make this procedure and its effectiveness still not fully understood and accepted.

More specific aspects will be dealt with below in order to highlight pros and cons of SHM, as well as any alternative solutions for AH. It will thus be possible to create the right context for the chapters to follow.

1.3.1 Data-driven vs. Model-driven approaches to SHM

The approaches to tackling an SHM procedure can be divided into two main classes: *model-driven* methods and *data-driven* methods. Data-driven approaches exploit monitoring data and adopt pattern recognition and ML, or other heuristic techniques, to create a statistical representation of the system from them (Worden & Manson, 2006).

In Model-driven methods instead, an inverse approach is applied to a law-based model, the most common method is Finite Element (FE) model updating (Friswell, 2007). This process involves adjusting some parameters of the model to reduce the residual between experimental measurements and model predictions; then simulations and tests on the updated model help to deduce the damage in the structure. However, a number of problems arise when applying these damage detection methods. For example, a Finite Element Model (FEM) is characterized by a large number of parameters, and their settings must be carefully evaluated. Those who set them should have thoroughly understood the underlying physics, checking that the values of the "healthy parameters" always maintain a physical meaning, as well as those set to simulate damage. The latter are very difficult to validate. The inevitable presence of errors, since the model by definition is a simplification of reality, is another issue that plagues this approach. Model-driven methods are also computationally heavy in that require multiple runs of a FEM to make predictions. Choosing the parameters to be calibrated will always imply that those not subjected to the same process are characterized by uncertainty. It must also be considered that even the best model may not reflect reality due to variations on the latter, compared to the data used in the calibration, for example due to environmental effects. These issues become even more serious when a historical structure is to be modeled. The uncertainties about the materials and their characteristics, the unusual geometry, the lack of knowledge on the connections, on the interventions undergone and on the present crack pattern, create difficulties in defining laws for a generalized application.

In this context, fundamental support can be given by historical information and the survey documentation. PERPETUATE, the European project for the proposal of a performance-based approach to earthquake protection of CH, in one of the several deliverables proposes guidelines for the seismic preservation (Lagomarsino et al., 2012). Tools to optimize the survey program are given, whose outcomes should be used in defining the structural model of the building and related artistic assets. Surveys involve the acquisition of numerous data relating to the geometry of the building, the foundations, the estimation of the mechanical parameters, the historical data of transformation and damage, the state of maintenance and the identification of the damage mechanisms, the dynamic behavior. Preliminary sensitivity analyses are also suggested to identify the main parameters to be investigated, which allows to finalize the investigation to few important points (limiting cost, time and destructive tests). However, albeit adequate tools, building an accurate model could turn out to be complicated. In conclusion, although models

can be an important support for SHM, one must bear in mind that the deviation of the results from the real behavior can be significant (Brownjohn et al., 1999; Zhang et al., 2001).

Data-driven approaches in SHM are usually applied to data coming from permanent or long-term monitoring systems as a lot of samples are available on which to base reliable statistics. In these methods the data can be studied and analysed already including variations given by the external environment or by noise. Differently from the previous methods, in these approaches knowledge of the phenomena that influence the structural behavior does not come from physical laws implemented in a model but they are deduced directly from the measurements. The response acquired under the frequent conditions of the structure is taken as a reference for a generic algorithm. Starting from this, the condition defined as "normal", or improperly "not damaged" (as the structure could have pre-existing stable damages, as in the case of architectural assets), is used to deduce the damage, because the latter will modify the normal parameters. In order to reach the maximum effectiveness, these methods would require data from each damage state to be used to set a generic pattern recognition algorithm. Obtaining them for structures such as architectural assets is very complicated or even impossible: this is a very relevant problem which will be discussed extensively in this thesis. An attractive idea is to appropriately exploit a FEM to overcome the issues that plague data-driven methods, in order to gain the advantages of both, and to implement in practice a mixed method, driven by data but to some extent supported by models.

1.3.2 Issues with monitoring of architectural heritage structures

Heritage buildings stand out from the rest of the building for artistic, historical, archaeological, ethno-anthropological aspects that outline their uniqueness. Many assets also combine these values with particular structural characteristics, to the point that the technical regulations for CH structures do not coincide with those for ordinary structures.

The objective of this paragraph is to highlight some differences between ordinary civil structures and AH, differences that make modeling of these buildings complicated, suggesting an approach to diagnosis based on monitoring.

Both ordinary and CH structures embrace sub-categories ranging from the most disparate geometries, to the simplest building materials to the most innovative ones, shaped with the most diverse construction techniques, typical of every era, culture,

geographical location, designer. Drawing up a complete list of the differences between these two classes of buildings would be practically unproductive, since the number of exceptions would also be greater than the items identified. This means that most of the claims that could be made on the structural differences could be denied by identifying within the two categories examples that do not agree with what has been said. Therefore, here, more than a list of differences, a framework is outlined within which to search for the most common differences, but which are not necessarily valid for each building.

A categorization that effectively summarizes the differences can be based on three macro aspects: geometry, materials and construction details. From a structural point of view, these are the aspects that most specifically define the structural behavior. In fact, even the Italian regulation for existing buildings (Ministero delle Infrastrutture e dei Trasporti, 2018, 2019) uses the same aspects and the depth of their knowledge to attribute a level of knowledge to the entire structure on which the mechanical parameters of the materials to be used in the assessments depends.

- **Geometry**. In many cases, CH structures have geometries that are distant from ordinary ones. This is due to two main reasons concerning function and social relevance. In fact, many CH structures necessarily had to assume particular shapes, different from ordinary buildings, because their function was also particular, e.g. stadiums, theatres, pavilions, towers, mausoleums, etc. In other cases, the design was influenced by other aspects, such as the political or religious role that often characterized these buildings: their projects were often entrusted to extraordinary architects or engineers who went beyond classic schemes to amaze and fascinate both the community and the client. Just to give some practical examples, domes, lanterns, arches, high ceilings not interrupted by floors, colonnades, slender towers, pinnacles, large spans, vaulted ceilings are aspects and elements that (with the due exceptions) are easier to find on CH structures than on ordinary ones. Neither the foundation nor their geometry is always “ordinary”. Often it can be variable as well as the characteristics of the soil; moreover, buildings are often connected to other constructions whose contribution must be taken into account in the modeling (Clemente & Buffarini, 2008). The geometric aspect also includes the variations that occurred after the end of the construction period. It is very common that historic buildings have been modified over time both for reasons related to reuse (adding spaces, eliminating elements, opening or closing doors and windows, etc.) and structural reinforcements (adding chains or other resistant elements,

hooping systems, etc.). Not infrequently the buildings are set on old constructions. In the general case, it is not immediate to understand how the modifications interact with the main structure, both at the structural scheme level, because they could change an ordered scheme that was conceived by the designer which could be easier to model, and at the level of interaction between different materials.

Straddling the geometry and materials aspects, the deformation and cracking state of the construction can be placed. Generally, it is reasonable to expect that an older structure, which has undergone various traumatic events, will be characterized by a more worrying crack pattern, especially if it is also associated to bold geometries, scarce material properties, structural schemes that are not optimal for resisting the events happened to that geographical area.

- **Materials.** This issue affects most ancient buildings, regardless of their cultural value. Speaking about materials, a clarification is necessary, the difference could exist for two main reasons: (i) because since the construction the building materials used had different mechanical properties from those commonly used today. Use of poorer raw materials, due to the availability of the place, or the non-optimal assembly of different materials, such as mortar and masonry or concrete and steel for the modern architectures, could mark the difference with the materials used today which instead are subjected to specific regulations and test; (ii) because their evolution over the years has led them to break away from those normally used today. The degradation of materials could be greater in historic buildings, both because they have undergone more seasonal cycles, because they may lack the surface treatments that are expected today and because a crack pattern could have favoured the access of harmful agents. In addition to this, it should be noted that destructive and semi-destructive tests on AH to evaluate the properties of materials are not always permitted or, at best, are subject to limitations. Therefore, the knowledge of the behavior of the material coming from a limited number of samples or tests is not always exhaustive. This will increase the uncertainty on the model adopted, considering also that often different materials are used for the same construction and each would require a model validated with an adequate number of tests.
- **Construction details.** The construction techniques have naturally evolved over the years, based on the evolution of technologies and of the experience

acquired from traumatic events. Furthermore, since there were no technical regulations in the past as they are conceived today, the construction techniques could vary considerably according to the place of construction, the designer and the type of structure. This means that, in addition to being a difference with ordinary structures given by the temporal distance, also differences between buildings of the same epoch could exist in the construction details. Different construction details lead to different structural behaviors that the modeling should reproduce. When technical drawings are not available, their knowledge must be achieved through destructive or non-destructive testing.

In addition to the differences themselves, it should be noted that while many similar examples are available for ordinary structures (e.g. reinforced concrete framed structures), it is much rarer to find structurally similar architectural assets: the limitedness of analogous models already analysed and resolved increases even more the uncertainty about the goodness of the formulated hypothesis for CH structures.

1.3.3 Definition of damage in heritage structures

In this document, the term "damage" will very often be raised. Everyone knows the generic meaning of this word but in this context, it takes on a particular connotation that should be made explicit.
Farrar and Worden (Farrar & Worden, 2012), in a global perspective of SHM define a damage as:

"Intentional or unintentional changes to the material and/or geometric properties of these systems, including changes to the boundary conditions and system connectivity, which adversely affect the current or future performance of these systems."

All damage begins on a material level and such damage is generally referred to as defects. Sometimes the damage to the material progresses and generates a collapse. Clearly, material defects, cracks, deformations are present in all structures at a certain level, especially in historic buildings, and they may not affect the function of the work. In terms of timing, damage can accumulate incrementally over long periods of time, as is the case damage associated with fatigue or corrosion, but it can also progress very quickly, as is the case of critical fracture; finally, transient

natural phenomena, such as earthquakes, can lead to sudden damage. That said, what kind of damage are we trying to predict / identify in a SHM procedure on AH?

First of all, the damage as it will be conceived in this thesis is on a structural level. If elements that do not contribute to the dynamic behavior of the structure suffer damage, they cannot be identified by this type of procedure. Architectural assets are very often characterized by pre-existing crack patterns that derive from past traumatic events, subsidence, unusual operating conditions, corrosion, deterioration or the combination of various factors. If these damages are stable, or do not evolve over time, they will not be identified by the monitoring procedure. The stability of pre-existing damage, or their absence (although rare for AH) allows a structural condition to be defined as "normal" and thus defines a reference condition for making comparisons and identifying, possibly, a "damaged" condition. The normal is generally the condition in which the structure is found at the time of installation of the monitoring system, the stability of which should be defined in a structural evaluation through tests and investigations. This is also referred to as “healthy” or (improperly, given the presence of pre-existing damage) “undamaged” condition, meaning that no new damage has been created nor the pre-existing ones are progressing. The damage detection algorithm would perceive that as a normal condition state.

The damages that the procedure aims to identify are of two types: with a noticeable trigger and with an unclear cause. In the first case, a traumatic event such as an earthquake, an exceptional climatic or operational condition affects the structure while it is being monitored. In that case, if the structure has not reported evident collapses, a difference is sought in the pre and post event parameters in order to understand if it may have generated anomalous variations. This is exactly what happened to Church of Monastery of Jerónimos in Lisbon (Masciotta et al., 2016) and to two Italian bell tower, the Gabbia tower in Mantova (Gentile et al., 2016; Saisi & Gentile, 2015) and the San Pietro bell tower in Perugia (Ubertini et al., 2018), which had the advantage of being monitored as the tremors took place. Clearly, little or even not visible damage or hardly identifiable by non-experts is sought, not disastrous collapses that would already be visible without the need to analyse data: in those cases, the monitoring would aim to support the decision process, the management of the emergency, the surveillance of temporary dangerous conditions (see 1.3). If the damage develops without an evident cause, (such as due to subsidence or the advancement of pre-existing cracks) its effects are not intentionally sought in the data and two moments to which to refer the

comparison are not defined, since the cause is not manifest or it extends over a long period. In this case, a warning should signal the achievement of an excessive variation of the diagnostic parameters with respect to the initial normal condition. An appropriate regression of the data could identify the trend of the parameter and estimate its evolution, also considering the possibility of a sudden worsening linked to the fragility of materials such as masonry.

To sum up, damage can be defined as a deviation from a condition which is assumed to be normal. Unless integrated with models or other tools, a monitoring procedure is not able to identify pre-existing damage, as data from the structure in its original condition ("undamaged") is not usually available, and therefore a comparison is not possible. However, a clarification is necessary. From the point of view of measurements, dynamic monitoring is nothing more than a series of dynamic tests under environmental conditions, repeated over a short period of time. A dynamic test leads to the identification of modal quantities, that are, frequencies, modal damping ratios and modal shapes. From the latter, it is possible to identify system weaknesses, e.g. parts that vibrate reaching much greater displacements compared to the main body of the structure. These could derive directly from the original design, in which most likely dynamic conditions were not considered, or weakening (cracks, deformations) that occurred after, which nevertheless remained stable. Only in this sense, an SHM procedure can highlight a previous damage, even if stable: in this situation the results of a dynamic test are exploited rather than the dense repetition of the measurements that a monitoring contemplates. The Figure 1. 3 shows the lantern of the *Santa Caterina* church in Casale Monferrato (AL), Italy, as an example; its relative deformability with respect to the main body is perceptible from the modal shapes of a FEM that has been calibrated on the basis of experimental modes (Ceravolo et al., 2016).

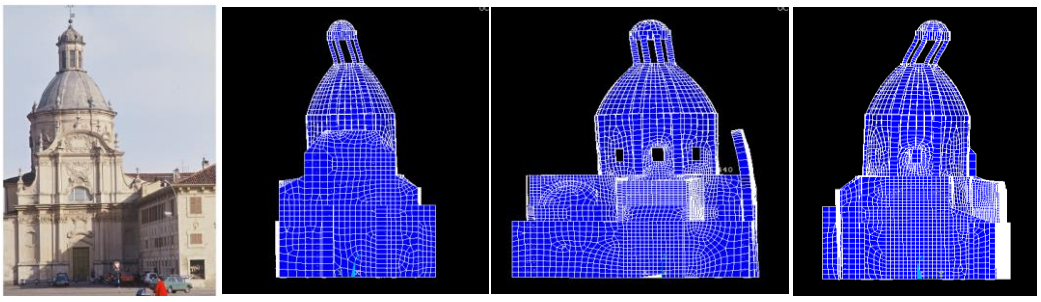

Figure 1. 3: *Santa Caterina* church and its FEM showing the first modal shapes

Within the sphere of identifiable damage, a further classification is possible based on the elements involved: damage can occur on a local or a global scale. Both are potentially identifiable by an SHM procedure. The former could involve single structural elements without affecting the integrity of the entire building. In that case, vibrating modes with limited participation mass would be involved. This situation is not uncommon for historical structures, in which the connections between elements are not always effective and the box-like behavior is not always guaranteed. Global damage is generally more serious and difficult to treat as a greater percentage of mass is involved in the vibration and anomalies in primary structural elements are expected. Despite this, both should be given appropriate importance as serious local damage could lead to collapses of the elements involved which could hit and damage primary elements in turn.

1.3.4 Definition of structural safety of architectural heritage

In assessing the structural safety of historic buildings, the thresholds or parameters of judgment used for new buildings certainly cannot be applied.

Buildings in the past were not “designed” as we understand today. The ancient builders referred to a “rule of thumb” such as geometric proportions and to rules handed down verbally, often kept as treasures by generations of builders. These rules were outlined by trial and error and evolved over the centuries until the birth of the first building regulations and survived until the mid-twentieth century (Beckmann & Bowles, 2004). In addition, compared to today, in ancient times it was customary to build accepting a greater risk. Therefore, in most cases historic buildings do not remotely reach safety levels that are required today by modern building codes (Zanotti Fragonara, 2012). This marked difference in safety standards, together with the specific structural characteristics of heritage structures already discussed in 1.3.2, motivates the fact that a further document, the Directive PCM (Recommendations PCM, 2011) in Italy is added to that used by engineers for standard constructions (Ministero delle Infrastrutture e dei Trasporti, 2018). The safety of AH is guaranteed by compliance with three limit states: two refer to the limit states defined by the NTC, while one is specific for CH.

The limit states to be considered for CH are, as a rule, SLV (Life-saving Limit State) and SLD (Limit State of Damage): they are part of SLU (Ultimate Limit States) and SLE (Operational Limit States) respectively, and are motivated by the desire to safeguard the safety of the occupants in the event of rare and high intensity

earthquakes and limiting damage to less intense but more frequent earthquakes. A further status is considered for CH, SLA (Limit State of damage to artistic assets), in order to admit only a modest damage to the artistic assets contained in the artefact, such that it can be restored without significant loss of cultural value. It is noted that assessment against the SLD is considered only in relation to loss of functionality (usability) of the building, as it is implicitly considered that the damage to a historic masonry building is inevitable, especially with regard to frequent seismic action and, as such, a consequence to be considered acceptable. The directive also highlighted a further aspect to consider for AH buildings: the category of relevance. In fact, historic structures can require particularly high level of seismic protection, especially if they have a pivotal role as CH. In particular, the first version of the Directive (Recommendations PCM, 2008) had set three different relevance levels for historic structures, namely: limited, average and high. Based on this, but also on their usage category (occasional, frequent, very frequent), the action had to be defined.

The European research project PERPETUATE (Lagomarsino et al., 2010) is precisely related to the application of the performance-based approach to earthquake protection of CH in European and Mediterranean countries. The project, led by the University of Genova, intends to develop European Guidelines for the evaluation and mitigation of seismic risk to CH assets, with innovative techniques for the seismic strengthening of historical buildings and the preservation of unmovable artworks. This project approaches the problem from two perspectives: for architectonic assets (historic buildings; macro-elements, which are architectonic elements that may be analysed independently from the rest of the building) and for artistic assets (frescos, stucco-works, pinnacles, banisters, statues, balconies, battlements, etc.). Within several deliverables (Abbas et al., 2010; Lagomarsino et al., 2010), the project suggests some criteria for the choice of target performance levels for the seismic retrofit of historic buildings, providing even more details than the directive, especially for what concerns the life safety and the safety of the artistic assets. Three levels of performance are proposed: Use and human life (U), Building conservation (B) (even in this case, the preservation from building damage is not related, as for ordinary buildings, to the costs of repair or rebuilding but to the possibility of restoration, due to the intangible value of a cultural heritage asset) and Artistic assets conservation (A).

Preserve the historical building without substantial changes or invasive retrofitting interventions, following the principle of “minimum intervention”, is another key concept underlying the directive. The debate on interventions and their

intensity is certainly not recent. More than 30 years ago, in 1986, the guidelines issued by the *Ministero dei Beni Culturali* (Ministero dei beni cultural e ambientali, 1986), reiterated the importance of "a multidisciplinary approach" and highlighted the critical issues that are still current today: *"Lack of clarity of the code with reference to the planning of the interventions, aggravated by the habit of use improper building regulations in force for standard buildings and not for monuments", "conflict between conservation problems and the need for seismic protection of the building (including its users), and relative assumption of responsibility", "lack of calibrated and reliable calculation and design procedures"* (Borri & Corradi, 2019).

The Directive of 2011 (Recommendations PCM, 2011), the previous Italian building codes of 2008 (Ministero delle Infrastrutture e dei Trasporti, 2008) and the current one, released 10 years later, distinguish between ordinary and listed buildings, but compared to the 1986 guidelines, require a numerical evaluation of the structural safety, which will be done before and after an intervention and must testify the achievement of a higher level of safety. Building Codes distinguishes three types of interventions for existing buildings:

- **adaptation:** interventions aimed at achieving the safety levels for by the same regulation;
- **improvement:** interventions aimed at increasing the existing structural safety, even without necessarily reach the levels required by the Code;
- **local repairs:** or interventions affecting isolated elements, and which in any case involve an improvement of pre-existing safety conditions.

Considering the invasiveness that adaptation interventions would entail, if it were possible to reach a level of safety required for modern structures, the legislation rightly provides that for CH the only interventions contemplated are those aimed at improving the pre-intervention level (*miglioramento* in Italian). This presupposes an adequate compromise between conservation and acceptable structural safety. The definition of "acceptable" safety levels, as well as the concept of "safety", still represents an open issue for monumental buildings.

In the directive this assessment is recommended by using FEM or similar methods, not available in 1986. Although it is clear that the scientific knowledge in the field of the analysis of historical structures, especially those in masonry, is significantly greater than in those years, there are cases in which the numerical

models are not able to capture the structural behavior of the building as difficulties and non-quantifiable errors could influence the analysis. In case one interfaces with particular constructive characteristics, whose contribution is difficult to evaluate in the analysis, the document provides *"the designer can make use of an adequately motivated subjective analysis"* and this, of course, is a critical point of the code.

Regarding safety, as opposed to the principle of minimum intervention, some comments are considered appropriate. This principle is shared not only by the rules but also by the International Council on Monuments and Sites (ICOMOS) in the Venice charter (ICOMOS, 1964) and in the most recent document (ICOMOS, 2003), in which it is explicitly reported:

> *"Each intervention should be in proportion to the safety objectives set, thus keeping intervention to the minimum to guarantee safety and durability with the least harm to heritage values".*

Carrying out a minimum intervention certainly does not mean not intervening or intervening less than necessary. It is already perceived in the definition that, once the safety objectives have been defined (which may certainly be lower than those of ordinary new buildings), the intervention that least affects the values of the asset, among all possible ones, will be put into practice. In fact, as well as heavy interventions are not tolerable since they would upset an asset that was not designed to meet current requirements, in the same way, preferring non-intervention in situations of proven necessity is not as acceptable: the collapse of a heritage structure or part of it is undoubtedly more dramatic than an intervention from many points of view.

SHM can be included in this debate because, if performed adequately, it gives the possibility to evaluate the evolution of the health of a structure. A lot of information can be gleaned from the dynamic identification of a structure. Weak or too deformable parts of the building can be identified by analysing the vibrating modes. Pre and post seismic events can reveal hidden damage to sight. The evolution of natural frequencies, net of the other factors that influence them, can reveal the propagation or birth of damage, even in the absence of an earthquake. A monitoring system implicitly increases its safety level thanks to the continuous knowledge of its state: small dangerous variations can be perceived immediately and precautions can be taken quickly, either by limiting the use of the asset or by providing temporary supports. Commonly instantaneous and anticipated

interventions will have less entity and would satisfy both the safety criterion and the minimum intervention. The close relationship between structural interventions and monitoring is effectively expressed in the Guidelines released within The Eu-India Economic Cross Cultural Programme (EU-India Economic Cross Cultural Programme, 2006) where it can be read:

> *"Strengthening and monitoring should be regarded as complementary activities. Monitoring may be used to limit the extent of a strengthening operation; the adequacy of the response of the structure and the maintenance of a required "safety" can be assessed via long term monitoring; monitoring will permit the detection of a unexpected inadequate behaviour and thus give the chance to implement future corrections or additional strengthening".*

However, despite being a very precious tool, monitoring remains a means of knowledge. If a new damage is identified, localized and assessed (i.e. the first levels of the Rytter hierarchy (Rytter, 1993)), monitoring should be integrated with additional methods of analysis to plan optimal low-invasive interventions.

Chapter 2

Issues, approaches and strategies for the monitoring of architectural heritage

Before going into the heart of the thesis, it seems appropriate to define some key concepts and in particular the meanings they assume in this document. In fact, although some of the concepts are known and usually employed in various disciplinary fields, here they will be projected in the context of the CH structures and will therefore take on their own particular meaning that should be specified.

In the sphere of AH, SHM terminology indicates the process of extracting structural information from records acquired on a structure of cultural interest and the definition of its diagnosis. In general, different types of measurements can be acquired in a monitoring procedure, which for convenience can be grouped into two macro categories: static and dynamic. They are acquired at relatively short intervals of time by sensors positioned on the structure in order to collect data in the points of relevant structural interest and maximize the extractable information. For the times that usually characterize a variation of structural condition, it is observed that, in ordinary cases, a daily sampling can be a good compromise between a tight control and an easily manageable computational burden. Nevertheless, sampling can always be thickened if the condition requires it, for example when the building has been heavily damaged by an earthquake and there is a risk of collapse or during

structural interventions, when it is advisable to promptly know any changes in the parameters. Some data, depending on the type of sensor, are processed in order to obtain so-called damage-sensitive characteristics, that is, those parameters that "react" to a structural change, such as damage, and which can therefore be used as health indicators.

In some situations, monitoring data alone would not be sufficient to understand the complex functioning of works designed and built tens, hundreds or thousands of years ago. Therefore, in order to reach a diagnosis that is as robust and precise as possible, measurements deriving from different sensors, Non-Destructive Test (NDT), historical and geometric information are integrated in a complex path of knowledge. This expresses all the multidisciplinarity of the conservation process of an asset, which implies the collaboration of restoration and geomatics experts, structural engineers, historians, archaeologists, etc. (Nayci et al., 2020).

In this document, particular attention will be paid to the so-called dynamic monitoring, that is the one that tries to define the condition of an asset starting from the study of its vibrations. It is currently applied to many engineering sectors, such as mechanics, aerospace, naval, electronics and many others (Boller, 2009; Chang et al., 2002; Farrar & Worden, 2012). In each sector there are specific issues, critical aspects related to their own case studies, which the research is trying to overcome. In the specific case of AH, aspects such as the unusual geometry, the uncertain connection details, the properties of the materials unknown and often altered over time, the interventions undergone represent sources of uncertainty that can significantly influence the diagnosis, both if carried out with traditional tests and by exploiting the dynamic monitoring series.

To these are added specific issues concerning dynamic monitoring, which will be discussed later. Basically, in this chapter the concepts of vibrational SHM will be explored from the CH perspective, highlighting the issues to which reference will be made throughout the document. Some Italian and international case studies that have been the subject of research in this sector in recent years will be shown.

2.1 Similarities and differences with the diagnostic process used in medicine

The analytical phase of the diagnostic process is typical of medicine and it is no coincidence that there are assonances with the same concepts used in SHM, but with important differences.

In fact, many terms coined and used in the medical field, such as *diagnosis, anamnesis, prognosis,* etc. are effectively re-proposed in SHM. The parallelism appears even more effective if we consider the monitoring of the AH: they give the whole idea of elderly patients, who wear the signs of time and lived experiences, which can be read through injuries, damage and decay. The juxtaposition of the two sectors is even proposed in the ICOMOS guidelines (ICOMOS, 2003), which states in point 1.6:

> *"The peculiarity of heritage structures, with their complex history, requires the organisation of studies and proposals in precise steps that are similar to those used in medicine. Anamnesis, diagnosis, therapy and controls, corresponding respectively to the searches for significant data and information, individuation of the causes of damage and decay, choice of the remedial measures and control of the efficiency of the interventions. In order to achieve cost effectiveness and minimal impact on architectural heritage using funds available in a rational way; it is usually necessary that the study repeat these steps in an iterative process."*

To assess the patient's health, many vital signs can be monitored. In many cases, a report that contains information relating the trend the pulse rate, respiratory rate, body temperature, blood pressure and saturation is enough to identify the presence of pathologies, at least the most common. Replicating this monitoring on a structure might seem strange because it apparently has no vital parameters that give information about its condition, clearly being an inanimate object. However, the structures also have a heartbeat, in a way. Each structure is in fact a system characterized by a certain mass and stiffness. The stiffness of the system is directly linked to the health of the structure as it varies when damage appears or interventions are carried out to increase safety. Mass and stiffness define the dynamics of the system, i.e. how the structure responds to inputs (displacements or

forces). Assuming that the mass varies very little, or that in any case a substantial mass variation does not occur spontaneously and unnoticed, one can indirectly monitor the stiffness of the structure ─ and therefore its health condition ─ by monitoring its dynamic parameters (Fan & Qiao, 2011; Salawu, 1997).

Probably the most important difference between the two types of patients, animate and inanimate, is the ability to communicate their malaise. A structure could continue to accumulate significant damage without anyone noticing. This is extremely dangerous as it, or parts of it, could come to a sudden collapse, without giving time and opportunity to intervene. A monitoring system acts as the sensory apparatus of the structure and the measurements that are extracted are what it communicates about its state of health in its language. SHM aims to translate records into diagnostic information using techniques for data analysis, statistics, models, ML algorithms, and so on.

In monitoring a person's vital signs, conceive a diagnosis just establishing threshold health values beyond which an "unhealthy" condition is expected is not an effective strategy. In fact, for example if we set the minimum and maximum breathing rate, we will have a false alarm every time the patient holds his breath or engages in a workout, absolutely harmless activities and reversible variations on vital parameters. Their danger lies in their potential to hide pathological manifestations by compensating with opposite variations for the anomalies the disease would create in the data. In such a situation we would have an ongoing pathology which however does not manifest itself at the data level, i.e. a *false negative,* which could delay and make less effective or even vain subsequent interventions / therapies.

Also, in the structural field there are conditions that temporarily and harmlessly alter the aforementioned diagnostic parameters and are precisely the environmental conditions. A brief clarification: to indicate these confounding effects, the SHM community refers to Environmental and Operational Variations (EOVs), since for mechanical, aerospace or even civil structures (e.g. bridges, platforms, tanks) with a distinctly functional rather than cultural character, operating conditions can heavily influence the response of the system; for AH, which by their nature are not subject to major operational variations, environmental conditions have a greater weight and that is why in this discussion the effect of the environment will be treated in more detail.

Like holding breath and workout for humans, environmental phenomena (reference is made to ordinary environmental phenomena) are harmless and reversible for structures but, temporarily modifying the dynamic parameters, increase the uncertainty of the diagnosis. For this reason, the study of their effect on the structural response is an important step in the constitution of an accurate monitoring procedure and finding an "health indicator" that is very sensitive to damage and as less sensible as possible to environmental effects is one of the main challenges of the SHM community. In this document these aspects will be explore in depth with focus on AH.

2.2 Vibration based SHM

The idea of studying the dynamic response of a structure to identify any damage is by no means new. There are traces of its implementation using acoustic or vibration-based techniques, no doubt qualitatively, already from past centuries, as reported in (Higgins, 1895; Stanley, 1995), where a tap test was used to detect cracks in railroad wheels.

However, only in the last decades, this sector has shown such a development to face the passage from the research phase to that of practical application. This has happened in some sectors more than in others where specific difficulties have hindered or slowed down effective executions. In civil engineering, this practice has mainly reached infrastructures such as bridges, viaducts, tall skyscrapers. The application is motivated by several unforeseen collapses of bridges that have resulted in loss of life and a desire to reduce the life cycle costs associated with these facilities through the use of condition-based maintenance (Farrar & Worden, 2012).

On the other hand, the application of vibrations based SHM on heritage structures is still, to date, a little beaten field, especially as regards practical applications. It may be due, in the first place, to the difficulties encountered in general in the monitoring of civil structures and infrastructures, given by the scale of the buildings which requires more extensive and therefore more expensive and carefully designed monitoring systems, the great uncertainties due to the heterogeneity of the materials, the cracking state, manufacturing defects, the uniqueness of each structure, exposure to environmental phenomena, unpredictability of operating conditions, etc. (De Stefano & Ceravolo, 2007; Peeters et al., 2004); to these are added a non-immediate visualization of the benefits that could bring to the AH sector. These systems are in fact designed to prevent

structural damage, or rather, detect structural damage in its initial state, so that actions can be undertaken before it becomes irreparable. And in general, even when it comes to human health, it is more difficult to devote effort and money to something that seems healthy, not understanding that prevention can avoid catastrophic events, as well as allowing economic savings after an initial investment.

Moreover, there is a general skepticism about the use of these modern vibration based SHM techniques, because, as anticipated, only a few years ago they landed in the world of real structures (Clementi et al., 2021). This is not so true for monitoring systems capable of measuring physical quantities such as the width of the cracks, the pressure in the material, the tension in a reinforcing element. It is a fact that some structures belonging to the AH, certainly the most relevant or with the most unsafe conditions, have been equipped with so-called "static" monitoring systems (Ottoni & Blasi, 2015). Probably it is because these provide more immediate and easier to interpret information than a dynamic monitoring system: everyone, experts and non-experts, understands the danger of a crack that is opening more than it should; not everyone has the same sense of danger when reading a natural frequency drop.

Yet, a very important concept should be highlighted: instruments such as crackmeters, pressure cells, load cells, return information that has a *local* value, that is, referring only to the point in which they are applied. This opens up two paths: (i) a very dense (and therefore very expensive) sensor network is set up, which is not the ideal case for buildings and AH, which often have extraordinary dimensions; (ii) a limited number of sensors are predisposed with the risk that, if a more extensive damage that does not involve the instrumented position is taking place, the instruments will not be able to register it. A dynamic monitoring system instead, coupled with a proper vibration-based procedure, will be able to provide information on the overall behavior of the structure, and therefore to capture significant structural changes that could lead to its collapse. In fact, vibration testing can be thought and considered as a *global* non-destructive health monitoring technique. Global methods typically use the lower modes of the structure as their "dynamic fingerprint": they can work with a much coarser network of sensors which is usually spread over the entire asset (Balageas et al., 2010). This certainly does not mean that a static local system is less effective, but on the contrary, integrating it with the dynamic one, following the discovery of a damage, one could have valuable information to locate it and understand its entity. In many cases, static

and dynamic measurements are coupled (Alaggio et al., 2021; Ceravolo et al., 2021; Gentile, Ruccolo, & Canali, 2019b; Gentile, Ruccolo, & Saisi, 2019; Kita et al., 2019; Masciotta et al., 2017; Saisi et al., 2017).

The concept of a vibration-based damage detection procedure is to get dynamic parameters, such as eigenfrequencies and modal shapes, from measurements acquired at predetermined time intervals. These quantities, which in a monitoring protocol are obtained through an identification procedure (among the most commonly used: (Overschee & De Moor, 1996)), analytically they are closely related to the mass and stiffness of the vibrating system. Stiffness, which is briefly defined as the ability of a body to oppose the elastic deformation caused by an applied force, depends on the material properties, on the constraints and on the shape. These characteristics could be altered due to those slow deteriorating phenomena or sudden shocks described in the previous paragraphs, endangering the health of the architectural asset. Therefore, observing the trend of the dynamic characteristics means supervise the evolution of the stiffness and of these characteristics and thus appreciate the structural condition. Unfortunately, it is not only structural health that influences its dynamic behavior but also specific environmental and operational factors can cause fluctuations in these parameters, which are called in the jargon EOVs (Sohn, 2007; Sohn et al., 1999; Xia et al., 2012). Their presence affects the damage detection potential.

Rytter (Rytter, 1993) defined 4 main tasks for a damage assessment procedure: *level I*: damage detection; *level II*: localization of the damage; *level III*: quantification of the damage and *level IV*: prognosis of the residual useful life. Level I only provide information on the occurrence of damage in the structure, which is absolutely sufficient for many real applications. The challenge at this level is just to obtain indicators as sensitive as possible to damage and as little as possible to other effects, such EOVs, being able to detect small damage in an early state without receiving too many false alarms. This, which is a fundamental aspect in SHM of civil structures and architectural assets, will be discussed extensively in paragraph 2.3 and in the following chapters.

The dynamic response of a structure can be measured continuously, periodically or once. In the first case, the sensors are permanently installed on the structure and the accelerometric signals are collected and processed in order to extract the aforementioned diagnostic characteristics. This is the most convenient paradigm from the point of view of monitoring, since the structural behavior towards the stresses given by the external environment can be viewed in full, anomalous behaviors can be detected immediately, from the first symptoms and

slow damage developments such as those from fatigue can be perceived as long time series are collected. This practice, if done in real time, also makes it possible to avoid catastrophes as, when anomalous behaviors occur, the structure could be promptly declared uninhabitable and subjected to an intervention in a short time. Obviously, this of the three is generally the most expensive and demanding solution, since it involves the long-term purchase or rental of the instrumentation, provides a protocol for data analysis and structural diagnosis that is implemented and managed by qualified personnel continuously.

Periodic monitoring, on the other hand, is a middle ground between continuous monitoring and real dynamic tests. It consists in measuring signals on the structure, periodically, therefore not leaving the system fixed on the object. It is a procedure that has the advantage of being able to monitor various structures in turn with the same instrumentation, perhaps maintaining a sufficiently short interval between one measurement and another so as not to risk losing the appearance of anomalies. The measurement on a structure can also last for a certain period in order to also obtain information on environmental variations, which however would always and in any case be segmented, if compared to continuous monitoring. A very useful application consists in comparing the diagnostic parameters pre and post traumatic event, such as an earthquake: if the measurements of a structure are available prior to the event, new tests can be made to understand if the dynamic response has changed and therefore the structure has been damaged. Obviously appropriate attention must be paid to the environmental conditions of the two tests since these could cause percentage variations of up to 10% during a year (Peeters & De Roeck, 2001; Xia et al., 2012).

The last option is one-time or *una-tantum* monitoring. This, rather than a monitoring can be seen as a non-destructive test. It returns the dynamic characteristics of the structure that can be analysed on their own or in combination with a numerical model; for example, by analysing only the extracted vibrating modes we can understand if there are particular, asymmetrical behaviors, e.g. caused by differences in stiffness or deformability in some areas. Instead, when a FEM of the structure is available, it can be updated with experimental results through proper model updating techniques, reaching a high degree of similarity with its real twin. The model can therefore be used for the optimal design of interventions or to predict the structural response to changes in external conditions. As this is an isolated procedure, many sensors can be used and a spatial resolution of the vibrating modes can be reached, as exhaustive as possible. On the other hand,

the parameters obtained are strictly dependent on the period and the conditions in which the signals were acquired, and there will be no way to understand the annual evolution of those parameters if not by repeating the test. In the next paragraph some examples of monitored architectural assets that follow these three paradigms are shown and some peculiarities are highlighted.

2.2.1 Dynamic identification: some relevant applications to heritage structures

As anticipated, in the world of civil structures the practice of dynamic monitoring has been facing the passage from research to practical application in recent years, and this is demonstrated by the fact that to date there are no regulations governing these practices.

Architectural assets are further behind than newly built infrastructures or skyscrapers in this transition, probably due to the reasons mentioned above, such as the unawareness of the benefits by those who manage these structures, the perplexity of facing an investment for the purpose of prevention and probably the idea that these structures can continue to last for centuries, as they have already done, even without proper care from a structural point of view. At the research level, however, many studies and applications have been made and documented and it is hoped that they can form a solid basis for future concrete applications and even for the drafting of guidelines. Among the assets which have been subjected to such tests, here, where possible, more space will be given to case studies on which the author himself has had the opportunity to work.

One-time monitoring – dynamic test campaign

Among the three solutions on which dynamic tests are combined, probably the una-tantum is the most common for AH, since it does not involve the permanent installation of sensors and acquirer, it is simpler to carry out and not so expensive as the others but it must be stressed that the results will be linked to the conditions in which the test is carried out.

In any case, having these data available, even through a single test, offers a term of comparison if a traumatic event happens, to compare the diagnostic parameters before and after the event, as one can always decide to repeat the test. The advantage of these techniques is that they can be applied to any type of architectural asset, to anything that vibrates, and in fact here will be reported examples of very different structures in terms of style, materials, history, function, artistic and cultural value.

The underground Pavilion V, located in Turin (Italy) is an example of application to the heritage of the twentieth century (Ceravolo, Coletta, et al., 2020). Especially following the collapse of the Polcevera bridge, questions have arisen about the very durability of consolidated materials and technologies, in particular prestressed concrete. The Pavilion is an iconic structure designed by Morandi, conceived in 1958 as an extension of the exhibition space that houses the industrial vehicles section of the Turin Motor Show. It consists of a single large space, 69 m wide and 151 m long, and is located 8 m below ground level (Figure 2. 1).

Figure 2. 1: internal view of Pavilion V, designed by R. Morandi

In this case, the dynamic characterization tests were considered necessary for the interpretation of the structural system in view of a possible reuse as a part of the Polytechnic of Turin. The tests had the objective of probing the structural and seismic reliability of this type of scheme, as well as its possible improvement and seismic restoration, to be designed with the support of a FEM calibrated thanks to the results of the dynamic identification (Figure 2. 2).

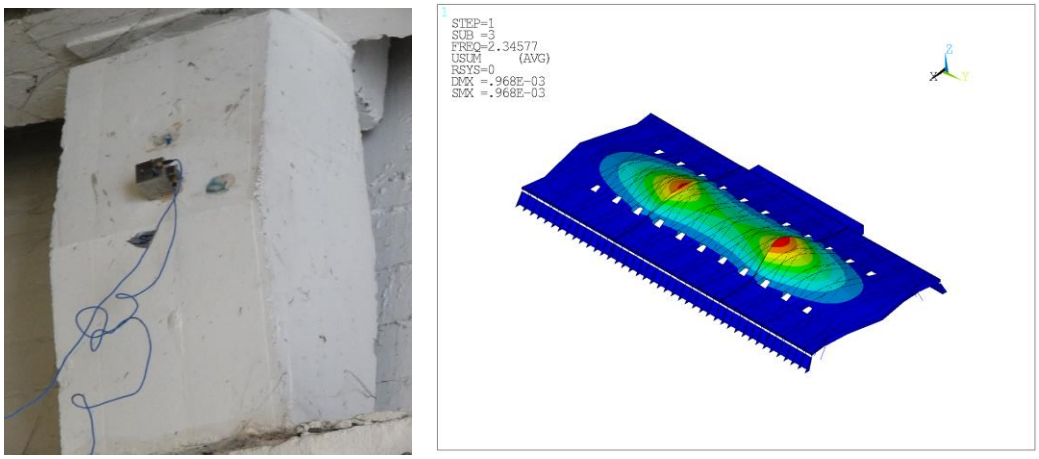

(a) (b)

Figure 2. 2: instrumented small connecting rod (a) and FEM of the Pavilion V (b)

As usual in these cases, a preliminary numerical model has been built for the optimal definition of the locations of the sensors: they are generally placed in the positions that have greater freedom of movement (Figure 2. 2a). Thanks to it, two setups were defined. The first configuration was designed to obtain information especially in the horizontal x-y plane while the second mainly investigates the vertical direction. The tests were conducted using both the environmental excitation and the impulsive excitation of a hammer. Two critical and characteristic aspects emerged from the tests on the pavilion: its great rigidity and the uncertain functioning of the expansion joints. The structure, in fact, being underground and squat, had shown a very low deformability which made the identification process problematic, as the amplitude of the accelerations recorded was very low. The second aspect concerned the uncertainty about the connection of the 3 macroblocks that compose it: the link was designed to disconnect the three bodies but it was not taken for granted that, over the years, it had remained so. The modal shapes identified thanks to these tests confirmed their functioning. It should be noted that this constitutes a weakness from the seismic point of view as the three independent blocks could hammer each other in the event of a seismic shock. And in fact, this will be an aspect to which great importance must be given in the interventions to make the structure safe and reusable. This is an example of how the dynamic tests have highlighted criticalities. Furthermore, the dynamic parameters identified were used, together with the results of mechanical tests, to calibrate the FEM on which the interventions for reuse will be designed (Figure 2. 2b).

Another asset subjected to dynamic tests, distinctly different from the previous one is the church *Santa Maria delle Grazie*, better known as *Santa Caterina*, located in Casale Monferrato (AL), Italy. It can be considered one of the most important Baroque religious buildings of that territory, built between 1718-1726 on a project attributed, in classical historiography, to Giovanni Battista Scapitta (Figure 2. 3).

Figure 2. 3: external view of the *Santa Caterina* church

From the geometric point of view, it is characterized by a large oval dome with the principal axes of about 10 and 15 m, which is supported by a 7-meter-high drum. The dome is built on eight arches and as many buttresses, which flow into a thin lantern, 5 meters high, consisting of eight masonry slender pillars, one for each buttress. The façade is one of the most richly decorated elements and it protrudes from the main body of the church by about 6 m, constituting a potential element of seismic vulnerability. As concerns had arisen about the condition of the church, some non-destructive tests were planned, including a dynamic test campaign (Ceravolo et al., 2016).

The dynamic tests were conducted in September 2010 and were divided into 4 sensor setups, in order to spatially cover all the more informative points of the

structure that had been indicated, as for the Morandi's pavilion, by the preliminary FEM. To merge modal shapes identified in the different setups, a subset of "links" sensors had been kept fixed during the dynamic tests: this operation maximizes the spatial resolution, even when a limited number of sensors are available with respect to the complexity of the geometry. It is clear that this process can be implemented only when the sensors are not fixed on the structure, therefore in a una-tantum, or at most in a periodic monitoring procedure, if the structural complexity requires a higher resolution. In this case, only ambient noise was provided to excite the structure. This procedure made it possible to clearly identify four vibrating modes of the structure which were exploited to update the preliminary model. Two main aspects were ascertained from this procedure: an excessive deformability of the lantern, implicitly detected by the equivalent modulus resulting from the updating and confirmed by the critical crack pattern of the pillars detected by the visual inspection; and in addiction, a substantial disconnection between the facade and the rest of the church. This information was invaluable in guiding the reinforcement interventions that were completed on the lantern (Figure 2. 4) and are being developed on the façade.

Figure 2. 4: reinforcement intervention on the lantern of the *Santa Caterina* church

Among the different examples reported in the literature, the following are mentioned: the *temple of San Nicolò* in Carpi (MO, Italy), example of 16th century

architecture, where the dynamic tests have allowed the design of an intervention for the reduction of seismic vulnerability by means of isolators and dampers (Figure 2. 5a) (Sonda et al., 2015); the bell tower of Fossano, which flanks the *Cathedral of Fossano* (CN) dedicated to Santa Maria and San Giovenale and dates back to the end of the 14th century, in which the dynamic tests confirmed the results of the non-destructive tests, which identified the central part as the weakest. As a result of these findings and the dangerous spread of a crack, it was declared unfit for use and a hooping operation was planned (Figure 2. 5b) (Ceravolo et al., 2016). Even much older works have been subjected to this type of test: as an example, the Colosseum (Pau & Vestroni, 2008), probably the most famous Italian monument in the world.

(a) (b)

Figure 2. 5: temple of *San Nicolò* (a) and bell tower of the Cathedral of Fossano (b)

Periodic monitoring

Reference can be made to the term monitoring even when the observation is not strictly continuous, but at a sufficiently high frequency with respect to the monitored process, so that any anomalies can be detected early.

There may be various objectives that lead to undertake periodic monitoring procedures. For example, in Portugal on the *Mogaduro* clock tower, a tower of the medieval castle of the same name, dating back to the 17th century, several tests were carried out between 2005 and 2007 (Figure 2. 6a) (Ramos et al., 2010). In particular, the first tests were made before the structural rehabilitation and the results were compared with those obtained after intervention. In this case, this monitoring was

aimed at verifying the effectiveness of the intervention consisting in lime injection for the consolidation of the walls, replacement of material with high level of degradation, filling of voids and losses and installation of ties (or steel belt) at two levels. After this it was also decided to install a periodic monitoring system to evaluate the environmental effects of temperature and relative air humidity on the dynamic behavior of the tower, and to detect any possible non-stabilized phenomenon in the structure, that it was not possible to investigate with isolated measures.

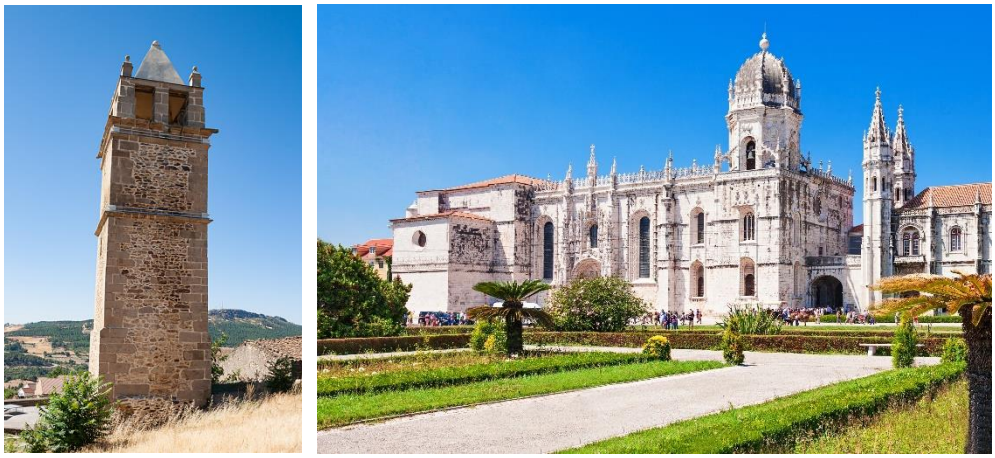

(a) (b)

Figure 2. 6: Mogaduro clock tower (a) and Church of Monastery of Jerónimos (b)

For a similar purpose, a dynamic monitoring system was installed on the Church of Monastery of Jerónimos in Lisbon (Masciotta et al., 2016), celebration of the most important historical period of the Portuguese nation, built in the 16th century in honour of Portuguese navigator Vasco da Gama (Figure 2. 6b). It recorded data for just under 3 years, thanks to which important considerations on the effect that the external environment has on the dynamics could be extract. For example, a strong positive correlation was found between temperature and natural frequencies, while a moderate negative linear correlation with the relative humidity emerged. The system was accidentally in operation when an earthquake of magnitude Mw = 6.1 and with epicenter offshore Southwest Iberia occurred. Therefore, a comparison between the pre and post-earthquake frequencies was possible and it was observed that a decrease, even if very limited, took place following the quake.

Another case involved in periodic dynamic monitoring is represented by the church of *Anime Sante* in l'Aquila (Italy), 18th century church whose collapse on

live television made it one of the symbols of the 2009 earthquake (Figure 2. 7a) (Boscato et al., 2012; Russo, 2013). A 2-year static and dynamic monitoring activity was performed to check the structural response and the actual level of damage after the earthquake. In this period the dome was subjected not only to the usual environmental excitation, but also to a series of tremors that were part of the seismic swarm of the previous earthquake. These excitations, undoubtedly greater than the environmental ones, were exploited to more accurately identify the dynamic parameters. This campaign was meant to analyse the residual yield and evaluate the ancient church. The dynamic monitoring of this asset provides also a way to indirectly check possible drops of tension in the cables and relaxation in the FRP belts used for safety.

(a) (b)

Figure 2. 7: damaged *Anime Sante* church and Saint Torcato church

Even for the Saint Torcato church, a *neo-manueline* 19th century temple in the North of Portugal (Figure 2. 7b) the effectiveness of anchoring systems was wisely evaluated on dynamic measurements before and after its activation. In this case, an increase in modal frequencies, linked to a strengthening in stiffness, was found (Masciotta et al., 2017).

Permanent monitoring

The number of heritage structures dynamically monitored on a continuous basis are still limited today. Some of the most relevant cases in the literature are reported here. Among the Italian monuments, the *Basilica of Collemaggio* in l'Aquila is mentioned, an ancient church of the 13th century considered the highest expression of the architecture of its region (Figure 2. 8). It is a masonry structure which was severely damaged, just like the church of *Anime Sante*, by the 2009 earthquake but it was rehabilitated and reopened in 2017. After rehabilitation, the monitoring

system has effectively become an essential tool for the implementation of the conservation plan (Alaggio et al., 2021). The conservation plan has the objective of evaluating the conservation status of the basilica, on the basis of its intrinsic vulnerability and the regional seismic risk. Research activities are attempting to evaluate reliability thresholds and to define damage detection and localization procedures. In addition to detecting the classic seasonal fluctuations, the continuous monitoring was able to capture evolution of the frequencies trend over years. And in fact, the analysis of the time series has led to highlight a decreasing of the natural frequencies over time, with almost 0.1 Hz frequency decrement in 2 years. One of the possible explanations lies in the in-plane stiffness decaying of the Cross-Lam timber roof due to superficial microcracking.

Figure 2. 8: external view of *Basilica of Collemaggio*

A few years ago, the bell tower of the *Basilica di San Pietro* in Perugia (Italy) was equipped with a continuous monitoring system (Ubertini et al., 2017). It is a 13th century polygonal-shaped tower, about 70 m high, with a tapered spire, which flanks the oldest basilica (Figure 2. 9). The acquired signals are currently analysed using an advanced SHM procedure in order to detect departures of the structural behavior from normal conditions. A procedure is envisaged for the removal of environmental confounding effects from time series of the extracted natural frequencies, based on adequate statistical modeling and, finally, a novelty detection is used to identify damage. The results of the research conducted both with the experimental data and with the FEM have shown that the minimum detectable damage is relatively small (i.e. such as not to compromise the safety of the structure) and it would not be easily detected by a visual inspection. Therefore, it proves to be, although still at the research level, an SHM system capable of enabling an early

detection of structural damage, thus providing the key information that is needed to promptly undertake remedial actions.

Figure 2. 9: bell tower of the *Basilica di San Pietro*

Other relevant Italian cases are represented by the *Basilica of Santa Maria Degli Angeli* in Assisi (Cavalagli et al., 2017), the *Carrobiolo tower* in Monza (Gentile, Ruccolo, & Saisi, 2019; Saisi et al., 2017), the much ancient *temple of Neptune* in Paestum (Zuchtriegel et al., 2020), the *Milan Cathedral* with one of the largest monitoring systems (Gentile, Ruccolo, & Canali, 2019a) the *Hagia Sophia Basilica* (Kasimzade et al., 2018) and last, not least, the *Sanctuary of Vicoforte* (Chiorino et al., 2011; Pecorelli et al., 2017). The latter and the data recorded by its monitoring system, will form the basis of the analyses carried out in the next chapters. Therefore, it seemed appropriate to dedicate a paragraph to it and report the details of both the basilica and the monitoring system installed. Below will be briefly reported the construction phases of the work, the main investigations conducted and summarized the results previously obtained, highlighting those that in some way contributed to the analyses presented in this document. This is not intended to draw up an exhaustive treatment but will give the reader a global vision of the structure and of what revolves around it. More attention will instead be placed on the two monitoring systems, whose characteristics directly affect the analyses

presented in the following chapters; their description is reported for convenience in chapter 3, where also the data collected by them are shown.

The Sanctuary of Vicoforte

The Sanctuary of Vicoforte, also known as the basilica *Regina Montis Regalis*, is a majestic Baroque architecture located in the homonymous town, in the northwest of the Italian peninsula (Figure 2. 10).

Figure 2. 10: external view of the *Sanctuary of Vicoforte*

Its construction is linked to a miraculous event that took place in 1592, when it seems that a fresco of the Virgin Mary depicted on a rural pillar began to gush drops of blood when it was accidentally hit by a hunter (Cozzo, 2002; Cozzo et al., 2017). This event shook the citizens, in which a strong Marian devotion is re-entered, so much so that it was deemed opportune and necessary to build a small chapel around the pylon. The interest, the devotion and the pilgrimage towards that pillar grew to such an extent that the duke Carlo Emanuele I at the end of the 16th century commissioned the construction of a large Sanctuary. The duke wanted the Sanctuary to become a large mausoleum of the Savoy. The project was entrusted to Ascanio Vittozzi, who reworked the solution already proposed by the court architect Ercole Negri di Sanfront, which already provided for an oval plan. Construction officially began in 1596, but various problems slowed the work progress. They largely depended on the constitution of the foundation soil, which is made up of silt and marl. The death of the architect in 1615 and a few years later of the duke, the lack of financial resources and various political events, decreed the

abandonment of the site. In fact, the attention of the Savoy in the years to come had shifted to the basilica of Superga in Turin, which effectively became the mausoleum of the dynasty. For decades the construction of the basilica stopped at the level of the impost of the dome. Only at the beginning of the 18th century, the project was taken up again by the architect engineer Francesco Gallo, who before embarking on the project of such a large and particular dome, studied for a long time the structure and the previous project in order to find an optimal solution. He was also supported and encouraged by the then royal architect, Filippo Juvarra. Gallo saw the construction of the high drum and the majestic dome, the largest oval-shaped masonry dome in the world with internal axes of 37.15 and 24.80 meters (Figure 2. 11). An iron ring system was also put in place, consisting of 3 rings of bars with a total section of about 140 cm^2 which was intended to absorb a component of the horizontal thrust. The dome was disarmed in 1732, with the concern and fears of all present who were certainly not used to seeing such bold works.

(a) (b)

Figure 2. 11: external (a) and internal (b) view of the dome of the Sancuary of Vicoforte

The religious, artistic and political interest for the Basilica has always been relevant to the extent that in 1880, it was proclaimed a National Monument. Since then, also given the structural problems that the basilica had from the earliest stages of its construction, many testing campaigns, research and analysis have been carried out in order to define an optimal plan for its protection and conservation.

The first structural investigations were carried out by the engineer Martino Garro in the middle of the century (Garro, 1962). He noted the widespread and troubling state of cracks in which the structure was in those years. The cracks, which are concentrated above all in the most vulnerable points, i.e. near the circular openings of the drum, date back to the first years of construction and were then

aggravated by the differential settlements of the 8 buttresses that carry the drum, with differences up to about 30 cm.

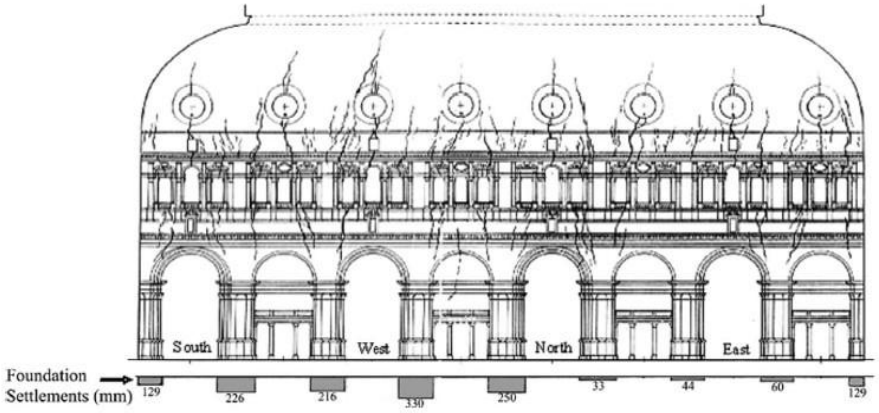

Figure 2. 12: crack pattern and settlements of the Sanctuary of Vicoforte in (Garro, 1962)

Garro even reconstructed the history of the subsidence over time, highlighting that they were already at a worrying level (more than 25 mm) when the structure reached its maximum height of 10 m. In fact, the clayey layer began to plasticise due to the flow of rainwater in the excavation and to yield as the weight of the masonry increased; at the time a drainage system was also built to allow the water to flow out. During the construction of the rest of the Sanctuary, the subsidence continued to evolve. Garro highlighted the difference between settlements of adjacent pillars, as they generate hazardous shear stresses in the masonry.

More recent surveys, divided into 3 campaigns from 1976 to 2008, shed light on the reasons that led to these large differences in subsidence. The campaigns included both geotechnical and geophysical tests (Chiorino et al., 2012; Lai et al., 2009). At first the stratigraphy of the ground beneath the basilica was defined, and on that occasion also the geometry of the foundation of the Sanctuary was modeled. The ground was also characterized by means of SPT (Standard Penetration Test), drilling and laboratory tests, and in a second campaign, its initial properties were also evaluated, i.e. before the construction of the structure. Tests such as Cross Hole and MASW (Multi-station Analysis of Surface Waves), REMI (Refraction Microtremor), Nakamura test, 3D electrical tomography and 2D seismic tomography were made to analyse the terrain from the geophysical perspective. Thanks to these campaigns, today it is known that the soil is characterized by two main formations, in marl and in silt-clayey, with variable thickness. The stiffer marl layer is inclined towards the southwest where it is covered by a thicker silt-clay

layer that reaches up to 5 m. To the east side, however, this layer with the worst mechanical characteristics is very thin and practically the 3 buttresses in that portion rest directly on the marl. The foundations are laid on a mechanically uneven laying surface, as shown in the Figure 2. 13.

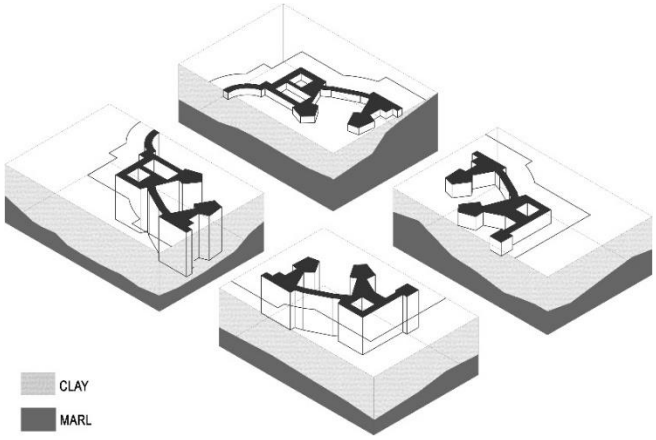

Figure 2. 13: reconstruction of the soil configuration under the Sanctuary

Other investigations of different nature have also been conducted on the Sanctuary in those years and more recently. For example, the precise definition of the three-dimensional shape of the oval dome was obtained thanks to modern 3D modeling techniques and a laser scanner campaign (Aoki et al., 2004) (Figure 2. 14), flanked by the study and comparison with archive drawings (Novello & Piumatti, 2012a, 2012b).

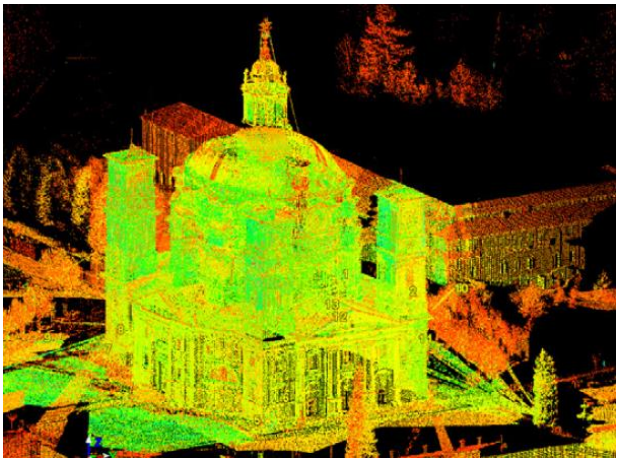

Figure 2. 14: points cloud by (Aoki et al., 2004) laser scanner campaign

The geometric model of the Sanctuary has formed the basis for numerous applications, such as different versions of the FEMs that have been developed over the years (Calderini et al., 2006; Ceravolo, De Lucia, et al., 2020; Chiorino, Calderini, et al., 2008). Each has specific characteristics in relation to the purpose for which it is realized. For example, in (Calderini et al., 2006) a continuum anisotropic non-linear constitutive model is used to conduct a non-linear FE analysis limited to the dome-drum system, under mass forces and a set of settlements of the foundations. In the following chapters, two FEM will be involved, built in *Ansys*® and *Diana FEA*® environments, which differ mainly in the size of soil modeled, as well as in the software. Both refer to linear elastic isotropic constitutive laws, assigned to each macro-element. The evident simplification is motivated by the objective for which the models were created, that is, global dynamic analyses under light environmental stresses.

At the same time as these investigations were carried out, a new strengthening system for the dome, in addition to the original, was designed and installed (Figure 2. 15a).

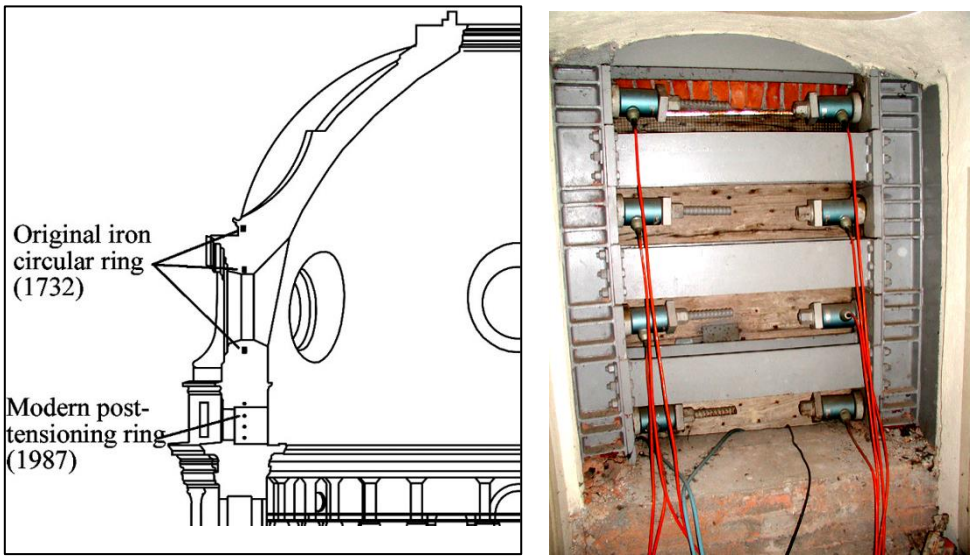

(a) (b)

Figure 2. 15: strengthening systems (a) and ends of eight post-tensioned bars on a steel frame

This system consists of 56 post-tensioned *Dywidag* high-strength steel tie-rods ($f_y \approx 1080$ MPa, 32 mm in diameter) inserted inside the masonry on top of the drum anchored in 14 points along the perimeter of the Sanctuary. The interface between two adjacent series of bars consists of a steel frame inserted in the masonry,

necessary to ensure continuity (Figure 2. 15b). The bars were equipped with tensioning devices operated by means of jacks and load cells for the instantaneous reading of the load values, placed at both ends. The system, following a significant initial tension loss, was re-tensioned in 1997, 10 years after it was put into operation.

2.3 The environmental effects

Unless there are particular situations, the heritage structures are totally or partially exposed to climatic events, such as rain, extreme temperatures (both positive and negative), wind storms, excessive humidity, snow, hail, etc., like all other civil structures. Unlike the latter, however, heritage structures are often characterized by greater fragility which may be due, depending on the case, to the age of the materials, the lack of protective systems / treatments or the audacity of the geometries that could make them more exposed than less unusual and valuable buildings.

These environmental phenomena, in addition to having a "direct" deterioration effect, which in most cases occurs over a fairly long period of time, also cause problems when trying to establish an accurate diagnosis based on monitoring data. In fact, it is found that some climatic phenomena influence the measures of both static and dynamic structural response (Bassoli et al., 2017; Boller, 2009; Cross, 2012; Deraemaeker et al., 2008; Kita et al., 2019; Ni et al., 2005; Sohn, 2007). For clarity, here we are not referring to sensor measurement errors caused by climatic events, but real changes in structural behavior, correctly recorded by the sensors. Then, if the structural behavior changes and the sensors successfully detect it, why should it be a problem for SHM? the answer is simple: the effects of environmental variations on the diagnostic characteristics of a structure are easily confused with those due to structural damage.

In fact, these effects, although (in most cases) harmless and completely reversible (that is, at the end of the climatic event the diagnostic parameters return as before), the variation they generate in the diagnostic characteristics can be comparable to that of the damage. Distinguishing between the two is paramount. In fact, those who manage a monitoring system are interested in the health of the structure and therefore in the dangerous permanent variations of its stiffness, as they need this information to establish any maintenance interventions, provide for limitations in the use of the property or even the temporary closure.

Confusing the two triggers could have two types of consequences:

- **False positive error:** i.e. when a climatic effect is confused with a damage. This condition could occur frequently if the "good health" thresholds of the structure have been set with a large margin of safety. Receiving a (false) alarm whenever a more or less extraordinary climatic event occurs (which could also last for several days) involves mobilizing each time a team of technicians to check the state of the structure on site, as well as the evacuation of people present, workers and visitors. This undoubtedly makes the monitoring protocol inefficient, expensive and unnecessarily limiting.
- **False negative error:** i.e. when the effect of the appearance of damage on the monitoring data is attributed to a climatic event. In the most fortunate cases, this could simply delay the necessary intervention, which however could increase invasiveness as the damage progresses. But in cases of particularly serious damage, the structure could be compromised before the error is recognized, nullifying the possibility of intervening and making monitoring fundamentally useless. This second scenario, although rarer than the first, could have dramatic consequences and cause losses in terms of heritage (the protected structure itself, cultural objects it contains, frescoes) as well as endangering the people inside and around the building.

Environmental factors can affect both the mass and the stiffness of the system. In fact, precipitations such as snow, rain and hail could be seen as a mass addition to the system, which could last for days, until the liquid stored in the cavities or porosities of the materials dries completely. Variations in temperature could affect stiffness, for example due to the effect of freezing which tends to stiffen the body (Peeters & De Roeck, 2001). Predicting the effect that these factors have on the structure is not trivial. In the literature, for those same assets monitored permanently or periodically (see chapter 2.2.1) relations have been found, for example as regards temperature and modal frequencies, directly proportional (Masciotta et al., 2017; Tronci et al., 2020), bilinear (Ramos et al., 2010), inversely proportional (Gentile, Ruccolo, & Canali, 2019a), with proportionality depending on the mode considered (Saisi & Gentile, 2015), or also, for the same structure, some modes are closely related to thermal conditions and others seem almost uncorrelated (Saisi et al., 2018).

These trends certainly strongly depend on the structural scheme and the material, but also on a series of contributing causes such as the contiguity with other buildings, the presence of reinforcing elements made in different materials, the way

in which environmental factors affect the building and also how this last modify the properties of the foundation soil. In fact, the vibrating system will also include a more or less large portion of foundation soil, whose properties (e.g. degree of humidity and temperature), which are also dependent on environmental factors, will affect the diagnostic parameters. Therefore, the first step of this study will be to study how environmental phenomena affect both the static and dynamic behavior of the chosen case study. This will be dealt with and taken up from the 3rd chapter of this document onwards.

2.4 Machine Learning approaches to SHM

As has happened and happens in most of the engineering sectors, also in SHM the technological advancement is gradually spreading, making improvements or replacing procedures that in the past were done manually by operators.

In general, progress is appreciated on different scales, ranging from the hardware component to the software, but also strategies and algorithms that are implemented to process the data. For example, in monitoring, technological development has led to the creation of increasingly advanced sensors, capable of recording the desired quantities at higher frequency and more accurately, which are collected and recorded in increasingly powerful and fast computers, forming moles of impressive data, which would be impossible for an operator to analyse. Thus, also in this sector, ML techniques have begun to spread, aimed at synthesizing and generalizing data by extracting information on which to base a decision-making process (Farrar & Worden, 2012; Figueiredo et al., 2011; Flah et al., 2020; Smarsly et al., 2016). ML emulates the learning ability of human by using computers to automatically acquire knowledge and skills and by learning to refine continuously its performance, achieving self-improvement. The goal of is to design some methods they can find effectively the intrinsic relationships in the data learning from known data, thus predicting unknown data or judge their characteristics. For example, in the monitoring of civil structures their application aims to associate certain diagnostic characteristics measured on a building with a structural condition, whether physiological or pathological. Generalization is the most troubling problem for ML.

From the perspective of the theory of knowledge, ML is very similar to human learning (Mitchell, 2000). Both machine and human learning are knowledge-

increasing processes and both algorithms and humans aim to become intelligent. However, the following differences could be highlighted:

- Human learning is a long-term process; ML is generally fast and short.
- Human beings are forgetful and can only remember some knowledge while machines can remember all knowledge it has learned.
- Knowledge is not transportable for human learning, i.e. a person's knowledge cannot be copied directly to another. ML can copy the knowledge learned into any other system.
- A distinct characteristic of human learning is generating ideas in a best way, while the ideas obtained by ML are usually not the best.
- The connection and inspiration of humans are complex to be simulated by a machine. Human learning can be of jumping style, while machines always follow rules docilely. This is caused by the different logics followed by human learning and ML, respectively.

When computers are applied to solve a practical problem, the methods to obtain the searched solutions from a set of input data usually must be explicit. This is not always possible. If particularly complicated problems are faced, the possibility that there is no valid method to solve them could happen. An example in this sector could be the modeling of a particularly dynamically complex structure, where not all the influencing parameters are evident: in such cases also the computational burden could represent a problem.

An effective strategy is to learn input-output functionality from examples in a similar way where children learn what sports cars are, by simply being told which cars are sports rather than receiving a precise specification of sportiness (Chu et al., 2008). The approach of using examples to synthesize associations is known as the learning methodology. Examples of input/output functionality are called *training data*.

In SHM, the basic idea is to learn from the training dataset a relationship between these characteristics and the presence / type of damage, and then reapply it thereafter on new, unknown data. Integrating these methodologies into a procedure for monitoring an architectural asset would lead to benefits from various points of view: it would allow the process to be automated by minimizing the intervention of an expert operator. A well-calibrated algorithm should even exceed the performance of an operator, having the speed and computing power of a

machine able to easily handle large amounts of data, even high dimensional ones, and not being subject to human error. The ease of management and the reduced cost could be incentives for the diffusion of structural monitoring systems for AH, with all the advantages of having continuous information on the health of these structures, as extensively explained in chapter 1. And it would not be strange if with their diffusion their efficiency also increased, given that today the scarcity of examples is one of the major obstacles to the improvement of these systems.

Some key concepts of ML from SHM point of view are recalled below. This discussion is not intended to be exhaustive but has the purpose of defining a unique terminology for understanding this document. For more detailed information on the general theory of ML and pattern recognition, reference can be made to (Bishop, 2006).

2.4.1 Supervised vs unsupervised

ML problems fall into two macro categories: those of *supervised learning* and those of *unsupervised learning*. The difference between them lies in the availability of the output, or *labels*, in the training phase of an algorithm.

If labels are available, we are dealing with a supervised learning problem. In this case the algorithm can learn a relationship between them and the measured data, with the intent of applying it to new, unknown data to predict their labels. Depending on the type of label, the algorithm can address 2 tasks: classification or regression. A supervised classification problem is faced when, given a single or multi-dimensional data set, the goal is to assign a categorical class (marked with a label) to each data; these classes are discrete: for example, in SHM they are generally represented by a structural diagnosis, for example "normal condition", "damaged condition" (in the most fortunate cases each class indicates a type of damage). In regression problems quite simply, labels are one or more continuous variables but the basic idea is exactly analogous to that of classification. Regression problems can be used in SHM, for example, to predict diagnostic parameters of a structure, on the basis of specific predictor variables, which can be represented by other diagnostic parameters (homogeneous or inhomogeneous with those predicted) environmental or operational variables. Predicting the behavior of a structure under normal conditions gives the opportunity to make a comparison with the one actually measured, from which important differences should emerge if the structure diverges from its usual behavior.

On the other hand, in an unsupervised problem there is no training label available, so the final goal cannot be, as in the previous case, to associate a concrete meaning to the data, since there is no already categorized data on which be based; nevertheless, an unsupervised procedure could allow to get relevant information from unlabelled data. Among the possible tasks, when there is no labelled data, there are clustering analysis and anomaly detection analysis. In clustering, the data is "observed" by the algorithm and a logical grouping is derived from it rather than forcing the grouping, as in the previous cases, according to the categories that we attribute to it externally. The other task, namely anomaly detection, also called novelty detection, or outlier analysis, is of great interest for SHM. If data is available that is known to come from the normal condition of a structure, a statistic can be constructed of such data. At that point, any data subsequently collected can be tested to see if it conforms in some sense with the model of normality; if it is not, then it can be said that the non-conformity will correspond to a damage. Intuitively, it can be seen as a two-class problem classification. This task is very convenient for SHM, as one of the major obstacles in this area is not having labelled data available, as will be discussed further on. Using an unsupervised algorithm allows you to minimize the initial information needed, while still implementing a reliable damage detection procedure. Obviously, it will have the limit of not being able to distinguish the type of anomaly that would arise but numerical models can be combined to go further in the Rytter hierarchy (Rytter, 1993).

2.4.2 Training data

In both supervised and unsupervised problems, initial data is needed to initialize the algorithm. In fact, in these problems three phases are generally defined as training, validation and test phase.

This initial data makes up the ML algorithm. The training dataset (TD) is supplied to the algorithm with or without the corresponding outputs, depending on the type of problem to be addressed. The model evaluates the data repeatedly and uses it to define its parameters. The goal is to build a model that generalizes well even new data, unknown to the algorithm, as well as of course those of the TD.

In some cases of supervised problems, a validation is expected on a small set of labelled data, which however are not used for training. This is mainly used to avoid the phenomenon of overfitting, i.e. that the algorithm adapts too tightly to the TD and therefore fails to generalize data other than those. The validation dataset is used to adjust some parameters of the algorithm, before it is final. A sort of test set,

but on which algorithm can have feedback and modify the parameters that regulate it. The testing dataset, on the other hand, is the set in which the algorithm, already trained and validated, will be applied in order to complete one of the previously mentioned tasks, then provide labels, discrete or continuous, define the cluster to which it belongs and detect a certain novelty.

Once the differences between the various sets have been clarified, it is important to clarify some aspects related to the world of structural monitoring. In a perfectly ideal situation, in which all data relating to every possible structural condition were available, the most intuitive thing to do would be to imprint a supervised classification problem. A dataset containing all possible conditions would be provided to the algorithm as training. It would be validated on another data set and then, in its final version, applied in real time or in near real time to the data that would be recorded continuously on the structure. If well fitting, the algorithm would be able to label any structural condition that would arise, since, having already seen it in the training set, it would already know the characteristics. The trivial question is: where could the data for any structural condition be taken from?

Is it possible to know in some way how the diagnostic parameters of a structure would evolve following a specific damage? The author tries to analyse each road and evaluate the obstacles that may arise.

Use of experimental data relating to past periods

This choice assumes that: (i) the structure, some time ago, has suffered that specific damage; (ii) the data relating to that condition has been recorded; (iii) the structure has been brought back exactly to the previous situation.

The practice of dynamic monitoring of AH is quite young and only a few structures boast historical data series that cover a period long enough to include an episode of damage and repair (indeed more than one and of various kinds for a complete training set). But this is not the main problem, as it could be solved after a few years. Obviously, this also presupposes that the structure naturally undergoes these damages, as it is not possible from a multitude of points of view (cultural, historical, artistic, economic, political, sociological, religious) to procure voluntary damage to these structures: there is a possibility that this will never happen. But yet, in case all of the above happened somehow, returning the structure to its previous conditions would be the biggest challenge. How would it be possible to repair a

structural element, perhaps requiring consolidation, use of higher performance materials, new connections, etc., and regain the same initial behavior? This is highly unlikely because while wanting to reuse the same material, it would have different properties, as the originals have most likely evolved over time, or the element had a crack pattern that cannot be replicated on the new one and many other differences that would be even difficult to list all.

Use data from another similar structure

This could represent a more than valid solution to strengthen a monitoring process of easily replicable, mass-produced structures.

In fact, by sacrificing one or a certain number of them to obtain data relating to damages, a training dataset could be created to build a model applicable in the future on all copy products. this would involve an initial investment which, however, would be recovered since the data could be exploited on all products of that type, unless there are manufacturing differences or production defects. Evidently, this is a process that can be applied to structures that are easily replicable and economically expendable in view of future recovery. One can think, for example, of mechanical structures, aeronautic or aerospace components. It is also equally evident that this concept is not applicable to civil structures but in particular to architectural assets, which, very concisely, are neither replicable nor economically expendable, as well as culturally, artistically, historically and morally. And therefore, how can an algorithm be trained if this data is not available?

In this thesis we will discuss this topic and some proposals will be presented such as that of creating damage data starting from other dynamically similar systems. Their data are clearly not directly usable to train the chosen algorithm because will present significant differences with the structure being monitored and therefore it will be shown how to "adapt" the data and make them usable for different (but similar) systems from those on which they were acquired. An alternative method will also be presented to collect data similar to those deriving from damage, obtained by implementing an indisputably reversible operation. In addition, a strategy will be shown that can be defined halfway between supervised and unsupervised: it starts from a supervised regression, to finally flow into a novelty detection problem, thus addressing the problem of the need for data from damage conditions. In this case the first operation is used to try to mitigate those environmental effects which, as previously explained, create uncertainty in the diagnosis.

Environmental effects are also an important issue for the choice of training data. In fact, if in the discussion on data in damaged conditions it was stated that the ideal would be to train the algorithm to recognize them all or as much as possible, the same applies to environmental condition. In fact, the more experience the algorithm accumulates with respect to the variations given by environmental conditions, the more easily it will be able to recognize them and distinguish them from damage. In fact, generally the best choice when selecting a training set within an available dataset is to include important climatic variations, such as snowfall, wide temperature and humidity ranges and other phenomena that will affect the behavior of the specific structure.

Also reflect on the fact that different environmental conditions and different damages (both with different levels of amplitude) could act simultaneously. Therefore, a training set to be almost exhaustive should contain the combination of all these factors, an unquantifiable amount of real data practically impossible to obtain.

2.4.3 Universality and customization of procedures

A significant aspect, on which it is appropriate to focus attention, is the generality of ML approaches, that is how data driven monitoring procedure based on AI algorithms interfaces with different structural systems. This is fundamental to make it clear that the work described in this document is not limited to (nor aims at) the detailed study of a case study, but is strongly projected towards the generalizability of the proposed methods, in order to involve most of the architectural heritage in a larger and more significant debate.

The analyses carried out mainly concern the Sanctuary of Vicoforte, which, as already specified, is a monumental masonry basilica dating back to the 18th century. However, its structural characteristics have in no way guided or constrained the proposed methodologies: the procedures that an operator entrusted with monitoring the Sanctuary should perform would be absolutely repeatable for a structure different in geometry, material and any other aspect that determines its response: obviously the TD will be different. In fact, ML algorithms work on the data that are given them as inputs, on which, (as their name suggests) they automatically learn and set their parameters. These parameters have no physical meaning, they are not associated with experimentally measurable or estimable quantities on the basis of results reported in the literature, but rather they define the shape of generalization

(classification or regression) within a path of mathematically complicated relationships that is not easy to govern. In fact, it is common practice, at least in the first instance, that the choice of the aforementioned parameters is entrusted to cross validation procedures that choose them on the basis of a compromise between accuracy and overfitting of the training data; subsequently, if necessary, small adjustments can be made to better adapt the generalization to the problem faced, with the awareness of how and how much each parameter influences the results. The automaticity of ML algorithms makes data-driven approaches very appreciable since the same series of operations can be replicated on different structures without the need for manual customization: the algorithm that will read and interpret the data will certainly adapt to the problem but automatically, without the need for an expert operator to intervene. This is an absolute advantage, for example, compared to model driven approaches, in which a different model must be built for each system, set on the basis of experimental measurements and the sensitivity of the operator who in this case plays a fundamental role.

Having clarified that the heart of the SHM procedure would remain practically unchanged, except for internal and automatic modifications of the ML algorithm, a generic monitoring scenario can be considered and examined. Slightly broadening the perspective, two stages can be identified within the entire monitoring protocol of a building in which an appropriate customization would bring substantial benefits: the initial phase of defining the sensor setups and the final phase of the definition of thresholds and decisions.

In fact, the first should be oriented towards the definition of the most sensitive measures possible to the expected damage and less sensitive (or which can more easily be made so) to all other harmless effects. The definition of the instrumentation can be guided by various criteria that include the material that constitutes the structure, the structural scheme, the presence of critical elements for safety as well as evaluations on the costs of the sensors, accessibility and invasiveness. Just to cite a few examples, generally speaking it will be important to keep an eye on the consequences given by thermal expansion in metal structures more than in other materials, as metals are more sensitive to temperature excursions; it is important to monitor possible hammering phenomena, for example through LVDTs, if you are dealing with structures divided into blocks or adjacent structures, such as church and relative bell tower; the tension inside chains, hooping systems, elements capable of absorbing thrusts should be kept under control through load cells; displacements or related quantities should be observed in soaring elements. The choice of position, as well as the type of sensor, also plays a

fundamental role in the damage detection process, since different positions could contain a highly different degree of information. If a dynamic monitoring system is to be installed on a structure, in addition to the individual optimal positions, the layout as a whole must be designed so that the spatial resolution of the modal shapes is exhaustive. In general, the latter problem is addressed with Optimal Sensor Placement (OSP) procedures. These aspects vary among different structures and currently there is no generally accepted protocol to guide the SHM system design.

As for the last phase instead, it should be highlighted and taken into account that, once the algorithm has been set automatically, a certain number of false positives or, more generally (depending on what kind of nature the ML procedure and what objective it proposes), misclassified data is expected, precisely due to the unpredictable and random nature of the experimental measurements. Clearly, the entire monitoring protocol should be able to manage these situations, i.e. take note of these data, but, in order to report an actual danger to the structure, it should reach a certain number at a certain frequency of occurrence. The latter could be specifically defined on the structure being monitored on the basis of criteria ranging from the stability of the measurement being analysed (opening of the cracks, modal frequencies, pressure / tension in structural elements, etc.) to the variability that characterizes the mechanical parameters of specific materials, the probability of occurrence of phenomena that could cause such harmless anomalies, etc.

To summarize, even if the heart of an ML-based SHM procedure is, so to speak, automatically versatile, the upstream and downstream operations, if appropriately modeled on the observed object, could have great positive influence on the efficiency of the entire monitoring protocol.

Chapter 3

Environment-dependent structural behavior of monitored cultural heritage buildings

The growing interest in preserving and protecting the historical CH has encouraged the application of modern structural monitoring techniques ─ sometimes developed in different fields, such as mechanical, aerospace and civil engineering ─ in the area of architectural assets. As a matter of fact, these techniques, which are based on the analysis and interpretation of the data acquired by the sensors, have proved to be very versatile and effective for various types of structures, clearly after an appropriate parameter setting (Sohn et al., 1996).

The reason for their success lies in the fact that a monitoring system, supported by an intelligent diagnostic features extraction, allows to keep under observation the overall health state of a building, evaluate the condition of conservation and even to readily establish the safety condition after sudden events such as earthquakes (Ashraf et al., 2020; Boscato et al., 2014; Ramos et al., 2013; Russo, 2013; Ubertini et al., 2018). As discussed in chapter 1, symptom-based methods for AH (Bartoli et al., 1996; Gentile et al., 2016; Lorenzoni et al., 2013) are sometimes preferable to approaches based on FEMs, especially when the accuracy of models is strongly affected by a high level of uncertainty regarding the effective properties of materials, their current state, the construction techniques, the possible interventions stratified over the years, the structure-soil interaction and so on (Bal

et al., 2021; Chiorino, Spadafora, et al., 2008; Forgács et al., 2018; Maria D'Altri et al., 2020). Moreover, these techniques are particularly appreciated in the heritage context as they prove to be practically non-invasive, reversible and in addiction, helping to increase the level of knowledge (Cappello et al., 2016; Masciotta et al., 2017; Zonta et al., 2014), they lead to compliance with the minimum intervention principle, as that introduced in the ICOMOS guidelines (ICOMOS, 2003).

However, even data-driven approaches have important issues to address. As discussed in (Deraemaeker et al., 2008; Kita et al., 2019; Sohn, 2007; Sohn et al., 2002; Ubertini et al., 2017) in most cases the structural diagnostic features are influenced by external environment which cause fluctuations that can be confused with the appearance of damage, or worse, hide it. Among all fields of SHM, the issue of environmental variations mainly concerns civil structures, which by their nature are totally exposed to climatic conditions and, in fact, many studies on these effects have been done on signals from historical structures and bridges (Barsocchi et al., 2020; Cabboi et al., 2017; Catbas et al., 2008; García-Macías & Ubertini, 2020; Gentile, Ruccolo, & Canali, 2019b; Ni et al., 2005; Ramos et al., 2010). Discriminating the EOVs from variations due to real damage on the data is crucial to avoid wrong diagnoses.

In this chapter, a large amount of heterogeneous field data related to the Sanctuary of Vicoforte (described in 2.2.1 paragraph) is systematically analysed to investigate which have the greatest influence on its structural behavior. Knowing how monitoring data depend on environmental phenomena allows to shed light on their annual fluctuations, giving us the extent of the values attributable to seasonal variations and actual anomalies which could be associated with changes in the structural system, i.e. damage. Environmental data, measurements of static sensors (Ceravolo et al., 2017) and modal natural frequencies (Ceravolo et al., 2015) collected in more than 10 years are scanned and crossed in order to discover any correlations.

The analysis of these time series, treated with mathematical and statistical tools, has led to some mechanical interpretations of the observed behavior of the Sanctuary and the results obtained, especially in terms of correlations between different factors affecting measurements, are deemed relevant in the practice of long-term monitoring of CH.

3.1 Statistical tools for monitoring time series

In the first part of this sub-chapter, reference is made to theoretical notions useful for explaining subsequent elaborations. They are simple and consolidated concepts of statistics, effective in analysing experimental data.

3.1.1 Correlation analysis

The analysis of correlation is a method of statistical evaluation used to examine the strength of a relationship between continuous variables. This particular type of analysis is useful for confirming possible connections between variables (Ezekiel, 1930; Taylor, 1997).

The existence of a correlation implies that if there is a systematic variation in a variable, it is also found in a variable related to it. The search for a possible correlation between the variables passes through the hypothesis, in this specific case, of the existence of a linear relationship between them. In general, data may also exhibit a more complicated than linear relationship. As a matter of fact, series that have a weak or no linear correlation might have a strong nonlinear relationship. However, checking for linear correlation before fitting any model is a useful way to identify variables that have a simple relationship. In addition, a slight deviation from linearity - which can be detected from the scatter plot of the data - will not heavily affect the measure of their linear dependence, i.e. the *linear correlation coefficient*.

In cases when the uncertainties can be estimated, it could be assessed whether the data approach the linear relationship, if so, the assumption of the linear relationship between the variables would be confirmed. Unfortunately, in many experiments it is not possible to have an *a priori* estimate of uncertainties and directly the raw data must be used to establish if they are linearly related. The linear correlation coefficient (or *Pearson correlation coefficient*) measures the extent to which a set of n data points $(x_1, y_1), \dots (x_n, y_n)$ supports the hypothesized relationship and it is expressed by:

$$r = \frac{\sigma_{xy}}{\sigma_x \sigma_y} \tag{3. 1}$$

where σ_x and σ_y are the standard deviations of the variables and σ_{xy} is their covariance. By considering the definitions of the indices, the Eq. 3.1 can be written in the following form:

$$r = \frac{\sum(x_i - \bar{x})(y_i - \bar{y})}{\sqrt{\sum(x_i - \bar{x})^2 \sum(y_i - \bar{y})^2}} \tag{3. 2}$$

r is a measure of how well the supposed function approximates the data; it is defined in the range $[-1, +1]$. The closer r is to the limits of the interval, the closer the data are to the supposed line. On the contrary, if $|r|$ is very low and close to 0, the points are said to be linearly uncorrelated. The sign of r specifies the slope of the relation: a high positive coefficient implies a *positive correlation*, i.e. the variable increases simultaneously with the other while a *negative correlation* is asserted when a variable decrease when the other increases. Nevertheless, if a strong linear relationship exists between data, there is no expectation that experimental measurements will be settled exactly on a line. For experimental measurements, such as structural monitoring data treated here, unit values can never be obtained. Similarly, as a discrete number n of points is contemplated, one should not expect to obtain perfectly 0 as a r between uncorrelated variables: when the measurements are really uncorrelated, this coefficient decreases as the number of observations increases.

In this chapter, the correlation analysis allows to identify which environmental aspects and structural monitoring variables are related, information that can generate usable insights as they are or even the starting points for further investigations aimed at modeling the physical phenomena that govern the system.

3.1.2 Selection of variables through Principal Component Analysis

If a large number of sensors are installed on the monitored asset, a pre-processing via *Principal Component Analysis* could alleviate the computational burden in view of the correlation analysis.

Principal Component Analysis (PCA), also known as *Hotelling* transform, *Karhunen-Loève* transform or orthogonal decomposition - mathematically speaking - is an orthogonal linear transformation that turn the data points by some scalar projection to a new coordinate system such that the greatest variance comes to lie on the first coordinate (called the *first principal component*), the second greatest variance on the second coordinate, and so on (Jolliffe, 2002). This analysis was first proposed in 1901 by Karl Pearson and then developed by Harold Hotelling in 1933. The aim is to reduce the number of variables describing a system to a smaller number of latent variables, limiting the loss of information as much as possible. This method identifies the most influencing variables through the *Singular Value Decomposition* (SVD) algorithm, a factorization that generalizes the eigen-decomposition for any $n \times d$ matrix through an extension of the polar decomposition.

In particular, given a matrix of *d* variables and *n* observations $[O]_{n\times d}$, the SVD decomposes it in three matrices, as:

$$[O] = [U][S][V]^T \tag{3. 3}$$

where $[U]_{n\times n}$ and $[V]_{d\times d}$ are unitary matrices which contains the *left-singular vectors* and *right-singular vectors* of $[O]$ respectively, and $[S]_{n\times d}$ is a rectangular matrix with real and non-negative terms on the diagonal known as the *singular values* which are sorted in descending order.

For instance, when a very large number of sensors are installed on a monitored structure, the SVD algorithm could be used to choose the most representative time series of the system, for each type of sensor. In particular, as many $[O]$ as the types of sensor installed on the structure are assembled, which collect the d time series in columns. Referring to the temperature data as an example, SVD was used to obtain the singular values of the setup of $d = 24$ thermometers; the most representative temperature devices have been selected starting from the Proper Orthogonal Mode (POM) with highest singular value. A representative device was thus selected which show the highest absolute amplitude of the first POM. This avoids processing a too large number of series containing redundant information, and reduce the data elaboration burden.

3.2 Case study: the Sanctuary of Vicoforte

The Sanctuary of Vicoforte, already described in (2.2.1), represents the benchmark of the analysis proposed in this chapter (Figure 3.1).

Figure 3.1: the Sanctuary of Vicoforte

The choice is guided by the fact that two monitoring systems are installed on the Sanctuary, both continuous, which measure static and dynamic quantities over time. These allow to have valuable information on the structural behavior, which can derive from the reading of the measurements of a single sensor or from the overlapping and crossing of different devices. Since these data will be the heart of this chapter and they will also be used in analysis in subsequent chapters, it is considered appropriate to go into detail and describe in the next two paragraphs the layouts of the sensors of the two continuous monitoring systems.

3.2.1 Static monitoring system

A first instrumentation to monitor the evolution of the significant crack patterns was installed on the Sanctuary in 1983. In the following years, several upgrades of the static monitoring system followed until 2004, when the latest monitoring system was installed and the procedure for the acquisition of data was automated.

The sensors composing the static monitoring system can be grouped into two main categories depending on the measurements recorded: *structural* sensors, which measures crack width, strains and stresses and *boundary conditions* sensors which acquire measurements that are not traceable to diagnostic parameters, but are useful for understanding the evolution of structural behavior.

The first group includes:

- 12 crack meters (of which 2 are damaged) (CM);
- 20 pressure cells to determine the stress in the masonry (CP);
- 56 load cells to monitor the force in the tie-bars (LC);
- 2 orthogonal wire gauges to measure the convergence of the axis of the dome (E).

In Figure 3.2, the layouts of the structural static sensors are reported:

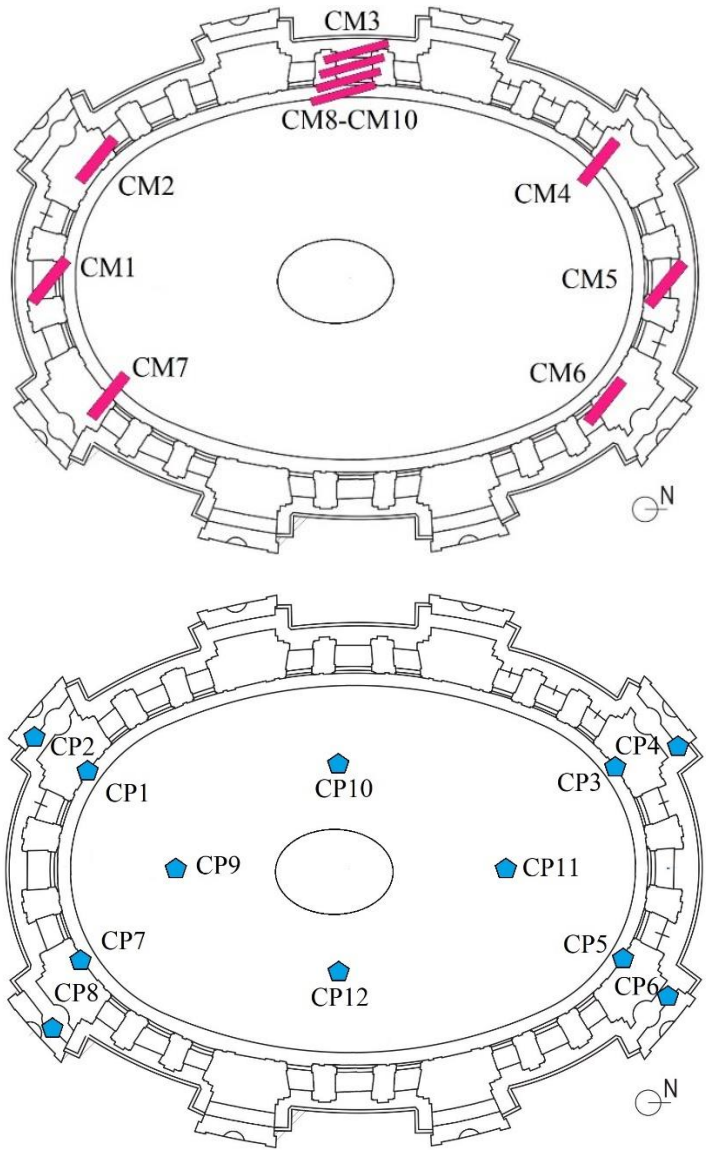

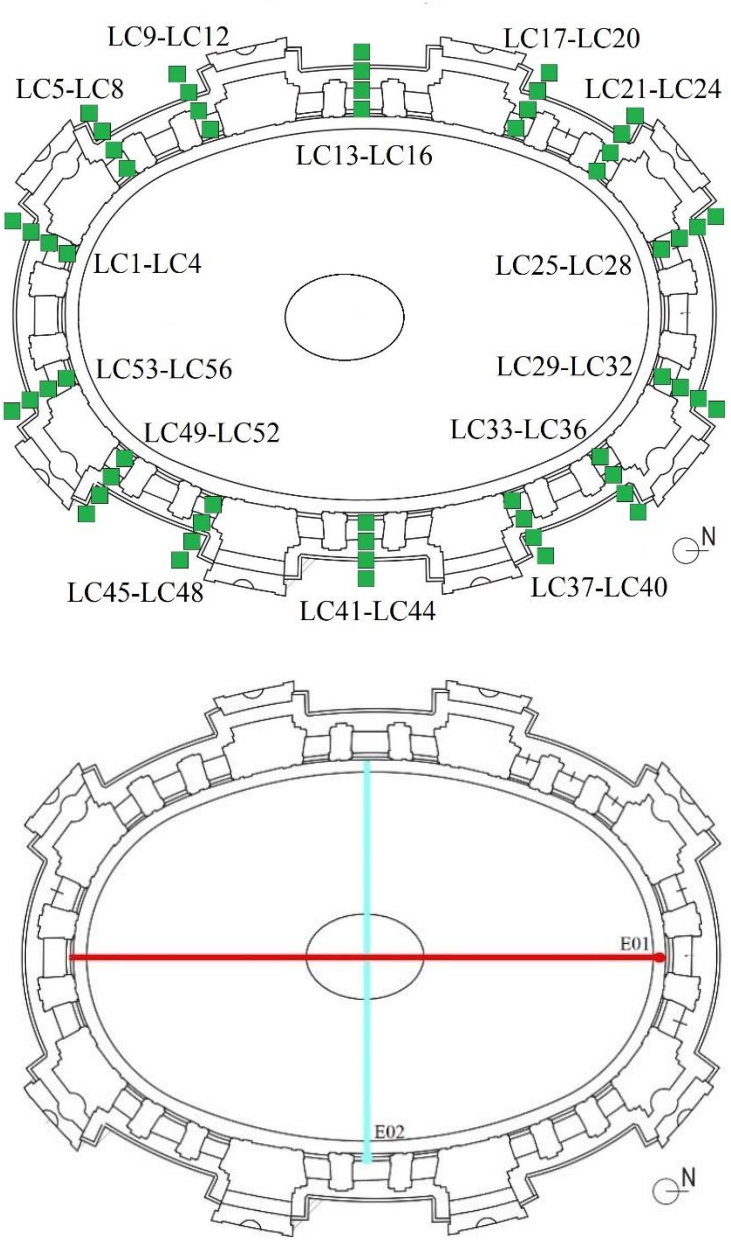

Figure 3.2: layout in plan of crack meters, pressure cells, load cells and wire gauges

The group of boundary conditions sensors includes:

- 24 temperature sensors;
- 3 piezometric electric cells.

Their layouts are reported in Figure 3. 3.

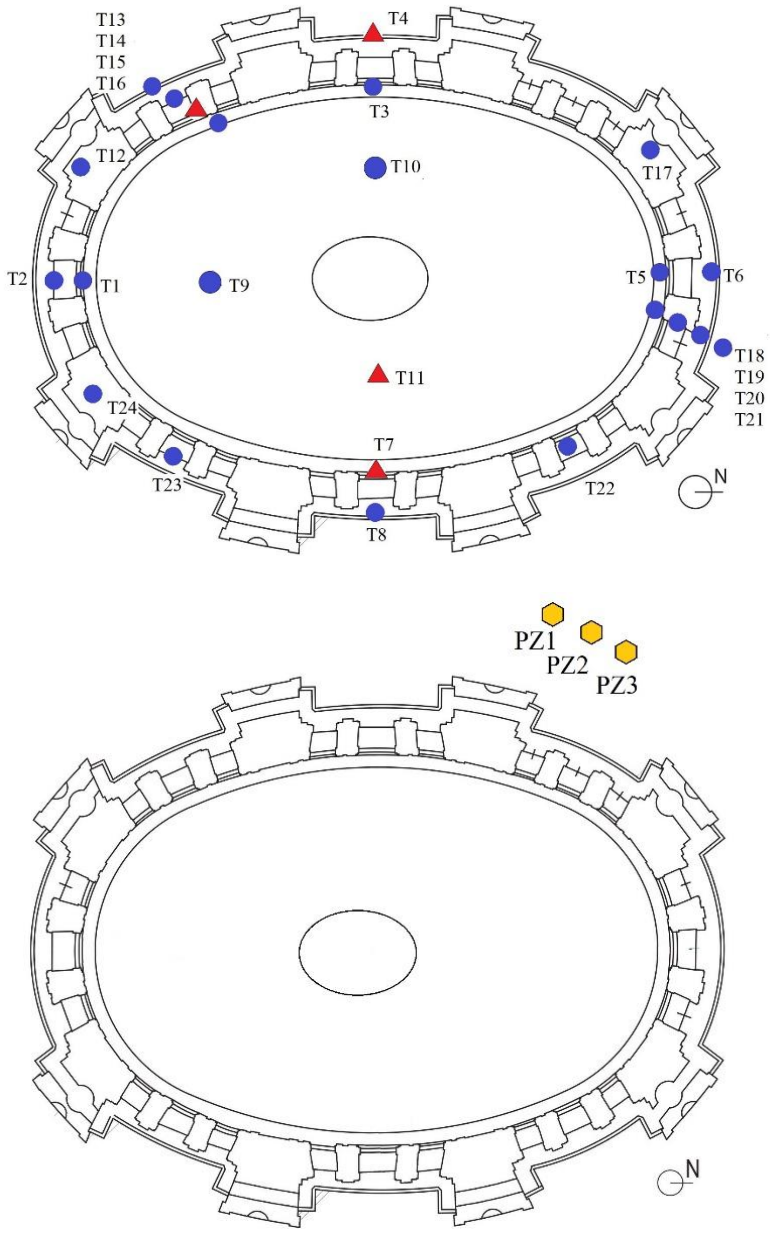

Figure 3. 3: layout in plan of temperature sensors and piezometric electric cells

The crack meters, that are nothing more than LVDTs (Linear Variable Displacement Transducer), check the evolution of the largest cracks and are installed at the bottom of the dome; the load cells monitor the load carried by the

tie bars of the modern strengthening system (Figure 2. 15); the wire gauges measure the elongation of the dome along its minor and major axes. The temperature sensors are installed both inside and outside the structure, in the hole of the staircases, on the bars and in the extrados of the dome.

This system began recording data in 2004, following the stipulation of a new research program between the Polytechnic of Turin and the administration of the Sanctuary, with the contribution of the CRC Foundation. The management was entrusted to the Turin-based company GDTest S.r.l. (https://www.gdtest.it/). All measurements acquired until 2015 were regularly processed and checked. Results showed the substantial efficacy of the reinforcing system in containing deformations of the dome and also revealing technical anomalies (not structural) in some devices (Ceravolo et al., 2017). The renewal of the static monitoring data acquisition and management system is scheduled for 2022, when the integration with the dynamic one will also be carried out.

3.2.2 Dynamic monitoring system

A permanent dynamic monitoring system was also installed on the Sanctuary at the end of 2015. It has the objective of returning so-called "global" information on the structural behavior of the Sanctuary, unlike the static one which instead returns information spatially limited to the point where they are installed. From a conceptual point of view, this is the major difference between the two monitoring systems. The actual data acquisition only started in December 2016, following a process of calibration and optimization of the procedure.

The system consists of 12 mono-axial piezoelectric accelerometers (PCB Piezotronic, model 393B12, seismic, high sensitivity, ceramic shear ICP® accel., 10 V/g, 0.15 to 1k Hz, Resonant Frequency ≥10,000 Hz, Overload Limit ±5000 g pk, Temperature Range −50 to +180 °F) distributed on the structure through an OSP procedure, in order to maximize the spatial resolution of the modal shapes (Ceravolo et al., 2015). Three orthogonal accelerometers are placed at the base of the crypt to keep the ground accelerations and the remaining sensors are located at different levels of the vibrating system, mainly on the lantern-dome-drum elements (Figure 3. 4).

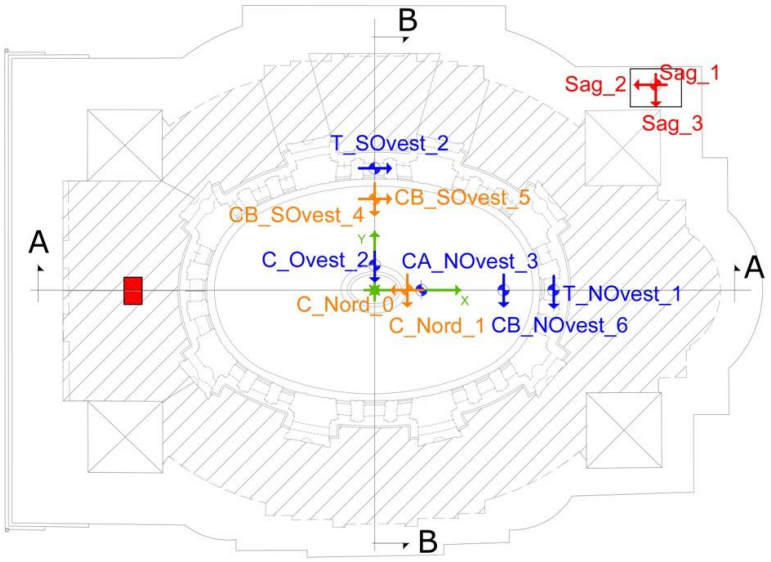

Plan

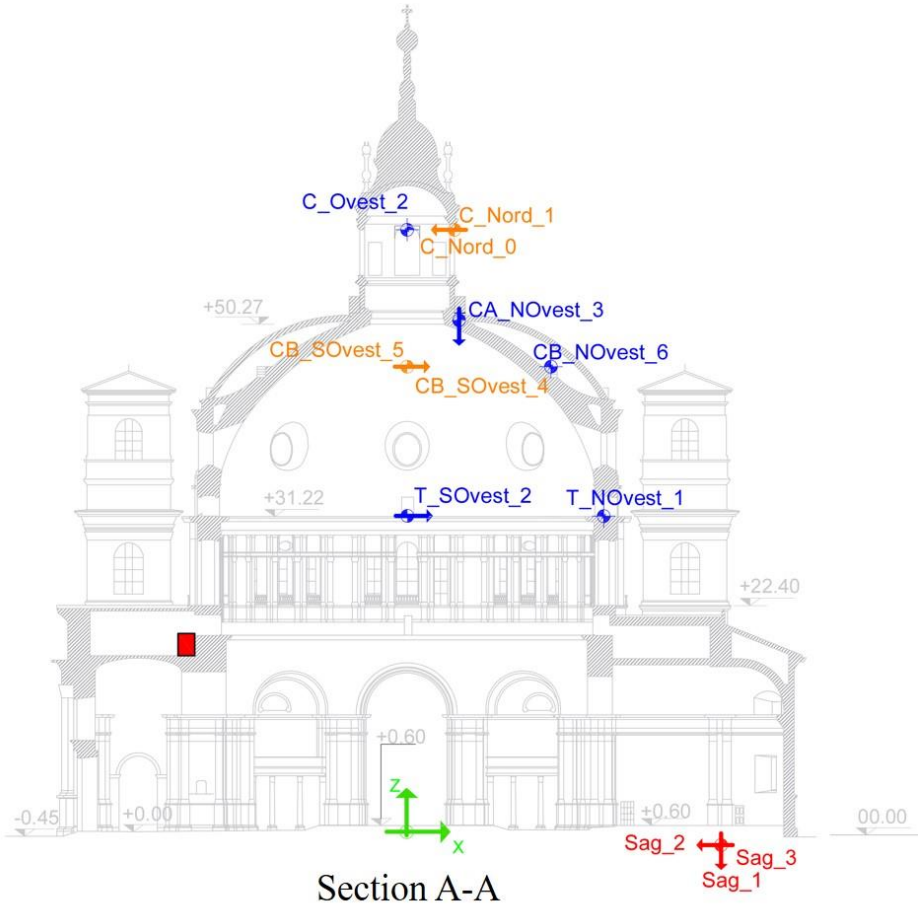

Section A-A

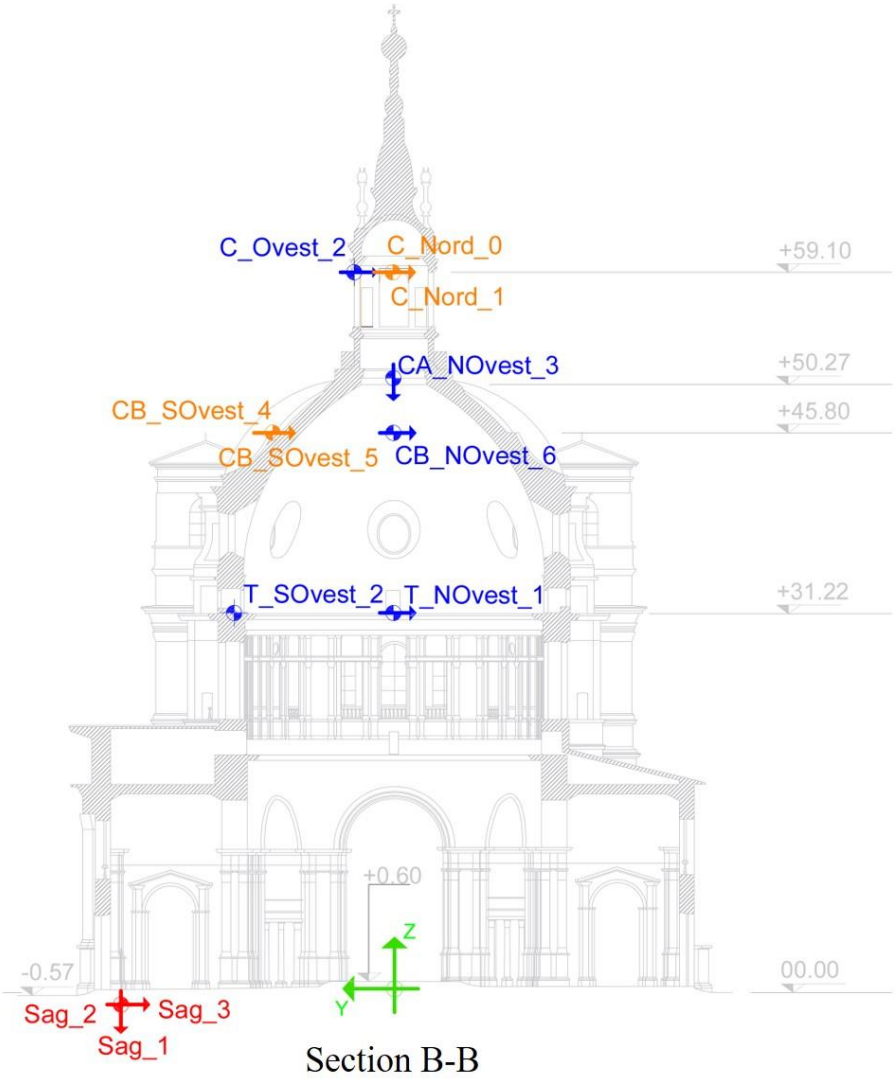

Figure 3. 4: location of accelerometers in plan and in sections A-A and B-B

In order to obtain diagnostic parameters of the structure, i.e. quantities that contain information on structural health, the accelerometric signals are subjected to a dynamic identification procedure which exploit an algorithm of the SSI (Stochastic Subspace Identification) family (Brincker & Andersen, 2006; Overschee & De Moor, 1996), optimized on the needs of the Sanctuary (Pecorelli et al., 2020).

3.3 Processing of the field data

The next paragraphs describe how the data collected directly in field are organized and processed, which is the first step of this analysis. Observations will be made on the plots of the measures and the reasons for which series have been selected rather than others will be clarified. In addition, environmental data measured by a weather station close to the Sanctuary, will also be plotted and described.

3.3.1 Environmental data

The environmental factors considered most significant for civil structures and in particular for this case study, also on the basis of the results of previous studies (Alaggio et al., 2021; Masciotta et al., 2017; Moser & Moaveni, 2011; Ramos et al., 2010; Saisi & Gentile, 2015), are involved in the correlation analysis.

Specifically, the following time series were selected:

- average daily temperature;
- maximum daily temperature;
- minimum daily temperature;
- humidity;
- rainfall.

These data were obtained following a request to *ARPA (Agenzia Regionale per la Protezione Ambientale) Piemonte* agency (Arpa Piemonte, 2000) and are referred to measures recorded in Mondovì (CN), the closest weather station to Vicoforte (about 8 km), in the period from 01/01/2004 to 31/12/2020. The trend over time with a daily sampling is reported in Figure 3. 5.

The graphs clearly show the seasonal trend of temperatures, which takes the form of an almost sinusoidal function. Humidity also seems to follow a seasonal trend, albeit in a much more modest way than the temperature. To study the influence of water phase variations on the structure (present both in the ground and in the pores of the masonry), two lines at 0 and 4 ° C were reported, two reference points for the properties of water: at atmospheric pressure, at 0 ° C the water shows the liquid / solid phase transition, while at 4 ° C it reaches its minimum volume and maximum density. These properties are related to pure water but can still be considered a reliable reference for the water enclosed in the system (Sandrolini et al., 2011).

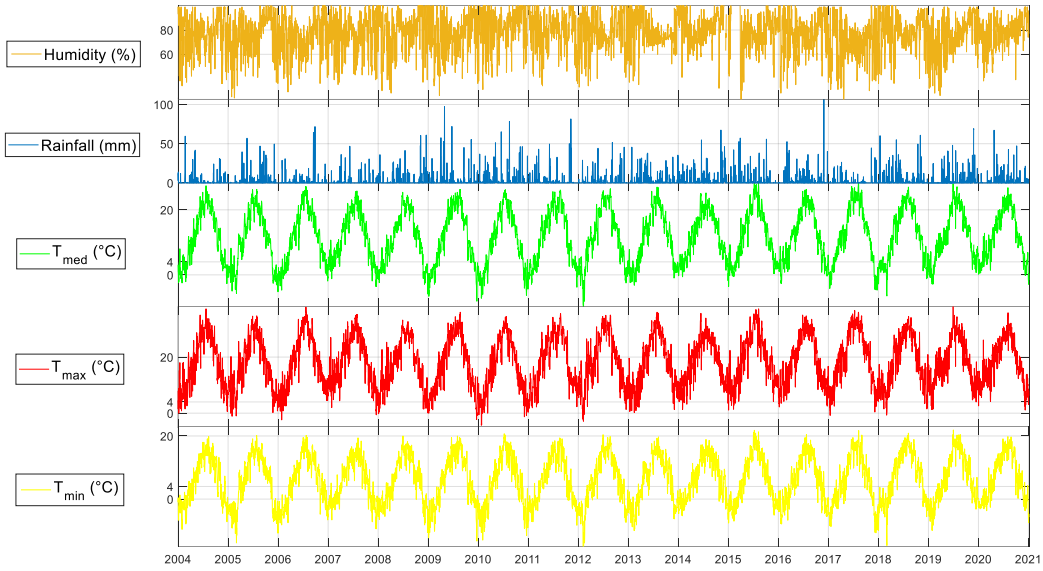

Figure 3. 5: environmental parameters. From the top to the bottom: humidity, rainfall, average temperature, maximum temperature, minimum temperature

3.3.2 Dynamic monitoring data

The accelerograms acquired by the permanent dynamic monitoring system installed on the structure are continuously processed thanks to the automatic identification procedure described in (Pecorelli et al., 2020). They record the response of the structure to environmental, traffic and geological excitation, i.e. no known artificial excitation is applied. Each sensor records signals of approximately 21 minutes starting from the sixth minute of each hour (e.g. at 12:06, 13:06, etc.). The data is stored and then loaded into the identification code, implemented in the Matlab® environment.

Briefly, the signals undergo pre-processing, which performs signal decimation, mean and trend removal, band pass filter, low frequency component removal and signal normalization; subsequently, the most information-rich signal interval, i.e. the 5-minute segment showing the highest Root Mean Square (RMS), is selected and given as an input to the dynamic identification process. Identifying signals with a length of 5 minutes instead of the total of 20 minutes recorded, allows to reduce processing times by minimally affecting the quantity of modes extracted: for the specific case of the Vicoforte Sanctuary, it has been verified that 5 minutes is a sufficiently long time to contain an adequate number of oscillations of the lowest structural frequencies; at the same time, it is not too long, a characteristic that allows

to keep the calculation time at a reasonable level. The identification procedure, as anticipated, uses a time domain technique, SSI. The outputs of the identification procedure are finally subjected to a statistical analysis, comparing different identification sessions and evaluating the stability of the modes when the order of the system increases. Final graphics of the procedure described applied on a single signal are shown in Figure 3. 6, as an example.

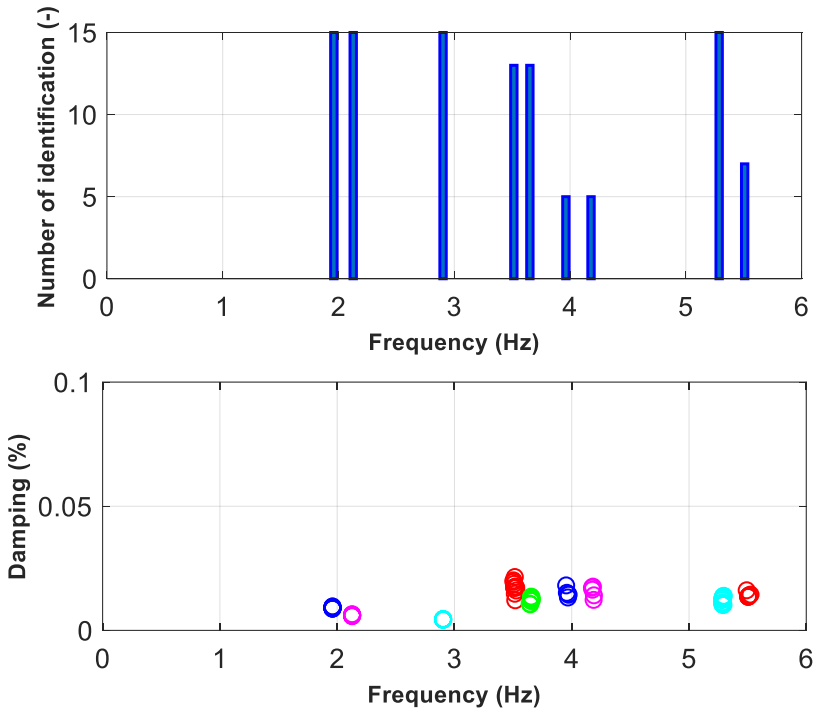

Figure 3. 6: stabilisation and cluster diagrams, output of the identification procedure

In view of an optimization of the identification procedure, the period of the day that statistically returned the greatest number of modes identified was sought. It has been noted that the signals recorded from 18:00 to 6:00 are the most unproductive since they return a much lower number of modes than during the day, probably due to the low level of nocturnal excitation related to the vehicular traffic. Therefore, the procedure processes only daytime signals. For more information on the procedure, please refer to (Pecorelli et al., 2020).

Exclusively as regards the correlation analysis, only one sample per day was considered in order to make the frequencies comparable with the environmental quantities that have daily sampling.

Figure 3. 7 shows the time series of the frequencies identified in the year 2018-2020.

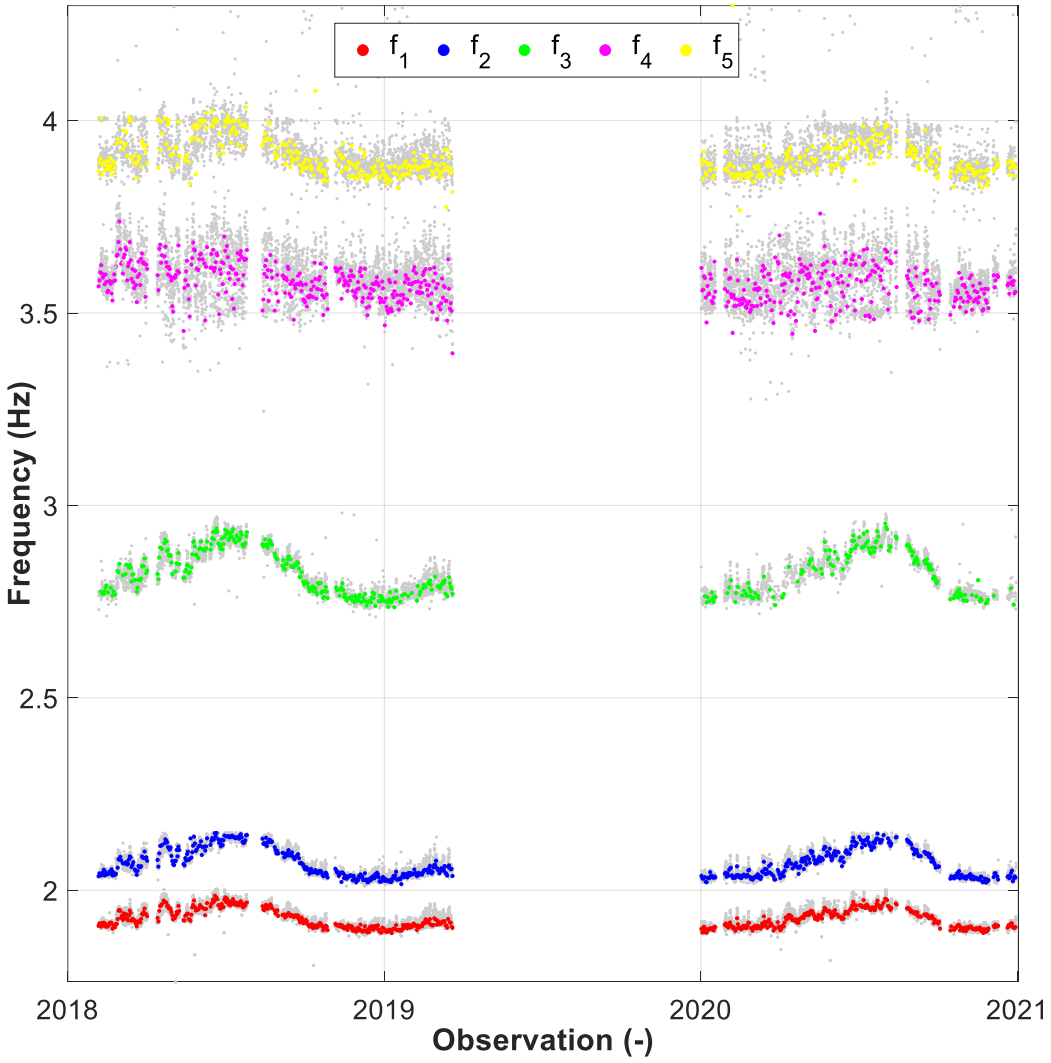

Figure 3. 7: dynamic monitoring data: trends of the first five frequencies of the Sanctuary

All the daily identifications are shown in grey and those of 12:00 of each day, used in the correlation analysis, are highlighted in color. The first one, f_1, corresponds to the first bending mode in the Y direction (the direction of the minor axis of the oval dome), the second one, f_2, to the first bending mode in the X direction (the direction of the major axis). The third frequency, f_3, refers to the first rotational mode, while the fourth and fifth ones, f_4 and f_5, are related to the second bending modes in Y and X, respectively. The minor gaps in the trends correspond

to missing identifications, as it is quite usual that some vibration modes are not identified under common operational conditions. The largest gap, on the other hand, which affects a large part of 2019, is the consequence of a system malfunction that compromised data acquisition. Attempts are currently underway to recover at least some of that data.

The frequencies show a seasonal trend, just like some environmental data. In particular, it seems that the frequency values increase in view of the summer and decrease in the colder months. As already highlighted, the natural frequencies represent a diagnostic parameter of the structure as it depends on the stiffness of the system, which changes with the appearance of damage. Here it can be clearly seen that their behavior is not stationary even in undamaged conditions, a characteristic that makes it difficult to recognize a possible occurrence of damage. The purification of harmless fluctuations in diagnostic parameters or alternatively the search for an associated parameter that is insensitive to these effects is one of the most relevant issues within SHM.

3.3.3 Static monitoring data

As previously mentioned, the static monitoring system was activated in 2004: the analysis of the data acquired in the following 10 years was presented in the paper (Ceravolo et al., 2017).

The static system has undergone periodic malfunctions over time, due to several environmental (thunderstorms and lightning) and technical factors (problems with the electrical box). In order that this study was not affected as little as possible by sensor errors, it was decided to involve only data already verified, i.e. acquisitions up to May 2015. However, this means that there is no temporal overlap between static and dynamic data, i.e. there is no period in which information is available from both.

The graphs in Figure 3. 8 refer, from top to bottom, to the data of thermometers, piezometers, crackmeters (above: the 8 time series; below: zoom on a time series to highlight the seasonal trend), strain gauges which measure the convergence of the dome, pressure cells introduced into the masonry (as before, above all the series, below the zoom on one) and load cells of the strengthening system.

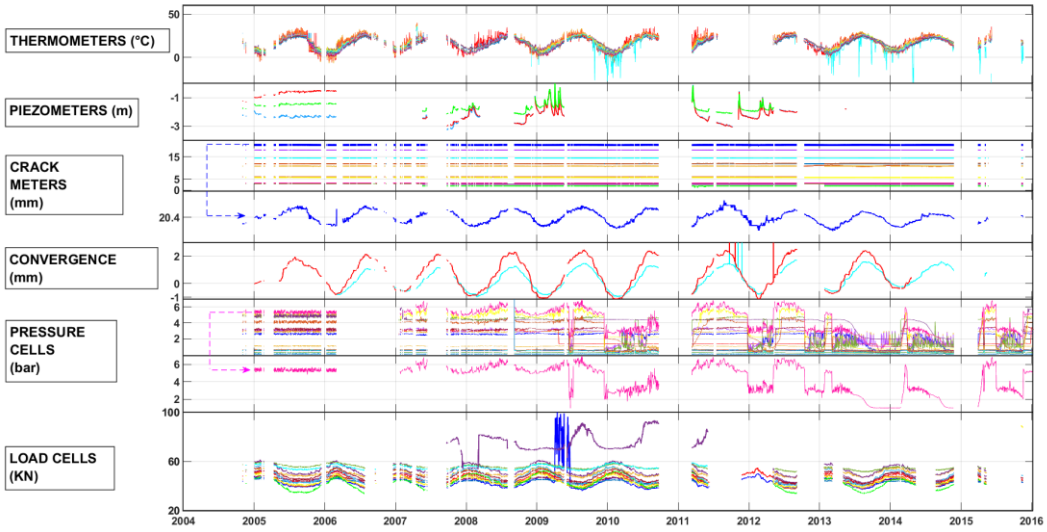

Figure 3. 8: static monitoring data. From the top to the bottom: thermometers, piezometers, crack meters (all and a selected time series), convergence, pressure cells (all and a selected time series), load cells

Many of the recorded static parameters show seasonal fluctuations. This is unquestionably true for the measurement of the temperature of the Sanctuary walls, which is a function of the external one. The thermometers exhibit trends of very similar measurements but shifted by a few degrees as they are installed at different heights both internally and externally. The piezometer data is scarce and following inspections the cause was discovered: the control unit was malfunctioning and therefore the data was not collected correctly. Therefore, it was decided to neglect the piezometric data in subsequent evaluations. The data from the cracks is very interesting: all LVDTs have seasonal trends which show that the cracks tend to open with the arrival of summer and close again as the cold months approach. The expansion of the dome also moves with the changing seasons and is consistent with the measurements of the crack meters: it widens in summer and tightens in winter. It can be observed that the "sinusoid" of the major axis has a greater amplitude than that of the minor axis: it has been noted that in the summer months, that is when the elongation of the axes is maximum, the ratio between the minor and major axis oscillates in the interval $0.6 \div 0.7$, in accordance with the ratio between the length of the axes, which is approximately 0.67: this indicates that the dome expands uniformly. The pressure cells seem to have collected reliable data up to about 2009; in the following years, some devices have completely discordant data from the others, an anomaly that could be caused by local phenomena or sensor failure. For

this reason, it was decided not to involve them in the correlation analysis. The measurements of the load cells all appear very consistent with each other and with themselves, tending to repeat the same movement over the years. Exceptions are the LC44 cell and a measuring section of another sensor (LC4) in spring 2009.

3.4 Correlation between environmental and structural monitoring data

In this paragraph the possible existence of correlation is verified, that is a statistical relationship between heterogeneous measures described in the previous paragraph.

A step before calculating the correlation coefficient and also a useful way to detect possible nonlinear dependence between variables is to visually examine the data within a scatter plot. This operation makes it possible to check the value of r obtained, both in terms of sign (i.e. positive or negative dependence) and value (i.e. measure of the strength of the relationship). It also gives the possibility to immediately detect any strongly non-linear dependencies, which would hardly be captured by the correlation coefficient, implicitly pushing to use another type of approach.

For slightly non-linear relationships, the linear correlation coefficient is still a significant index since it generally does not change in magnitude. Furthermore, a visual examination of the data allows to identify any outliers and evaluate whether to eliminate them if they are physically unreachable, as they could significantly influence the aforementioned coefficient. Static data were used first, combining them with environmental data. Not all devices were involved in this analysis: for each type of measurement one or a subset of sensors representative of the system was selected, following engineering and mathematical evaluations (PCA).

For example, as regards the 28 thermometers installed on the Sanctuary, they were grouped by level and exposure (inside or outside the building) and only one per category was selected thanks to PCA. In particular, the thermometers 4, 7, 11 and 15 were chosen, positioned respectively on the external and internal side, on the extrados of the dome and on the reinforcement system. As anticipated, the strengthening system is composed of 56 post-tensioned bars spread over 4 levels and 14 positions of the oval (see chapter 2.2.1 and Figure 2. 15). Among these, only 5 were examined: among the cells on the highest segmented ring, the LC48 was selected by applying the PCA on the entire level and also the cells close to the

attachment of the strain gauges (i.e. LC04, LC16, LC32, LC44) were selected. PCA was also used for crack opening data, and the LVDT was selected on the West side, located on one of the most important lesions. All possible combinations were studied and the correlation coefficient was calculated for each (see Table 3. 1). For reasons of space, only the most significant dependencies are shown in Figure 3. 9.

Table 3. 1: correlation between environmental parameters and each type of static sensor

Combination		***r***				
Thermometer 4, 7, 11, 15	**T_{med}**	0,94	0,94	0,93	0,89	
	T_{max}	0,92	0,93	0,91	0,86	
	T_{min}	0,89	0,9	0,87	0,87	
	Rain	-0,10	-0,13	-0,08	-0,06	
	Humidity	-0,16	-0,17	-0,17	-0,12	
Convergence minor and major axis	**T_{min}**	0,80		0,43		
	T_{med}	0,80		0,40		
	T_{max}	0,76		0,37		
	Humidity	-0,03		0,06		
	Rain	-0,01		0,15		
Crack meter	**T_{med}**	0,72				
	T_{min}	0,71				
	T_{max}	0,69				
	Humidity	-0,06				
	Rain	0,04				
Load cell LC04, LC16, LC32, LC44, LC48	**T_{med}**	-0,34	-0,87	-0,75	-0,70	-0,73
	T_{min}	-0,34	-0,86	-0,75	-0,67	-0,73
	T_{max}	-0,32	-0,83	-0,70	-0,66	-0,69
	Rain	0,09	0,08	0,04	0,04	0,05
	Humidity	0,02	0,01	-0,02	0,01	0,01

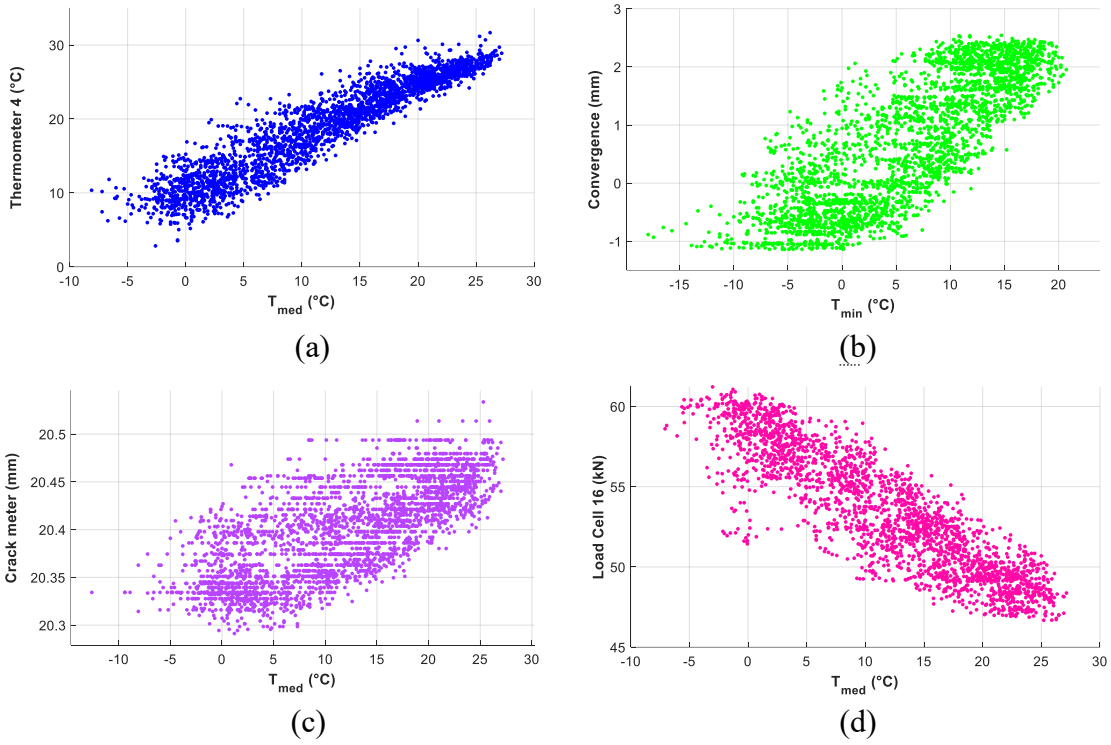

Figure 3. 9: correlation between static sensors and T_{med}

The same procedure was applied on the dynamic monitoring data, and the respective results are shown in Table 3. 2. As above, in Figure 3. 10 the scatter plots with the most significant dependencies are reported.

Table 3. 2: correlation between environmental parameters and frequencies

	Rain	**T_{med}**	**T_{max}**	**T_{min}**	**Humidity**
f_1	0,0560	0,8271	0,8074	0,7636	-0,1839
f_2	0,0435	0,8663	0,8375	0,8131	-0,1479
f_3	0,0239	0,8764	0,8575	0,8176	-0,1840
f_4	0,1112	0,2812	0,3118	0,2076	-0,0755
f_5	0,1372	0,5818	0,5700	0,5344	-0,1215

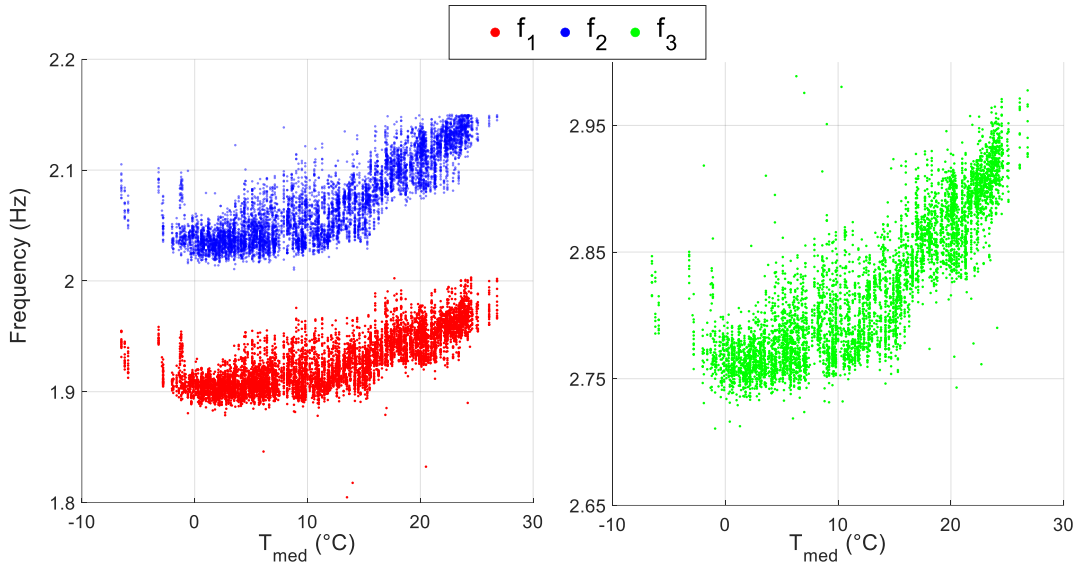

Figure 3. 10: stronger correlation between environmental parameters and frequencies

The results of the correlation analysis indicate that both the static and dynamic behavior of the Sanctuary are greatly influenced by variations in the ambient temperature. In fact, the series of monitoring data do not show a significant correlation with other environmental phenomena taken into consideration, such as humidity and rain. The highest coefficients among the static data relate to the measurement of the temperature of the masonry, of the load in the bars and of the crack gauges. The coefficients indicate that the increase in the external temperature corresponds to an increase in that of the internal masonry (Figure 3. 9a) and a delay is observed in the time series that varies from 10 to 30 days depending on the position of the sensor. This is most likely due to the thermal inertia of the material. The increase in temperature causes the opening of the cracks at the level of the balcony which is accompanied by a decrease in the load in the bars (Figure 3. 9c and Figure 3. 9d). This could be motivated by the fact that the steel of the bars expands more than the masonry, as indicated by the difference in their coefficients of thermal expansion. In this situation the bars tend to compress and consequently the tension decreases (Ceravolo et al., 2017). Strain gauges recordings suggest that the masonry of the dome expands in the summer months and closes in cold periods, i.e. the measurement of the elongation of the axes shows a trend directly proportional to the external temperature, (Figure 3. 9b).

The first five frequencies tend to increase with increasing external temperature, except for very low values: a bilinear behavior with slope inversion is observed for negative temperature values, as also observed in other case studies (Gentile, Ruccolo, & Saisi, 2019; Kasimzade et al., 2018; Peeters & De Roeck, 2001). A simple superimposition of dynamic and thermal series, following a normalization in which each distribution has been centered and scaled to set the mean to 0 and standard deviation to 1, obtaining the so-called z-score for each, allows to make some observations (Figure 3. 11).

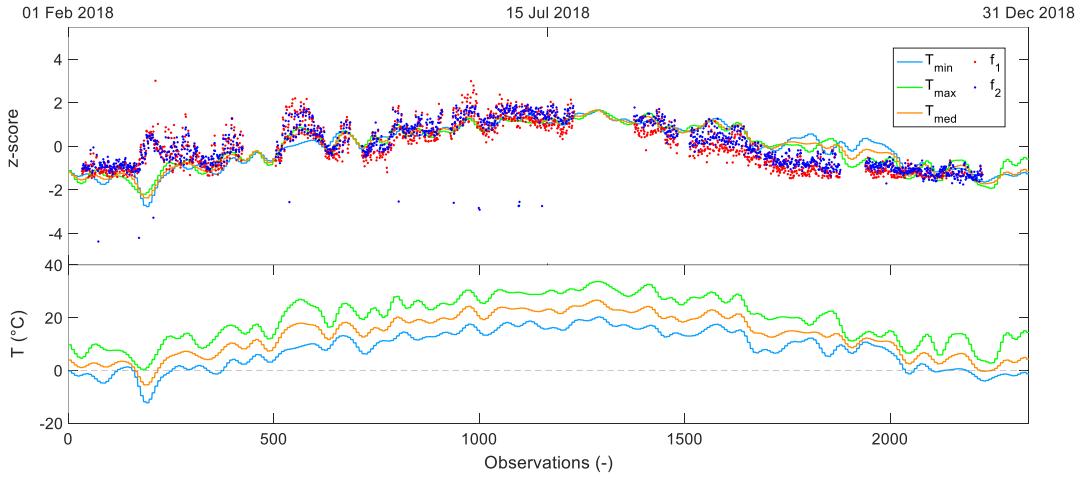

Figure 3. 11: above: normalized time series of frequencies with superimposed external temperatures. Below: original external temperature data

An annual cycle (2018) has been reported as an example. The trend of the frequencies seems to follow precisely that of the temperatures in almost the whole set with an evident exception of the first part. Around observation 200, the dynamic data show a peak while the temperatures show the same shape but inverted: it is observed that in all the other peaks the two measures seem to move in parallel, but in this period, they have opposite behavior. Comparing with a graph of non-normalized temperatures, it is highlighted that this is the only range in which the degrees drop drastically below 0 ° C. This is a further indication of the bilinearity of the frequency-temperature relationship as it approaches negative values. A plausible interpretation, already suggested in a previous research on the dynamic monitoring of the same asset (Coletta et al., 2019b), concerns the effect of ice, which is known to significantly increase structural rigidity (Peeters & De Roeck, 2001). An explanation for this effect could be found in the diversity of the thermal expansion coefficients of water / ice and solid material. They may be able to create

a kind of "stress-tightening" effect at the microscale, such as to cause an increase in the elastic modulus at larger scales. Therefore, since the thermal expansion coefficient of the liquid is higher than that of solid materials, variations in stiffness and natural frequencies could be associated with the variation of the thermal expansion coefficient of water with temperature. Another possible interpretation could concern the foundation soil and its stiffening due to the freezing of the water contained within it. However, the reasons are not yet known and understanding this relationship is still a challenge for the author and the research group that deals with the Sanctuary: the hypothesis should be verified with experimental tests. Figure 3. 11 also indicates a greater dispersion of frequencies when the three temperature measurements diverge, that is, there is a greater temperature excursion during the day.

Another aspect worth mentioning. A counterinuitive relationship emerges if dynamic and static data are juxtaposed. In fact, even if a direct comparison is not possible, not having contemporary data available, it is noted that the increase in the frequency for high temperatures corresponds to the increase observed in the opening of the crack and the decrease in the load in the post-tensioned bars, as if the strengthening system was less effective in the summer. Generally, when the cracks open and the strengthening system is less strained, a system should weaken and therefore register a decrease in frequencies, yet the opposite would seem to happen (Figure 3. 12 next page). Probably other factors such as the stiffness of the foundation soil, its humidity linked to the depth of the aquifer and the effect of temperature on the parameters of the materials as mentioned above, etc. affect the dynamic response of the Sanctuary and in particular the lower vibration modes.

3.5 Conclusions

This chapter presents the systematic study of heterogeneous monitoring data in order to obtain valuable information for the SHM.

An indication of which phenomena can affect the structural behavior, how and to what extent, is provided thanks to an orderly and systematic intersection of all the environmental and monitoring measures available for the Vicoforte Sanctuary. Having to deal with heterogeneous measurements, coming from devices for static, dynamic and environmental monitoring, the data analysis was organized methodically, creating a first study by sensor category, in which the variables as a function of time are examined.

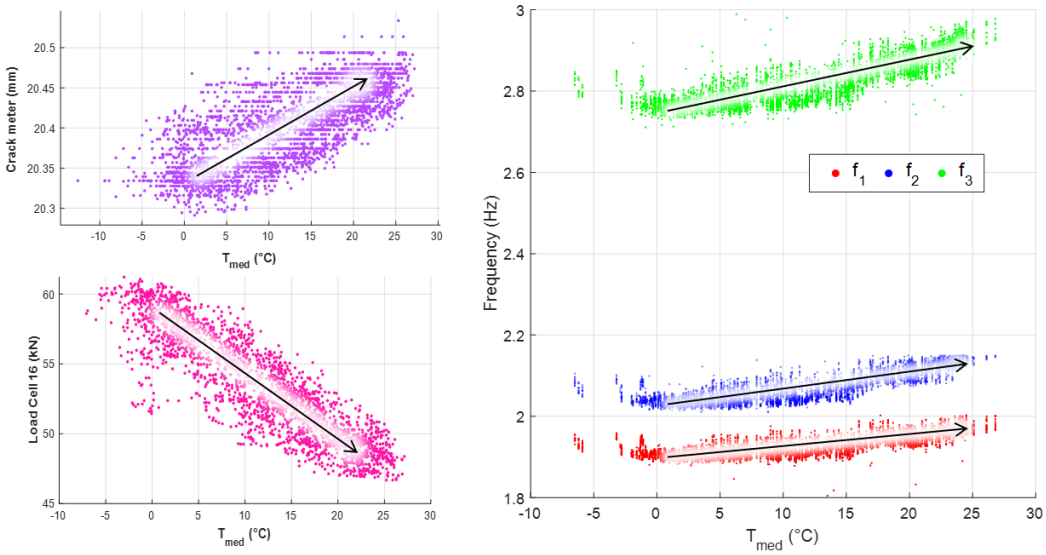

(a) (b)

Figure 3. 12: counter-trend that emerged from the comparison of the results of the analysis of static (a) and dynamic (b) monitoring systems

In this phase it is possible to select the data to be conveyed in the second phase, thanks to mathematical tools and engineering evaluations, in cases where more than one sensor of the same type is available that return redundant information. The intersection of the different types of data represented the second phase of this study. In particular, the measures of the static and dynamic monitoring system with respect to environmental data were examined, revealing both correlations already found in the literature, such as that between temperature and frequencies, and unexpected ones, such as that between temperature and crack width, or that between the latter and the frequencies.

This research and the correlations found could represent a point of reference for historical structures with similar dimensions or geometries. The followed path has the advantage of being easily generalizable and applicable to data other than those treated here, depending on the type of monitoring system installed on the asset. The results obtained also represent a tool to guide the decision on which devices to install / restore / upgrade to optimize the structural monitoring of the specific building and for structures belonging to the same category, naturally to be associated with economic evaluations.

Part of the work described in this chapter was also published in a journal paper (Ceravolo et al., 2021).

Acknowledgments: This research was partially supported by the Amministrazione del Santuario di Vicoforte and the Fondazione Cassa di Risparmio di Cuneo.

Chapter 4

Removing environmental effects from monitoring records

As seen in the previous chapter and in many researchers conducted specifically on AH (Alaggio et al., 2021; Masciotta et al., 2017; Moser & Moaveni, 2011; Ramos et al., 2010; Saisi & Gentile, 2015), environmental factors represent a source of uncertainty in the definition of the diagnosis based on the analysis of monitoring data. In fact, as can be clearly observed in the plots of the time series of diagnostic parameters such as frequencies (Figure 3. 7), opening of cracks, expansion of the dome (Figure 3. 5), etc., environmental factors generate seasonal fluctuations that make the data non-stationary. This erratic pattern could be mistaken for structural damage, or worse, it could offset the variation given by real damage, thus hiding it.

A smart strategy to get rid of those confounding effects consists in creating a reliable model of the healthy structural behavior of the system, accounting and predicting these reversible and harmless variations. To model the health behavior, innovative techniques in SHM have exploited statistical tools and ML algorithms (Farrar & Worden, 2012; Figueiredo et al., 2011). Here the word "model" refers to relationships that are extracted directly from measured data, without the need to study the underlying physical phenomena. In their strongest sense, the goal is to predict the future response of the structure and to identify occurrence, type, entity and/or location of possible damage in real or near real time. Quite recently, Cross *et al.*(Cross et al., 2011; Cross & Worden, 2012), proposed and applied the concept

of *cointegration* for SHM problem. This property, commonly used in econometrics in relation to economic indicators, is the element that allows to give an order and systematize the process of condition assessment and damage detection, in combination with an appropriate regression method. The outcome of this procedure strongly depends on the quality of the regression that takes place. There are manifold methods to perform a regression on experimental data, from the simplest to the most complex and the choice generally depends on the shape of the data and on a balance between the computational weight and the target required by the problem. In this chapter, an interesting class of machine learners based on statistical learning theory and Bayesian variants is used to model structural behavior. Specifically, the algorithms of Support Vector Machines (SVMs) and Relevance Vector Machines (RVMs) have been considered to generalize structural diagnostic features.

In many of these procedures (Doebling et al., 1996; Erazo et al., 2019; Farrar et al., 2001; Salawu, 1997), the structural frequencies are taken as diagnostic features, as they depend on global stiffness, which change when significative damage occur. However, even measurements with a more "local" significance, e. g. width of cracks, load in a strengthening system, pressure in certain elements, can be taken as a reference for assessing structural health, especially if considered as an enrichment of global parameters, a sort of zoom in a certain area of the structure.

Moreover, for each diagnostic feature, different combinations of predictor variables will be considered, also on the basis of the results obtained in the previous chapter, and any improvement in the accuracy of the technique will be measured. However, as it is easy to conceive, any model approximates a much more complex reality and it must be based on a reasonable number of components, whose selection might turn out complicated. To cover this issue, the study of the correlation between environmental parameters and diagnostic characteristics made in the previous chapter is fundamental to have an idea of which environmental series are important for modeling the behavior of the system and for discarding the less relevant ones. For this reason, as well as for the great availability of data, the Vicoforte Sanctuary constitutes the case study of this proposed procedure.

The layout of the chapter is as follows: Sections 4.1 and 4.2 discusses the relevant background theory, covering the cointegration property and the basic theory of SVM and RVM. Section 4.3 reports different applications of the above property to different types of monitoring data, considering both healthy and

damaged conditions of the considered case study: the latter, being unavailable, are simulated using a FEM of the structure. In Section 4.4 the conclusions are drawn.

4.1 Cointegration for SHM

As highlighted previously, the property of cointegration is used in this context to remove trends in diagnostic features over time, in order to identify a stationary indicator related to the health of the structure.

Having a set of nonstationary time series referred to the healthy condition of the structure, subjected to environmental effects, the aim of this approach is to define a combination of them which is stationary when the structure is healthy, and that can be used as a control parameter. If this stationary combination exists, the time series of the diagnostic features considered are termed *cointegrated*. This control parameter can be seen as a damage indicator as it should be stationary under different environmental and operational conditions, while its mean and variance should vary when a damage occurs or it evolves over time. Here below the key concepts are reported to allow the understanding of the procedure for SHM; for a more mathematically rigorous treatment of cointegration, reference can be made to (Engle & Granger, 1987).

In order to measure the extent of the non-stationarity of a variable, it is fundamental introducing the *order of integration*. A nonstationary time series, x_i (here, for the sake of brevity, it will be considered $x_i = x(t_i)$), is said to be integrated of order d, indicating it as $I(d)$, if its d-*th* difference is stationary. Thus, given a time series $x_i \sim I(1)$, it should be differenced only once in order to get a stationary process, which will be indicated as $I(0)$. In the econometric context, usually a linear relationship between economic variables is sought, so for example, a set of economic variables over time $\{x_i\}$, are co-integrated if a vector $\{\alpha\}$ exists such that,

$$u_i = \{\alpha\}^T\{x_i\} \sim I(0) \tag{4. 1}$$

So u_i is a stationary process and $\{\alpha\}$ is the co-integration vector. However, of course not all variables are linked with simple linear relation. In some cases, series are related to each other through nonlinear relations, so their most suitable combination should be found in order to reach stationarity.

Between the series of monitoring data, it may happen that the structural characteristics of a system exhibit a non-linear dependence with external parameters linked to environmental and operating conditions. To clarify the concept, taking for example a set of two time series associated with the same system, namely $x_{1,i}$ and $x_{2,i}$, and assuming that one depends nonlinearly and other depends linearly on some external parameters (for example temperature), any linear combination of them will be nonstationary. However, if a nonlinear combination of them exists which produces a stationary process, like, just to give an example:

$$u_i = \alpha_1 x_{1,i} + \alpha_2 x_{2,i}^2 \sim I(0) \tag{4. 2}$$

Variables $x_{1,i}$ and $x_{2,i}$ are said to be nonlinearly cointegrated.

In this chapter the variables considered are the trends over time of the natural frequencies and of the load measured in the reinforcement system of the Sanctuary. In an ideal case, in a controlled environmental condition, such as during a laboratory test, unless damage occurs, the values of the natural frequencies and the load in the bars of a system remain unchanged over time (unless there are slow phenomena of aging that are not the focus of this study), therefore their trend would be stationary and would already be indicators of damage themselves. Clearly, this reasoning clashes with the real world, in which many other factors intervene. Consequently, the onset / evolution of damage will have to be sought in a new variable, stationary in healthy conditions of the structure and which starts to vary in value when the health of the system fails. In this approach, the above parameter is represented by the residual of the regression model of one of the diagnostic characteristics of the system, ε_i, that is the difference between the observed data and its predicted value. The latter is obtained through a regression process (linear or non-linear, depending on the case) implemented using a class of ML algorithms (Shi et al., 2016) based on statistical learning theory. The basic theory of the algorithms considered, SVM and RVM, is reported in Subsections 4.2.1 and 4.2.2. In the immediate next paragraph instead, the Augmented Dickey-Fuller (ADF), a statistical test commonly used to establish the stationarity of the time series, a fundamental step of the procedure of cointegration, is exposed.

4.1.1 The Augmented Dickey-Fuller (ADF) test

Since for this procedure, the starting variables should have the same integration order, the first step in applying this theory consists in verifying the integration order

of the time series to be treated. In the econometric sector this check is usually performed by testing each series for a unit root; if the test detects the presence of a unit root, it will be inherently non-stationary. The ADF test is one of the most popular root unit tests for checking the stationarity of variables. It is effectively applied to determine how many times the difference operator should be applied to make the time series stationary (Fuller, 2009).

The test involves the fitting of a model of the variable with the form:

$$\Delta x_i = \rho x_{i-1} + \sum_{j=1}^{p-1} b_j \Delta x_{i-j} + c_1 i + c_2 + \varepsilon_i \tag{4.3}$$

where: ρ is a parameter that regulates the stability and therefore the stationarity of the model; b_j are the coefficients of the autoregressive process; p is the lag order of the autoregressive process; $\Delta x_{i-j} = x_{i-j} - x_{i-j-1}$; ε_i is the model residual, $c_1 i$ is a deterministic trend term and c_2 is a constant. Both the latter terms are optional additions which are dependent on the complexity of the real model.

The concept of the ADF is to test a null hypothesis on ρ, i.e. $\rho = 0$. This because if ρ is statistically near to 0, the process can be considered as nonstationary and integrated of order 1, i.e. $I(1)$. The null hypothesis can be assessed using the test statistic,

$$t_\rho = \frac{\hat{\rho}}{\sigma_\rho}. \tag{4.4}$$

The t_ρ statistic is now compared to the relevant critical value for the Dickey–Fuller test, which can be found in tables reported here (Fuller, 2009). For a generic time series, the following cases arise:

- $t_\rho < t_\alpha$ the null hypothesis can be accepted: the time series is nonstationary $I(1)$;
- $t_\rho > t_\alpha$ the null hypothesis can be rejected in favour of the alternative hypothesis.

The ADF test is a crucial step to confirm the existence of a cointegration relationship between the data, in our case those measured by the monitoring system.

In fact, in addition to performing the test on the starting time series to ascertain that they have the same order of integration, it is essential to repeat it on the residual of the model, ε_i after having defined the regression model of one of the variables which, as anticipated, in this work will be implemented with ML algorithms.

4.2 Regression models for SHM

A regression analysis generally aims to build a map between two or more number series. The variable to be regressed is called *dependent*, *predicted* or *estimated* variable, while the one (or more) on which the model will depend is called *independent* or *predictor* variable.

To make the concept intuitive, an example can be made using the monitoring quantities. In the previous chapter, a correlation was found between some structural parameters and the ambient temperature. In this case, the regression would consider the structural data as a predicted variable and the environmental one as a predictor variable, since (even if mathematically the opposite case could work and give an accurate model, in undamaged condition), it is not physically credible that a monitoring parameter influence an environmental one: an anomaly in the structural measurements does not cause the ambient temperature to vary. This situation will be referred to by the letter (a).

In addition, another situation must be mentioned: a structural parameter can also be predicted as a function of another structural parameter, both affected by the same external conditions. For example, the opening of the cracks on the dome is directly linked to its expansion and therefore to the measurement of axis convergence. Or the frequency of the first bending mode in one direction is related to that in the other direction, or to the second mode in the same direction. In this case, even if one is not the cause of the other, these measures are inextricably linked and one can be modeled as function of the other. This situation will be referred to by the letter (b).

In this SHM procedure, the regression will serve to fit a model of a structural variable under healthy conditions, which could be univariate or multivariate depending on the number of predictor variables chosen, which is good enough to produce a stationary residue (which will be their cointegration relationship u_i in Eq. (4. 1) and (4. 2), depending on linearity or non-linearity) when environmental parameters change. In fact, once the variables that come into play have been appropriately chosen and the model fitted using one of the many techniques

proposed in the literature, it is possible to obtain the residual of the regression model by subtracting from the measured data, those predicted by the model.

In this specific case, the residual of an appropriate regression model (i.e. that produces a stationary residual, certifying cointegration between the variables) of one of the diagnostic parameters would take on the meaning of damage or health indicator. This is because, being the model created on the basis of data collected in healthy conditions, it will always predict the chosen structural parameter in healthy conditions. Therefore, by applying this model to new data of the predictor variable, we will have an estimate of what the monitored structural parameter should be if healthy. By comparing this estimate and the actually observed structural parameter, precisely through the model residual, i.e. their difference, it will be possible to guess if a healthy behavior is being observed (estimate and observed almost coincide and therefore the residue is close to 0) or if something abnormal is happening (the difference between the estimate and the observed data increases in modulus).

This is very intuitive for (a) situation, since the predictor will not contain any information on the damage, being an environmental parameter, and therefore will in no way be able to transmit it to the estimate of the structural parameter. As a consequence, the difference between the “healthy” estimated parameter and the “damaged” observed value diverge greatly.

What changes for situation (b) is that the predictor variable, being also measured on the structure, could also vary with the damage. But what still makes this application feasible is the fact that it is very unlikely that the damage will affect both structural parameters in the same way. Consequently, the relationship that had been modeled on a healthy condition will change with the appearance of damage, and therefore the distancing between estimated and observed value in damaged condition will still be visible. This is due to the fact that damage is often a focused, asymmetrical phenomenon, so it is very unlikely that several diagnostic characteristics will be affected by keeping their relationship constant, equal to that in the healthy condition. On the other hand, using a structural parameter as a predictor of another can have the advantage that it already contains the effects of all phenomena that influence them. For example, an error could be made if only environmental parameters are used as predictors of a structural variable that is also highly sensitive to operational aspects: the only environmental parameters used to predict its trend would not be able to explain the operational fluctuations, which consequently could be mistaken for damages. A good strategy could be a model that considers both environmental and structural variables as predictors.

To interpret the results on the residual plot, a tool from the *statistical process control* (SPC) or *statistical quality control* has been applied. A kind of control chart, the *X-chart* (Montgomery, 1996), has been overlapped to the trend of the model residual $\varepsilon(t)$, by plotting its mean value $\mu(\varepsilon)_{TD}$ and the upper and lower control limits, called UCL and LCL respectively, at $\mu(\varepsilon)_{TD} \pm 3\sigma(\varepsilon)_{TD}$. The subscript TD indicates that these quantities are computed over the range of training data, the data used to fit the regression model. When the ε_{TD} distribution is close to a Gaussian (it can be checked through the Kolmogorov-Smirnov Test), this range contains 99.7% of the samples.

So, through this tool, the SHM procedure ends in a real novelty detection or outlier analysis. In fact, by testing the regression model on new data and getting its residuals, if the structural condition has not changed, almost all observations of the residual should fall between the UCL and LCL. If damage appears, there may be a deviation from the aforementioned range and an unusual number of observations exceeding the control limits.

In the next two paragraphs the two regression techniques used are reported.

4.2.1 SVM regression

Support Vector Machines are supervised-learning models combined with a specific learning algorithms from Statistical Learning Theory, designed to address classification and regression analysis (Boser et al., 1992). While here the formulation for regression problems is briefly reported, a full discussion can be found in (Drucker et al., 1996).

Assuming a training dataset composed by a number *N* of inputs $\{x\}_i$ (where curved brackets denote vectors), and outputs y_i (i.e. the *label*, which in regression problems is a continuous variable). The objective is to find the function $y = f(\{x\})$ which better generalize on new data, i.e. with minimum error in predicting new data. SVM considers the following linear function:

$$f(\{x\}) = <\{w\}, \{x\}> + b \tag{4.5}$$

where {w} and b are the parameters to be adjusted to reach the best fit. In order to do this, SVM follow the so-called Structural Risk Minimization (SRM) principle, which imply the minimization of an upper bound on the generalization error, as

well as the minimization of the empirical error on the training dataset. This allows to avoid overfitting on new data. In formulas, the structural risk to be minimized can be expressed as:

$$R(f) \leq R_{emp}(f) + \lambda||\{w\}||^2 \tag{4.6}$$

where the empirical risk, a kind of loss function, is expressed as:

$$R_{emp}(f) = \frac{1}{N}\sum_{1}^{N} L(f(\{x\}_i) - y_i) \tag{4.7}$$

λ is a regularization parameter. Among several types of loss functions, SVM uses the δ-insensitive function defined as:

$$L(f\{x\} - y) = \begin{cases} |f(\{x\}) - y| - \delta & if \ \ |f(\{x\}) - y| \geq \delta \\ 0, & else \end{cases} \tag{4.8}$$

where δ is called *insensitive parameter*. Substituting the loss function in the structural risk, it leads to the minimization of:

$$\frac{1}{2}||\{w\}||^2 + C\sum_{i=1}^{N}(\xi_i^* + \xi_i) \tag{4.9}$$

subject to the constraints (for each $i = 1, \dots, N$),

$$\begin{gathered} \xi_i^* \geq 0 \\ \xi_i \geq 0 \\ y_i - (<\{w\}, \{x\}_i> + b) \leq \delta + \xi_i \\ (<\{w\}, \{x\}_i> + b) - y_i \leq \ \delta + \xi_i^* \end{gathered} \tag{4.10}$$

where $\{\xi^*\}$, $\{\xi\}$ are slack variables, C (the *trade-off,* or *regularization parameter*) is a constant which combines the effect of N and λ and determines the trade-off between the flatness of $f(\{x\})$ and the empirical error. The solution to the

minimization problem in Eq. (4.9) under the constraints in (4.10) is given by the saddle point of the Lagrange function:

$$L = \frac{1}{2}\|\{w\}\|^2 + C\sum_{i=1}^{N}(\xi_i^* + \xi_i) - \sum_{i=1}^{N}\alpha_i[(<\{w\},\{x\}_i> +b) - y_i + \delta + \xi_i] - \sum_{i=1}^{N}\alpha_i^*[y_i - (<\{w\},\{x\}_i> +b) + \delta + \xi_i^*] - \sum_{i=1}^{N}(\eta_i\xi_i + \eta_i\xi_i^*) \quad (4.11)$$

where η and α are Lagrange multipliers. Now, deriving L with respect to $\{w\}, \xi_i, \xi_i^*$ and b to find the saddle point and substituting back the relations in L, the following objective function to maximize results:

$$-\frac{1}{2}\sum_{i=1}^{N}\sum_{j=1}^{N}(\alpha_i - \alpha_i^*)(\alpha_j - \alpha_j^*) <\{x\}_i\{x\}_j> -\delta\sum_{i=1}^{N}(\alpha_i^* + \alpha_i) + \sum_{i=1}^{N} y_i(\alpha_i - \alpha_i^*) \quad (4.12)$$

which is subjected to the condition:

$$\sum_{i=1}^{N}(\alpha_j - \alpha_j^*)\{x\}_i = 0 \qquad and \qquad C \leq \alpha_j - \alpha_j^* \leq 0\,. \quad (4.13)$$

The solution for α_j, α_j^* is thus obtained from (4.12). It allows to find $\{w\}$ (from the derivative of L with respect to $\{w\}$):

$$\{w\} = \sum_{i=1}^{N}(\alpha_j - \alpha_j^*)\{x\}_i \quad (4.14)$$

$\{w\}$ is fully described as a linear combination of training samples $\{x\}_i$. Only a small subset of the $\{w\}$ will in many cases be different from zero: these will define the *support vectors*. Substituting into the (4.5), the regression function is finally obtained:

$$f(\{x\}) = \sum_{i=1}^{N}(\alpha_j - \alpha_j^*) <\{x\}_i\{x\}> +b\,. \quad (4.15)$$

b is instead calculated using the Karush–Kuhn–Tucker (KKT) conditions.

The linear formulation can be generalized to the case of non-linear regression exploiting the so-called *kernel methods*: thanks to a mapping function, the data of the original space (where could there could be difficulties in generalizing) are mapped into a high-dimensional space, where they can be regressed more simply. The linear SVM algorithm is then conducted in the new feature space, which represents a nonlinear operation in the original space and thanks to the popular *kernel trick*, the computational burden is drastically reduced as the calculation of the high dimensional sample coordinates can be avoided.

4.2.2 RVM regression

Another kernel-based approach for classification and regression is represented by the Relevance Vector Machine, formulated by Tipping (Tipping, 2001). The SVM shows excellent generalisation property but it suffers from several disadvantages: (i) the generalizations are not probabilistic; (ii) the estimation of the trade-off (C) and the insensitivity parameter (δ) is necessary; (iii) there is a need to use "Mercer" kernel functions; (iv) the number of support vectors could be high. RVM shares the sparseness capacity and preserves the excellent generalization performance of the SVM without suffering from any of listed limitations. It exploits a Bayesian approach to learning, where a *prior* over the weights (governed by a new set of hyperparameters), is introduced. The hypothesis consists of choosing the most probable configuration of the weights, resulting from an iterative process on the data set. Sparsity is achieved, since the posterior distribution of many of the weights are often peaked around 0. The remaining non-zero weights are named *relevance vector*s, in deference to the principle of Automatic Relevance Determination (ARD), on which the approach is based.

Considering a data set of predictors $\{x\}_i$, and target t_i, variables, one can follow the standard probabilistic formulation and assume that the targets are samples from the model with additive noise: $t_i = y(\{x\}_i; \{w\}) + \varepsilon_i$, where ε_i is Gaussian noise with mean 0 and variance σ^2. Then $p(t_i|\{x\}) = \mathcal{N}(t_i|y(\{x\}_i), \sigma^2)$, where the notation specifies a Gaussian distribution over t_i with mean $y(\{x\}_i)$ and variance σ^2. The mean of this distribution, is modelled as for the general prediction case of SVM (which considers Kernel) with the general basis functions parameterised by the training vectors:

$$y(\{x\}) = \sum_{i=1}^{N} w_i K(\{x\}, \{x\}_i) + b \tag{4.16}$$

while the likelihood of target distribution is calculated as:

$$p(\{t\}|\{w\},\sigma^2) = (2\pi\sigma^2)^{-N/2} exp\left\{-\frac{1}{2\sigma^2}\|\{t\} - \boldsymbol{\Phi}\{w\}\|^2\right\} \tag{4.17}$$

where $\{t\}$ is the vector of the N targets, $\{w\}$ is the weight vector and $\boldsymbol{\Phi}$ is a matrix of dimension $N \times (N+1)$ named "design matrix", where each term is defined as $\Phi_{im} = K(\{x\}_i, \{x\}_{m-1})$ and $\boldsymbol{\Phi}_{i1} = 1$. As generally the estimate of $\{w\}$ and σ^2 from the previous equation leads to overfitting, it is preferred to impose some a priori information over the weights, which is modelled as a 0-mean Gaussian prior probability distribution:

$$p(\{w\}|\{\alpha\}) = \prod_{i=0}^{N} \mathcal{N}(w_i|0,\alpha_i^{-1}) \tag{4.18}$$

where $\{\alpha\}$ is a vector of $N+1$ hyperparameters. It is important to observe that an individual hyperparameter is provided for every weight: this is the basic feature of RVM as it is responsible for the sparsity properties of the model. The posterior over the weights is given by Bayes' rule,

$$p(\{w\}|\{t\},\{\alpha\},\sigma^2) = (2\pi)^{-(N+1)/2}|\{\Sigma\}|^{-1/2} exp\left\{-\frac{1}{2}(\{w\} - \{\mu\})^T\{\Sigma\}^{-1}(\{w\} - \{\mu\})\right\} \tag{4.19}$$

where the quantities (posterior covariance and mean) are defined as:

$$\{\Sigma\} = (\boldsymbol{\Phi}^T\{B\}\boldsymbol{\Phi} + \{A\})^{-1} \tag{4.20}$$

$$\{\mu\} = \{\Sigma\}\boldsymbol{\Phi}^T\{B\}\{t\}. \tag{4.21}$$

$\{A\}$ is a defined as $diag(\alpha_0, \ldots \alpha_N)$ and $\{B\} = \sigma^{-2}\{I\}_N$. σ^2 is considered as a hyperparameter to be estimated from the data set. So ML becomes a search for the hyperparameters posterior most probable. By integrating out the weights, it is possible to attain the "*marginal likelihood",* or *"evidence"* for the hyperparameters:

$$p(\{t\}|\{\alpha\},\sigma^2) = (2\pi)^{-N/2}|\{B\}^{-1} + \boldsymbol{\Phi}\{A\}^{-1}\boldsymbol{\Phi}^T|^{-1/2} exp\left\{-\frac{1}{2}\{t\}^T\left(\{B\}^{-1} + \boldsymbol{\Phi}\{A\}^{-1}\boldsymbol{\Phi}^T\right)^{-1}\{t\}\right\}. \tag{4.22}$$

To reach an ideal Bayesian inference, hyperpriors should be defined over $\{\alpha\}, \sigma^2$, and integrated out. However, RVM adopt a pragmatic optimization of the marginal likelihood with respect to $\{\alpha\}, \sigma^2$, based on MacKay (Tipping, 2001). Essentially, the maximum of $p(\{\alpha\}, \sigma^2|\{t\})$ is sought assuming a uniform hyperprior.

The key characteristic of the RVM approach is that, as well as providing good generalisation performance, the inferred predictors are highly sparse as they contain relatively few non-zero w_i parameters. During the learning phase, most of the weights are automatically set to 0, therefore the procedure is very effective to select the basis functions that are "relevant" for good predictions.

4.3 Application to field data

It was decided to apply the SHM procedure based on cointegration and ML regressors on two types of monitoring data, one deriving from the static monitoring system of the Sanctuary, the other from the dynamic one, the natural frequencies of the system. Both parameters are considered 'diagnostic', as they are supposed to change when damage appears. The structural frequency is linked to the dynamic response of the entire structure and therefore has a more global meaning than the static monitoring parameters. The load supported by the tie bars, on the other hand, is a measure that is spatially limited to the area in which it is acquired. However, since the strengthening system is a very delicate intervention carried out on the dome of the Sanctuary, and being based on the balance of the compressive forces applied to the masonry by the post-tensioned bars, even the anomalous measurement of only one of the cells could be an indication of much more expanded damage. Both situations exposed in 4.2, (a) and (b), will be evaluated, also by considering both types of predictors.

4.3.1 Application to static monitoring data: Load Cells

The graph in the Figure 4. 1 shows the trends of all the LCs, in the period from 2004 to 2014 (as anticipated, subsequent data were not considered reliable and therefore neglected).

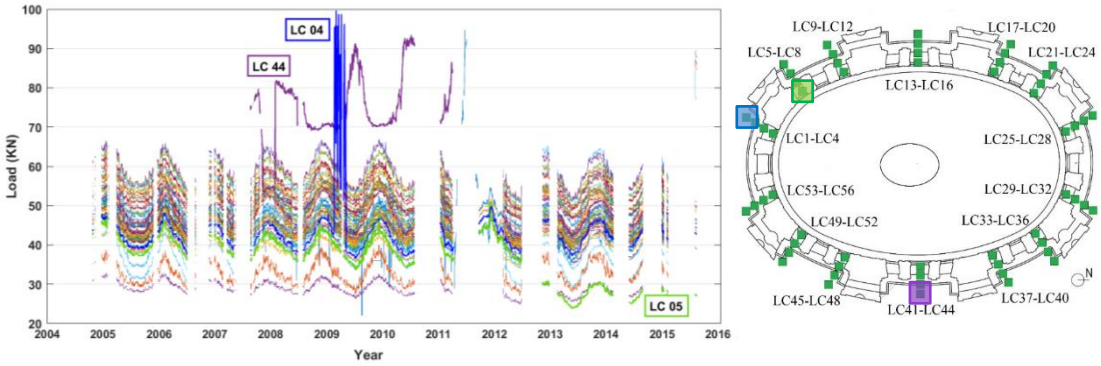

Figure 4. 1: time series of the load cells and their layout in plan

In the plot, it is possible to note that there are some highlighted cells, which during that period exhibited anomalous measurements. Following inspections and checks, it was ascertained that they did not correspond to real load variations, but to measurement errors due to (i) loss of oil in the sensor and (ii) infiltration of humidity which had temporarily damaged the control unit. Nonetheless, it was thought to exploit these anomalous measurements to test the method, treating these measurement errors as structural anomalies.

The first step is to select appropriately a set of training data, of course related to healthy condition. Since these parameters have shown a seasonal trend, the ideal would be to have a full cycle available for training and, in addition, when available, it is convenient to choose a range of observations in which exceptional events, although harmless, cause large variations in the data (for example heavy snow, downpour, hail, etc.). In this way, if similar events happen, the model succeeds in estimate values close to those observed.

In the following graphs the trend of the Load Cell 44 (LC44) has been modeled through SVM by exploiting different predictors: another structural parameter, the load measured in LC48 (Figure 4. 2), i.e. the adjacent tie-bar; the most correlated environmental parameter found in chapter 3, T_{min} (Figure 4. 3); and ultimately both (Figure 4. 4). For convenience they were named respectively *I, II, III*. Here, approximately the first two years of the series have been selected, when the anomaly had not yet occurred. It is observed that, although this anomaly is appreciable even just by observing the temporal trend of LC44, here we want to highlight a comparison between different models by optimizing the prediction. This could be crucial in view of an automatic damage detection procedure, i.e. without the data

being previously viewed by an operator, to be applied even in cases of more modest anomalies and difficult to detect by visual examination.

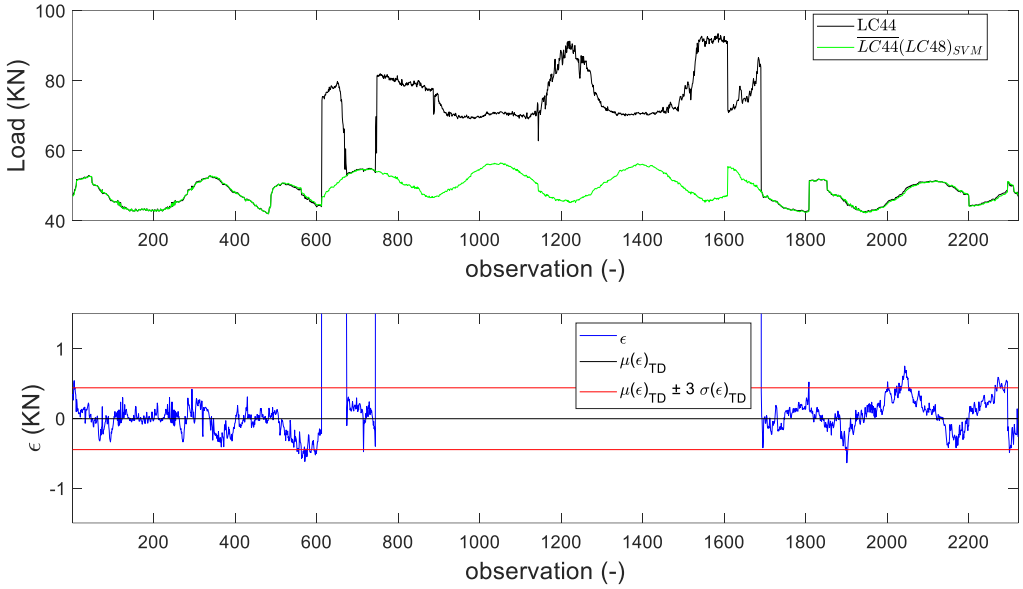

Figure 4. 2: LC44 SVM model using LC48 as predictor and its model residual (I)

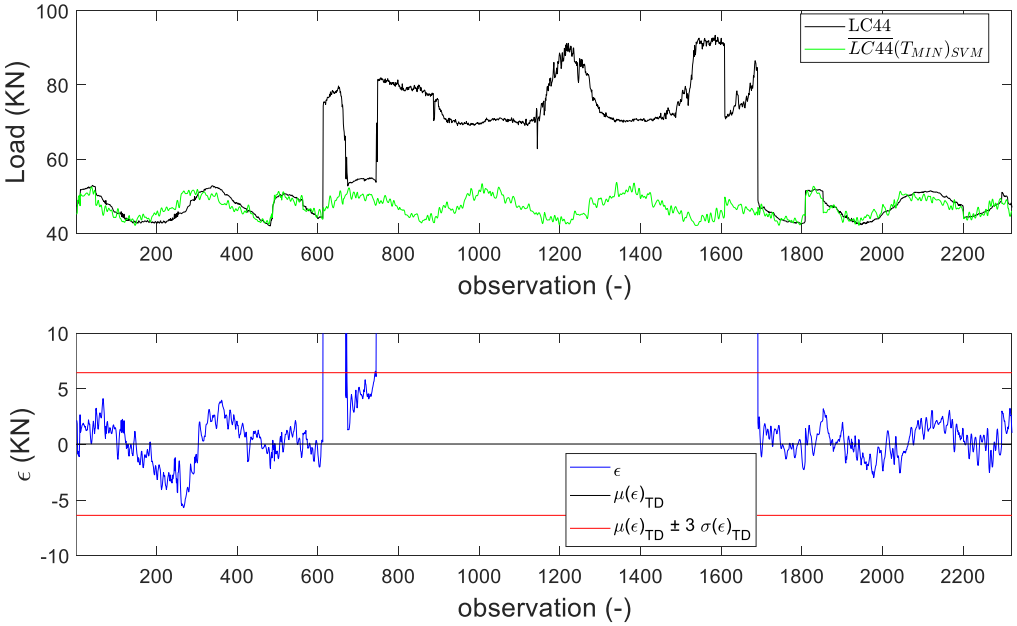

Figure 4. 3: LC44 SVM model using T_{min} as predictor and its model residual (II)

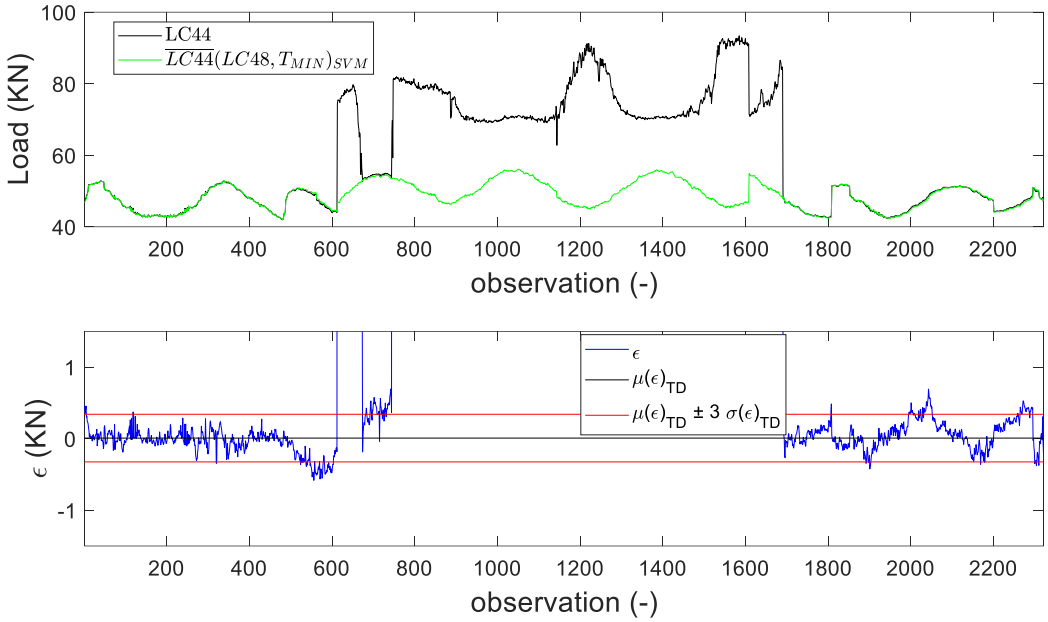

Figure 4. 4: LC44 SVM model using LC48,T_{min} as predictors and its model residual (III)

The residual graphs have been limited at the top to allow a better view of the healthy observations, since those relating to the anomaly correspond to very high residual values (as mentioned, the one in question is not a structural damage but a technical sensor damage and is already evident in the time series of the parameter). Each model has been fitted by optimising the all the hyperparameters, i.e. box constraint, Kernel scale, insensitive parameter, Kernel function, through a Bayesian optimization with the aim to minimize the 5-fold cross-validation loss. In Table 4. 1 the main characteristics are summarized:

Table 4. 1: characterisics of models built on static monitoring data

ID	Predictors	Predicted	Kernel Fun.	$RMSE_{TD}$	SV/N_{TD}
I	LC48	LC44	Linear	0.148	443/500
II	T_{min}	LC44	Linear	2.137	199/500
III	LC48, T_{min}	LC44	Gaussian	0.111	466/500

From the graphs and data shown in the table, the following can be observed. All the models are able to derive a cointegration relationship: the initial series are

all non-stationary, in the range of TD, with integration order 1, and all the residuals of the models are stationary in the same range.

The II model has a higher Root Mean Square Error (RMSE) of the 3 implemented: this indicates that it is the one that reproduces the observed behavior less accurately. In fact, this aspect is also observable from the first graphs in Figure 4. 3, in which it seems that the time series of the estimate is "ahead" of that of the observed series. This could be due to the thermal inertia of the bar: the II model is in fact based on the temperature, which, being most likely the cause of the oscillations, precedes the effect. The model III, involving both types of predictors, structural and environmental, is the one that best estimates the load in LC44, slightly exceeding I, the one based only on the structural data of LC48.

As far as the identification of the damage is concerned, so the comparison of the residual with the error bars of the X-chart, all the models are able to identify it: the data relating to the accuracy of the detection of this kind of binary classification (i.e. how a novelty detection can be considered) are shown in the Table 4. 2.

Table 4. 2: outcome of the procedure on static monitoring data

ID	% FP	% FN	Accuracy
I	6.52	6.58	0.9345
II	0	6.86	0.9681
III	12.16	2.22	0.9246

Analysing the accuracy values, the second model seems to be the best performing. This is due to the fact that its residue in the TD range is the most dispersed, with the highest standard deviation $\sigma(\varepsilon)_{TD}$, effectively widening the range between UCL and LCL. This decreases the false positive (FP) and would increase the false negative (FN), which is not the case here since the anomalous load measurements are much higher than those in normal conditions. However, if dealing with real damage, the greater width of the control limit range would imply greater difficulty in detecting milder and structurally realistic anomalies than that found in this series. And it should be noted that, as already discussed in, a FN is much more dangerous than a FP, which at most involves inefficiency of the monitoring system.

Following these arguments, among those proposed the best model turns out to be the last one, characterized by the best RMSE, intermediate accuracy and lower number of false negatives.

4.3.2 Application to dynamic monitoring data

Natural Frequencies in undamaged condition

Unfortunately, under general operational conditions, not all of the frequencies are always identified, especially those relating to higher frequency modes. For this reason, it was decided to treat only the first 5 frequencies identified in the Sanctuary, as in the previous chapter. In fact, in this analysis it is necessary that each observation contains each of the characteristics involved (in this case the first 5 frequencies) and involving time series of frequencies marked by many gaps would mean sacrificing many "incomplete" observations. In this case, two models are proposed made with the same predictors but with the two aforementioned algorithms, SVM (Figure 4. 5) and RVM (Figure 4. 6), named as *IV* and *V*. In this case it was decided to model the trend of the 2nd frequency.

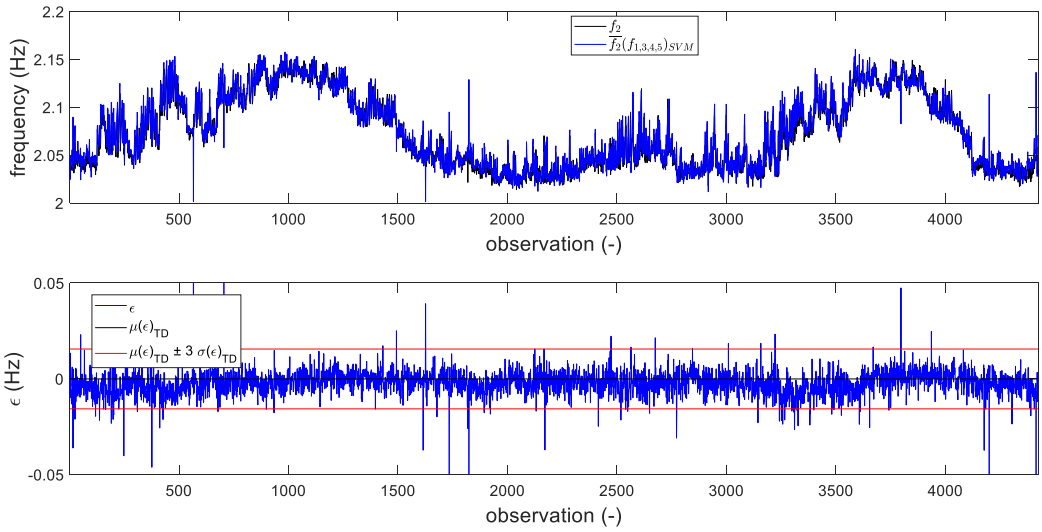

Figure 4. 5: f_2 SVM model using f_1, f_3, f_4, f_5 as predictors and its model residual (IV)

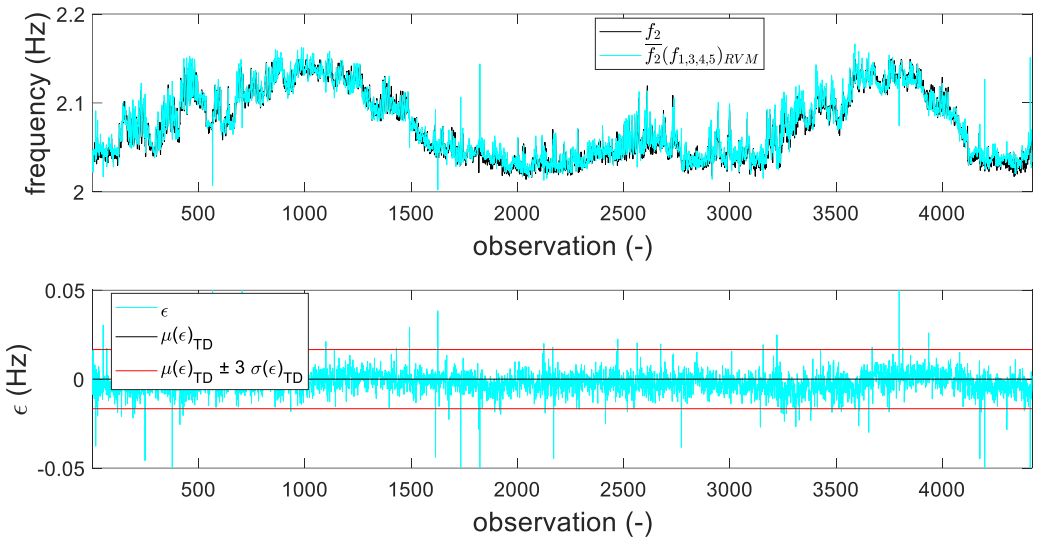

Figure 4. 6: f_2 RVM model using f_1, f_3, f_4, f_5 as predictors and its model residual (V)

The data between [1100 1700] have been chosen to train the algorithms as it is a range in which a conspicuous variation is observable. This set roughly correspond to the data collected in the autumn of 2018, the season in which the transition from high to low values of temperature is recorded, with the concordant variation in frequency.

Table 4. 3: characterisics of models built on dynamic monitoring data

ID	Algorithm	Predictors	Predicted	Kernel Fun.	$RMSE_{TD}$	V/N_{TD}
IV	SVM	f_1, f_3, f_4, f_5	f_2	Gaussian	0.0052	578/600
V	RVM	f_1, f_3, f_4, f_5	f_2	Gaussian	0.0055	4/600

From the point of view of the quality of the goodness of the fitting, as shown in Table 4. 3 the two models show a very similar RMSE. However, looking at the difference in the information points used to fit the model, RVM has a significantly lower number of relevant vectors than the support vectors, as anticipated by his theory.

In this case, since there is no damage in the dynamic measurements, the residuals of the models, plotted on the X-chart, are compared just on the basis of FP: V in this case, V lead to less errors than IV, see Table 4. 4.

Table 4. 4: outcome of the procedure on dynamic monitoring data

ID	% FP	$\mathbf{RMSE_{TOT}}$
IV	2.10	0.0070
V	1.72	0.0071

To the trained eye, it should already be clear that those single spots in the residue plot that cross the bars do not represent damaged conditions. In fact, they are isolated and sudden points, which in the subsequent observation immediately return to the range of good health, which would not happen if the structural scheme were irremediably changing. However, since they could still be a source of uncertainty, a way to reduce them is to apply a moving average to the trend. This was done by contemplating 5, 10 and 20 points for both models and recalculating the UCL and LCL, with the least dispersion (Figure 4. 7 and Figure 4. 8). This average moving window allows to drastically reduce isolated peaks, increasing the efficiency of the monitoring procedure, even more if the original error bars are kept as a reference.

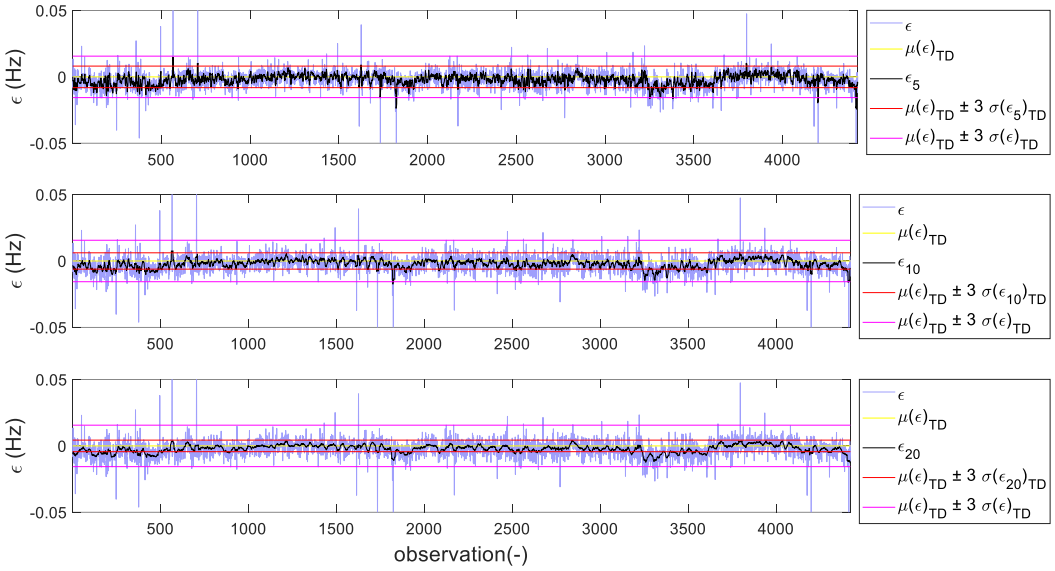

Figure 4. 7: SVM model residual mediated through moving windows at 5, 10, 20 samples

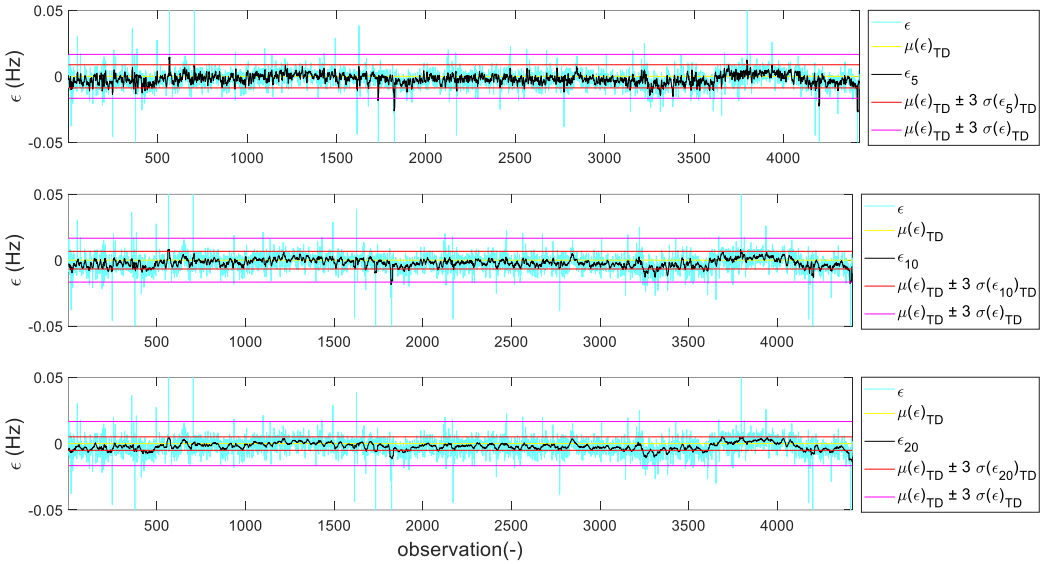

Figure 4. 8: RVM model residual mediated through moving windows at 5, 10, 20 samples

Natural Frequencies in damaged condition

Another case was explored with the dynamic data of the Sanctuary, that is the one that includes heterogeneous predictors as in the case of the load cell data. Even in this case, the environmental data with the strongest correlation, found in the previous chapter, was selected, namely T_{med}. Compared to the previous case, only the first two modes will be involved as structural parameters. In fact, their trends appear strongly correlated, because of near-symmetries of the structure. If the plant was perfectly circular, one might expect that both of these coincident frequencies would experience the same variations due to operational and environmental variations. Because the dome is actually elliptical rather than circular, two frequencies that are similar, but not coincident: however, one might expect that the dependence on environmental conditions will still be very similar in the them, and therefore cointegration is expected to be effective carried out on the frequency pair.

In this application, the ability to detect damage has also been tested: (luckily) not having available data relating to a damaged condition, as the data available come exclusively from healthy conditions, they have been virtually simulated. The FEM of the Sanctuary was used, that was available from previous researches (Ceravolo, De Lucia, et al., 2020), which was calibrated on the experimental frequencies (Figure 4. 9). It is modeled in Ansys® environment. The materials are characterized by isotropic linear elastic constitutive laws, as this FEM is mainly

used for global dynamic analyses in which the response derives from very low excitations such as environmental ones.

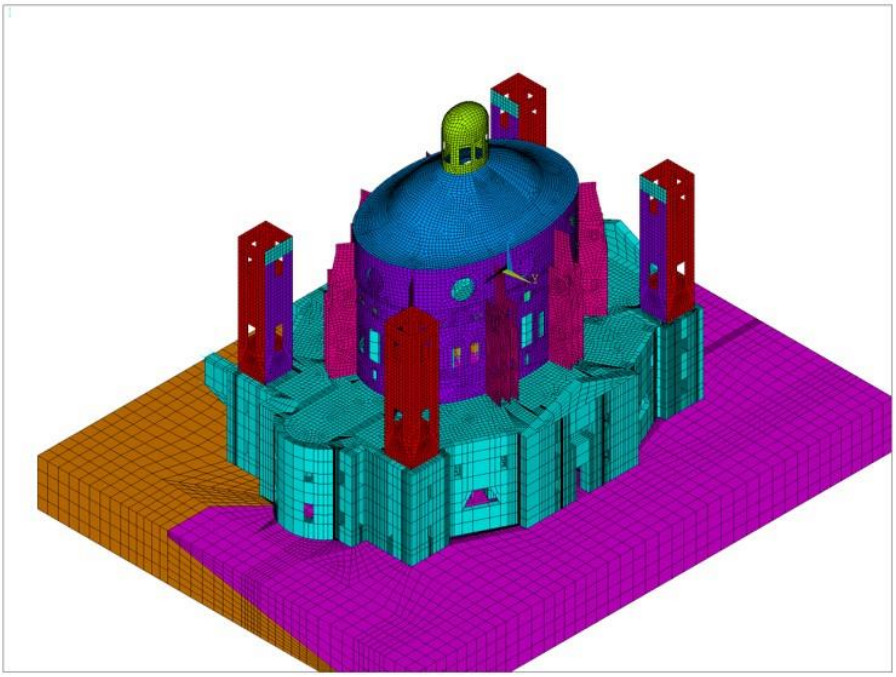

Figure 4. 9: FEM of the Sanctuary of Vicoforte

Table 4. 5: FEM calibrated parameters

Macro-elements	E (GPa)	υ (-)	ρ (Kg/m^3)
Basement	2.00	0.35	1800
Drum	2.30	0.35	1700
Bell Towers	4.50	0.35	1800
Dome	5.50	0.35	1700
Buttresses	5.50	0.30	1700
Lantern	5.60	0.35	1800
Steel	210	0.35	7800
Marlstone	5.00	0.35	2100
Clay	0.75	0.35	1900

The damage in the model was simulated by reducing of the Young's modulus of the zones more subjected to stress due to the self-weight load, in order to make the virtual damage location as realistic as possible (see Figure 4. 10). These zones

are located at the base of the buttresses, so the Young's modulus of these vertical elements was reduced to 60% to its initial value.

It is noted that the modeling of damage in this application has been extremely simplified. In a real scenario, the beginning of a damage would result in a series of low amplitude sudden damages, which could give rise to a smoothed drop of natural frequencies. In these situations, a nonlinear model is often required to get not misleading results and it would be exploited to simulate gradual variation of structural characteristics. In future, when the FEM will be aided with such information, more realistic situations will be reproduced in order to test the damage detection capabilities of the procedure even in those scenarios. Nevertheless, even with a simplified modeling, the goal of demonstrating the effectiveness of the damage detection procedure can be pursued. The proposed approach applies between a reference (initial) state and a damaged (final) state then the sharp Young's modulus reduction could be seen as a "snapshot" of that evolution. The simplified damage modeling lead to relative low percentage of frequency variation, which was kept constant for all the damaged observation since modeling a damage worsening (in addition to requiring refinements of the current FEM) would facilitate damage detection.

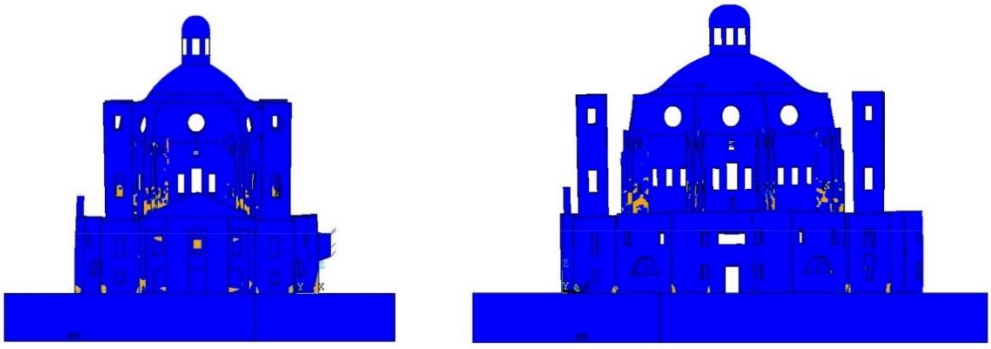

(a) (b)

Figure 4. 10: Von Mises' stresses under self-weight load: south transverse view of the FEM (a); east longitudinal view of the FEM (b)

The reduction of the buttress modulus results in a reduction of the numerical frequencies. By defining f_{da} and f_{un} the frequencies of damaged and undamaged model, the index D is assumed to be the normalised difference between the undamaged and damaged frequencies:

$$D = 1 - \frac{f_{da}}{f_{un}}; \tag{4.23}$$

the obtained indices are reported in Table 4. 6**.**

Table 4. 6: FEM dynamic paramethers *pre* and *post* damage to buttresses

Mode	f_{un} (Hz)	f_{da} (Hz)	D (%)
f_1 **(1st bending Y)**	1.925	1.885	2.08
f_2 **(1st bending X)**	2.109	2.079	1.42

At this point, an equal reduction in percentage has been applied to the experimental frequencies, starting from observation 5500 when the damage is supposed to occur (Figure 4. 11). Both the algorithms have been tested on this data.

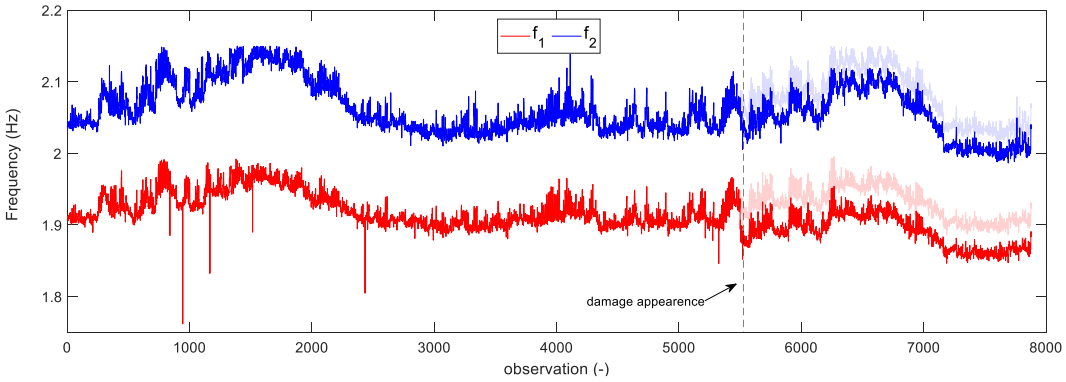

Figure 4. 11: application of the virtual damage to the time series of the first frequencies

It should be noted that in these last graphs there are more observations because, since only the first two frequencies were used as structural characteristics, far fewer "incomplete" observations were discarded compared to the previous paragraph, where it was required that all 5 frequencies be included in each sample.

The ADF test performed on those trends, in the range of TD (i.e. [1000:2000]), proves they are nonstationary with integration order equal to 1. In this case, the predicted variable is the frequency of the first vibrating mode, being the one most sensitive to the damage imposed (see Table 4. 6) therefore the one on which it should be easier to detect the damage. In order to make immediately clear the need to look for a health indicator for damage detection which is insensitive to

environmental variations and also to demonstrate that the modeled damage would not be immediately identifiable from the starting variables, in Figure 4. 12 the *X-chart* was implemented directly on the first frequency trend.

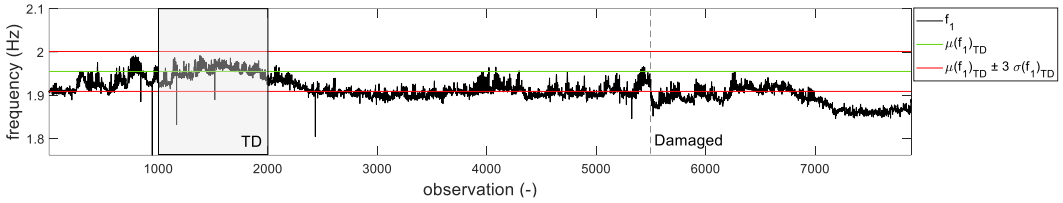

Figure 4. 12: X-Chart plotted directly on the virtually damaged frequency series: f_1

It is easy to observe that a very high number of FPs would occur before the appearance of the damage (observations that exceed the LCL) and, much more worryingly, the frequency increases given by high temperatures (approximately the range of observations [6000÷7000]) compensate for the variations generated by the damage (FN), hiding it. With this awareness, the methodology was tested on these data in damaged condition: in

Figure 4. 13 and Figure 4. 14 the models obtained using the SVM and RVM and the respective residual ε are reported (see a summary in Table 4. 7). They will be referred as VI and VII.

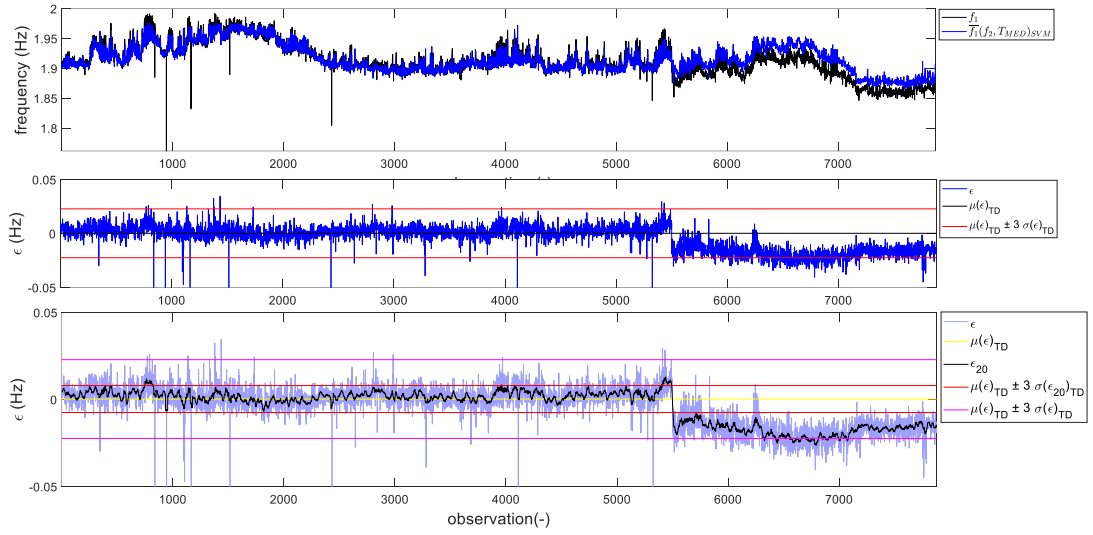

Figure 4. 13: f_1 SVM model using f_2, T_{med} as predictors and its model residual (original and mediate through a 20 samples average moving window) (VI)

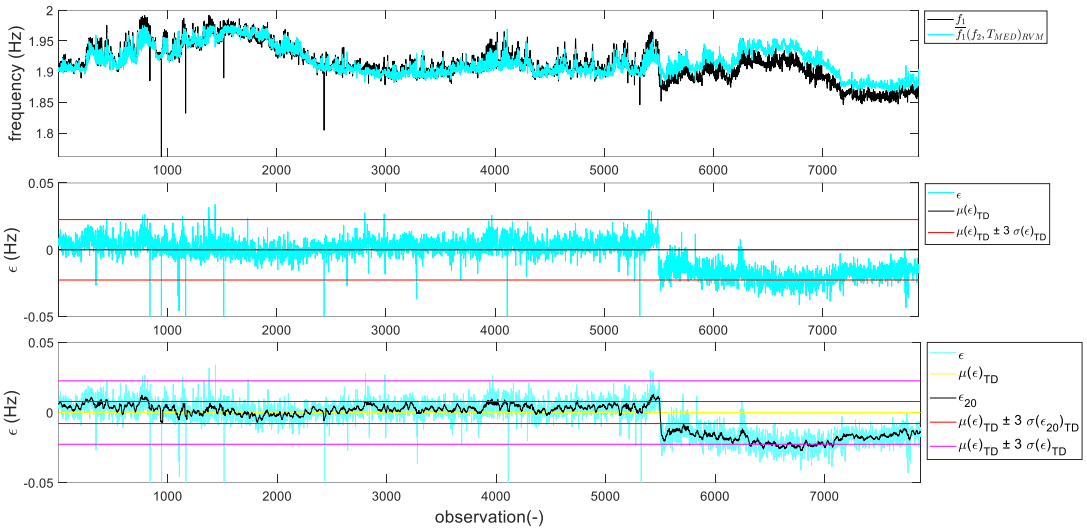

Figure 4. 14: f_1 RVM model using f_2, T_{med} as predictors and its model residual (original and mediate through a 20 samples average moving window) (VII)

Table 4. 7: characterisics of models built on virtually-damaged dynamic monitoring data

ID	Algorithm	Predictors	Predicted	$RMSE_{TD}$	V/N_{TD}
VI	SVM	f_2, T_{med}	f_1	0.0075	1000/1000
VII	RVM	f_2, T_{med}	f_1	0.0075	3/1000

Both the regression models produce a regular low residual before the damage introduction (observation 5500) while it moves away from zero after its appearance. Following 5500th sample, many points exceed the LCL, hence the strategy report satisfying results in the damage investigation, especially once the moving average is applied, which increases the accuracy of the classification between healthy and damaged condition (see Table 4. 8).

Table 4. 8: outcome of the procedure on dynamic monitoring data with virtual damage

	Original residual (ε)			**Averaged residual (ε_{20})**		
ID	**% FP**	**% FN**	**Accuracy**	**% FP**	**% FN**	**Accuracy**
VI	0,49	79,5	0,76	2.93	0.29	0.9787
VII	0,5091	75,6	0.77	5.49	0,168	0.9612

The graphs clearly show the difference between false positive samples and true (or better, virtual) occurrence of damage. In the first case ε exceeds the UCL or LCL but it returns to stationarity immediately for subsequent observations. On the

contrary, when the damage occurs, ε moves away from 0 indefinitely, and probably, in a case of actual damage, it would continue to diverge as the damage would continue to progress.

4.4 Conclusions

In this chapter a procedure for damage detection in SHM is proposed and applied, based on the cointegration property associated with ML algorithms for regression, the residue of which is judged using a tool, the X-chart, from SPC literature. The whole process leads back to a novelty detection.

The procedure was successfully applied to both static and dynamic monitoring data, by exposing and comparing the choice of different predictors, algorithms and post-processing of the damage indicator parameter obtained.

This procedure is deemed convenient for SHM as (i) it is based on a simple and versatile idea, then it can be used on several assets with different schemes, material, age and kind of damage expected; (ii) it only requires that the regression model should be set on data related to the normal condition of the building. The major issues are just about the choice of this set: a wrong selection of training observations or predictors can lead to errors in damage detection. Therefore, the training data must be chosen with great care. If one knows that any normal environmental/operational condition causes a strong variation in the monitored response, data from such events must be included in the training set to avoid a FP indication if a similar event occurs later.

Part of the work described in this chapter was also published in a journal paper (Coletta et al., 2019a).

Chapter 5

Transfer learning to gain labelled data from different structural conditions

5.1 The lack of labelled data for SHM

To date, it is a fact that the use AI has spread widely in many engineering sectors including SHM, where ML algorithm are applied to extract information from large amounts of data and perform predictions, as seen in the previous chapter. Classical ML algorithms exploit statistical models that are calibrated, or better *trained*, on previously recorded data whose output, the *labels*, may or may not be known, going towards *supervised* and *unsupervised* learning problems respectively. In the middle of these approaches there is another class, the *semi-supervised* learning problems, where the scarcity of labelled data leads to the implementation of methodologies that make use of both labelled and unlabelled data to train the selected algorithm.

In the SHM of AH, these labels should be obtained by evaluating the structural condition of the building from which those specific data come, then by means of investigations, visual inspections, measurements and tests carried out by personnel with advanced and specific professional knowledge in structural engineering (Boller, 2009). These are quite expensive operations, especially if you think you have to repeat them for different combinations of environmental and operating

conditions, just for the undamaged condition. As for the observations of the damage conditions, the difficulty of materializing those conditions is added even before carrying out the inspections to get the labels. As discussed in 2.4.2 in reference to "Use of experimental data relating to past periods", it is very unlikely that damage to an architectural asset will occur while the structure is lucky enough to be under monitoring (at least to date, since the very reduced dynamically monitored architectural assets); it is even more unlikely than that the damage is perfectly repaired by returning the structure to its initial in order to exploit that damaged data as TD for the future. Just to imagine it, theoretically all the elements of a building should be damaged and perfectly repaired one at a time to have a rich and complete training dataset.

In fact, all these mentioned ML problems are based on the idea that these data are extracted from the same distributions: in the case of SHM of buildings, it means from the same structure and approximately in the same period (so that there are negligible effects of degradation between the measures).

One idea to solve this problem could be to create this dataset using the damage data of several very similar structures (Bull et al., 2021). This idea could be very convenient for mass-produced structures (*homogeneous* population), such as mechanical components, prefabricated structural elements, parts of aerospace or naval aircraft: in practice, economically expendable objects. One or more items would be sacrificed in view of exploiting their data to train algorithms to monitor their copies.

However, it is difficult to conceive this vision within the building sector and the reasons for this are different: (i) the practice of dynamic structural monitoring of building is relatively young and therefore the available datasets are neither many nor very large; there are very few datasets containing data relating to real buildings in damaged conditions; (ii) the data of one structure (if not with the use of specific data processing techniques) are difficult to reuse for another due to the geometric differences, the materials, the state of deterioration and cracking, the interventions undergone, the foundation soil which are reflected in a different dynamic behavior. This aspect is further accentuated for architectural assets, which by their nature are geometrically original, unique and which are characterized by greater uncertainties as regards materials and stratifications; (iii) even if, in the remote case, very similar CH buildings could be found, the hypothesis of deliberately causing damage to one of them to build a dataset is not even contemplated, it would be inconceivable from a cultural, artistic, historical and economic point of view.

Therefore, at first glance it would appear that the idea of using data acquired on one system to build the training dataset to monitor another it is hardly applicable for heritage structures: a system very similar to the monitored one, which is economically and technically expendable, should be identified, as well as a method for matching the data which will inevitably present discrepancies.

Here a strategy for CH structure based on Transfer Learning (TL) is proposed to compensate for insufficient labelled data by exploiting datasets acquired on similar but certainly not identical structures. It addresses the problem for which domains, distributions and tasks (these concepts will be explained in the next paragraphs) do not correspond in training sets and test sets, manipulating them using methodologies such as the so-called Domain Adaptation techniques (Pan et al., 2011; Pan & Yang, 2010).

5.1.2 Transfer Learning idea for SHM

The concept behind TL is very intuitive and is subconsciously used by people in many daily actions. For example, gaining experience (or, as they say in ML lingo, *training*) riding a motorcycle simulator in a video game can definitely help you ride a real motorcycle. This is because video game and motorcycle are two systems, obviously different, but similar, from which common information can be extracted which can be used to face both *tasks* that are represented here by riding situations. TL is a very convenient strategy for dealing with problems involving with a new, little-known system (*target*), exploiting information available or more easily obtainable from another system (*source*), which is somehow related to the first. The graph in Figure 5. 1 (next page), from (Pan & Yang, 2010), visually explain the TL idea.

So far, TL has only seen a few isolated applications in the more general field of structural engineering. In the context of deep learning, some research has used TL to improve the performance of neural networks in the identification of cracks in images of damaged structures. For example, Dorafshan et al. compared the AlexNet Deep Convolutional Neural Network (DCNN) architecture in classifiers, fully trained and TL modes, on a set of 19 high definition images (3420 sub-images, 319 with cracks and 3101 without) of concrete (Dorafshan et al., 2018).

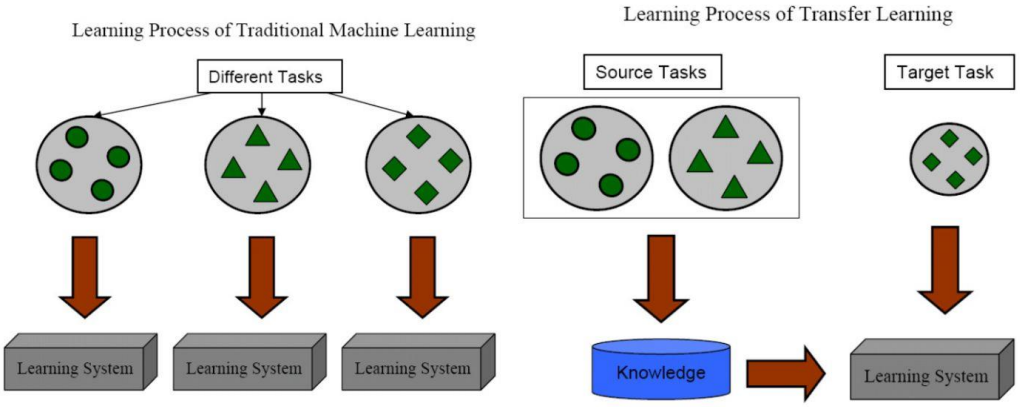

Figure 5. 1: different Learning Processes between Traditional Machine Learning and Transfer Learning (Pan & Yang, 2010)

Still, on concrete structures, Jang et al. applied TL to repurpose the GoogLeNet deep neural network architecture and achieve automated identification and visualization of cracks from hybrid images that combine visual images and infrared thermography (Jang et al., 2019). Tronci et al. exploited a rich acoustic dataset to gain experience to address a damage classification problem on simulated data of a 12 degrees of freedom benchmark shear-building structure (Tronci et al., 2022). Gao et al. proposed the concept of the Structural ImageNet with four baseline recognition tasks, using a TL approach based on the variant VGGNet (Visual Geometry Group) through feature extractor and fine-tuning to achieve well-performed classifiers according to different detection task (Gao & Mosalam, 2018). To make up for the lack of training data, Chakraborty et al. proposed a translated inductive TL-based classifier, demonstrating its effectiveness in the classification of fatigue damage in an aluminium lug joint (Chakraborty et al., 2011). More recently, Gardner et al. proposed to employ TL via domain adaptation techniques for the subclass of heterogeneous populations in which two structures are defined topologically similar. A first case concerns the multisite damage location, and a second case demonstrates the applicability of TL between numerical simulation and the experimental structure. Furthermore, they provided a discussion on the applicability to case studies considered not topologically similar (Gardner et al., 2020).

In SHM of CH structures, as can be easily understood at this point of the discussion, the use of the TL is motivated by the lack of labelled data relating to damaged conditions, but also to particular operating conditions which for some reason are not present in the training dataset of the algorithm. Since here a vibration

based SHM procedure is to be undertaken, the similarity between the structures between which to apply the TL will have to be found at the level of dynamic behavior.

A system that certainly resembles the architectural asset to be monitored from a dynamic point of view and on which, without doubt, it is easier to obtain damage data, is the FEM of the structure. It is a valuable tool in this scenario because it allows to perform many simulations corresponding to a large number of structural conditions, obtaining data of conditions that the structure has never experienced, without the real structure being affected.

However, although in some cases they are very close, the data provided by the model cannot be considered extracted from the distribution of field data, even if the model has been experimentally calibrated. The reasons concern both the simplifications that are inevitably considered by the model (not all parameters are calibrated; not all parts of the structure are geometrically modeled, especially in the case of structures as complex as architectural assets; due to the compromise between computational burden and modeling accuracy that must necessarily be found when defining the mesh; for crack and deformation patterns that can hardly be reproduced faithfully) and for complications that can occur in reality (the real system could be subject, for example, to different environmental factors in the monitoring period, i.e. the test set, compared to the data used to calibrate the FEM which would therefore produce altered training data; also operating conditions could change, as well as the geotechnical properties of the foundation soil).

Precisely because of this inevitable discrepancy between the two systems, virtual and real, the domain adaptation algorithms could prove to be fundamental to move the data closer together, thus making the FEM data exploitable in the implementation of a better generalization on the real monitoring data. In a way, it is a procedure that resembles model updating.

Once an adaptation is achieved, a classifier can be trained and tested on the adapted data. Here a RVM classifier was considered (Tipping, 2001), which was trained on FEM data and tested on unlabelled monitoring data, before and after transformation to compare results and evaluate any improvements in accuracy.

The chapter is organized as follows: in the next section the basic theory of domain adaptation techniques is reported with particular attention to the Transfer

Component Analysis (TCA). Section 5.3 presents the case study, exposing the construction of both domains. The comparison between a classification between original and adapted data is evaluated and presented in 5.4. Finally, the concluding remarks are presented.

5.2 Domain Adaptation for SHM

Domain adaptation is a sub-sector of TL that attempts to transfer knowledge across different systems which are connected in some way, associated to domains of data (Pan et al., 2011; Pan & Yang, 2010). The term *domain* includes these two components:

- feature space of inputs $\mathcal{X}$;
- marginal distribution of a sample set of inputs $X = \{\boldsymbol{x}_1, \dots, \boldsymbol{x}_n\}^T \in \mathcal{X}$, $P(X)$.

In TL problems, two domains are defined, referred to the different systems: a *source* and a *target* domain indicated as $\mathcal{D}_S$ and $\mathcal{D}_T$. Each of them is associated to a *task,* defined by $\mathcal{T} = \{\mathcal{Y}; f(\cdot)\}$, where $\mathcal{Y}$ is the label space and $f(\cdot)$ is the objective predictive function that can be used to predict the corresponding label (which can also be seen as a $P(y|x)$). To summarize:

- $\mathcal{D}_S$ contains the labelled data, i.e. the information intended for transfer. It is mathematically defined as:

$$\mathcal{D}_S = \left\{\left(\boldsymbol{x}_{S,1}, y_{S,1}\right), \dots, \left(\boldsymbol{x}_{S,nS}, y_{S,nS}\right)\right\}^T; \tag{5. 1}$$

- $\mathcal{D}_T$ contains data that comes from the system to be investigated, which are unlabelled or only partially labelled:

$$\mathcal{D}_T = \left\{\left(\boldsymbol{x}_{T,1}, y_{T,1}\right), \dots, \left(\boldsymbol{x}_{T,nT}, y_{T,nT}\right)\right\}^T. \tag{5. 2}$$

In these definitions, $\boldsymbol{x}_{S,i} \in \mathcal{X}_S$ are the n_S observations and $y_{S,i} \in Y_S$ are the corresponding output which in case of SHM are the structural conditions. On the other side, $\boldsymbol{x}_{T,i} \in \mathcal{X}_T$ are the n_T observations in the target domain, where the data can be partially labelled or unlabelled, i.e. $y_{T,i}$ may or may not exist for all feature observations $\boldsymbol{x}_{T,i} \in \mathcal{X}_T$.

In domain adaptation methods, it is supposed that the feature and label space are the same for both domains, i.e. $\mathcal{X}_S = \mathcal{X}_T$ and $\mathcal{Y}_S = \mathcal{Y}_T$, that in the SHM sector it means that the same diagnostic characteristics and the same structural conditions are considered for both systems. Instead they differ in the marginal and (in some cases) in the conditional distributions: i.e. $P(X_S) \neq P(X_T)$ and $P(Y_S|X_S) \neq P(Y_T|X_T)$, so the diagnostic features are differently distributed and also the probability that the structural conditions (the labels) will occur, knowing that these features have occurred could be different between the two domains

Because of these differences, a classifier may make mistakes if trained on the source domain and tested directly on the target domain. To remedy this, numerous techniques have been developed to shorten the distance between the densities of the domains, taking advantage of a nonlinear mapping function $\phi(\cdot)$ which aims to match the distributions in order to get $P\big(\phi(X_S)\big) \approx P\big(\phi(X_T)\big)$ and $P\big(Y_S|\phi(X_S)\big) \approx P\big(Y_T|\phi(X_T)\big)$.

It this study, a recently developed learning algorithm, the TCA, has been applied to reduce the distance between data distributions from a continuous monitoring set of data collected on a real structure, the Sanctuary of Vicoforte, and its corresponding numerical model.

5.3 Transfer Component Analysis

TCA is a domain adaptation technique proposed by Pan *et al.* in (Pan et al., 2011) about ten years ago. The algorithm tries to learn some transfer components across the previous defined domains in a Reproducing Kernel Hilbert Space (RKHS) using the Maximum Mean Discrepancy (MMD) as an embedding criterion. This leads the data distributions of the different domains to be approached in the subspace spanned by these transfer components. In this new subspace, on the transformed data, ML algorithms can be trained for classification or regression problems exploiting data from the richer source domain and then tested on the unlabelled or partially – labelled target domain.

TCA is based on the assumptions that $P(X_S) \neq P(X_T)$ but $P(Y_S|X_S) = P(Y_T|X_T)$. The strategy by which TCA proposes to find the mapping function $\phi(\cdot)$ is based on the minimization of the distance between the marginals $P\big(\phi(X_S)\big)$ and $P\big(\phi(X_T)\big)$ and the requirement that $\phi(\cdot)$ retain the important properties of the

original distributions X_S and X_T. This approach avoids explicitly defining the nonlinear transformation $\phi(\cdot)$.

The MMD distance between two distributions can be empirically measured by the distance between the empirical means of the two domains. This can be written in this form:

$$Dist(X_S', X_T') = tr(KL) \tag{5. 3}$$

in which X_S' and X_T' are the transformed inputs from the source and target domains, K is the Kernel matrix, containing the kernel matrices of source, target and cross domains (i.e. $K = k(X, X')$ where $X = \{X_S, X_T\}^T$) and L is the MMD matrix, expressly defined as:

$$L(i,j) = \begin{cases} \frac{1}{n_S^2} & if\ x_i, x_j \in X_S \\ \frac{1}{n_T^2} & if\ x_i, x_j \in X_T \\ \frac{-1}{n_S n_T} & otherwise. \end{cases} \tag{5. 4}$$

By a decomposition of the kernel matrix, the empirical kernel map can be obtained using a $(n_S + n_T) \times m$ matrix of weights, W, which transforms and reduce the feature vector into a m-dimensional space,

$$\widetilde{K} = \left(KK^{-\frac{1}{2}}\widetilde{W}\right)\left(\widetilde{W}^T K^{-\frac{1}{2}}K\right) = KWW^TK. \tag{5. 5}$$

The distance between the empirical means of the two domains can then be rewritten replacing $\widetilde{K}$ in the distance:

$$Dist(X_S', X_T') = tr(W^T KLKW). \tag{5. 6}$$

In the minimization of the distance, a regularisation term is introduced to check the complexity of the weight matrix. The kernel learning problem becomes:

$$\min_{W} \; tr(W^T KLKW) + \mu \, tr(W^T W) \quad \text{s.t.} W^T KHKW = I \tag{5. 7}$$

where μ is a *trade-off / regularization* parameter, H is a centring matrix, I is an identity matrix and the constraint on $W^T KHKW$, that represent the variance of the projected samples (a property that TCA aims to preserve) avoids the trivial solution $W = 0$. Then, writing the Lagrangian of the latter equation and going through a short mathematical demonstration, it can be proved that the Eq. (5. 7) can be efficiently solved by the following equivalent trace optimization problem:

$$max_W \; tr((W^T(KLK + \mu I)W)^{-1} W^T KHKW). \tag{5. 8}$$

The solutions for W in equation (5. 8) are the m leading eigenvectors of $(KLK + \mu I)^{-1} KHK$, where $m \leq n_S + n_T - 1$, which are used to define the space of the transformed features through $Z = KW$, where $Z \in \mathbb{R}^{(n_S + n_T) \times m}$.

5.3 Case study

The concept of adaptation between the data coming from real structure and its numerical model can be put into practice for many kinds of structure, and therefore is extendable to several research fields.

As anticipated, the case study is represented by the Sanctuary of Vicoforte. It represents an ideal case study since, in addition to having a permanent static and dynamic monitoring system, the data of which have already been analysed in the previous chapters, it has a very advanced mechanical FEM. It was briefly introduced in the previous chapter (4.3.2), where it was used to derive percentages of reduction of the structural frequencies in presence of a damage, that were used to test the novelty detection procedure; so here, more details will be provided. The FEM, whose latest version was developed in another research work (Ceravolo, De Lucia, et al., 2020), will constitute the source domain in this TL application. In this framework, the two systems are considered to belong to a homogeneous population since they are intended to be identical in topology, geometry and materials (Gardner et al., 2020).

Given that the dynamic monitoring data have already been presented in the previous chapters, it should already be clear that they do not show anomalous variations as, fortunately, to date the Sanctuary has not encountered any damage.

Aiming at demonstrating an improvement of a classifier trained on FEM and tested on real data, among the cases without and with domain adaptation, more than one class (or structural condition) are necessary. Therefore, here, for once, much-hated variations due to environmental effects have been used in favour.

In fact, this application will aim at improving the recognition of different environmental conditions, expressed by a temperature variation, within the distribution of the natural frequencies. Obviously, the final practical purpose of this practice is not to indirectly detect a temperature variation from the classification of diagnostic dynamic parameters of a building, since this could be done very trivially with a thermometer.

This research instead represents a sort of test field for a future TL application in a damage identification perspective. The temperature, as seen in chapter 3, have a strong influence on the dynamics of a system (Cabboi et al., 2017; Ramos et al., 2010; Ubertini et al., 2017), so that in some cases it generates data alterations comparable to damage (Peeters & De Roeck, 2001; Sohn, 2007; Xia et al., 2012). This similarity of effects is exploited here to outline two classes and test a transfer of information from the FEM to the real structure.

This is done because large amounts of data are available associated with environmental changes, whereas no real data are available for damaged data, therefore the effectiveness of the procedures could not have been tested in a damage detection context. In fact, a positive result would suggest that the procedure can provide a valuable tool for identifying damage in real monitoring programs, by appropriately changing the source domain: it would be enough to add to the classes used here, which are "not damaged at 3°C" and "not damaged at 10°C", with classes related to damaged conditions whose data would come from the FEM.

5.3.1 Source Domain

The FEM is used to compose the source ddomain. It is a numerical linear model already calibrated through experimental dynamic data before the development of this study for other research objective (Ceravolo, De Lucia, et al., 2020); in spite of that, the data from this FEM showed some inevitable differences with the experimental data distribution, here selected as the target domain, in addition to the fact that the former are constant, since the model is not influenced by any external phenomena, while the real Sanctuary suffers EOVs. The diversity of domains can be attributed to: (i) model calibration residue; (ii) uncertainty due to dynamic

identification (which includes potential sensor failures, distortions of the acquired signal, non-uniqueness of the identification result, which is ultimately subjected to a statistical analysis); (iii) influence of all other environmental and operational factors on the experimental frequencies, which are not present in the experimental data set used to calibrate the model; (iv) slight evolution of the dynamic behavior from the moment the model was calibrated to the current monitored response.

This turns out to be an opportunity to demonstrate that TL can be applied to deal with situations like this. In (Gardner et al., 2020), for example, the strength of this approach is demonstrated in the use of models which are not perfectly validated and are potentially influenced by model-form errors, which are still able to grasp, to a certain extent, the fluctuations in the characteristics caused by damage.

To compose the source domain, and therefore to give the FEM data a distribution, the eigenvalues problem has been solved several times by slightly varying the mechanical parameters. Specifically, a Gaussian distribution has been attributed to the elastic modulus of each macroelement. Its average was set equal to the calibrated value (Ceravolo, De Lucia, et al., 2020) while the variance was set on the basis of literature values for the same material (Saloustros et al., 2019) and also considering the variability of the results of the available experimental tests (Aoki et al., 2011). For example, the distribution of the elastic modulus of the steel of the strengthening modern system has been assigned a much smaller variance than that of the modulus of the historical masonry, since the properties of the current steel are certified before being put on the market. Elastic moduli randomly extracted from these distributions were assigned to each eigen-analysis, resulting in a slight variation in the frequencies and modal shapes extracted. One hundred eigen-analyses were solved with as many combinations of elastic moduli: half of these analyses were labelled as a healthy condition at a temperature of 10 ° C, as the dynamic data used for the calibration of the model had been collected at an average temperature corresponding to about 10 ° C.

An excursion of 7 ° C was assumed for the second class, the effect of which was mechanically reconstructed and applied to the second half of the dataset. To obtain the effect of the temperature excursion a simplified model has been developed, which is shown below. The procedure involved only the first 3 vibrating modes the Sanctuary, corresponding to the first bending modes in the y and x directions, which are the directions of the minor and the major axes respectively and to the first torsional mode. These experimental frequencies could be considered

the most reliable as they show less variance in their estimated values and a higher identification rate.

Simplified frequency-temperature model

Considering a symmetric portion of a homogeneous and isotropic linear elastic material with uniformly distributed porosity filled by liquid, e.g. water, under the hypothesis of a uniform distribution of temperature over the liquid and solid materials. Initially, it is considered free to expand. Heating the material with some kind of source, the increased volume, V, is evaluated through $V = V_0 + V_0\alpha_s(T)T$, where V_0 is the volume corresponding to the reference temperature of 0 Kelvin, while $\alpha_s(T)$ and T are the thermal expansion coefficient of the solid (which depends on the temperature) and the absolute temperature in K, respectively. At the same time, the liquid phase will undergo an expansion at constant pressure and an increase in pressure at constant volume, since it can realistically be assumed that the rigidity of the solid phase is much higher than that of the liquid phase. Assuming initially the incompressibility of the solid phase, one can calculate the pressure increase in the liquid, p_l, with respect to the reference state p_0, as:

$$p_l = p_0 + p_0\alpha_l(T)T \tag{5. 9}$$

where $\alpha_l(T)$ is the thermal expansion coefficient of the liquid. Since the portion is free to expand, the pressure in the matter is not the same as that of the liquid, but it should be purified by a certain amount p^*. It represents the pressure hypothetically accumulated if the portion was not free to expand, and it can be calculated as $p^* = p_0\alpha_s(T)T$, being function of $\alpha_s(T)$. Therefore, the actual pressure in the portion of material, uniformly distributed over the solid and liquid phases:

$$\begin{aligned} p &= p_l - p^* = p_0 + p_0\alpha_l(T)T - p_0\alpha_s(T)T \\ p &= p_0\big[1 + \big(\alpha_l(T) - \alpha_s(T)\big)T\big]. \end{aligned} \tag{5. 10}$$

At this point, considering that the portion of material investigated is far from the boundaries of the body to which it belongs, it can be assumed that zero deformation occurs at the macroscopic scale, since the deformations are concentrated for the most part at the boundaries. Under these new assumptions, the relationship between stress and strain becomes,

$$p = E\varepsilon_0 \tag{5. 11}$$

from which, by substituting the (5. 10), the elastic modulus E can be obtained as a function of temperature and expansion coefficients:

$$E(T) = \frac{p_0\left[1 + \left(\alpha_l(T) - \alpha_s(T)\right)T\right]}{\varepsilon_0} \tag{5. 12}$$

rewriting the (5. 11) for p_0, as $p_0 = E_A\varepsilon_0$, and thus setting $E_A = p_0/\varepsilon_0$, the previous equation becomes:

$$E(T) = E_A\left[1 + \left(\alpha_l(T) - \alpha_s(T)\right)T\right] \tag{5. 13}$$

where $E(T)$ represents an equivalent elastic modulus, which considers the effect of the different thermal expansion coefficients of the solid and liquid phase of a portion of material (i.e. indirect thermal effect), valid for a portion of matter far from the boundaries of the system. E_A would be equal to E_0 if only this effect were considered. However, more generally, it is known that temperature also has a direct effect on the Young's modulus of materials, due to the thermal agitation of the particles which increases with increasing temperature. This $E - T$ relationship is commonly inversely proportional and non-linear but for temperatures close to environmental values, within the range -50/+50 °C, a linear variation can realistically be adopted. Therefore here, in order to take into account the variation of Young's modulus due to the direct effect of the temperature (i.e. to the thermal agitation of the particles), a linear contribution in the parameter E_A can be introduced, as a function of the parameter r, so that $E_A = (E_0 - rT)$:

$$E(T) = (E_0 - rT)\left[1 + \left(\alpha_l(T) - \alpha_s(T)\right)T\right] \tag{5. 14}$$

where r is the tangent at small relative temperatures (i.e. around 273.15 K, 0 °C) of the $E - T$ relation describing the thermal agitation effects, while E_0 is a fictitious 0 Kelvin elastic modulus (fictitious as the law is linearised at small relative temperatures).

Generally, being $\alpha_l(T) \gg \alpha_s(T)$, then $\alpha_l(T) - \alpha_s(T) \approx \alpha_l(T)$. Moreover, as the Sanctuary is a masonry structure, in a first approximation, the contribution due to the direct effect of thermal agitation in the variation of the elastic modulus within the range of values of environmental temperatures is considered negligible. Accordingly, r is assumed to be null. Finally, as the liquid contained in a masonry civil structure is mainly constituted by water, the relation becomes:

$$E(T) \approx E_0[1 + \alpha_{H2O}(T)T] \tag{5. 15}$$

where $\alpha_{H2O}(T)$ is the water thermal expansion coefficient, whose values are reported in (https://webbook.nist.gov/chemistry/) and plotted in Figure 5. 2.

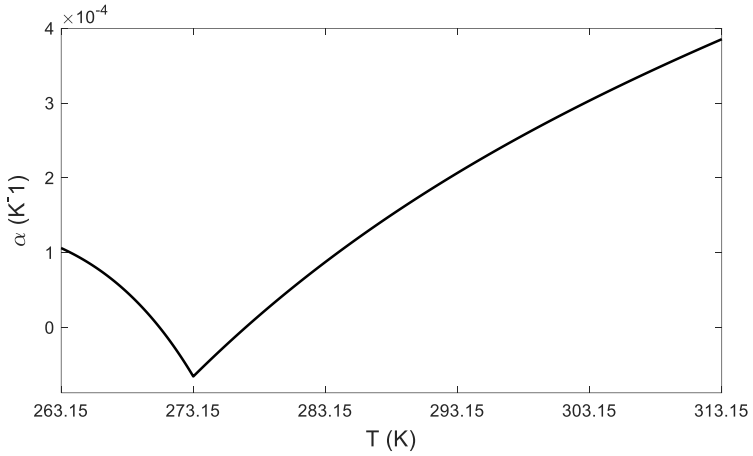

Figure 5. 2: thermal expansion coefficient of water as a function of temperature $\alpha_{H2O}(T)$

Following the hypothesis of uniform temperature on the entire solid-liquid system analysed, the solution of the eigen-problem performed on the structural mass and stiffness matrices, gives an estimate of the natural frequencies of the system as the temperature varies, $f_k(T)$, for the k^{th} vibrating mode:

$$f_k(T) \approx f_{0,k}\sqrt{1 + \alpha_{H2O}(T)T} \tag{5. 16}$$

where $f_{0,k}$ is the fictitious 0 Kelvin frequency for k^{th} mode. Figure 5. 3 shows the first two experimentally-identified frequencies of the Sanctuary, overlapped to the assumed model (5. 16), both plotted as a function of the external temperature. In Figure 5. 4a, the resulting distribution of the frequencies at 3°C and 10°C is illustrated.

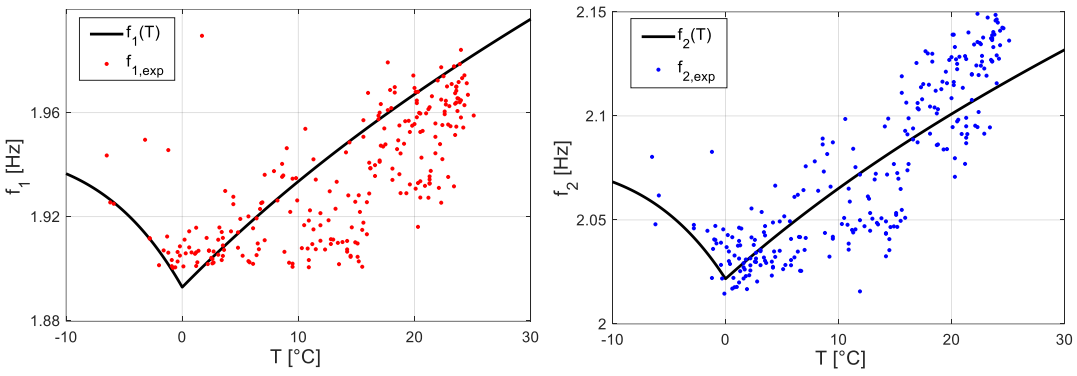

(a) (b)

Figure 5. 3: simplified frequency-temperature law for the first (a) and second (b) vibrating modes of the Sanctuary

5.3.2 Target Domain

The first three experimental frequencies of the Sanctuary with the relative distributions constitute the target domain (Pecorelli et al., 2020). A dataset close in time to that used as a reference to calibrate the FEM was considered [2017-18], in order to exclude any evolution of the parameters in the following years. Each observation is associated with a temperature value, which corresponds to the average temperature recorded in Vicoforte on the day of acquisition of the signal from which the modal frequency is obtained. These data, as in chapter 3, was obtained following a request to Piemonte (Arpa Piemonte, 2000). Among all these samples, those associated with temperatures of 3 and 10° C were selected, corresponding to the two classes to be separated in this classification problem (Figure 5. 4b).

From the examination of the two domains it can be observed that the numerical one is much more regular and the classes are already easily separable at first sight. The target domain, i.e. experimental, is much more disordered and although it is evident that the decrease in temperature is associated with a decrease in frequency, since the class at 3 °C is positioned for the most part on values of the three frequencies lower than those of the class at 10 °C, it can however be noted that the classes intersect. This is because temperature may not be the only factor affecting frequencies in reality, whereas in the model, in this case, it is the only factor modeled.

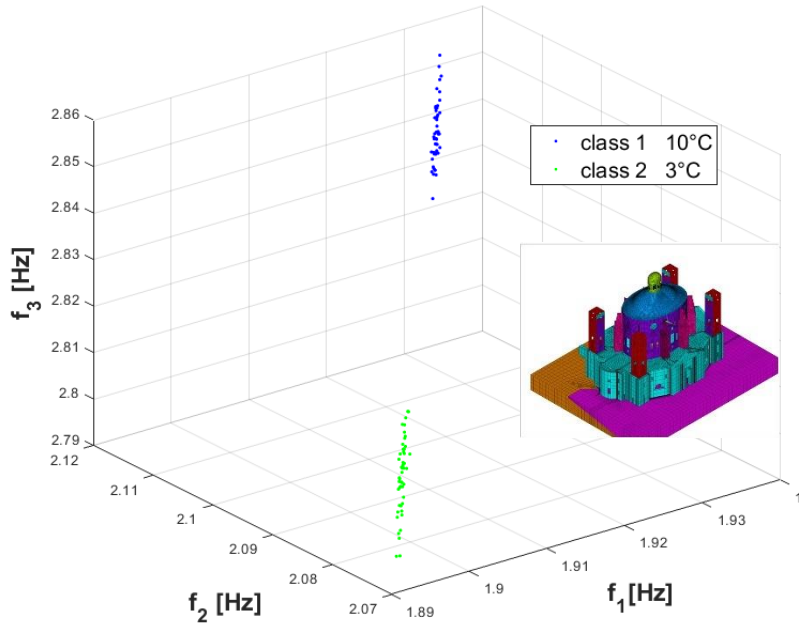

(a)

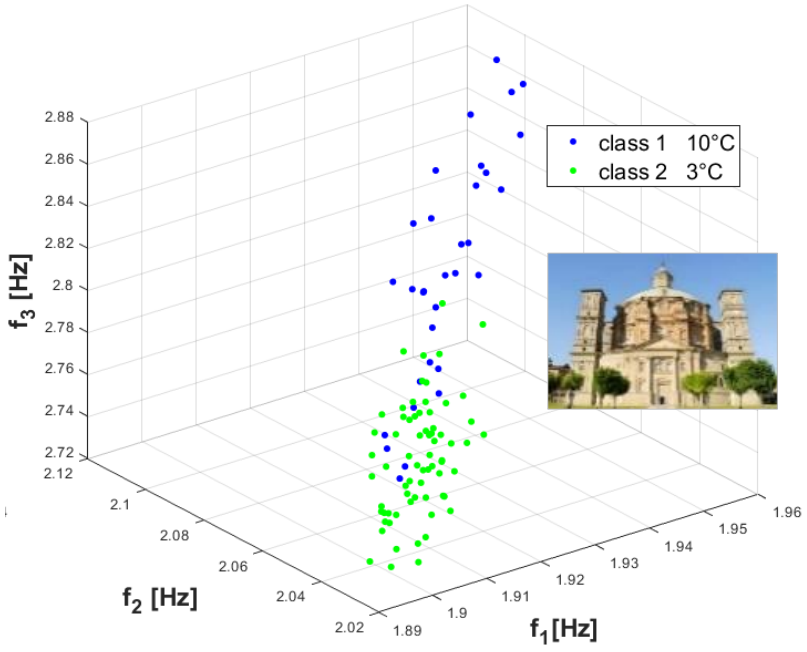

(b)

Figure 5. 4: source (a) and target (b) domain samples

In other words, a sample of class 1, colored in blue, which however seems more similar as values to class 2, could be the product of a particular operating condition

(or environmental condition in addition to the temperature) that led the values of the three frequencies to lower, even though there is an external temperature of 10 ° C. This difference in the data, although the FEM of the Sanctuary is geometrically modeled in a very accurate way for real structures of this complexity and also calibrated with the experimental frequencies, motivates the adoption of a domain adaptation technique.

5.4 Classification

5.4.1 Original dataset

An RVM classifier (Tipping, 2001) has been applied on the Sanctuary data, before the use of the domain adaptation technique. A radial basis function was chosen for this problem. In addition to the source data, a small subset of labelled target data has been selected and used for defining the kernel scale parameter that maximises the average classification accuracy, applying a five-fold cross validation procedure ($\sigma = 0.3$). The final classifier was trained on a set consisting of all the source data and a part of the first class of the experimental data (the samples that are not circled in the Figure 5. 5) and was tested on the remaining target data. In Figure 5. 5a, the results of the classification are graphically illustrated while in Table 5. 1, the classification accuracy is reported.

5.4.2 Adapted domains

The domain adaptation technique was applied to the data of the Sanctuary of Vicoforte. A quadratic kernel was used for the transformation. Again, a five-fold cross-validation procedure was performed and the hyperparameters which returned the highest average accuracy were selected.

Adaptation resulted in a number of transfer components m equal to 2, a regularisation parameter $\mu = 10^{-7}$ and a kernel scale equal to 15, while $\sigma = 2.9$ has been selected for classification, still with a Gaussian kernel. In Figure 5. 5b the outcome of the RVM classifier trained in the transformed feature space is shown, and its accuracy is presented in Table 5. 1. The application of TCA led to an almost 20% improvement in the classification of the experimental data of the Sanctuary, subjected to two different temperatures.

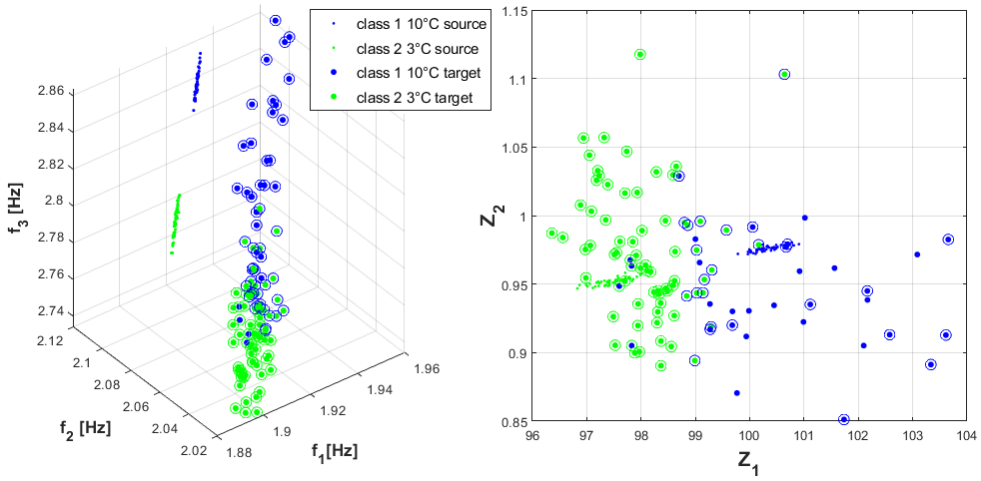

(a) (b)

Figure 5. 5: RVM classification in the original (a) and transformed feature space (b)

Table 5. 1: classification accuracy

	RVM	TCA-RVM
Accuracy	62.8%	79.1%

As always with ML algorithms, attention must be paid to the results, over which it is difficult to have direct control since the parameters that regulate the algorithms have no physical meaning. For example, just maximising the accuracy in the classification which follow the domains adaptation, without proper control over the results, leads to the transformation in the Figure 5. 6.

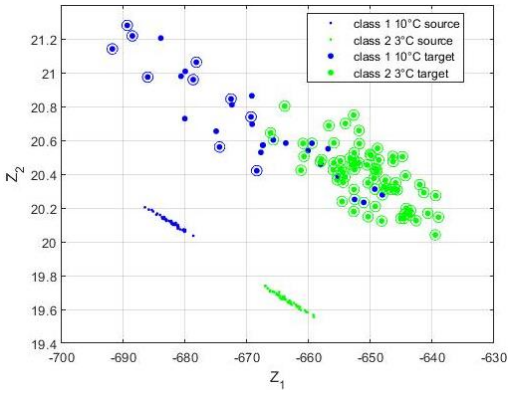

Figure 5. 6: result discarded because potentially misleading on new data / classes

Although it has a higher classification accuracy than the previously shown, it has been discarded because it is considered valid only for this particular

configuration of the classes. For example, the addition of a new class is quite likely to undermine the classifier trained on these transformed characteristics.

5.5 Conclusions

The lack of labelled data coming from structural damaged conditions represents a very significant problem in the field of SHM. Especially for those areas, such as that of AH, in which obtaining them is technically difficult, economically inconvenient and culturally inadmissible. Numerical models, due to inevitable simplifications, potential errors and not validated behavior do not always aid the interpretation of experimental measurements, unless a proper "bridge" between the systems is conceived.

The application of the TCA led to a clear improvement in classifying the experimental data of the Sanctuary of Vicoforte, subjected to two distinct environmental temperatures. The good outcome obtained in the recognition of different environmental situations encourages the use of TL for the purpose of damage identification, in which the FEM would be useful in producing data related to virtual damage conditions that would otherwise be impossible or difficult to obtain. Insights will be needed to define the optimal composition of this virtual data domain and to determine the extent to which model simplifications can be decisive for improving SHM methods.

A comment regarding the characteristics of the FEM used for this application seems appropriate. Accurately modeling the behavior of masonry structure is a very complex task. In this research, a model of a masonry structure characterized by elastic-linear constitutive laws was considered: this could seem a very important approximation, as masonry is known to be subject to more complex behavior which very often does not have proper physical laws suitable to describe them. In this specific case, having been simulated a structural response to very light stresses, i.e. variations in temperature, it is reasonable to assume such a simplification but it could turn into an oversimplification if other scenarios are contemplated, so an alternative strategy should be searched. Hybrid models, i.e. mixing physical model tested in laboratory with numerical model, would be extremely helpful in those situations (Miraglia, 2019). In these methods, highly uncertain structural behaviors are directly tested in laboratory over subparts of the structure or on scaled samples, while behaviors characterized by less uncertainty are modelled with numerical tools and mixed with data provided by the tests in a quasi-real time configuration. This

would be even more useful if one wants to involve damaged conditions classes, which, thanks to hybrid methods, would be simulated much more faithfully than using a totally virtual model.

Finally, a further necessary clarification should be dedicated to the $E-T$ relationship used in this chapter. The relationship between the elasticity of the FEM materials and the temperature is in fact a key point of this specific application and the results obtained depend strictly on this model. The simplified $E-T$ model was to a certain extent conceived on the basis of the analyzes conducted in chapter 3: the bilinear shape of the experimental data, with a change in slope around 0 ° C suggests a connection with the water state diagram. As highlighted in paragraph 2.3, where some examples and relative references have been reported, this $f-T$ trend is not universally valid but it varies from structure to structure. This difference could depend on factors of different nature, such as (i) the type of material, its porosity and how different materials interact with each other; (ii) the exposure of the structure which determines internal-external temperature differences, between the cardinal points and at different height levels; (iii) type of soil, the level of influence of T on it (the case of bare ground and asphalted ground should be distinguished), in combination with other geophysical phenomena; (iv) the geometry and constraints of the structure (including adjacent buildings) and the possibility of thermal expansion of the elements; (v) the presence of metallic structural elements with a strong influence on the global stiffness. Operationally, predicting and modeling all these effects triggered by environmental conditions (i.e. the healthy behavior of a structure under varying environmental conditions) could be very complex and misleading in the event that the structural response at different temperatures is not available a priori to be used for a validation. Therefore here, observing this relationship directly from the measured data seemed be the most reliable way; then, aware of the measured behavior and knowing the system in detail, the physical mechanism that produces that trend has been identified in the phenomenon of water expansion inside the masonry elements, which produces responses very similar to those measured.

Anyway, it should be noted that in this application the two temperature classes have been modeled only for research purposes, in order to have a concrete confirmation in terms of classification accuracy on data already labelled, since, as already mentioned, experimental data have never been measured regarding damage to the Sanctuary, fortunately. In a real application, the ultimate purpose of this kind of procedure should be to detect damage and possibly its type / location. In the author's view, under this circumstance it would be appropriate to have at least data

available regarding the healthy behavior of the structure under varying environmental conditions before the monitoring procedure is operational: they could be collected continuously or through temporary campaigns over a year, in order to collect a full cycle of the ambient temperature. Once collected, they could form the basis on which to calibrate the FEM, providing, depending on the case, different combinations of parameters for different temperature ranges: e.g. 4 calibrations could be provided for the 4 seasons. On these models, the damage could be simulated, perhaps by taking advantage of hybrid modelling, generating virtual measurements that take into account both the variations due to temperature and damage. Their inevitable deviation from the experimental data would be bridged by an adaptation of the domains: data of the healthy structure at different temperatures could be used to define the parameters of the transformation (since present in both domains) which would then be applied also to the data in damaged conditions. Finally, having data for different classes (damaged and healthy at different temperatures) adapted to the new features space, ML classifiers could be trained directly on them (with a TD composed of both source and target domain data), similarly to what was done in this chapter, and tested on unknown (adapted) experimental measurements.

Part of the work described in this chapter was also published in a paper (Coletta et al., 2020).

Chapter 6

Producing labelled data from experiments: a test simulation

In Chapter 2, the difference between supervised and unsupervised learning in ML was exposed with reference to SHM of architectural assets. It is essentially linked to the availability of data labelled in the training phase of the ML algorithm which then leads to different tasks that the chosen algorithm has the possibility to undertake.

In chapter 4, positive results have been obtained with the novelty detection based on cointegration and ML regression, which came to distinguish the healthy condition, from a condition that moves away from health, even without being able to define it. However, sometimes this may not be enough. For example, if the training set is not chosen to contain a broad spectrum of examples of structural conditions as the external environment changes, the ML algorithm could mistake an environmental condition it had never seen before for damage (in classification) or failing to predict it (in regression problems). In fact, as widely discussed in chapter 3 and following, the dynamic parameters are strongly influenced by harmless environmental and operational factors, as well as by damage; it is therefore essential to associate data diversity with the right conditions to avoid so-called false positives and negatives. In order for the algorithm to not only recognize diversity, but also label it, it needs to have experienced these conditions (damaged, not damaged, environmentally / operationally different from normal ones). It was

seen in the previous chapter how to manipulate the data of a FEM in order to be able to build an efficient dataset to train a classifier to be applied directly on the real data. However, it is observed that the results depend heavily on the models used to simulate the environmental, possibly operational variations, the damages and their evolution.

This chapter suggests an original way to get data from an anomalous condition directly on the real structure. Taking advantage of a visit to the Vicoforte Sanctuary of the students of the Einaudi College of Turin, scheduled for April 2020, it was decided to involve them in an experiment with the aim of obtaining results to be exploited for Vibration-Based SHM. The visit was postponed for reasons related to the epidemiological emergency from COVID-19 and to date it has not yet been rescheduled due to the persistence of the emergency. Time was therefore used to better define the details of the experiment, which are reported in this chapter. In particular, each paragraph of this chapter will aim to answer the following questions:

i) *why*: what is the purpose of the experiment?
ii) *who*: who will be the people involved?
iii) *where:* what are the best locations?
iv) *how*: what are the modalities of the test?
v) *when:* what is the optimal period to carry out the test?

To answer these questions, a highly multidisciplinary work was set up which included simulations on the FEM of the Sanctuary, already mentioned in the previous chapters, statistical analysis of the historical series of measurements collected on the Sanctuary and from environmental stations, on site measurements and definition of anthropometric and motor parameters.

6.1 Motivations

As suggested in the introduction, the purpose of the experiment is to obtain experimental monitoring data relating to an anomalous condition of the structure, possibly attributable to structural damage. This is because, as highlighted several times, obtaining monitoring data relating to a real damaged condition is very difficult for civil structures and practically impossible for architectural assets.

It seems appropriate to re-propose at this point (already reported in 1.3.3) the definition of damage introduced by Farrar and Worden (Farrar & Worden, 2012) as “an intentional or unintentional change to the material and/or geometric properties

of a system, including variations to the boundary conditions which adversely affect the performance of the system". In most practical scenarios of vibration based SHM, changes to a structural system due to damage manifest themselves as variations to the mass, stiffness and energy dissipation characteristics of the system. When dealing with monumental, massive structures such as the Vicoforte Sanctuary, damage that is to be identified by monitoring is generally more likely attributed to a variation in stiffness, for example caused by the propagation of a previous crack, the creation of a new one or from a failure of a structural element etc. Many of the techniques proposed in the SHM field are based on the analysis of structural frequencies (Salawu, 1997), just like those seen in the previous chapters. This is because the structural frequencies directly depend on the stiffness of the system, and therefore a variation of the latter is immediately noticeable in the frequency trend (obviously unless the confounding effect of EOVs). One could therefore think of simulating structural damage data by temporarily varying the stiffness of the system, in order to appreciate an anomalous condition. Unfortunately, however, varying the stiffness of a system such as the Sanctuary is not a simple, immediate nor a reversible operation. If one wanted to contemplate a damage that increases the deformability of the system (which happens in most cases, but not always (Sohn et al., 2002)), for example, it would be necessary to insert devices that increase its deformation capacity.

As an alternative, it was decided to exploit the inverse relationship that frequencies have with the mass of the system, here shown for a SDOF:

$$f = \frac{1}{2\pi}\sqrt{\frac{K}{M}}. \tag{6. 1}$$

Quite simply, instead of reducing stiffness, it was decided to increase the mass of the system, just like ballasting (Worden et al., 2001). This operation is certainly more simply achievable and is certainly more easily reversible. Furthermore, instead of providing for the positioning of real ballasts, which should have been purchased / rented, positioned by technical personnel and then eventually removed from the same, it was decided to exploit an intrinsically mobile mass, that of people.

In particular, as anticipated, about 30 students from the Collegio Einaudi in Turin were involved, who in April 2020 should have made the usual visit to the largest oval masonry dome in the world and its monitoring systems, on the event entitled *"Sustainability between engineering, architecture and cultural heritage:*

The Vicoforte Sanctuary, the largest elliptical dome in Europe between history and technology".

Using people as a ballast allows, from a technical point of view, to be very flexible with their positioning, to be able to change it and create new configurations immediately and also contemplate the possibility of giving a slight force without the use of machinery such as vibrodine or shaker. From an economic point of view, it avoids the involvement of technicians and the rent or purchase of ballast.

Moreover, placing a ballast even only temporarily would require special permits from the supeintendence, while visits such as that of the college are made periodically on the Sanctuary by visitors of the *magnificat* route (*Santuario Di Vicoforte (Magnificat) - Kalatà!*, 2022) . As a disadvantage of this approach there is undoubtedly the limited mass: in fact, among the students and staff, including the researchers who worked on this project, a maximum of 40 people could be reached. Furthermore, some spaces of the Sanctuary, possible locations of the mass, are narrow or not very easily accessible: in those cases, a body with a specific weight greater than that of a person, would certainly be more effective in exploiting cramped spaces.

It should be noted that varying the frequencies of such a thick and massive structure by adding a mass corresponding to about 40 people was a very ambitious goal even before setting up any analysis. In fact, obtaining an estimate of the total mass of the Sanctuary from its FEM, in which the density of the materials is also calibrated on the basis of experimental data, it is easy to deduce that the additional mass reaches about 0.012% of the total mass of the Sanctuary.

Despite this, the project was still undertaken in order to have an order of magnitude of the number of people to be involved and if reasonable, evaluate to integrate their mass with that of ballast. Furthermore, as will be seen below, the project leads in any case to obtaining useful information on the sensitivity of the sensors, on the most effective sequences of movements, on the optimal periods for obtaining more stable frequency values.

6.2 Static load definition

On the basis of statistics and regulations, a representative "individual" of the group of people involved in the experiment is defined here, in order to identify some of its useful characteristics in the test project. Anthropometric values have been

obtained on the basis of the indications provided by the UNI CEN ISO / TR 7250-2: 2011 standard ("UNI CEN ISO/TR 7250-2:2011," 2011), which reports the study relating to 10 different population samples from as many countries around the world, including Italy, to which reference has been made.

6.2.1 Mass of the individual

This sample consists of 4020 subjects aged between 18 and 65 years and was analysed in the period July 1990 - September 1991.

Considering the average age of a university student, the 18-29 age range was considered. In light of this, based on the information provided in Table 3 in section 4.2 of the aforementioned standard (UNI CEN ISO/TR 7250-2:2011: Table 3, 4.2 - Information on secular change) about the tendency to change anthropometric values within the population for combined effect of secular trend and age, the value of mass is calculated. The mean mass values on a sample is equal to 68 kg (Figure 6. 1) (UNI CEN ISO/TR 7250-2:2011: Table 4, 4.1.1 – Body mass (weight), kg).

Table 4 — Italy — Statistical summary

No.	ISO 7250-1 measurement			Sample size *n*	Mean	SD	P1	P5	P50	P95	P99
		Age	Male	2 011	38	13	19	20	37	60	64
			Female	2 011	36	13	19	19	35	59	64
			Total	4 021	37	13	19	19	36	60	64
1	4.1.1	Body mass (weight), kg	Male	1 974	76	10	54	60	75	93	103
			Female	1 980	60	9	43	48	59	78	88
			Total	3 954	68	12	45	50	67	83	96
2	4.1.2	Stature (body height)	Male	2 011	1 716	69	1 563	1 601	1 714	1 834	1 883
			Female	2 011	1 592	64	1 443	1 490	1 590	1 695	1 757
			Total	4 021	1 654	91	1 463	1 512	1 652	1 806	1 862

Figure 6. 1: extract from Table 4 of the UNI EN ISO/TR 7250-2: 2011

Since this sample considers a population aged 18 to 65, it was decided to apply a variation based on the stature trend by age classes (UNI CEN ISO/TR 7250-2:2011: Table 3, 4.2 - Information on secular change) which intrinsically considers the tendency of change that combines "secular trend" and "aging". Specifically, given that the under-29 age group is approximately 1.75% higher than the sample average for males and females, this same increase was applied to the average mass, implying that mass and height vary proportionally. An average mass value of 69 kg was therefore obtained.

6.2.2 Encumbrance of the individual

In order to define the distance between the points of application of the mass and the maximum number of students that can be placed in each position, the size of a single individual was estimated. The same standard used for the mass was also used to calculate the encumbrance, increasing the values by the same percentage to consider the difference in average height between the class <29 and the whole population. In particular, references for the anthropometric measures come from UNI EN ISO 7250-1:2010 ("UNI EN ISO 7250-1:2010," 2010), while the average values still come from UNI CEN ISO / TR 7250-2, Table 4.

To leave enough space between each individual to move freely, the overall dimensions were calculated on the position shown in Figure 6. 2a. In addition, in order to make the most of the available space, another less spaced configuration of the individual is defined, less comfortable, in which the arms are closer to the body. In this configuration, therefore, only parking is envisaged, without carrying out any movement. Its measures are also defined in Figure 6. 2b. All the average measurements of each part of the body increased by the aforementioned percentage have been added up, obtaining the values reported in Figure 6. 2 and based on these, each individual is schematized as the ellipse that circumscribes its shape.

These measurements will define the number of people occupying the chosen positions, their distance, jump points and station points.

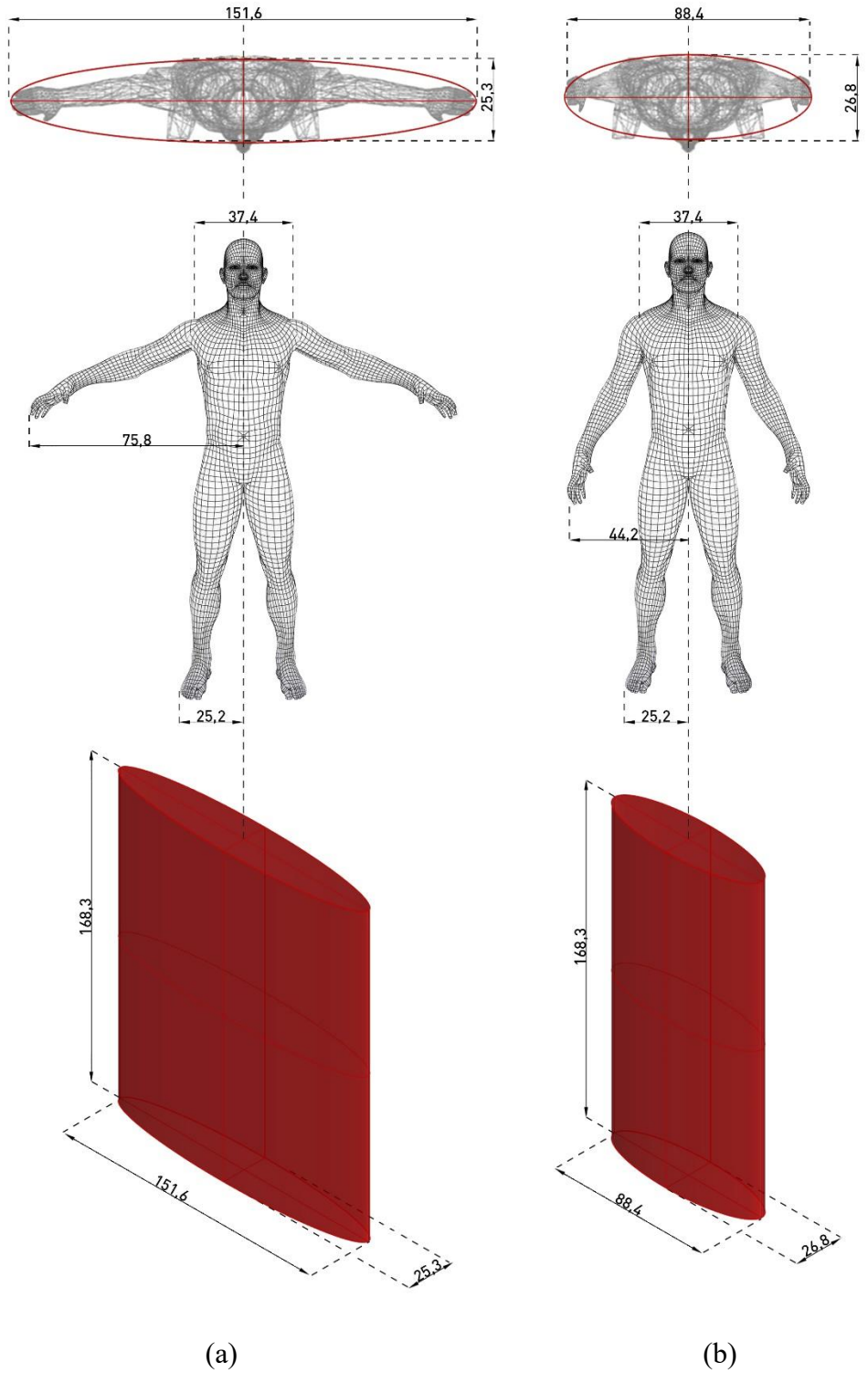

(a) (b)

Figure 6. 2: anthropometric measures for the considered sample and space of occupation for normal (in which the jump is allowed) (a) the less comfortable configuration (b)

6.3 Locations

The drum-dome-lantern system of the Vicoforte Sanctuary is characterized by two planes of almost perfect symmetry, orthogonal to each other. For the purposes of the study of the structure, a reference system was therefore defined whose X and Y axes run respectively along the direction of the major and minor axis of the base oval of the dome, the same used in the FE software. The vertical direction, marked as the Z axis, is therefore out of the plane of the sheet in Figure 6. 3. The origin of the reference system is positioned so that each point of the structure is characterized by coordinates with a positive sign.

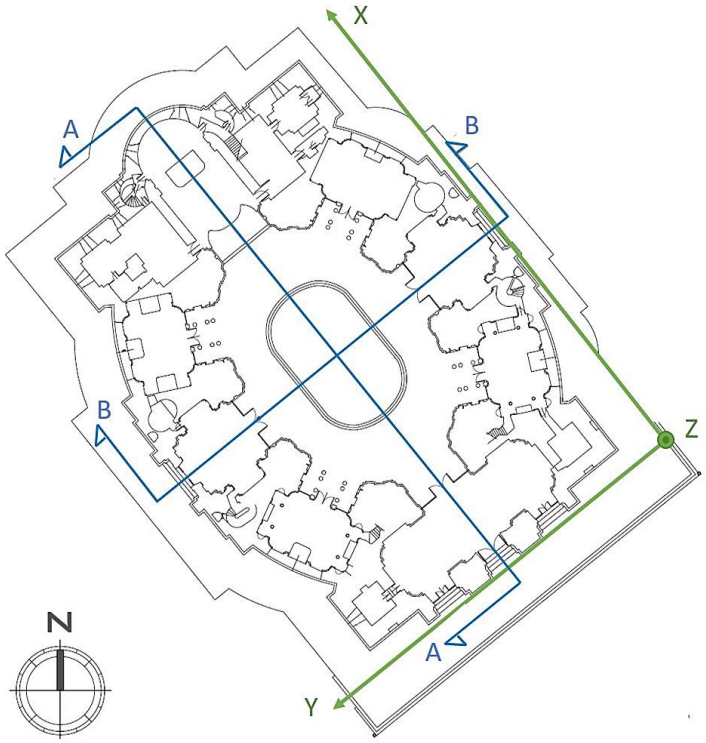

Figure 6. 3: plan of the Sanctuary and sections considered (A-A, B-B)

Two main sections have therefore been identified, along which to conduct the analysis.

- **Section A-A** develops along the major axis of the oval; it is a lightly (from a structural point of view) asymmetrical section with respect to the vertical axis passing through the center of the oval at the base of the

dome, characterized on one side by the presence of the apse and on the other by the main entrance to the Sanctuary.

- **Section B-B** develops along the minor axis of the oval; even this section turns out to be (slightly) asymmetrical with respect to the vertical axis of the oval base of the dome due to the different inclination of the cover on the North-East and South-West sides of the structure.

The positions chosen and shown below are briefly described and listed in ascending order with reference to their height. They are represented in Figure 6. 4 and Figure 6. 5.

LOCATION 1: This is the lowest position among those identified, at an altitude of about 5.80 m from the ground level. It is located about half the height of the main buttresses and corresponds to the point where the colonnades support the balconies.

LOCATION 2: It is located at the level of the impost of the arches that connect the buttresses; this is the most external position in plan with respect to the center of the oval of the dome.

LOCATION 3: Position at an altitude of about 19.50 m; this is the height at which the basement of the Sanctuary ends and the development of the drum begins. It represents a point of marked structural importance, in which the vertical bending stiffness along the two main directions varies significantly.

LOCATION 4: This is the height of the top of the drum, located approximately 31m high. The modern strengthening system (1987) made up of 4 levels of post-tensioned dywidag bars is installed at this height. Moreover, various sensors are also installed at that height, which are part of both static and dynamic monitoring systems.

LOCATION 5: At this height the dome is divided between the internal structural part and the copper roof that can be seen from the outside. It is approximately 42 m; here the geometry of the section is particular as there is a change in curvature that creates a small, almost horizontal plane over the extrados of the masonry layer.

LOCATION 6: It is located about halfway between position 5 and the highest point of the dome, where the lantern is inserted, at an altitude of about 46 m. Here

a horizontal plane, on one of the sections, is obtained thanks to a staircase leading to the lantern.

LOCATION 7: Altitude of the base of the lantern, at about 50 m. It is a structurally important position as it is the highest point of the dome and the point of contact between two different structural elements.

LOCATION 8: Is the height at which the internal and external balcony of the lantern is located. They are at about 53 m.

LOCATION 9: It is the highest point considered, at an altitude of about 60 m. geometrically it corresponds to the impost of the small dome of the lantern.

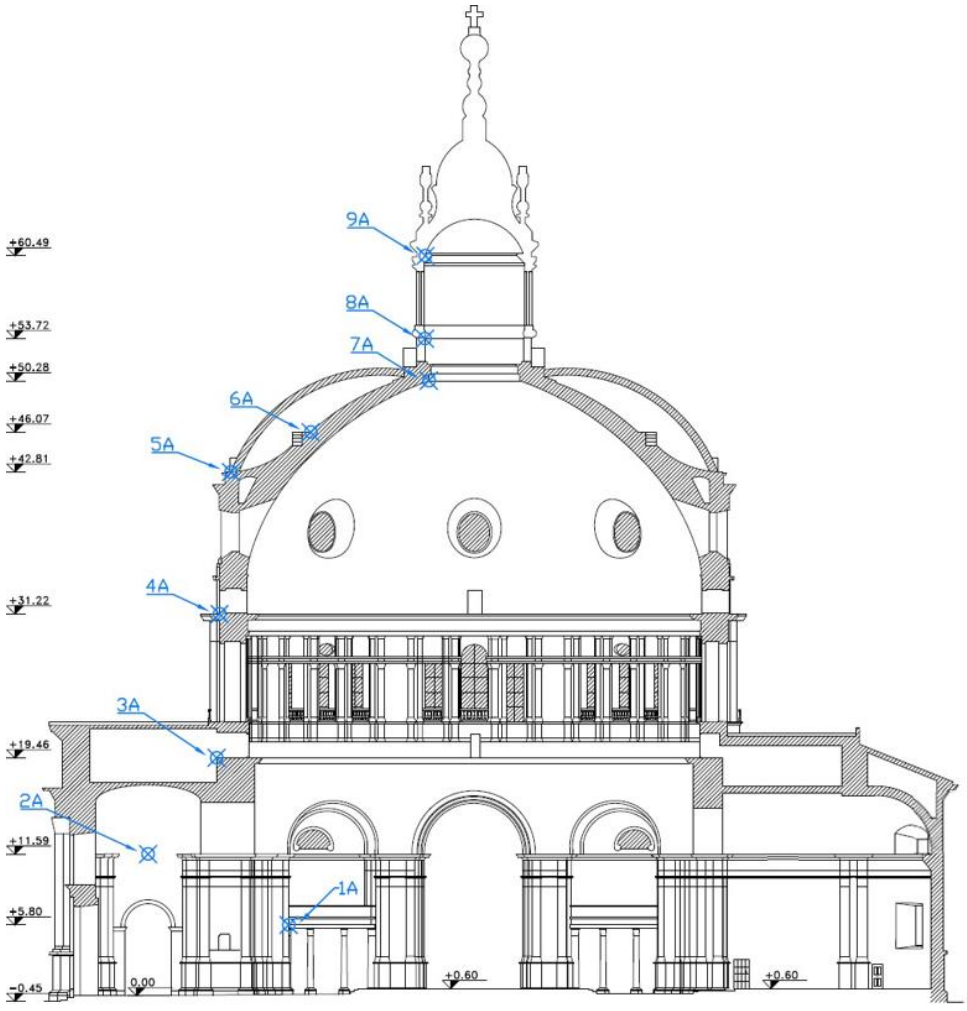

Figure 6. 4: longitundinal section A-A, parallel to X axes, and locations

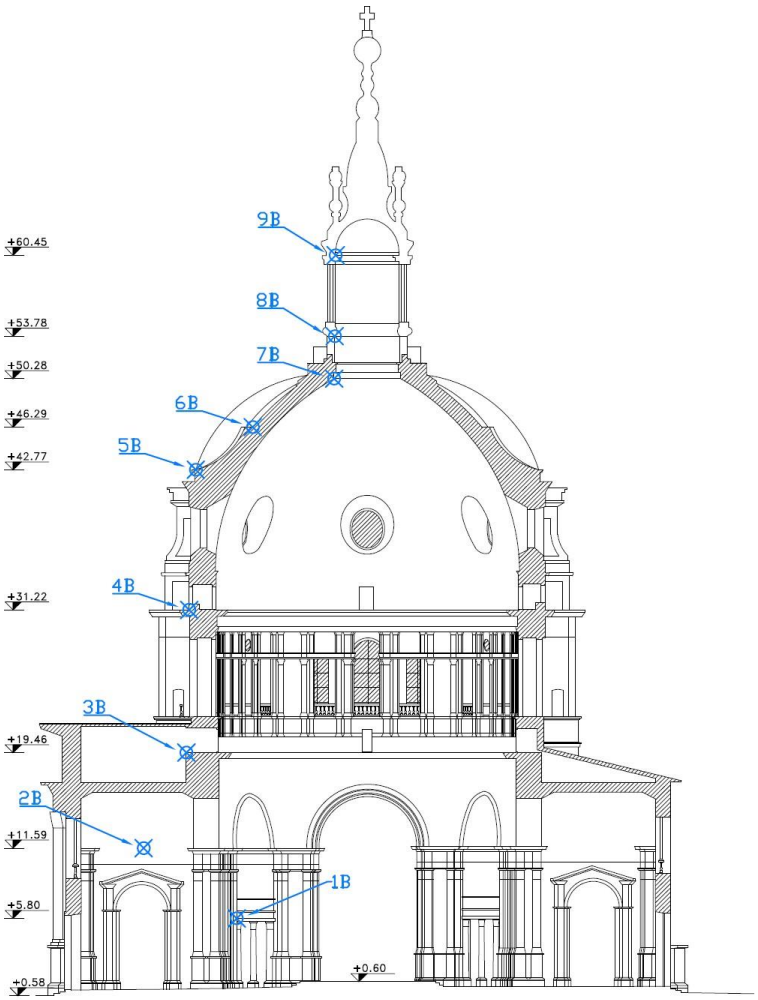

Figure 6. 5: transversal section B-B, parallel to Y axes, and locations

As anticipated, the FEM of the structure is used to perform the analyses, the same model described in chapter 4 and 5. The model by its nature is based on a compromise between accuracy and the required computational burden, optimizing the number of elements used for the discretization. In fact, aiming above all at global structural analysis of the structure, this model leaves out the geometric details of lesser interest for the global dynamics.

6.3.1 Location Sensitivity analysis

In this phase, the sensitivity of each position was explored, loading them one at a time with increasing mass values. Since the aim was to identify trends with respect

to load height and eccentricity, even unrealistic masses were considered and the encumbrance of individuals neglected in this phase.

For each position and number of added people, an eigen-analysis was solved obtaining the frequency values corresponding to the loaded model. They were compared with the frequency values of the unloaded model (shown in Table 6. 1), obtaining a percentage of variation defined as:

$$\Delta f_i = \frac{f_{i,unl} - f_{i,load}}{f_{i,unl}} \cdot 100\,. \tag{6. 2}$$

Table 6. 1: original numerical frequency values (unloaded FEM)

	f_1 (Hz)	f_2 (Hz)	f_4(Hz)	f_5 (Hz)
$f_{i,unl}$	1,93	2,11	3,89	4,18
Mode features	1st bending in Y	1st bending in X	2nd bending in Y	2nd bending in X

This was done for the bending frequencies, that is f_1, f_2, f_4 and f_5, which are numerically more stable, easier to excite than the torsional ones, and, especially the first 2, more easily identifiable (they show a higher percentage of identification (Pecorelli et al., 2020)). The results are reported in the form of graphs. Having repeated the same process for each position and section, for the sake of brevity only the most significant graphs are shown, followed by related comments.

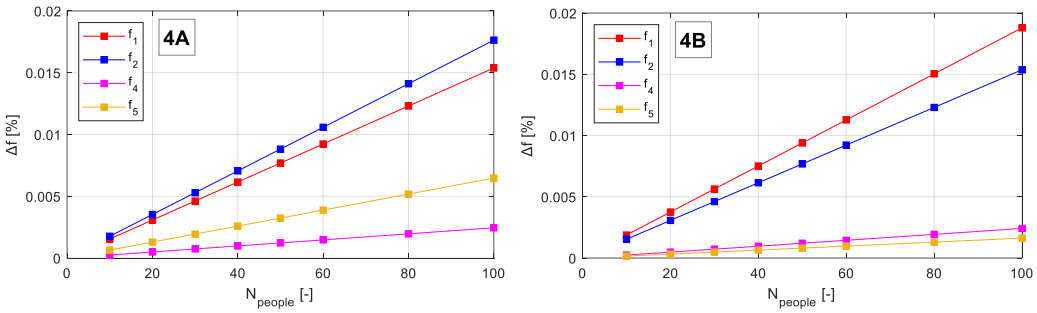

Figure 6. 6: frequency variation related to the number of people placed in location 4, in both sections, A and B

The graphs related to the position 4, in the two sections have the same general trend but inverted: the first 2 frequencies show higher variations with respect to the higher ones and while loading section A, the greatest variation is found in the modes in X direction (2 and 5), loading 4B, there are major variations on the modes in Y (1 and 4).

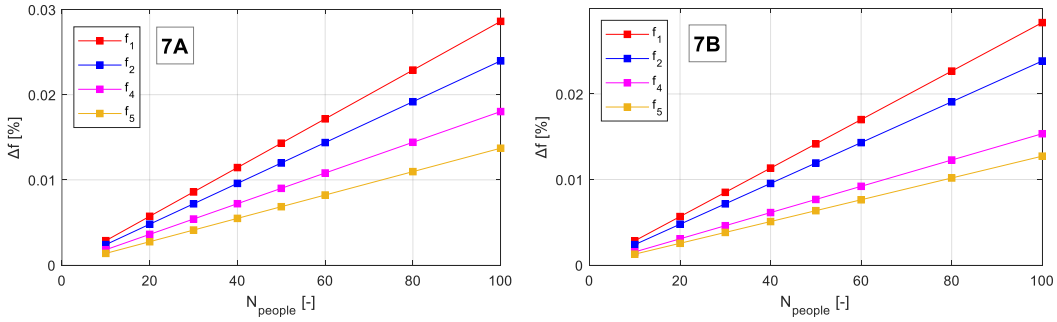

Figure 6. 7: frequency variation related to the number of people placed in location 7, in both sections, A and B

Analysing the positions at higher locations, such as 7 shown here, it is observed that the order of the frequencies from the most to the least sensitive remains unchanged even if the loaded section is changed. The same comment remains valid for all locations higher than 5th except the 9th, the highest. In the 9th location a greater variation in the higher frequency modes is noticeable (Figure 6. 8) while the order between modes in X and Y remains unchanged: the modes in Y, direction with lower inertia, are increasingly sensitive to the addition of mass of the corresponding ones in X. The locations 9A and 9B are so close in plan that the results are practically coincident.

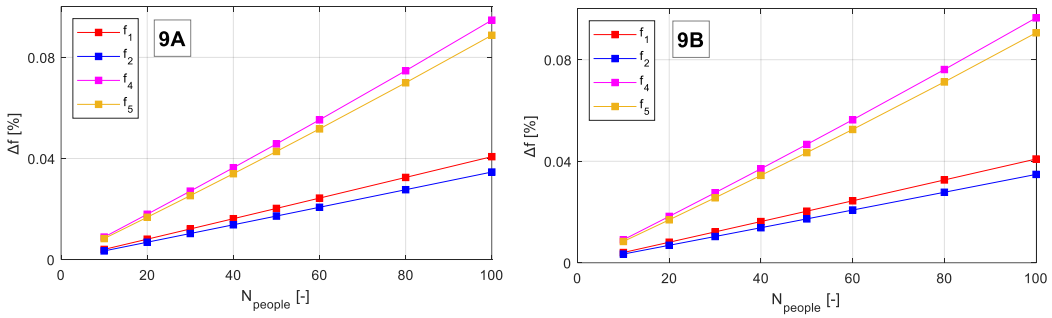

Figure 6. 8: frequency variation related to the number of people placed in location 9, in both sections, A and B

Looking at all the results of the analyses, the following information can be extracted which will serve as guidelines for defining the final configuration:

I. in general, the first two modes are always the ones that show the greatest variation in frequency;
II. for a fixed location, variations increase with increasing load;

III. for a fixed load, the variations increase with increasing height of location;

IV. the variations referring to a realistic number of people are very limited, practically imperceptible. As an example, by loading the location 7, the frequency of the first mode undergoes a variation of just over 0,01%, corresponds to less than one thousandth of a Hz.

The following diagram (Figure 6. 9) shows a summary of the results obtained, with reference to the placement of 40 people on the Sanctuary, in each location; it has the purpose of highlighting the differences in an easily readable figure: for the frequency variation values refer to the previous graphs.

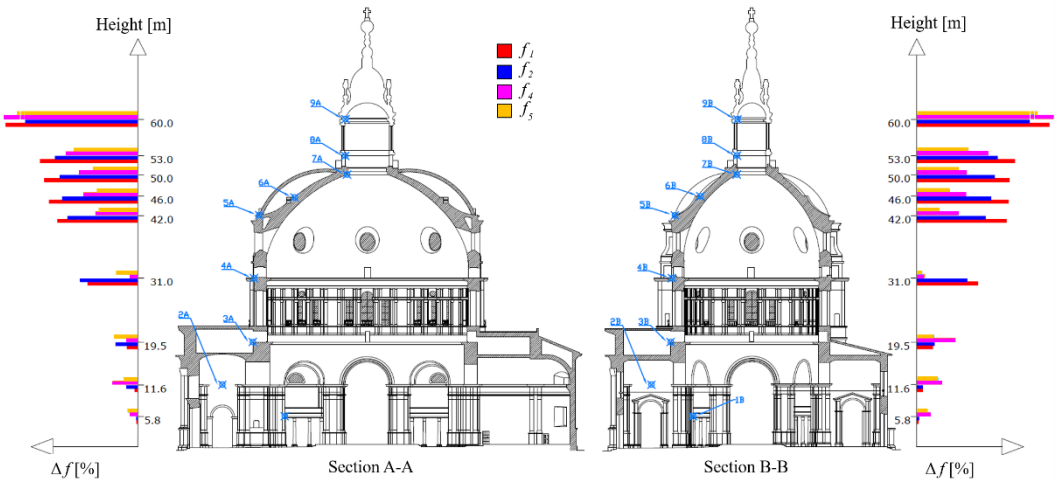

Figure 6. 9: comparison of the variation in frequency generated by the addition of the mass of 40 people in different locations

6.3.2 Actual eligible locations

In order to verify their employability, size and any logistical constraints, the locations described and explored in the previous analysis were the subject of an inspection on 21/05/21. Here some photographs taken on that occasion are reported and some aspects considered significant are highlighted. The lower positions, given the less influence they can get on dynamics, have been neglected. Starting from location 4 the paragraph proceeds towards the higher locations.

At an altitude of 31 m, which characterizes location 4, two horizontal surfaces can be occupied: the interior and the exterior. The external is made up of several masonry and metal balconies (depending on the side). The latter, rest on the structure through punctual supports (Figure 6. 10a). All these balconies are

potentially accessible, even if access to some, due to poor security measures, is not suitable for the safe passage of a group of people; it would need to be secured before the experiment (Figure 6. 10c).

(a) (b) (c)

Figure 6. 10: external balconies in location 4: metal (South side) (a) and masonry (West side) (b). Dangerous access to the West balcony (c)

At the same height, there is the internal balcony which offers the best view on the inside of the dome, and in fact it is an essential stop for those who visit the Sanctuary. It is accessible without particular difficulty along the entire internal perimeter of the drum; the only problems could concern the narrowness of the surface, partly occupied by the cables of the monitoring systems and the height of the railing (barely 100 cm) (Figure 6. 11).

(a) (b) (c)

Figure 6. 11: internal balcony in location 4 walked by visitors (a), detail of the usable area (b) and the railing one meter high (c)

Proceeding upwards is location 5, practically between the structure of the dome and its external cover. Here the usable space is larger but not all sides of the basilica are passable: some are cordoned off due to the presence of bats and poor hygienic conditions. The main issue of this location (and the higher) is its accessibility: people are harnessed and have to climb a steep ladder (Figure 6. 12).

(a) (b)

Figure 6. 12: location 5 and a detail of the steep ladder

Position 6 is located a little higher, approximately in the middle of the arch of the dome. Here a not too wide horizontal plane is offered by the plane of the staircase leading to the lantern (Figure 6. 13).

Figure 6. 13: location 6: the ramp and stairs leading to the lantern

Positions 7 and 8, which on the geometric model could seem distinct, in reality can be traced back to a single horizontal plane, that is the plane of the base of the lantern which offers an external and internal surface. The outer part can be walked on along the entire perimeter of the element while the inner part is only about ¾ (Figure 6. 14).

(a) (b)

Figure 6. 14: locations 7-8, the base of the lantern: external (a) and internal space (b)

Location 9 is not reachable except by suitable means. Therefore, it will not be considered for the experiment.

6.4 Dynamic Load definition

As highlighted in previous chapters, where the temporal trend of the frequencies identified experimentally was shown, not always in ordinary operating conditions and with the available environmental stress it is possible to sufficiently excite all the frequencies of interest of the structure. In fact, in Operational Modal Analysis (OMA) as the continuous monitoring of the Sanctuary is considered, the modal properties of a structure are identified based on vibration signals collected when the structure is under its normal operating conditions and no initial excitation or known artificial excitation are applied. In these situations, the vibrations of the structures are randomly generated by wind, precipitation, terrestrial vibrations, vehicular traffic, etc. Since the intensity of the combination of these phenomena is unpredictable, it could unfortunately happen that on the day of the experiment it is

particularly low so as not to make the frequencies of interest identifiable, making the test useless. Regarding this issue, several analyses had been made (Pecorelli et al., 2020) specifically for the Sanctuary to identify the hours of greatest excitement of the day, in order to optimize the identification process. This resulted in the exclusion of the evening and night hours (19:00 - 06:00), which had a lower percentage of successful identifications, most likely due to the lower intensity of traffic. The daytime hours are characterized by several successful identifications, but it may still happen that particular conditions are created which amplify the structural modes too little, making them imperceptible. Therefore, to remedy the possible low excitation, it was decided to exploit the ability of the students to impart a light force to the structure through their movement. The force that can be generated by an individual has been numerically reconstructed, so that it can be included in the simulations and optimize its effect.

6.4.1 Jumping

The anthropogenic forcing has been modeled by taking reference (McDonald et al., 2017). This is a study that addresses in detail the problems that arise in the process of modeling a forcing generated by human, a source which is by its nature very aleatory. The article focuses, in particular, on vertical movements performed using the *jumping* technique. This action is characterized by a cycle consisting of a "contact phase" and a "flight" phase.

In general, jumping can be performed by a human being at frequencies contained in the 1Hz-4Hz range (Pernica, 1990; Rainer et al., 1988). In order to amplify the response of the structure, it was thought to apply a forcing at a frequency close to the natural ones of the structure, benefiting from the effects of the resonance phenomenon; therefore, the first two bending frequencies of the Sanctuary of Vicoforte have been considered, since the second two are very close to or even higher than the maximum jump frequency that can be easily performed by human. Jumping allows for the generation of amplified forcing with respect to the weight of the person performing the jump, with increase factors in the range 2.0-4.5 (Sim et al., 2005), however this aspect has not been exploited. The forcing was used only to increase the vibration of the Sanctuary to make the frequencies more easily identifiable and not to increase the effect of the mass, as this would occur only in the moment of landing, a time too short to extract the modal parameters related to that condition.

The parameters necessary to uniquely describe the stress due to jumping are:

- the period T,
- the contact ratio time CR,
- the peak force F.

CR is the portion of the cycle in which there is contact between the person and the stressed structure. By normalizing the peak force F with respect to the weight (W) of the person who, by jumping, generates the stress, the parameter A is defined as:

$$A = \frac{F}{W}. \tag{6. 3}$$

The first two numerical frequencies of the Sanctuary, just like the experimental ones, are very close, $f_1 = 1{,}93\ Hz$ and $f_2 = 2{,}11\ Hz$. Then, to maximize the amplification of the structural response, two different periods should be contemplated corresponding to the inverse of the natural frequencies of the system, that is $T_1 = 0{,}52\ s$ and $T_2 = 0{,}57\ s$.

Numerically, two forcing with the aforementioned periods can be modeled without particular effort, but in reality, these two would be practically indistinguishable, as delays or advances are inevitably created in the jump even using a dynamometer to synchronize the movements of students.

For this reason, it was decided to model a single forcing with intermediate parameters, $f = 2\ Hz$ and period $T = 0.5\ s$.

To determine the amplitude, reference was again made to study (McDonald et al., 2017), in which the jump of 8 volunteers, male and female of different stature and weights, was recorded and analysed (Figure 6. 15a). An average curve was obtained from the points of the frequency-amplitude graph and from this, entering with the frequency of 2 Hz, an amplification factor equal to 3.25 was obtained. The CR is a very important parameter for the severity of the dynamic action: the lower its value, the sharper the shape of the forcing. The average curve was considered also for this parameter and the value corresponding to 2 Hz was extracted (Figure 6. 15b), i.e. CR = 0.58.

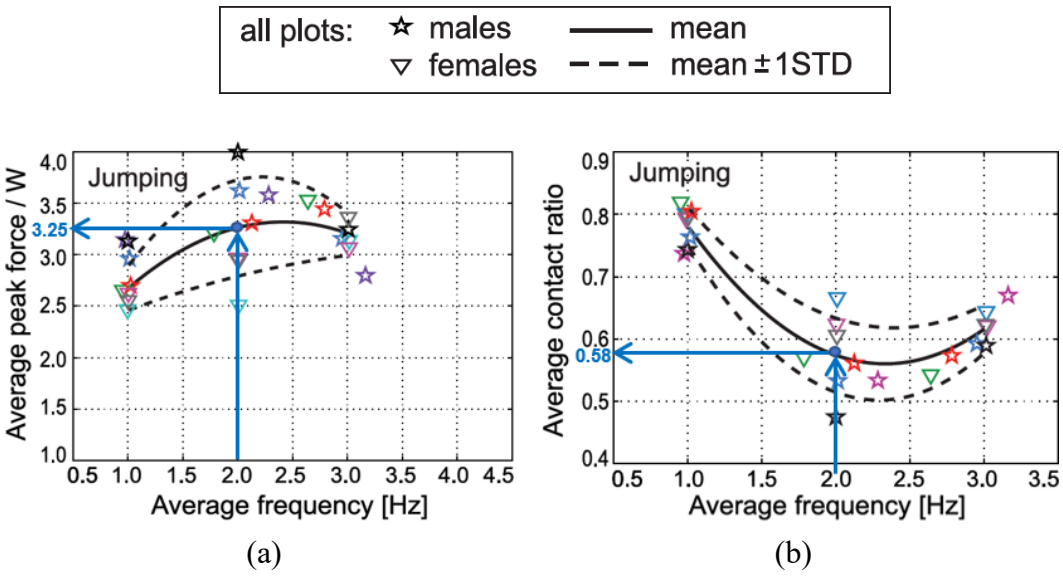

(a) (b)

Figure 6. 15: normalized average peak force (A) (a) and average contact ratio (CR) (b) as functions of the average frequency of jumping (McDonald et al., 2017)

Summing up, the parameters useful for modeling the anthropic forcing are reported in Table 6. 2.

Table 6. 2: anthropic forcing parameters

A (-)	CR (-)	f (Hz)	T (s)
3,25	0,58	2	0,5

6.4.2 Jump position optimization

Some simulations were carried out by applying the forcing, modeled with a sen^2 function, in some positions of the structure. In particular, they had the purpose of defining the most convenient positions for the application of the forcing, that is, they would generate a greater dynamic response of the Sanctuary. The evaluation took place through the analysis of the acceleration signals collected in precise coordinates of the Sanctuary, where the accelerometers of the monitoring system are installed (Figure 6. 16 and Figure 3. 4)

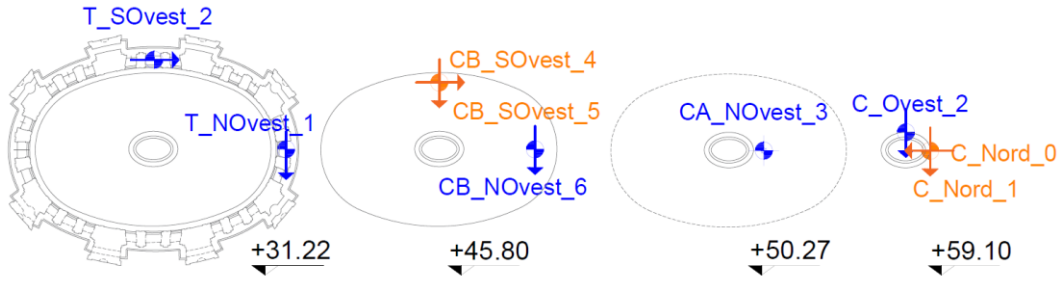

Figure 6. 16: layout of accelerometers in plan

In this way, the positions that would generate the greatest structural response read by the accelerometers were selected. The comparison was made in terms of accumulated energy, around the first two natural frequencies of the system. These will constitute just a guideline for the choice of the definitive jumping positions as in the final decision other elements will intervene, such as limitations related to safety, the protection of valuable elements, the practicability of the position, etc.

The forcing corresponding to the movement of 40 people is applied, for a duration of 5 minutes, separately in all the positions of greatest interest for the experiment, that are from the 4th to 8th (Figure 6. 17) which cause the greatest variations in frequency if loaded by mass (see paragraph 6.3).

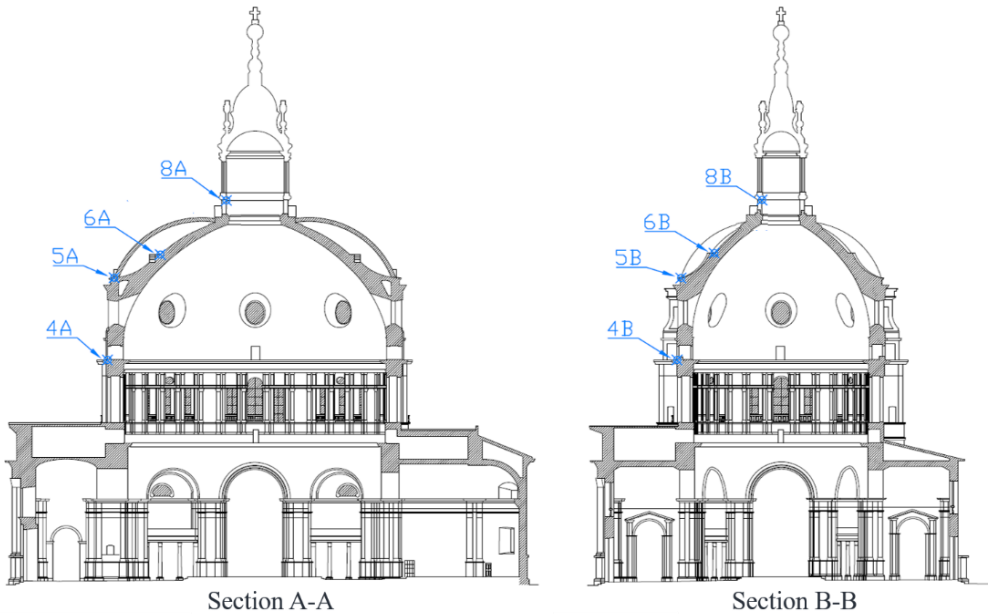

Figure 6. 17: more convenient locations for the static application of the mass, according to static analyses and employability

It should be highlighted once again that this is still an analysis under ideal conditions: each identified position represents a single physical point of the real structure in which undoubtedly the dynamic action produced by the jump of 40 individuals cannot be enforced at the same time, and it is also unlikely that an individual would be able to jump continuously for 5 minutes. Operationally, for each position of forcing application (discretized on the basis of the sampling time of the sensors) 9 signals of the structural response were obtained in the points where the accelerometers are installed, neglecting the triad at the base because it is minimally affected by the effects of the forcing. The Fourier transform was calculated for each like-accelerometric signal and the energy accumulated between 1,5 and 2,5 Hz, a range that includes the first two natural frequencies of the system, was calculated as:

$$E = \int_{1,5}^{2,5} |A(f)|^2 \, df \tag{6. 4}$$

The calculated energy is influenced by the resolution frequency used for the analysis, which is equal to the inverse of the signal length, which is remembered to be 5 min. The use of a longer signal would have led to more accurate peak values but with a greater computational burden. Given that an absolute value is not the objective of this analysis and that this approach involves all the cases investigated, the results of the comparisons are still significant. For a better visualization of the results, the graph in Figure 6. 18 reports a histogram showing the jump positions characterized by the greatest influence on the response of the structure (which maximize the read in the coordinates of the accelerometers) and the energy contribution for each sensor, implicitly showing which is most sensitive to the application of force in a given position.

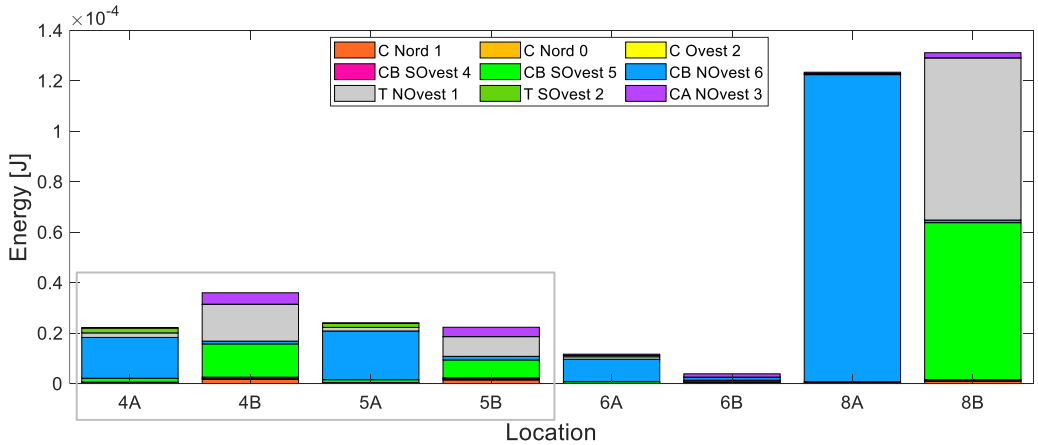

Figure 6. 18: energy virtually recorded by accelerometers for each jumping position

It would seem that location in 8 is the most convenient for positioning students to jump. However, it must be pointed out that the greatest contributions, out of scale with respect to the others, are given by the closest accelerometers and which are therefore affected by the local effect of the force application. Therefore, a zoom that allows a better visualization of the higher energy positions is shown in Figure 6. 19.

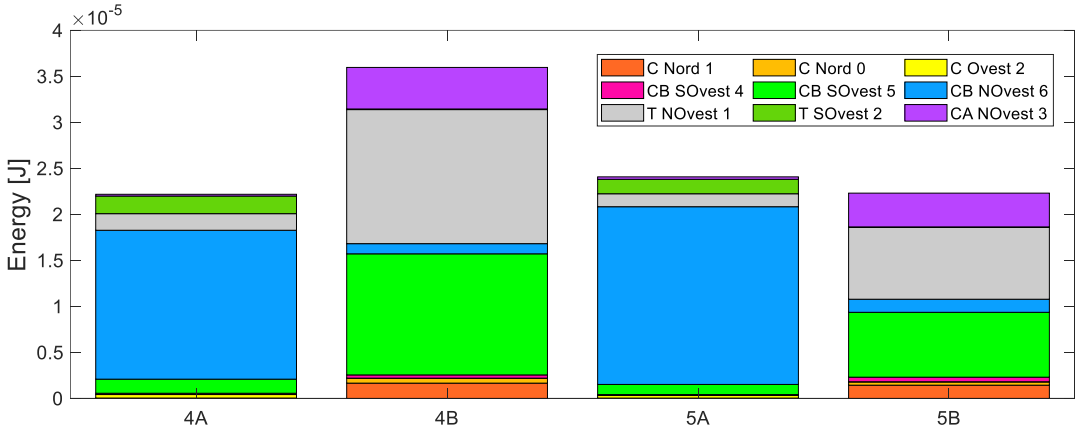

Figure 6. 19: energy virtually recorded by accelerometers for location 4 and 5 (zoom of graph in Figure 6. 18)

Focusing on positions 4 and 5, it can be observed that the highest altitudes are always recorded by accelerometers that measure in the direction of the minor axis of the dome, which has lower inertia: the accelerometers TN_Ovest_1, CB_NOvest_6 and CB_SOvest_6 are the most sensitive to the application of anthropogenic stress. Accelerometers directed parallel to the long section appear to suffer very little from the excitation. The vertical accelerometer CA_NOvest_3, on the other hand, seems to discreetly perceive the force when it is applied in the A-A section, much less in the orthogonal direction. Based on these observations, some recordings of the experiment day will be considered more relevant than others in the dynamic identification phase, in which environmental stresses will also intervene.

6.5 Choice of the period and of the optimal environmental conditions

As highlighted several times in this document, it is now known that environmental and operational conditions affect the dynamic parameters of a structure. In the case of the Sanctuary, for example, there are annual variations that reach almost 6% of

the minimum value identified for the first mode and about 7% for the second mode. These high variations refer to data collected from 2018 to 2020, thus encompassing entire seasonal cycles that were brought to light in previous chapters. Obviously, in a single day, the variation is significantly lower but still high enough to compensate for the variation due to the addition of mass, which is very limited as seen in paragraph 6.3.1.

Therefore, here we faced the question of understanding which was the period, or the environmental conditions, most suitable for carrying out the experiment, that is the one characterized by greater stability in the identified frequency values that would allow to notice the reduction due to the load of students. It was decided to divide the research into two phases: in the first, the historical series of frequencies were analysed, gross of all the phenomena that could affect, in the not entirely realistic hypothesis, that these are almost repeatable over the years (increased traffic at certain times of the year, concentration of precipitation in certain seasons, greater daily temperature variations, more intense program of visits at certain religious events, etc.); in a second phase, the time series were compared with the environmental ones, similarly to how it was done in chapter 3, but this time with the intention of understanding whether, statistically, a lower / greater variability corresponds to certain environmental episodes.

6.5.1 Selection of the period with low frequency variability

In this analysis, the time series of frequencies from 2018 to 2020 were statistically analysed in order to find the periods with the lowest variability. This does not necessarily mean that in the year in which the experiment will be rescheduled this trend will be repeated, due to the unpredictability of operational and climatic events, but it helps to outline a pattern on those conditions that repeat themselves, approximately in the same period, every year. For example, particular operating conditions dictated by a greater flow of tourists in the summer or linked to the greater use of the Sanctuary in conjunction with periods of a strong religious character, periods characterized by more or less intense rainfall, etc. It should be noted that the choice of meteorological conditions will be based on the subsequent analysis, but in this phase, periods could be highlighted in which, e.g., precipitation does not act directly but its effects affect the dynamics of the structure indirectly: the humidity conditions of the soil or of the structure itself that absorbs water are considered indirect effects. The graphs in Figure 6. 20, Figure 6. 21 show, for each of the 52 weeks of the year, the distributions of frequency data for the three-year period 2018-2020.

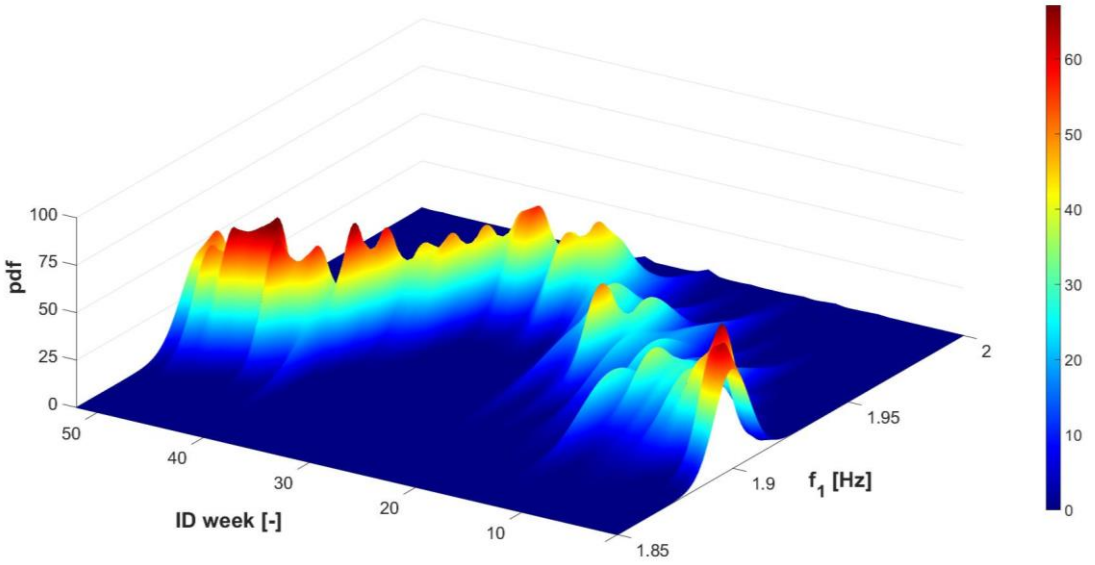

Figure 6. 20: juxtaposition of the weekly probability density functions of historical data (2018-20) of f_1

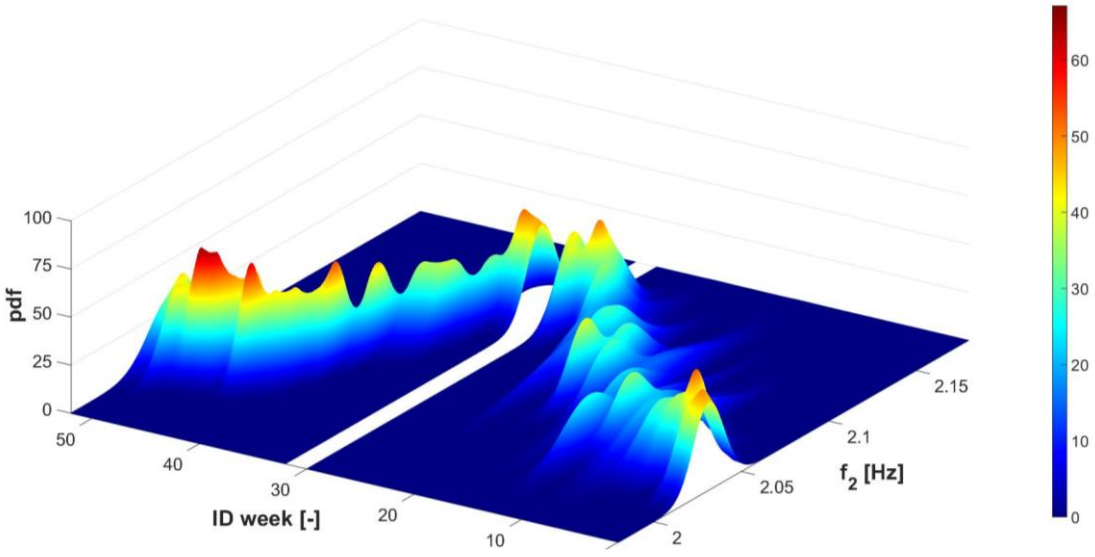

Figure 6. 21: juxtaposition of the weekly probability density functions of historical data (2018-20) of f_2. The blank is due to the limited availability of f_2 data identified during the weeks 31-32, considered not sufficient to build a reliable statistic

The periods in which there are more sharp distributions, and therefore less dispersion, are the first and last weeks of the year, and those around the 30th. These correspond to the periods in the height of the hot and cold season, excluding the

transition seasons, i.e. autumn and spring, in which the dispersion is evidently greater. Undoubtedly, using 3-year data could lead to greater dispersion in the event that the years showed a high difference between them: by merging 3 years, a large variance results notwithstanding no high variances occurred within the single week of the specific year. However, the purpose of this analysis is to choose a period of the year *a priori* and to make a statistic on different years of measurement leads to a more robust choice, less conditioned by events that characterized the individual year.

6.5.2 Selection of optimal environmental conditions

After analysing the frequency trend alone, the search for a trend or link between the dispersion of its value and some environmental conditions followed. In chapter 3 the relationship between environmental variables and dynamic parameters from the point of view of their value was evaluated. Here instead, it is evaluated how these can influence their dispersion, so attention will be paid to the color of the last graph in Figure 6. 22, which is the union of Figure 6. 20 and Figure 6. 21 but seen "in plan".

As it is reasonable to expect from the previous results, the sharpest curves correspond to the stationary points of the temperature cycle, i.e. when it reaches its annual maximum and minimum. Given that temperature was found to be among the most influential factors, it is reasonable that when its trend is changing its slope and therefore stays on the same values for a longer time, the value of the frequencies settles. As for the other phenomena, it seems that these periods also correspond to low rainfall, for example in the case of the first weeks of the year and the 32-34^{ths}. However, in those close to the 50th, although the average rainfall is not as scarce as the aforementioned periods, these have not influenced the sharpness of the frequency curves. The other environmental factors, humidity and thermal excursion, seem not to have a particular link with the variability of frequencies.

Downstream of this, it seems that the most convenient times to carry out the experiment are the month of January, the central weeks of August and the months of November and December, possibly on days without heavy rainfall.

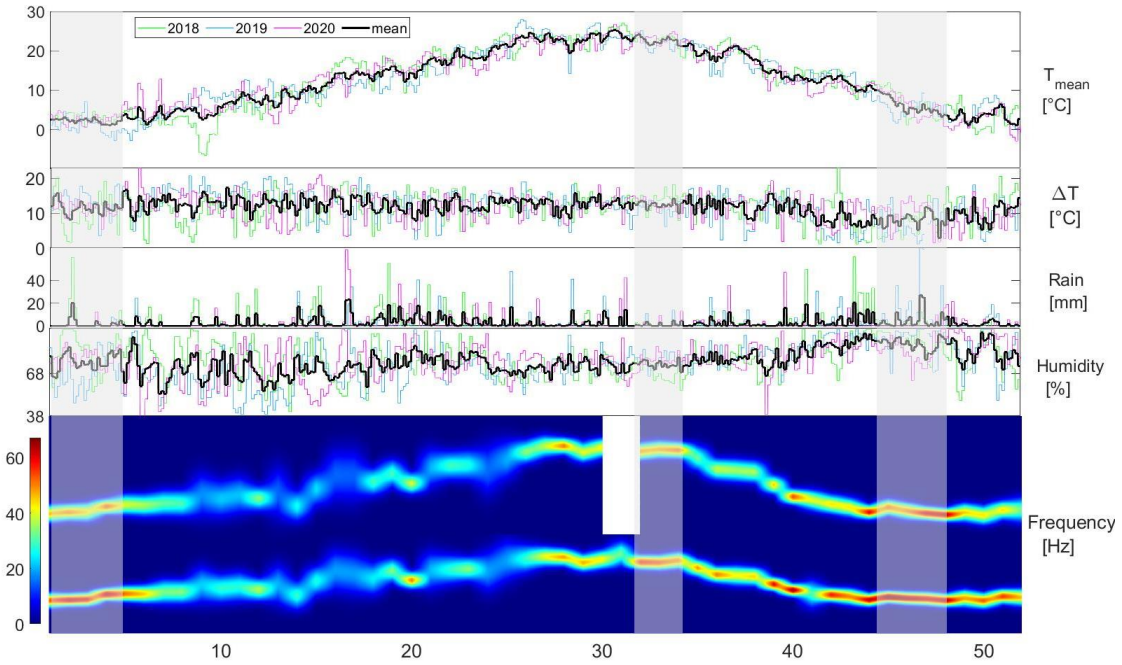

Figure 6. 22: annual data (2018-2020) superimposed (from top to bottom): temperature, daily excursion, rain, humidity. At the bottom: colormap of the weekly probability density functions of historical data (2018-20) of f_1 and f_2

6.6 Test FE simulations

After building a basis for defining the answers to the questions posed in the introduction of this chapter (*why*, *who, where, how* and *when*), some simulations of the test were carried out on the FEM. In particular, realistic configurations of the group of students have been defined, which respect the spaces they occupy in relation to that actually available in those parts of the Sanctuary.

Specifically, 3 particularly interesting configurations were simulated: the first with the aim of maximizing the obtainable frequency variation, which therefore follows the guidelines drawn from the analysis in 6.3 as a priority. The second maximizes the response acceleration of the system, which therefore focuses more on the conclusions of the dynamic analyses. The third, a little different from the previous ones, explores a logistically simpler configuration than the others: the students would in fact be positioned along the path travelled daily by visitors, the ascent to the dome called *Magnificat*. This would be the logistically and economically most convenient solution, as the spaces in question would already be in hygienic and safety conditions suitable for hosting people. Their layout is reported in Figure 6. 23.

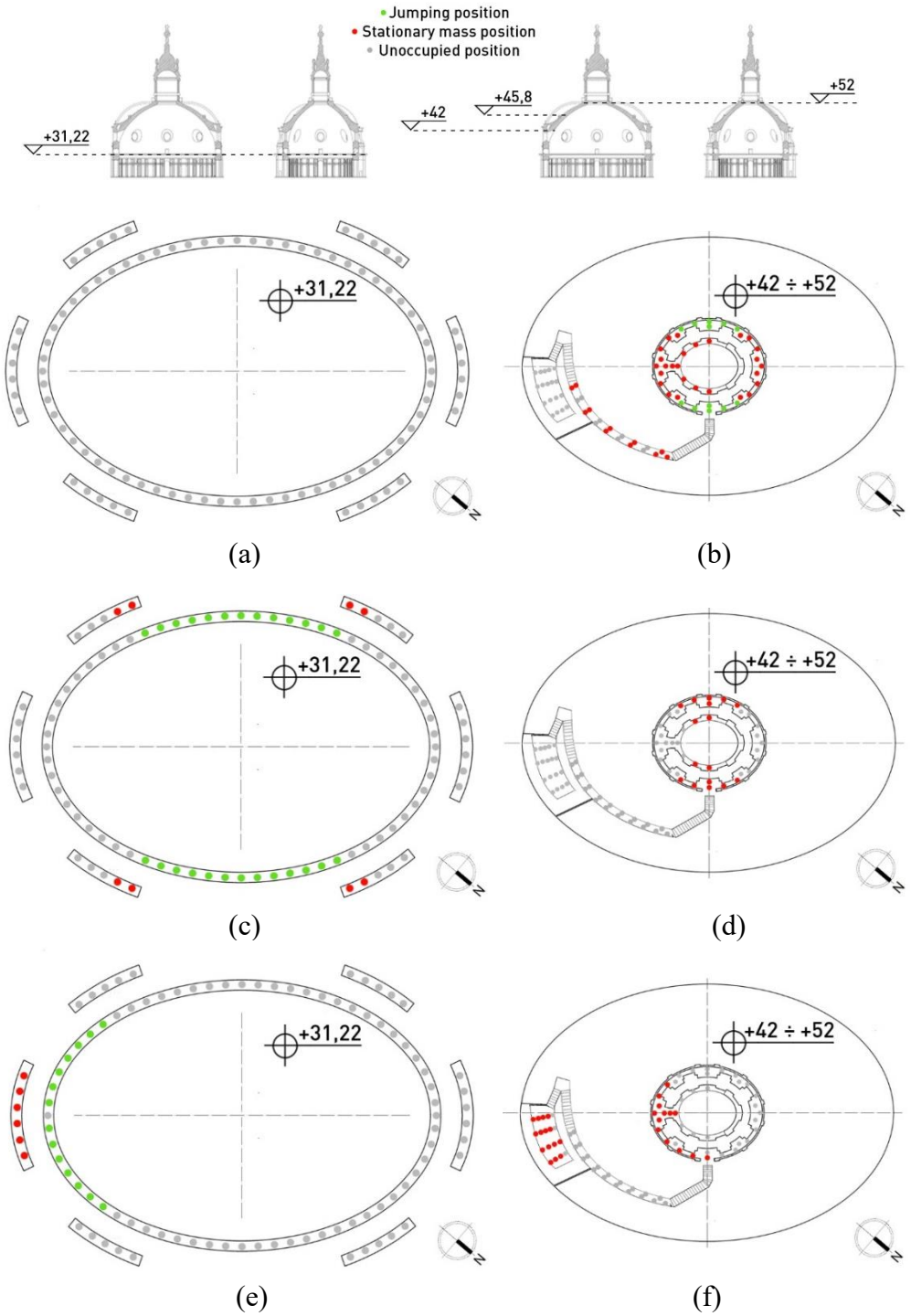

Figure 6. 23: three load configurations: 1st maximizes the frequency variation (a,b), 2nd maximizes the response acceleration (c,d), 3rd follows the *Magnificat* path (e,f)

In these simulations, some precautions have been added to make the result more realistic. The total load is no longer concentrated in one point, but each highlighted position in the layouts in Figure 6. 23 has been loaded with the mass of an individual. In the positions where jumping is expected, a forcing has been applied which takes into account the "not ideality" of the source. Specifically, a 5-minute forcing was modeled, in which 30 s of jump and 30 s of rest alternate, being a reasonable time for which a young person, on average trained, can jump. Furthermore, since it is unlikely that the jump parameters will be maintained all the time, a coefficient of variation was applied, extracted from a normal distribution with mean 1 and variance 3.7. The latter has been applied exclusively to the parameter T, since, accordingly to (McDonald et al., 2017), it is the factor that gives the greatest difference in the response between an ideal condition with constant T and the result of an experiment with inevitably variable T.

For each configuration, the frequency variation and the energy perceived by the 9 accelerometers were calculated. The first is calculated considering the mass of all 40 individuals, since, although in some positions the jump is expected and therefore for some time the mass does not act on the structure, it is expected to use the signal immediately following the 5 minutes of the forcing for the identification phase. It can be seen as a sort of free decay to which environmental noise is added, in which all individuals rest on the structure. The results are summarized and compared in the graphs in Figure 6. 24 .

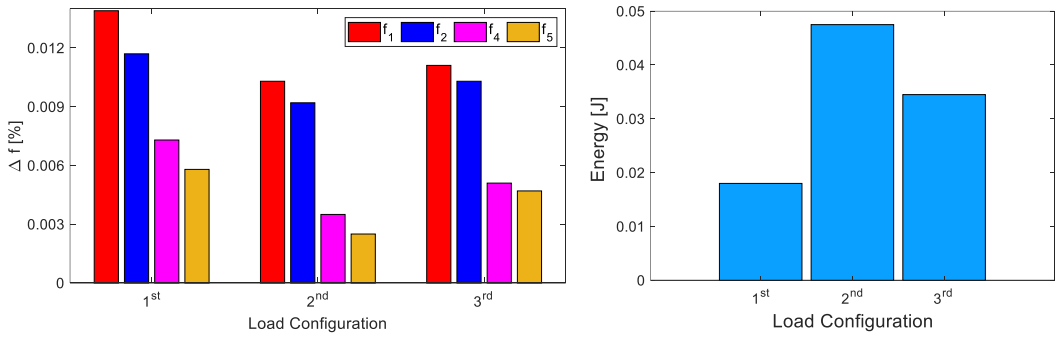

(a) (b)

Figure 6. 24: comparison of variation in frequency (a) and energy perceived by the system (b) between the three designed configurations

Indeed, the hypothesized configurations respect the intended objectives: the first is the one with the maximum variation in frequency, while the second is the one that gives the system the greatest acceleration, at least in the sensors locations. On the other hand, the first is the one that would provide less energy to the system

while in the second, the variation in frequency, already very limited, would be even lower. Configuration 3 is a good middle ground of the previous ones, as it produces intermediate results between them. It is noted that in these analyses the environmental or operational effects that would inevitably occur on the structure on the day of the experiment were not simulated. This is because the intent is to find the best configuration among those proposed regardless of those effects, which in any case would affect each of the configurations in the same way.

6.7 Conclusions

This chapter presents the project of an experiment on the Sanctuary of Vicoforte, aimed at obtaining data relating to an anomalous structural condition to be used for research in the SHM field. The following questions were addressed in sequence (i) motivations and objectives of the experiment; (ii) people to be involved and definition of their characteristics for the simulations; (iii) places in which to place the mass; (iv) modality of the test, definition of the movement; (v) period and optimal conditions for the experiment. Finally, some configurations with specific intentions were simulated.

From the results obtained to the simulations with the FEM of the Sanctuary, it emerges that the variation in frequency given by the addition of a mass corresponding to that of 40 people is too limited to be identified. Surely once the experiment has been carried out, no damage detection techniques will be omitted, for example those based on the difference in reaction to the damage of the various modes, rather than on the value of the abatement alone. However, it should be noted that the variation calculated for 40 people, for example in the latest simulations, does not reach 0.015%. of the unloaded frequency, a variation of the order of a tenth of a mHz, which would be covered both by the uncertainty that afflicts the identification process and by the usual environmental and operational factors, characterized by variations of greater orders of magnitude. This is due to the fact that the Sanctuary is a massive structure, with a squat structural scheme, which would require a much greater mass than is available: the group of students reach about 0.012% of the total of the Sanctuary, estimated on the FEM. Just to get a rough estimate of the number of people needed to make the change in frequency noticeable, the differences between one observation and the adjacent (measured one hour later) across the entire available data set. The distribution of these difference values ($\Delta f_{i,hourly}$) is shown in Figure 6. 25. From the statistics obtained, it can be stated that the variation between the observation under unloaded conditions preceding the experiment and the loaded condition should exceed 0.02175 Hz to

overcome the UCL value set at $\mu + 3\sigma$. This value corresponds to a percentage of f_1 of 1.127% which is associated, e.g., with a load of about 5000 people in location 4B (see Figure 6. 26). Repeating the calculation on f_2, in the same position it would take 6000 people to overcome (with a very high safety margin) its hourly variability. The average of the hourly variation, considering all the absolute values, is 0.0042 and 0.0049 Hz for the first and second frequency respectively. The frequency abatement values for large (and unrealistic) numbers of people are shown in Figure 6. 26.

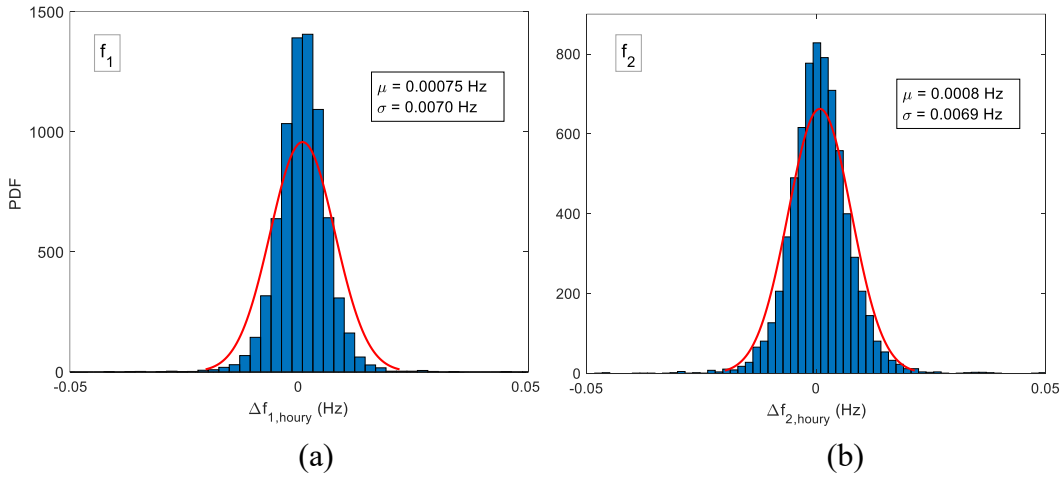

Figure 6. 25: Probability Density Function (PDF) of differences between frequency values identified one hour apart: f_1 (a) and f_2 (b)

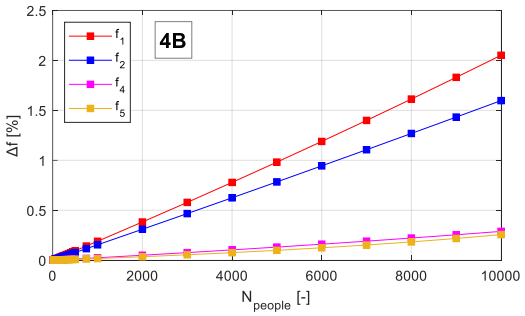

Figure 6. 26: frequency variation related to the number of people placed in location 4B: results of adding an unrealistic number of people

However, this does not mean that the experiment is to be considered useless. In fact, the accelerations that the group of students would give to the structure, with a frequency close to the first two natural frequencies, would amplify the response allowing to identify very accurately the dynamic parameters such as frequencies and damping, on which the uncertainty is greater. These new estimates, perhaps

made in one of the periods in which the variability is minimal, could be used to recalibrate the FEM, making it even closer to reality. Furthermore, given the results of the statistical analysis of the optimal period, two models could be calibrated, one corresponding to the "summer" and to the "winter" condition. Such accurate FEMs could therefore serve to reproduce damages that could train the ML algorithms to recognize them, perhaps going through a TL procedure to bring the two domains closer together.

The configuration that appears to be the most advantageous from the analyses is the one that follows the Magnificat path. It represents a good compromise between energy and frequency variations obtained. Although the latter are in any case very low, and it would be reasonable not to consider this parameter in the choice, configuration 3 instead of 2 (which carries more energy) is preferred because alternative techniques to identify the effect of the mass will be applied which perhaps would succeed to identify effects, through a comparison between identifications just prior to the experiment on the unloaded structure. This will be a very challenging goal for the procedure. Furthermore, the third configuration is the logistically simpler and easier to create, as well as the safest for the asset and for people, providing locations ordinarily occupied by visitors. This configuration is also the only one that does not provide for the occupation of positions to the West side of the Sanctuary, the area where the dome is most affected by cracks caused by the differential failure of the buttresses (see Figure 2. 12). However, movement on an already damaged structure could be dangerous and the distance from the cracks does not guarantee their protection. Therefore, before carrying out the test, a detailed inspection would be advisable to evaluate the current crack state, perhaps using the measurements of the crack meters of the static monitoring system, which, as anticipated in chapter 3, will be renewed in 2022. Following the updated crack mapping, local analysis could be conducted to examine the effect of the impressed stresses and its extent. Clearly not wanting to admit any damage caused by the experiment, high safety coefficients will be adopted and the configuration would be corrected if the slightest danger was foreseen. In that case, a less impetuous movement could even be contemplated in place of the jump, such as the tapping of one foot while remaining on the ground with the other or standing on tiptoes mimicking a jump without leaving the floor.

Chapter 7

Combining local and widespread information: geophysical satellite data for Structural Health Monitoring

The influence of the foundation soil, its characteristics and evolutions on the diagnostic parameters of a structure is another of the main issues of the SHM of buildings. Unlike the other structures typically monitored (e.g. aeronautical, mechanical, aerospace, etc.), the civil ones are in most cases based directly on the ground and involve it, in a more or less intense way, in their vibration. Like the external environment and the operating conditions, the foundation soil is also subject to annual variations that may be intrinsic or caused by the same environmental and operational factors that also act directly on the structure. These variations in the properties of the foundation soil, like the environmental ones, could cause fluctuations in the dynamic properties of the structure which, even if harmless, are source of uncertainty in the diagnosis process and in damage detection.

This issue could be even more complicated for ancient and particular buildings such as some CH structures. For newly built structures, the foundations are designed and built according to current codes and assessments, often based on

geotechnical tests, are made to establish whether the ground is suitable to accommodate the future load or if it can be made so through geotechnical interventions. For ancient buildings this is not always true. The reasons may be different ranging from the limited geotechnical knowledge to the inevitably less advanced technical and technological tools of the time. Moreover, often monumental architectures that we admire today are the result of overlapping projects over the centuries: the foundation soil has therefore been subjected to progressive stresses that were not properly controlled. But not all motivations are congenital. Over the years, foundations may have suffered damage or degradation caused by the change in the surrounding urban or natural context, for example, e.g. the construction of new neighboring buildings, subways, natural or artificial geomorphological changes, etc. All of this could have caused less stability, a less firm grip between the soil and the structure, which would have made vibrations more sensitive to changes in soil properties.

Changes in soil properties can be intrinsic, i.e. dictated by changes in conditions that come from the soil itself (for example deriving from changes in the flow rate of neighboring watercourses, consolidation conditions due to new constructions, structures or infrastructures) or be a consequence of environmental variations. In fact, environmental phenomena act both *directly* on the structure, modifying its mass and stiffness, and on its "constraint", the foundation soil, *indirectly* generating variations in its dynamic characteristics (Figure 7. 1).

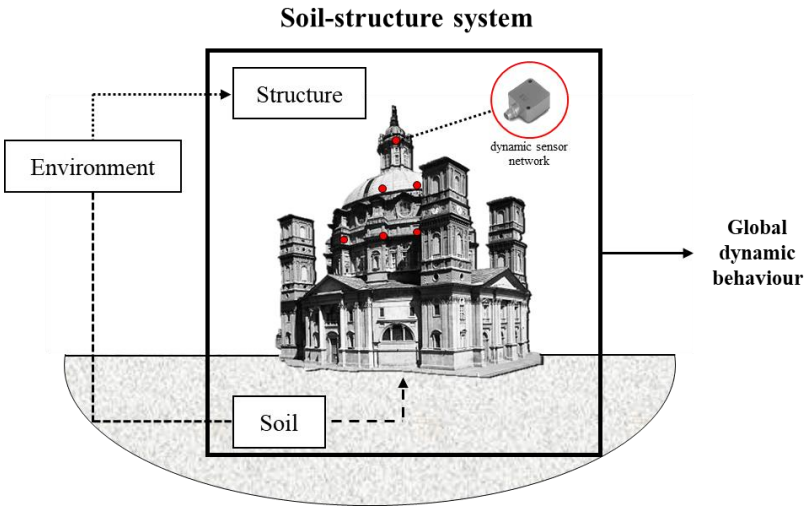

Figure 7. 1: scheme of soil-structure interaction and dependencies on environmental phenomena

In the literature there are many techniques that aim to remove the effect of environmental variations from monitoring data, this same document proposes one, instead the importance given to the variable soil properties is currently very limited due to a series of motivations.

First of all, SHM of AH is a relatively new research field, and this being an aspect that affects every work differently, an adequate framework has not yet been modeled. In addition, in most cases the foundation soil is not carefully monitored due to high costs, infeasibility, difficulties integration of soil data into structural monitoring, etc., or in the best cases geotechnical test results are available but spatially limited and not continuous over time.

This gap could be filled by using appropriate data measured by remote systems such as satellites, and this is what is investigated in this chapter. The aim is to integrate and enrich the in-situ monitoring data with *geophysical satellite data*, in order to investigate the effects of the soil on structural dynamics. Understanding the effect of soil on diagnostic parameters would allow to minimize the uncertainty or errors that characterize a data-driven diagnosis.

A thorough search of the relevant literature yielded no studies which have investigated the employment this kind of satellite data for civil SHM. Therefore, in the present chapter, this new application is proposed and investigated, starting from the data selection and processing aimed to the SHM context (7.1). Then a first data analysis to evaluate the connection between structural, environmental and geophysical satellite data is reported (7.2) and finally some preliminary FE simulations merging all the monitoring information is addressed (7.3). The case study is again the Sanctuary of Vicoforte as a lot of monitoring data are available that can be used for research. Moreover, it is particularly suitable being characterized by a critical geological configuration, which in centuries has caused differential settlements and consequent cracks to the structure. The foundation soil is likely to play an important role in the dynamics of the Sanctuary: it was identified among the possible explanations of the inconsistency between the static and dynamic monitoring system data, as highlighted in chapter 3 (Figure 3. 12).

7.1 Satellite data for SHM

Satellite remote sensing measurements are becoming increasingly relevant in observing and monitoring various terrestrial phenomena. They are currently widely used to monitor the effects of climate change such as melting glaciers, drought,

fires, and other phenomena, but the measured quantities are of interest to various other sectors, as highlighted by Milillo et al., (2018), including the field of structural engineering.

Of course, there are different types of data, which return measurements of different physical quantities, depending on the sensors a satellite is equipped with or how the data is processed and integrated with other types of information. For example, very recently *interferometric* satellite data has been employed for monitoring of aggregated buildings in urban areas (Bonano et al., 2013; Cavalagli et al., 2019; Cigna et al., 2014; Lenticchia et al., 2021; Ponzo & Ditommaso, 2020; Ubertini et al., 2018; Zhu et al., 2018), the effects of land subsidence in built environments (Arangio et al., 2014; Bozzano et al., 2018; Ubertini et al., 2018), and the anomalies detection in single structures (Meng et al., 2004), or infrastructures (Gentile et al., 2016; Lazecky et al., 2015; Meng et al., 2004; Zhu et al., 2018). These data identify displacements of points on the earth's surface and are obtained from radar instruments, e.g., Synthetic Aperture Radar (SAR). Instead, any application of *multispectral* and *hyperspectral* data was found in the literature of SHM: the latter can provide useful information regarding the geophysical properties of the soil, such as its temperature and water content.

For this analysis, the Land Surface Temperature (LST) and the Soil Water Index (SWI) data were selected, which will be better described in the following paragraphs. They belong to the European environmental program Copernicus of the European Space Agency (ESA) which provides a series of accurate, timely and readily accessible information, which enables environmental monitoring and assures civil safety (ESA 2020). Most of the measurements collected in Copernicus come from missions called Sentinel, some of which arise from collaboration with other European missions, such as those of the European Organization for the Use of Meteorological Satellites (EUMETSAT). First, the selected data will be subjected to systematic examination to investigate whether or not they contain useful information for SHM and, secondly, their usability from a technical-logistical point of view will be evaluated, i.e. if their acquisition parameters (spatial resolution, sampling frequency, percentages of missing or anomalous data) are suitable for SHM or can be rendered such by appropriate processing.

7.1.1 Land Surface Temperature

LST is defined as measure of the effective radiant temperature of the Earth surface or as thermal radiance emitted from the land surface, as respectively reported in ESA, (2013b) and Oyler et al., (2019). Not to be confused with the air surface temperature measured by thermometers (Hulley et al., 2019), LST is an index of the radiometric temperature of the ground surface which is a central aspect of biology and climate. In fact, its main applications concern biogeographical and ecological studies, agricultural ecosystems, and the analysis of the surface moisture status of ground.

Satellite data are classified according to the level of processing. LST is associated with a processing level 2, which indicates parameters obtained from level 1 data, i.e., measurement data and annotations. In particular, the LST parameter is obtained through a Split Window (SW) algorithm (Hulley et al., 2019; Remedios, 2012) that takes into account the thermal radiation measured by the Sea and Land Surface Temperature Radiometer (SLSTR) with an about 1 km spatial resolution, which provides multispectral measurements (Ferrato Lisa-jen, 2012; Hulley et al., 2019). In addition to SLSTR (which measures the Brightness Temperature, BT), the SW algorithm also takes into account atmospheric water vapor, satellite angle view, and land surface emissivity by means of biome and fractional vegetation (ESA, 2013a). Considering this, the LST can also be defined as the effective radiometric temperature of the ground surface in the SLSTR field of view (Remedios, 2012).

The data collected by two satellites are made available by the platform CREODIAS which collects most of the data and online services of Sentinel and other European satellites (CloudFerro, 2019): Sentinel-3A (S3A) and Sentinel-3B (S3B) whose data starts from March 2019. Due to the greater availability of data, the satellite S3A was considered for the following analysis. There are generally two acquisitions per day, acquired in the morning and in the night, which correspond respectively to the descending and ascending orbit of the satellites. The software gives the possibility to download the data in Not Critical Time (NTC) or in Near Real Time (NRT). For this study, the latter option has been chosen, allowing downloading data acquired from satellites just a few hours earlier, in the perspective of the integration with the almost real time in-situ structural monitoring.

The measuring points are spaced about 1 km apart, and they do not remain constant in the various acquisitions. While this kind of sampling is quite exhaustive

for the type of environmental monitoring for which they are designed, the same is not true for an application in SHM, in which the structures to be monitored are relatively small. At present, this is one of the most challenging issues of the application of geophysical satellite data to the SHM sphere. In fact, while the interferometric satellite data have a very dense spatial sampling but are recorded even after months, the geophysical ones provide at least one (but usually two) measurements per day, which however are spatially wide if compared with the usual dimensions of the civil structures. Actually, the recent rise of the remote sensing sector and the extensive use of Copernicus data for various objectives feeds good hopes that a tightening of the measures will be prepared, also given the new scheduled space missions (a constellation of nearly 20 additional satellites is expected to be put into orbit by 2030 (*https://www.copernicus.eu/it/informazioni-su-copernicus/copernicus-breve*)). If promising results were achieved by integrating these data into an SHM procedure, even specific refinements could be set up near the asset to be structurally monitored, perhaps by placing specific targets on the ground.

Clearly the measurement points currently captured by the satellite sensors not always coincide with the coordinates of the asset to be monitored, and, by varying from observation to observation, it is difficult to evaluate the trend over time of the geophysical parameter referred to a limited space, since the data it could be missing in many observations (that appends when they are acquired in different, but not too far, coordinates). To overcome these issues, here a basic interpolation operation was carried out. A "regularization" of the measures on a regular network with a constant step of 1 km (which is about the distance that the measuring points have) seemed like a good strategy to reconstruct the trend of the parameters over time in some reference coordinates. A process of triangulation-based linear interpolation, schematized in Figure 7. 2 has been adopted.

This operation implies the hypothesis of a linear trend between contiguous measuring points: on the one hand, in some specific cases it could be too simplistic and unrealistic (e.g. where sudden ground changes take place) but in most situations a linear variation is the most appropriate and impartial assumption, in the absence of more specific information about the trend between one measurement point and another.

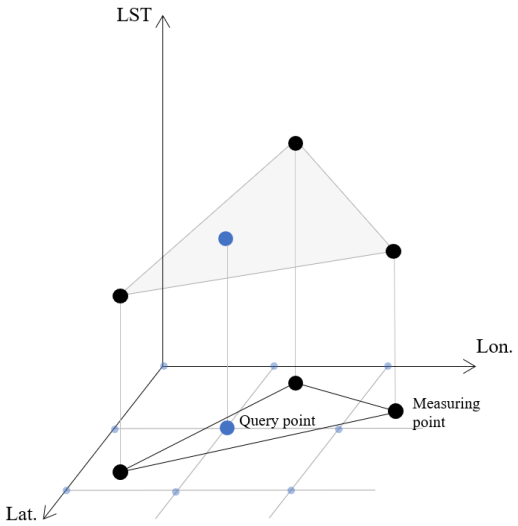

Figure 7. 2: process of triangulation-based linear interpolation performed on every point of the network (here named query point) and for every moment of observation

In any case, it must be specified that in this regularization, the maximum distance between a measured and a query point is only 700 m, i.e. when it is exactly in the center of 4 measurement points (a rather extreme situation): in any other case the query points are closer to the measurement points. Therefore, if the composition of the soil does not change abruptly, this interpolation could be considered acceptable, also because the environmental phenomena that generate the variations of the geophysical parameters, have generally more gradual spatial variations than a km. The interpolation also allows to get more robust and less sensitive data to eventual anomalous measurements, as well as making the data coordinates consistent among the acquisitions. All observations in the dataset were interpolated and then ordered, obtaining time series of the LST value for some selected coordinates. The main objective was to reconstruct the LST trend of the Sanctuary soil, but a much larger area than its footprint was processed in order to evaluate any differences or particularities compared to neighboring places. In particular, the data of a 121 km^2 surface have been extrapolated and reported in as many reference coordinates, i.e. the nodes of the regular network established. Figure 7. 3 shows the considered area, the network, and the LST mean value along two years, 2018-2019 (S3A morning data), while Figure 7. 4 shows the LST time series in the Sanctuary coordinates (the central node of the network) and its PDF.

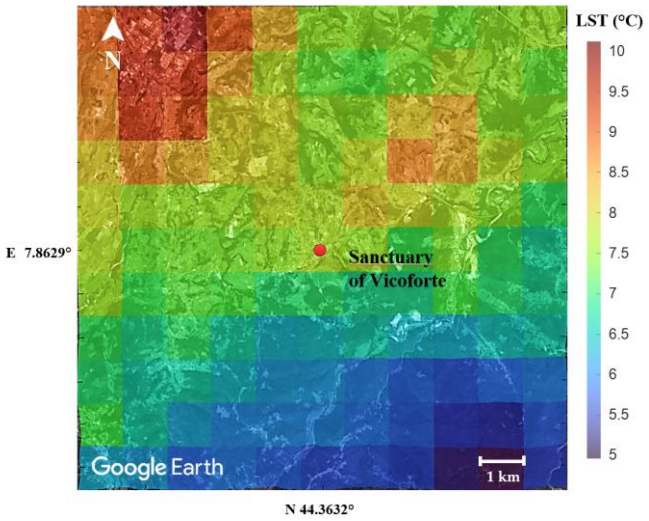

Figure 7. 3: two-year (2018-19) average LST interpolated on 121 points in the 11 km x 11 km grid around the Sanctuary (a) superimposed on Google Earth view

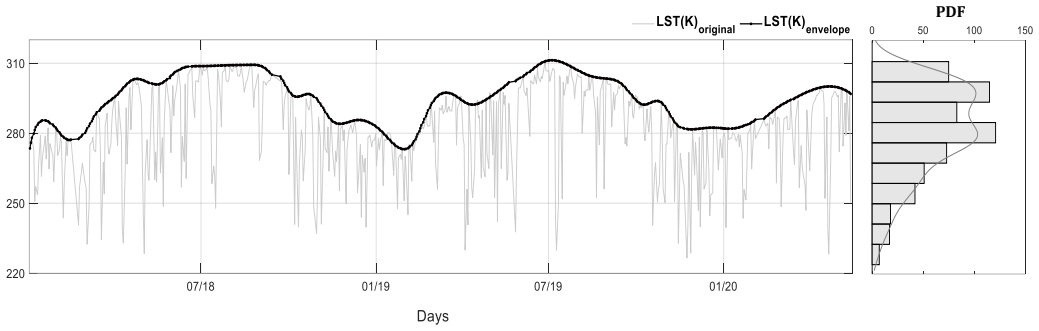

(a) (b)

Figure 7. 4: LST corresponding to the coordinates of the Sanctuary of Vicoforte: time series (a), histogram and PDF (b)

From the analysis of the data in the considered area, it can be highlighted that in general, the two-year average LST is higher in the built-up areas (North-West of the net, corresponding to the town of Mondovì, CN) and lower in the areas where the vegetation is denser (South of the net): the Sanctuary is located in the intermediate area with an average value between 7 and 8° C. For clarity, the time series of the parameters are not directly available on the mentioned platforms: they have been reconstructed by rearranging the data of the various acquisitions to evaluate their temporal evolution, an aspect of fundamental importance for SHM. In fact, structural monitoring requires data referring to specific coordinates, the ones of the structure, and pays attention to even the slightest changes, such as those after

24 hours, as it aims to identify evolutions that are generally faster than the environmental ones.

At a first visual examination, it can be seen that the series shows a clear seasonal trend that seems disturbed by sudden drops and different peaks with very low values. The latter probably does not represent an actual change in soil temperature as values of about -40°C are unlikely for the latitude of the Sanctuary, but instead, they are believed to be related to low BT values, from which LST derives.

7.1.2 Soil Water Index

SWI describes the soil moisture conditions in the first meters of depth, assuming values between 0% and 100%. It can be defined as percent saturation and is linked and driven by precipitation through the infiltration process (CGLS, 2013). Unlike LST, this parameter has a processing level 3, i.e. it is obtained from at least one level-2 parameter, which has been obtained from annotations and measurements. In particular, it derives from the fusion of 25 km Metop Advanced Scatterometer (ASCAT) of EUMETSAT Surface Soil Moisture (SSM) and 1 km Sentinel-1 SAR SSM. The latter parameter, SSM, describes dry and wet conditions, representing the degree of saturation of the first 5 cm soil layer (Bauer-Marschallinger et al., 2018, 2019; Bauer-Marschallinger & Paulik, 2019b; EUMETSAT, 2017). SWI data have a daily sampling time and a spatial resolution of 1 km.

From VITO Earth Observation of Copernicus Global Land Service (CGLS) (CGLS, 2014a) data from January 2018 to May 2020 has been collected. In addition to the SWI data, different information, such as the Quality Flag (QFLAG) and the State Surface Flag (SSF), is also provided.

Eight SWI values and eight QFLAG values are available, depending on the characteristic time length T, which can assume a value of 2, 5, 10, 15, 20, 40, 60, and 100. T should relate SWI and soil depth, but it must be pointed out that the algorithm for calculating SWI does not require the stratigraphy and soil properties, hence the relationship between T and the actual soil depth in the monitored points is not explicit (Bauer-Marschallinger et al., 2020). In fact, many studies have tried to validate the T-depth relation through soil moisture values measured in situ (Bauer-Marschallinger & Paulik, 2019a; Bauer-Marschallinger & Stachi, 2019; Paulik et al., 2012). In this study, reference will be made only to the extreme values of T, i.e., 2 and 100. The lowest T is able to somehow capture the phenomena that occur on the soil surface (as better explained in the next section), while T = 100 is the recommended value provided in the SWI validation report (Bauer-

Marschallinger and Paulik, 2019b) to be used when further information is not available for the specific case study.

Concerning the QFLAG, it is computed for each value of T, and it describes the quality of SWI depending on the input SSM data density: if enough SSM data are available, the QFLAG assumes a higher value; otherwise, its value is low. There is a specific threshold for each T-value: when the QFLAG exceeds it, the SWI value is considered as normal; otherwise, it is not reliable. Finally, the SSF shows freeze / thaw information (CGLS, 2014b) and it can assume different values based on the surface state at the observation time (SSF=0 unknown, SSF=1 unfrozen, SSF=2 frozen, SSF=3 melting, and SSF=255 data missing).

Compared to the LST data, the SWI data are sampled on a more ordered mesh because it has a higher level of processing. The process already used on LST is also applied on SWI to obtain suitable data for the purpose of this research, and the values on the same fixed network have been interpolated. Figure 7. 5 reports the mean value of SWI (for T=100) on the network, while Figure 7. 6 shows the times series and the PDF of SWI (for T=2 and T=100) corresponding to the area of the Sanctuary.

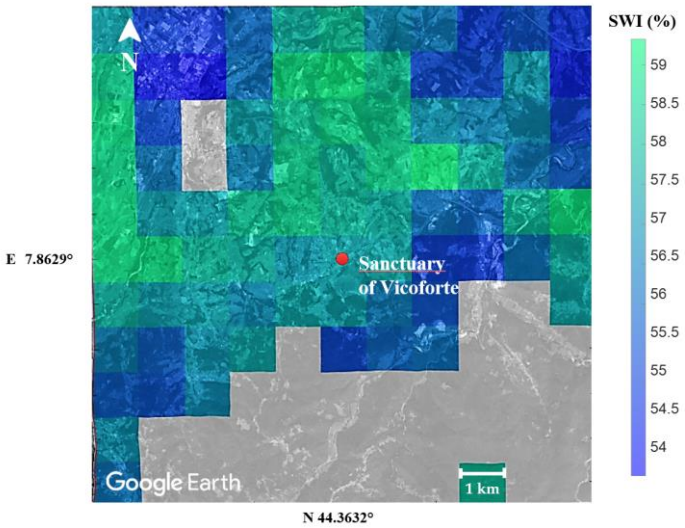

Figure 7. 5: two-year (2018-19) average SWI (for T=100) interpolated on 121 points in the 11 km x 11 km grid around the Sanctuary superimposed on Google Earth view.

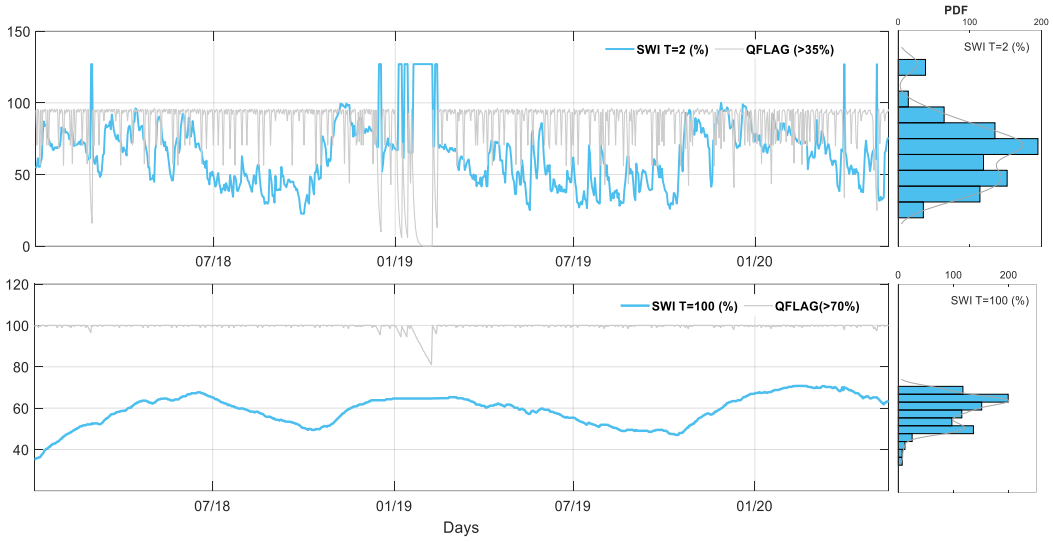

Figure 7. 6: SWI corresponding to the coordinates of the Sanctuary of Vicoforte. SWI and QFLAG time series(a) with its histogram and PDF (b); above T=2, below: T=100

Some considerations emerge from the visual examination of the average SWI (T=100) values in 2018 and 2019. Firstly, some areas appear to be missing data (south-east of the network). This derives from data series that show SWI values greater than 100% for the entire interval considered, which corresponds to a QFLAG=254. In Bauer-Marschallinger et al., (2020), such a value of QFLAG, indicated by the name "LowQFLAG", is associated with the error "*QFLAG value is low, indicating SWI value is less reliable*" and in fact, that area is characterized by a certain altimetric variation which is presumably the cause of this outcome. It should be noted that the time series of all points have been purified of unrealistic SWI values even before carrying out the interpolation, and therefore they do not affect the averages shown in Figure 7. 5. The north-west area, which as before corresponds to the coordinates of the inhabited center closest to that of Vicoforte, is characterized by the lowest annual average values of the entire surface considered, while the highest values are found in the areas covered by vegetation. As before, the data series relating to the Sanctuary coordinates have been assembled in the same interpolation process used for the rest of the network, as it represents one of the nodes. Figure 7. 6 show the resulting time series of SWI from January 2018 to May 2020, for T= 2 and T=100. In these figures, the SWI values higher than 100% have also been maintained for illustrative purposes. The trends of QFLAG for both T value is also reported. As the T-value rises, the fluctuation of SWI is attenuated, making the series smoother and the seasonal trend more easily

readable. In T=2 series, there are SWI values greater than 100% that are physically impossible since SWI=100% is the upper limit of the parameter and means fully saturated soil. These values correspond to QFLAG value below the reliability threshold, and, in several observations, they are also associated with SSF=2, which means frozen covered soil. These physically impossible values disappear entirely for high values of T.

The most frequent SWI percentages found are similar for the two series, and they are included around 45 and 70%. The annual trend of SWI with T=100 is much less dispersed than that with lower T. It appears that the index is subject to faster and deeper variations on the surface, while it is more stable at greater depths, less and more slowly influenced by the external environment. This hypothesis is reinforced by the comparison between the rainfall data in the area of the Vicoforte Sanctuary that will be discussed later.

7.1.3 Environmental and in-situ SHM data

In this paragraph, a brief summary of the environmental and on-site monitoring data is provided.

The environmental data, i.e., the daily rainfall and average temperature records had already been shown in the chapter 3: they come from the database of ARPA Piemonte (Arpa Piemonte, 2000). In particular, they are recorded from the station of Mondovì, CN, about 8 km away from the Sanctuary.

The structural monitoring data, i.e., the natural frequencies of the structure already analysed in the previous chapters, derive from the acquisitions of the permanent dynamic monitoring system installed on the Sanctuary (Ceravolo et al., 2021). In the analysis implemented in the present study, the first two frequencies of the Sanctuary were considered. They correspond to the first and second bending modes of the system in the direction of the minor and major axis of the oval dome, respectively. It was decided not to involve the higher frequencies for several reasons: (i) it was hypothesized that the lower frequency and bending modes are more strongly related to changes in the properties of the soil than the higher ones and those with high rotational components; (ii) in the specific case of the Sanctuary, the selected frequencies have a much higher identification percentage (Pecorelli et al., 2020) than the higher ones allowing better observations. Regarding the consistency with the satellite data acquisitions and their sampling, the identification of the accelerometric signals acquired at about 12:00 were used.

As mentioned in the previous chapters, this structure has suffered from significant structural problems, also due to the foundation settlements, since the beginning of its construction. They were caused by the particular configuration of the underlying soil; in fact, on the east side, the monument is mainly founded on a bedrock of marl inclined in the south-west direction, where it is covered by a silt-clayey layer (Chiorino et al., 2012) (see Figure 2. 13). Hence, the foundation rests on a heterogenous disposition of material; in fact, two of the eight buttresses are located on the marl layer and the others on the silt. This situation was also reproduced in the FEM that was used in this study, which is built in DIANA FEA® 10.2 (Figure 7. 7) and compared to that used in the previous chapters, it has a deeper soil layer of about 15 m, in accordance with a sensitivity analysis conducted (Dabdoub, 2021).

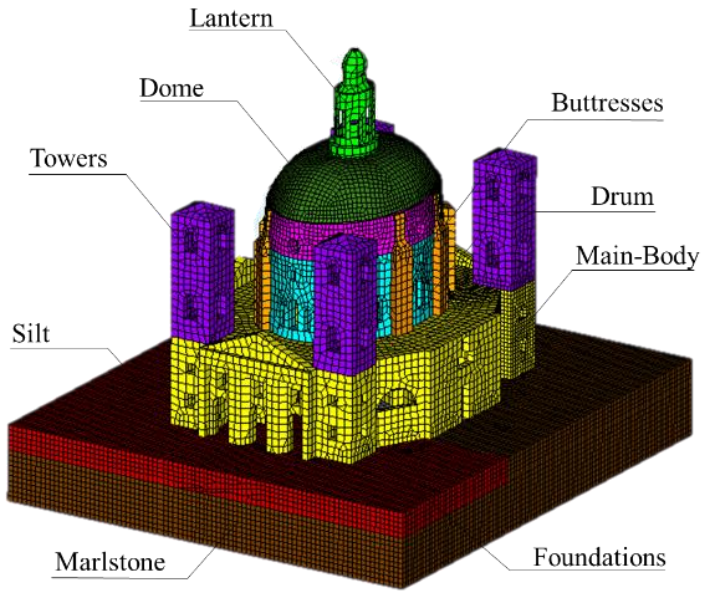

Figure 7. 7: FEM of the Sanctuary of Vicoforte and macro-elements

Even this model has been calibrated on the experimental dynamic data acquired at the temperature of 10°C and considers linear elastic constitutive laws for each macro-element, including the soil. Thanks to the calibration, the model reproduces the actual dynamic behavior of the Sanctuary and can be used to evaluate the response of the system to varying conditions imposed by the user. For the sake of brevity, only the information used for the analyses are reported, while a better description of the modeling strategy is reported in (Dabdoub, 2021). In Table 7. 1, the calibrated mechanical parameters of the macro-elements are shown.

Table 7. 1: FEM updated parameters of the main macro-elements

Element	Young's Modulus [GPa]	Mass Density [Kg/m^3]	Poisson Ratio [-]
Silt	0.53	1900	0.35
Marl-Stone	3.99	2100	0.35
Foundation	1.42	1800	0.35
Main-Body	1.42	1800	0.35
Drum	1.63	1700	0.35
Buttresses	3.91	1700	0.30
Dome	3.99	1800	0.35
Lantern	3.99	1800	0.35
Towers	3.21	1800	0.35

7.2. Processing and crossing of satellite and environmental data

As highlighted before, the LST trend presents many peaks with very low values corresponding to temperatures around -25÷-40 °C and reach up to -50 °C. Although these values may find significance for analysis in other fields, they were considered less significant for use in the context of structural monitoring because they probably refer to a low value of BT (from which LST is derived) rather than a sudden and drastic drop in soil temperature. In addition, such fast peaks are unlikely even considering the thermal inertia of the ground. For these reasons, it has been considered appropriate to process the data in order to draw the information contained therein useful for supporting on-site structural monitoring. The upper envelope of the LST original series has been computed in order to neglect the sudden peaks and keep the seasonal trend of the data (Figure 7. 4). This is obtained using a spline interpolation over local maxima divided by at least 10 samples.

Once the enveloped trend was obtained, it was compared with that of the air temperature (T_{air}) to highlight their connection. In particular, the series have been normalized and superimposed in Figure 7. 8a. They refer to the period 02/18 to 01/19.

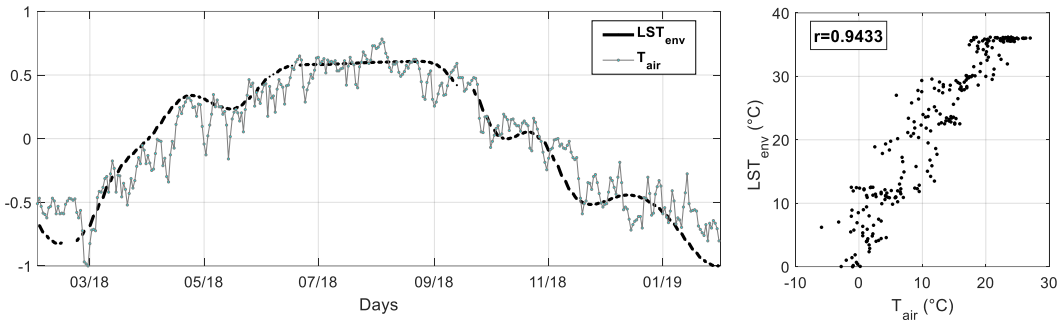

(a) (b)

Figure 7. 8: overlapping normalized time series: LST of S3A envelope and T_{air} (a) (in the plot LST_{env} is represented by a solid line with missing plots that create the effect of dashed line); LST of S3A envelope and T_{air} scatterplot (b)

It is evident that the two quantities are strongly connected, and this is also confirmed by examining their scatterplot (Figure 7. 8b) and their linear correlation coefficient, calculated as:

$$r(x,y) = \frac{cov(x,y)}{\sigma_x \cdot \sigma_y} \tag{7. 1}$$

in which $cov(x,y)$ is the covariance, σ_x and σ_y are the standard deviation of x and y respectively (Ezekiel, 1930; Taylor, 1997), in this case represented by T_{air} and LST_{env} data. It measures how strong a linear relationship is between two variables and it oscillates between -1 and +1. The higher $|r|$, the stronger the relationship between the variables, whereas the sign tells about the nature of the bond, i.e. positive or negative correlation. A coefficient of 0.94 was found between the two series, which is a very significant value, especially when related to experimental data. It would seem that the envelope of LST traces exactly the same trend of the average environmental temperature but more smoothly. This difference is undoubtedly due in part to the processing undergone by the variable, essential to get rid of those unrealistic values below -40 ° C. It is reasonable to think that less general processing, designed specifically for the series considered, would lead to a better match even on faster fluctuations. Regarding the values, which can be seen unnormalized in the scatterplot, those relating to the T_{air} are lower than those of LST: the difference is accentuated in the summer months where it reaches values that are around 10 ° C.

7.2.1 Autocorrelation analysis

In order to examine the trend over time of the two satellite parameters, an autocorrelation study is carried out (Box et al., 2015).

This analysis allows understanding how similar a parameter is to itself after a certain period of time by comparing the signal starting from a given observation with another delayed and evaluating how much it correlates as time goes on. Considering several k lag values, the autocorrelation coefficient ρ_k for a general time series $y(t)$ is calculated as:

$$\rho_k = \frac{\frac{1}{D}\sum_{t=1}^{D-k}(y_t - \bar{y})(y_{t+k} - \bar{y})}{\sigma_y^2} \tag{7. 2}$$

where D is the length of the series while $\bar{y}$ and σ_y^2 are its mean and variance. Given the available sampling, attention was paid to seasonal and annual fluctuations. For this purpose, the SWI (T=100) series, linked to slower changes, and the LST enveloped, which neglects sudden events, are suitable. In Figure 7. 9 and Figure 7. 10 the seasonal plot containing the superimposed annual trends and the Auto-Correlation Function (ACF), which displays ρ_k for multiple lag values, are reported for LST and SWI, respectively.

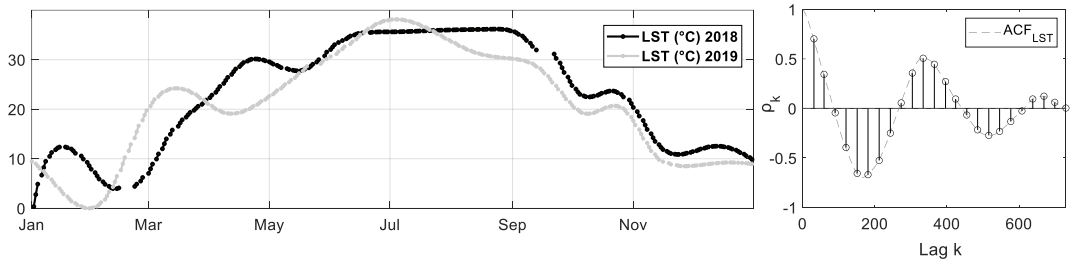

(a) (b)

Figure 7. 9: LST envelope overlapped time series (a) (in the plot LST envelope is represented by a solid line with missing plots that create the effect of dashed line) and ACF (b)

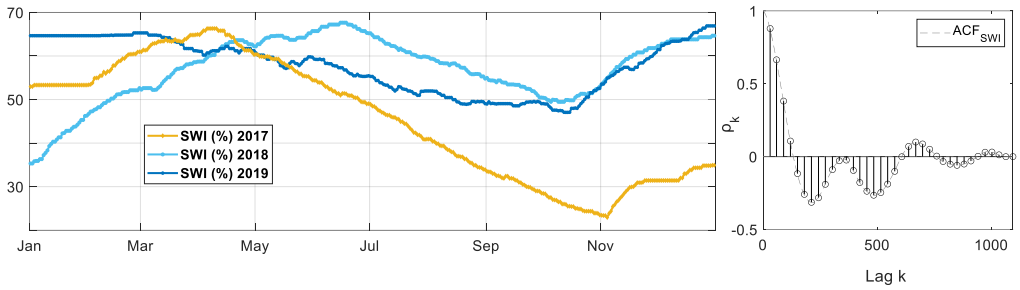

(a) (b)

Figure 7. 10: SWI (T=100) overlapped time series (a); ACF (b)

For the SWI parameter, data from January 2017 to December 2019 are considered, while for LST, only data of the last two are used (as anticipated, the LST data for the entire 2017 are not available on the platforms considered). The LST trends are very similar over the time considered; the greatest differences are found between the end of February and the beginning of March, with a maximum difference of about 13 °C. This parameter seems to show a clear seasonal trend, which increases in the summer months and decreases in view of the winter. This is confirmed by the ACF values, which reach peaks close to delays of about one year.

SWI seems to have a different behavior. Initially, the SWI data had been collected and analysed since January 2018 for consistency with LST. But the relevant disparity between the first months of 2018 and 2019 led to searching for the cause in previous records, and therefore, the entire 2017 series was also involved in the data analysis. In all three years, high SWI values were recorded in spring and abatements close to October and November, with the subsequent ascent. The particularity of 2017, which affects the values at the beginning of 2018, is in the value of that autumn dip, which is significantly lower than that of the following years, it is about a half. It is due to the period of low rainfall between the summer and autumn of 2017 (Arpa Piemonte, 2017) (observable in Figure 7. 11), which was interrupted in the first week of November, the week in which the SWI ascent begins. The strong dependence on rainfall, which is partly connected to seasonality and partly to less recursive environmental factors, makes SWI less cyclical than LST, and therefore the annual series are less correlated. This is also highlighted by the ACF graph, which does not show peaks in correspondence with lags of 1 year. In Figure 7. 11 the time series of SWI (T=2) and rainfall are compared: the SWI peaks are found in correspondence with heavy rainfall.

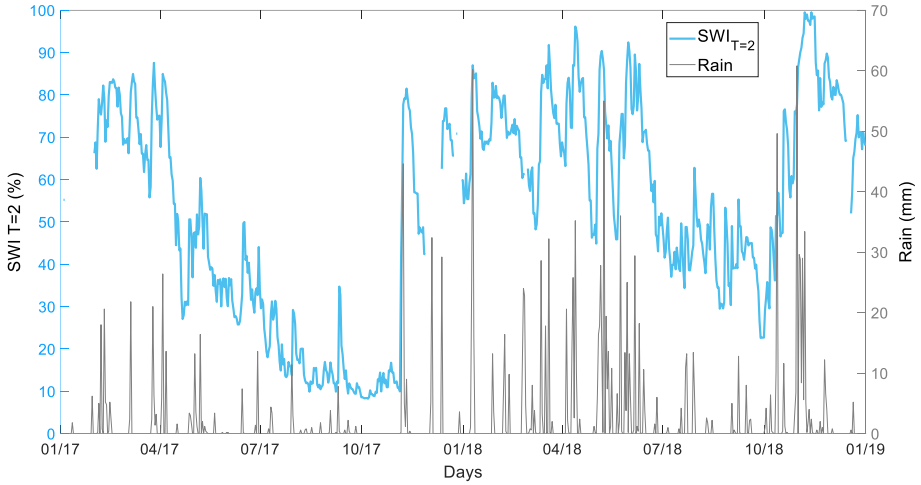

Figure 7. 11: comparison between rainfall and SWI (T=2) time series

Even by superimposing the normalized series of T_{air} and SWI of 2018, as previously done for LST, and calculating their linear correlation coefficient, it is easy to realize that the T_{air} is not the only phenomenon able to explain the trend of SWI of the soil (Figure 7. 12).

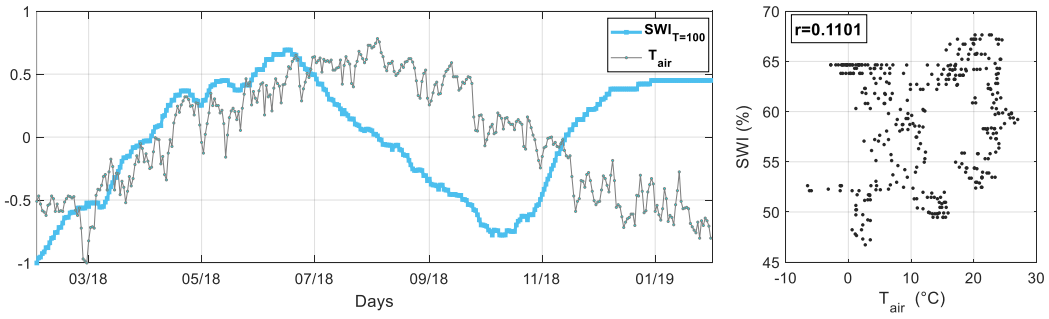

(a) (b)

Figure 7. 12: overlapping normalized time series: (a) SWI (T=100) and T_{air}; (b) SWI(T=100) and T_{air} scatterplot

7.2.2 Correlation between SHM and remote sensing data

After having independently examined the satellite geophysical data and processed them conveniently for the purpose of this study, they were crossed with the series of the first two natural frequencies of the Sanctuary. In this phase, it would be worth evaluating the possible presence of a cause-effect relationship. However, this problem could be very complicated given the interaction of the various phenomena:

as known and observed, SWI is linked to precipitation, which modify the properties of the soil as well as those of the structure, as it could lead to an increase in mass by wetting the masonry of the overlying structure; in the same way, the external temperature affects the structure and its frequencies both directly and indirectly by modifying the mechanics of the ground. Separating all these effects is not easy, even considering the fact that some relations are non-linear. For greater clarity, the influence of the mechanical parameters of the ground on the dynamics of the structure is not questioned here (it is already a fairly consolidated concept (Lou et al., 2011; Wong Hung Leung, 1975)) but rather, the possibility of reading this information within the series of satellite data considered and therefore of their usability for SHM is tested.

As a first step, the series were overlapped by removing their mean and scaling to their maximum absolute value in order to focus the analysis on their fluctuations: Figure 7. 13 shows the overlaps of the two frequencies with LST and SWI and their 3D scatterplot, while Figure 7. 14 show the 2D scatter plots for a better visualization.

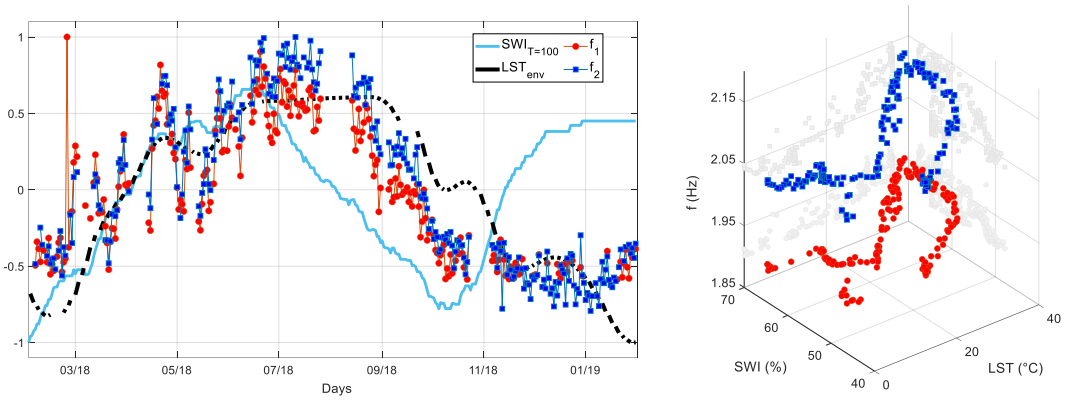

(a) (b)

Figure 7. 13: overlapping normalized time series (a) and 3D scatterplot (b): SWI(T=100) - LST envelope -f_1 - f_2 (LST_{env} is represented by a solid line with missing plots that create the effect of dashed line)

The Figure 7. 13a show that the LST arises in the warmer months, as do frequencies (see chapter 3), thus these quantities seem to be somehow related. This result agrees with what was expected, having ascertained the strong relationships between LST - T_{air} and T_{air} - f. A gap between the frequencies and LST at the beginning and at the end of the datasets is also appreciable, when the temperatures are more rigid: it is probably due to the bilinear trend of the frequencies (see chapter 3) (Ceravolo et al., 2021) with respect to the temperature, which inverts the slope

for negative values. Both figures have the sole purpose of analysing a long-term trend, as both satellite data have been purified of fast fluctuations (LST through an envelope and SWI considering the series at T = 100).

SWI tends to grow for the first half of the year considered in accordance with the dynamic parameters. However, it begins a rapid descent from mid-June 2018, earlier than those of the other variables. Finally, from mid-October onwards, the trends seem to completely diverge, contrary to what happened in the previous months.

From the simultaneous observation of the series over time, it is not immediate to understand whether one parameter is more closely related to dynamic behavior than the other. In fact, while in the first half of the year, all the series seem to grow quite consistently, in the autumn period, it is noted that the frequency trends deviate from both series of satellite data. In particular, it seems that the seasonal decrease in frequencies anticipates that of LST, and then also that of the ambient temperature, whereas lags behind the beginning of that of SWI.

To better visualize the relationship between the collected measurements, they were represented in 2D scatterplots (Figure 7. 14 reports the 2D projection of the 3D scatter in Figure 7. 13), and their linear correlation coefficient is calculated (Table 7. 2).

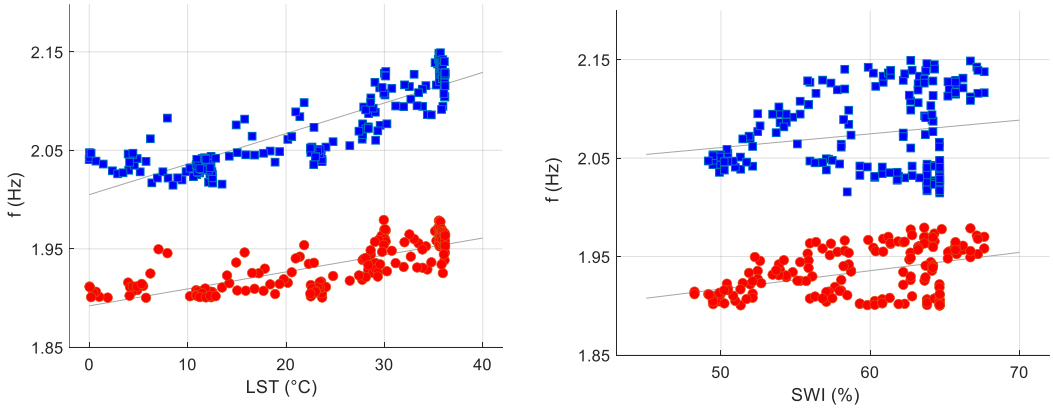

(a) (b)

Figure 7. 14: 2D scatterplot: (a) LST envelope – f; (b) SWI(T=100) – f.

Table 7. 2: linear correlation coefficients: SWI(T=100) - LST envelope - f_1 - f_2

	f_1	f_2
LST	0.78	0.87
SWI	0.44	0.19

In this regard, two clarifications are necessary: (i) the correlation coefficient measures the strength of a linear relationship and therefore fails to capture the presence of (strongly) non-linear relationships. This should be evident from a visual examination of the scatterplot. However, for slightly non-linear relations, the coefficient is still useful since the order of magnitude of the correlation does not change; (ii) correlation does not imply causation; this means that even if two variables show a high correlation, they could not be linked by a cause-effect relationship, but they could both be generated by the same phenomenon, without influencing each other, according to the debate on spurious and non-spurious associations. Taking the temperature as an example, having already verified the correlation between T_{air}-f (Ceravolo et al., 2021) and T_{air} -LST (Figure 7. 8), it would be natural to expect a correlation even between f and LST, being consequences of the same phenomenon. Hence the correlation does not prove that changes in soil properties are themselves a cause of frequency variations. In particular, this aspect will be examined in the next section.

On the other hand, although it is clear that LST variations are partially caused by T_{air} and SWI by precipitation, if mechanics of the soil played a fundamental role in the dynamics of the system (and that satellite data can quantify it with adequate accuracy), an even stronger relationship could be found between frequencies and satellite data compared to that with the aforementioned environmental causes. In fact, it must be highlighted that the soil properties expressed by satellite data could not only be influenced by the environmental factor with the more immediate association (LST by T_{air} and SWI by precipitation) but be the result and the combination of many phenomena (for example, LST could be influenced not only by T_{air} but also by exposure, cloudiness, rain, snow, wind, humidity, soil type, etc.). Accordingly, satellite data would represent a measure that is closer to the system than the pure environmental data, being the direct measure of their effects on a portion of the system, the soil. For this, their integration into a behavioral model of the structure would be reasonable, as well as convenient. With these premises, the intersection of the data was analysed.

Among the correlations obtained, those between LST and frequencies are quite interesting. Between these variables, the correlation reaches a value of 78% and 87% for f_1 and f_2, respectively, both in the same order of magnitude for that calculated between frequencies and T_{air} (72% and 75% as reported in Ceravolo et al., 2020 or more than 80%, as resulted in chapter 3 with updated datasets). As concerns SWI, equally significant values were not obtained. Theoretically, an inversely proportional relationship is what one would expect between SWI and the frequencies. In fact, as also reported in Bukkapatnam Tirumala, (2008); Pham et al., (2017) and Dong and Lu, (2016), the variations in soil stiffness show a non-linear relation with the degree of saturation, which in general implies a non-linear decrease of stiffness as the saturation increases. This is not reflected in the positive values obtained as correlation coefficients. An in-depth analysis aimed at modeling the relationship between the degree of saturation and the soil stiffness would deserve to be carried out and a validation on experimental frequency data suitably purified from the effect of temperature would be appropriate.

7.3 Analysis of thermal variations with FE simulations

Simulation on the FEM were conducted to investigate the consequential relationship between the satellite data and the dynamics of the Sanctuary. They are limited to thermal conditions, since the greater complexity that emerged from the discussion on SWI leads to the view that a separate study is appropriate.

In particular, in order to improve the interpretation of the phenomenon of thermal variation (both on the ground and in the air) on the dynamics of the Sanctuary, it was applied to the FEM of the Sanctuary. To do this, the following two approximate models were considered: one aimed to build the temperature distribution along the depth of the soil (Section 7.3.1) and the other to apply the temperature variation to the material of the Sanctuary and its mechanical parameters (Section 7.3.2).

7.3.1 Soil depth temperature model

Temperature of soil and foundations was estimated along depth starting from the enveloped LST data. An approximate solution of the following spatial damped diffusion equation was applied (the damping effects in time have been neglected for the purpose of the study):

$$\frac{\partial \Delta T}{\partial t} = \alpha \frac{\partial^2 \Delta T}{\partial z^2} + \beta \frac{\partial \Delta T}{\partial z} \tag{7. 3}$$

where $\alpha > 0$ and $\beta > 0$ are material constants; z is the depth ($z > 0$ downward) and ΔT is the absolute temperature amplitude (in K) around the mean value. Assuming the amplitude of LST as a boundary condition at surface, i.e. z=0, for any time, and $\frac{\partial \Delta T}{\partial z}(0, t) = 0$, the following equation is obtained:

$$T(z,t) = \overline{LST} + \Delta LST(t) \cdot e^{-\frac{\beta}{2\alpha}z} \left[\cos\left(z\sqrt{\frac{\lambda}{\alpha}\left(1 - \frac{\beta^2}{4\lambda\alpha}\right)} \right) + \frac{\beta}{2\alpha\sqrt{\frac{\lambda}{\alpha}\left(1 - \frac{\beta^2}{4\lambda\alpha}\right)}} \sin\left(z\sqrt{\frac{\lambda}{\alpha}\left(1 - \frac{\beta^2}{4\lambda\alpha}\right)} \right) \right] \tag{7. 4}$$

where $\overline{LST}$ is the mean value of LST in the observed time, $\Delta LST(t) = LST(t) - \overline{LST}$, α is the thermal diffusivity, $\beta = 2\sqrt{\pi\alpha/D_0}$ (Florides & Kalogirou, 2004) with D_0 fundamentals period of ΔLST, theoretically $\lambda = -\partial \Delta LST/\partial t/\Delta LST$ and it has been set equal to the median value of the observations after rejecting the negative results. D_0 can be estimated from the experimental data. In order to introduce these results in the FEM, the temperatures of the different layers of soil have been obtained as the average values between the thickness of the layers used to discretize the soil in the FEM:

$$T_{z_i z_{i+1}}(t) = \frac{\int_{z_i}^{z_{i+1}} T(z,t)\, dz}{z_{i+1} - z_i} \tag{7. 5}$$

where z_{i+1} and z_i are the coordinates of the boundary of the soil layer i with $z_{i+1} > z_i$. The value of α, thermal diffusivity in Eq. (7. 4), has been obtained exploiting the temperature at $z = 3.6\,m$ recorded during the inspection of 17/12/2020, i.e. 15°C: α which minimizes the error in the prediction of $T(z,t)$ given by (7. 4) was adopted. The optimization is carried out on the range of [0.1e-7 m^2/s and 100e-7 m^2/s], in accordance with the typical literature thermal diffusivity values for marlstone and silt (Florides & Kalogirou, 2004; VDI, 2000) and using the normalized error as cost function. The values of α obtained from the minimization process is reported in Table 7. 3 together with the other estimated parameters.

Figure 7. 15 and Figure 7. 16 show the results of the temperature-depth model. For the minimization operation, the LST data up to December 2020 were employed, given the date of the inspection.

Table 7. 3: temperature-depth model parameters

D_0 [s]	λ [1/s]	α [m²/s]
2.7034e+07 (about 312 days)	2.2451e-07	9.8000e-07

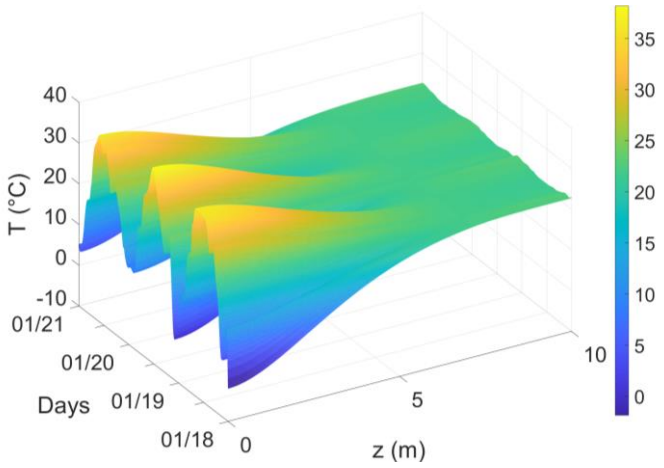

Figure 7. 15: time-depth distribution of soil temperature

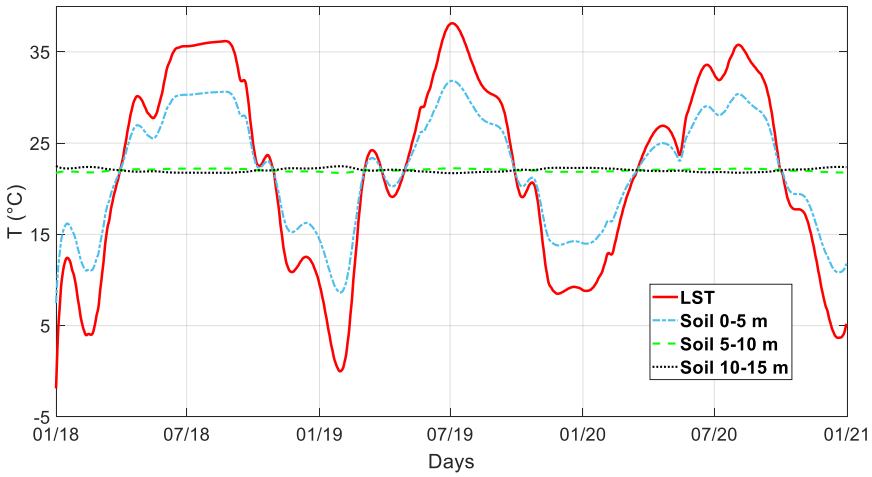

Figure 7. 16: mean temperature at different soil depth (sections of Figure 7. 15)

7.3.2 Temperature dependent elastic parameters

Once the soil temperature has been calculated from the LST data and the temperature of the materials of the other macro-elements is known, a simplified model is exploited to apply the temperature variations to the mechanical parameters of the system.

The simplified model for the Young's modulus $E(T)$ and temperature T is the same as reported in paragraph 5.3.1 used to build the source domain in the application of TL. For the sake of brevity, only the final relation is reported:

$$E(T) \approx E_0[1 + \alpha_{H2O}(T)T] \tag{7. 6}$$

where E_0 is a fictitious zero Kelvin Young's modulus, defined as fictitious because the law is linearised at small relative temperatures, $\alpha_{H2O}(T)$ represent the thermal expansion coefficient of the water as a function of absolute temperature T. It should be highlighted that this model has not yet been experimentally validated.

7.3.3 FEM analysis under different thermal conditions

Having the soil and masonry temperature, by the Eq. (7. 5) and (7. 6), it has been possible to obtain the elastic moduli of each material of the model at different temperatures. Hence, the relationship between natural frequencies and temperature can be explored starting from the FE eigen-analysis. The Young's modulus relative to a specific temperature according to the described laws was assigned through the FEM. For each element, the maximum, the minimum, and the average values of temperature (recorded between 01/02/2018 and 31/01/2019), were considered for consistency with the experimental frequency data. The temperature variation was analysed independently in each material, then applied to all elements of the model together. In these simulations, only the temperature effect is considered for the variations of the elastic modulus, neglecting all other EOVs that could influence the dynamic response of the structure. The results in terms of frequency variations are reported in Figure 7. 17.

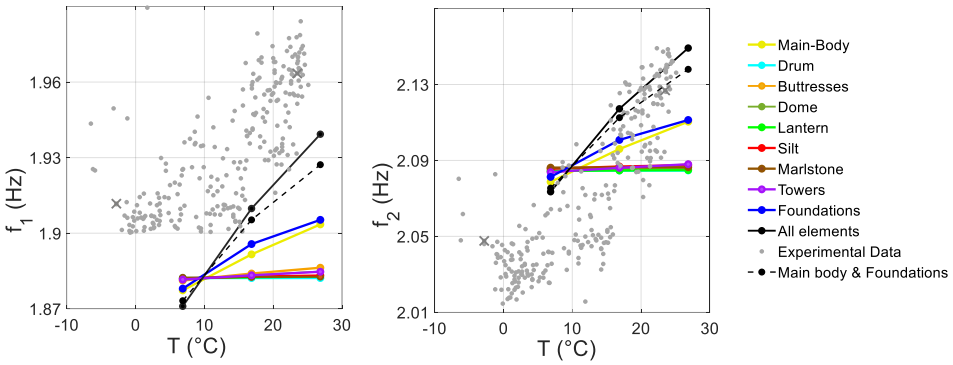

(a) (b)

Figure 7. 17: frequency-temperature relation for each macro-element, for main body and foundations together and for all structural elements: f_1 and T (a), f_2 and T (b)

Most relationships tend to be horizontal, indicating that the temperature change of these elements has a very limited effect on the frequencies of the structure. By applying the temperature variation to all macro-elements at the same time, the frequency trend is strongly inclined and tends to follow the slope of the experimental data. It is worth clarifying that the vertical discrepancy is related to residual calibration errors, which in this analysis has little relevance, given that the aim is to explore the sensitivity of frequency with respect a variation in temperature of the soil and on the structure itself. The elements that individually correspond to the most marked variations are the foundations and the main body: a further analysis was carried out by applying the temperature variation to both together (dashed black line in Figure 7. 17) in order to compare it with the analysis which implies the variation on all elements (solid black line in Figure 7. 17). The result shows that the frequency trends are very close but do not overlap. This indicates that the two elements at the base of the Sanctuary are the main, but not the only ones, responsible for the dependence of the dynamic response on temperature.

7.4 Results and discussion

Some considerations can be drawn from the general observation of all the analyses carried out on the LST and SWI data.

Both exhibit high spatial variations that can be noticed already in the observation of a relatively small analysed surface (11 km x 11 km). This can be seen as an advantage on the one hand because the instruments are able to capture even slight differences, but care must be taken in choosing the point of interest if this data are applied for structural monitoring instead of environmental monitoring,

the purpose for which have been designed. In an attempt to mitigate any local anomaly and make the time series more reliable and robust, spatial interpolation between the coordinates closest to the observed point was implemented. This operation, in the specific case, was considered reliable also because the annual average values of the parameters in the points adjacent to the Sanctuary are very close (Figure 7. 3 and Figure 7. 5), but this is not always guaranteed. In cases where the type of soil (and therefore how it responds to climatic variations) varies abruptly between two measurement points, the interpolation could lead to incorrect estimates of the intermediate points: carry out an investigation on the foundation soil of the structure to monitor and acquire information on the ground around a few hundred meters could help to understand if a linear interpolation is the most appropriate choice. Abrupt variations could moreover be identified by examining the data on a regular network, as in Figure 7. 3 and Figure 7. 5: if sudden color variations occur near the asset, more accurate analyses would be appropriate to use the reprocessed remote sensing data.

For the coordinates of Vicoforte, the LST presents a trend over time characterized by fluctuations towards very low temperature values. Since, for SHM purposes, the parameter is applied as a measure of the soil surface temperature, and as it is evident that those temperatures are considered unrealistic for the terrain at that latitude and altitude, they have been discharged by isolating the upper pattern of the series. This operation implies a certain degree of uncertainty, as any data conditioning operation; then, although this envelope operation may represent a valid solution to eliminate unrealistic values, its parameters should be carefully calibrated on a case-by-case basis.

The SWI parameter is very conditioned by the choice of the reference T. In particular, it was noted that for very low T, SWI seems to be strongly influenced by the rainfall trend. Also in this case, this choice involves a considerable degree of uncertainty; although document (Bauer-Marschallinger & Paulik, 2019a) recommends the choice of T=100 in cases where more precise information is not available, this may be questionable in the case of application of such data to SHM. Even in this case, the most desirable solution would be to evaluate the optimal T case by case, perhaps based on the depth of the foundations of the considered structure.

Although the LST seems to follow a fairly clear seasonal trend, which is repeated for 2018 and 2019, the same is not true for SWI. In fact, it appears much less predictable, and the overlapping of the series relating to 3 different years (2017-

19) does not seem to identify a common pattern, except for a common reduction of the parameter in autumn months.

The cross between the frequency trends with the satellite data highlighted the following aspects: LST follows the same seasonal trend as the on-site monitoring data. A higher correlation coefficient with the envelope of LST than with T_{air} was obtained for the frequencies. However, despite this high correlation, the FEM simulations highlight a weak dependence between the dynamics of the system and the temperature variation applied only to the ground element, lower than that shown by applying the thermal change to the material of the structure. There is no doubt that the soil has high thermal inertia, and especially the deeper layers are subject to very low thermal variations during the year compared to the emerging structure, directly exposed to climatic phenomena. However, undoubtedly, this result depends on the simplified $E(T)$ model adopted: other driving mechanisms could exist, which are not considered here. It should be reiterated that just the primary effect of the temperature on the ground has been modeled. Secondary effects, such as evaporation triggered by temperature and the consequent variation in saturation degree and mechanical properties of the soil, have not been considered and would require further analysis.

About SWI, it does not reach such high correlation values, but this does not exclude the connection with the dynamic behavior. Clearly, the datasets of frequencies that have been used are the result of all the phenomena that influence the stiffness, among which the temperature (environmental or related to the soil) stands out, as has been highlighted. This very important effect could have "covered" the influence that soil saturation could exert on the ground so as to make it invisible in the scatterplot. The question could ideally be resolved by investigating the evolution of the dynamic behavior of the Sanctuary as a function of the degree of saturation of the soil, keeping the temperature constant. This, technically not feasible on a structure the size of the Sanctuary, could also be simulated on the FEM in future research.

The poor identifiability of the relationship between SWI and the frequencies of the structure could find an explanation even in the presence of a drainage channel. In fact, the Sanctuary is entirely circumscribed by a channel about one meter high, which conveys the infiltrated water into an expansion tank, in order to keep the foundations and the ground just below the structure dry, avoiding instability of the clayey-silt layer (Figure 7. 18).

Probably the channel acts as a screen and weakens the frequency dependence on SWI in the case of the Sanctuary, but it may not be as weak for other types of civil structures. Furthermore, the choice of T, in our case T = 100, influences the search for the *f*-SWI relationship and it should be well thought out before drawing any conclusions on the independence of the parameters.

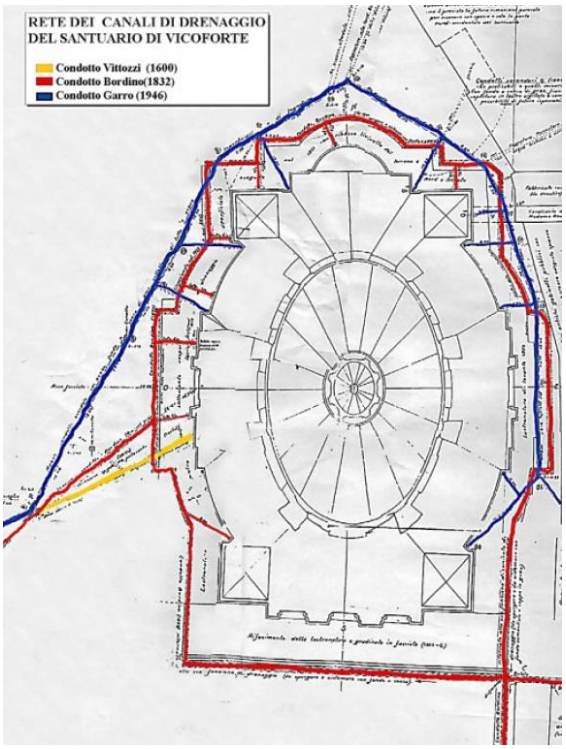

Figure 7. 18: plan of the network of drainage channels of the Sanctuary of Vicoforte

7.5 Conclusions

Despite the long list of challenges and limitation of this first study, satellite data have the potential to become a useful source for SHM when continuous information about the soil are not available. A key aspect of this research is the application of satellite data designed for environmental monitoring to support structural monitoring. The hypothesis driving this research is that these data contain information related to the stiffness of the soil-structure system, therefore partly responsible for the variation of the dynamic parameters identified. If confirmed, the simultaneous reading of the time histories and the application of techniques

developed within the SHM field could support the damage detection procedure, as many of the variations of the diagnostic parameters could be justified with the variations of the above parameters. This would allow reconstructing accurately the dynamic behavior of the system in a "healthy" condition, reduce the level of uncertainty and, therefore, to sharply notice the appearance of an anomaly.

Geophysical satellite data represent a solution for continuous and systematic soil monitoring at a reduced cost as they can be quickly and easily downloaded through platforms at no charge, within 1-3 days from acquisition and for the entire Earth's surface (Chuvieco, 2009). Given their global coverage, obtaining data for any building could be possible avoiding the high costs of in situ tests. After an initial effort in understanding and processing satellite data, the procedure could be automated and data included in dynamic monitoring protocol of structures. Moreover, satellite monitoring allows obtaining data without directly intervening on the monitored asset, not interfering in the least with the activities of the structure. Future studies could be focused on solving aspects emerged from this first approach of satellite data in structural monitoring and could improve the modeled link between the physical parameters included, even on multiple case studies, aiming at consolidating their use.

Part of the work described in this chapter was also published in the papers (Coccimiglio et al., 2022, 2021).

Acknowledgments: This research was partially supported by the Amministrazione del Santuario di Vicoforte and the Fondazione Cassa di Risparmio di Cuneo.

Conclusions

This thesis work aims to explore the encounter between the sphere of AH and the discipline of SHM. Irrefutable benefits emerged by considering both ordinary circumstances and some particular structural scenarios, such as the advent of earthquakes, the implementation of structural interventions, emergency management: in these, monitoring systems and the techniques for data analysis would offer continuous information on the evolving condition of the asset. Broadening the perspective, the awareness on the state of health of the CH structures deriving from the diffusion of the monitoring practice, would also allow an optimization of the resources of public or private authorities to devote to interventions. A scale of priorities, which takes into account the urgency of the intervention to be carried out, as well as other criteria (artistic, historical and political value, use, role within the community, consequences of non-intervention, etc.) could be a decisive step towards achieving more resilient cities and a new concept of *optimized conservation*. The great interest of communities and countries for their AH should encourage research to develop in this direction.

Three most relevant technical limitations emerged from this study, namely (i) the confounding influence of environmental and operational factors, (ii) the lack or limited availability of training data relating to damaged conditions and (iii) the limited attention paid to the variability of soil conditions: some strategies have been proposed and evaluated to address them, based on data-driven approaches which, however, are in some way supplemented by information from models.

Following the clarification of the role of SHM for CH structures, the reconstruction of the state of research to date and the definition of key concepts, the dissertation traced the following path. The environmental factors that influence the case study, the Sanctuary of Vicoforte, were systematically investigated, gaining awareness of how and to what extent these influenced the static and dynamic quantities of the system. In light of the outcomes, a novelty detection strategy based on cointegration and ML regressions was designed to remove the fluctuations due to these factors from the static and dynamic parameters monitored. This has led to an indicator of structural health only sensitive to so-called pathological changes. TL was subsequently applied, for the first time on such complex structures, in order

to integrate the data of the FEM into a data driven paradigm, that is a ML classification of real data. The FEM allows to simulate situations never experienced by the structure but its data must be adapted to the real ones because they always present divergences, especially for complex structures such as architectural assets. The obtaining of data from condition that the structure has never experienced, or due to damage, is also the goal of the experiment on the Sanctuary, the project of which has been reported: it would lead to a more accurate understanding of the dynamic response that would be used to better interpret future monitoring data. Finally, a first study of geophysical satellite data, usually conceived for environmental monitoring, was conducted in order to evaluate their potential contribution to SHM. This is an interesting prospect, especially in view of the growing development and improvement of remote sensing data. This research path has led to the achievement of a broader vision of the problem of the implementation of SHM for CH structure and to a greater awareness of the criticalities that hinder its evolution. Precisely the latter could direct, in a sense, the prospect for future research.

An aspect that has not been explored here and which could be the subject of future research is the optimal design of a monitoring system. The success of a data-driven monitoring approach, from the most basic to one based on the most complex algorithms, largely depends on the quality of the input data. Their suitability in this sense can be assessed both on the variety of environmental or operational situations to which they refer (the more complete the training set, the greater the experience the algorithms will have) and, strictly speaking, on the quality of the measurement. The latter could be incremented through the systematic evaluation of the instrumentation and its characteristics, e.g. acquisition frequency, accuracy, position, direction, composition of sensors, etc., aimed at optimizing the quality of monitoring with respect to costs and computational burden. A sensitivity analysis of the accuracy of the monitoring procedure with respect to each of the aforementioned aspects would lead to highlighting the most influential factors and which, consequently, should have particular attention in the design phase of the system. In this regard, both purely virtual studies (e.g. simulating acquisitions in different points of a FEM to optimize position and direction) and analyzes that exploit experimental signals (e.g. treating the signals with different sampling settings, adding different levels of artificial noise) could be conducted to derive guidelines for the installation of a monitoring system.

A considerable effort will be needed in this research field for to move forward in the damage detection scale defined by Rytter. In fact, to date, various researches

have been developed to identify the presence of damage (level I) but the structural complexity of the architectural assets and the variety of damage they could face make any further progress difficult, such as the localization or the quantification of damage and residual life. These certainly will represent challenging objectives of future studies, which will have to convey advanced experiences both in the field of structural engineering, architecture and science aimed at the management and understanding of large amounts of data. In the author's view, a fruitful combination of model-driven and data-driven approaches should be developed in such a way that it reaps the benefits of both approaches. On the one hand, investigating various case studies could help to understand to what extent the models can make up for the lack of experimental data and, consequently, help to define which environmental / operational situations should be acquired experimentally and which ones it would be enough to simulate numerically; on the other hand, the flexibility of ML procedures could direct the modeling process towards those aspects which need to be given greater importance and on which to invest in experimental tests, defining a minimum level of geometric and mechanical accuracy.

Finally, an aspect that will certainly deserve further investigation in the future is the involvement of satellite data for SHM. Satellite monitoring is a constantly evolving practice and new products, both in terms of instrumentation and algorithms for processing measurements are continuously being developed. This suggests that improvements in the acquisition procedures will take place, in terms of accuracy, spatial and temporal sampling. Data other than those considered in the research reported could be crossed with the structural data collected on site, in order to find new connections and then exploit them for large-scale SHM; moreover, a growing interest of the SHM community for these data could lead to a collaboration between the two parties aimed at defining ad hoc satellite instrumentation and measurement requirements.

In conclusion, it is undeniable that there is still a long way to go and issue to unravel to project these studies into practical application, but considering the really recent emergence of this research field and the high growth potential of instruments and methodologies, the prospects are strongly encouraging and the idea of a smart built environment that communicates with people is becoming more and more realistic.

List of abbreviations

ACF: Auto-Correlation Function
ADF: Augmented Dickey-Fuller
AH: Architectural Heritage
AI: Artificial Intelligence
ARD: Automatic Relevance Determination
ARPA: Agenzia Regionale per la Protezione Ambientale
ASCAT: Advanced Scatterometer
CGLS: Copernicus Global Land Service
CH: Cultural Heritage
CM: Crack Meters
CP: Pressure Cells
DCNN: Deep Convolutional Neural Network
E: wire gauges
EOVs: Environmental and Operational Variations
ESA: European Space Agency
EUMETSAT: European Organization for the Use of Meteorological Satellites
FE: Finite Element
FEM: Finite Element Model
FN: False Negative
FP: False Positive
ICOMOS: International Council on Monuments and Sites
KKT: Karush–Kuhn–Tucker
LC: Load Cells
LCL: Lower Control Limits
LST: Land Surface Temperature
LVDT: Linear Variable Displacement Transducer
MASW: Multi-station Analysis of Surface Waves
ML: Machine Learning
MMD: Maximum Mean Discrepancy
NDT: Non-Destructive Test
NRT: Near Real Time
NTC: Not Critical Time
OMA: Operational Modal Analysis
OSP: Optimal Sensor Placement
PCA: Principal Component Analysis
PDF: Probability Density Function
POM: Proper Orthogonal Mode
QFLAG: Quality Flag
REMI: Refraction Microtremor
RKHS: Reproducing Kernel Hilbert Space
RMS: Root Mean Square
RMSE: Root Mean Square Error
RVMs: Relevance Vector Machines
S3A: Sentinel-3A
S3B: Sentinel-3B
SAR: Synthetic Aperture Radar
SHM: Structural Health Monitoring
SLSTR: Sea and Land Surface Temperature Radiometer
SPC: statistical process control
SPT: Standard Penetration Test
SRM: Structural Risk Minimization
SSF: State Surface Flag
SSI: Stochastic Subspace Identification
SSM: Surface Soil Moisture
SVD: Singular Value Decomposition
SVM: Support Vector Machine
SW: Split Window
SWI: Soil Water Index
T: characteristic time length
TCA: Transfer Component Analysis
TD: Training Dataset
TL: Transfer Learning
UCL: Upper Control Limits
VGGNet: Visual Geometry Group

References

Abbas, N., Calderini, C., Cattari, S., Lagomarsino, S., Rossi, M., Corradini, R., & et al. (2010). Classification of the cultural heritage assets, description of the target performances and identification of damage measures. *Deliverable D4, WP No1, PERPETUATE Project (FP7), European Research Project on the Seismic Protection of Cultural Heritage.*

Abruzzese, D., Micheletti, A., Tiero, A., Cosentino, M., Forconi, D., Grizzi, G., Scarano, G., Vuth, S., & Abiuso, P. (2020). IoT sensors for modern structural health monitoring. A new frontier. *Procedia Structural Integrity*, *25*, 378–385. https://doi.org/10.1016/J.PROSTR.2020.04.043

Alaggio, R., Aloisio, A., Antonacci, E., & Cirella, R. (2021). Two-years static and dynamic monitoring of the Santa Maria di Collemaggio basilica. *Construction and Building Materials*, *268*, 121069. https://doi.org/10.1016/j.conbuildmat.2020.121069

Aoki, T., Komiyama, T., Tanigawa, Y., Hatanaka, S., Yuasa, N., Hamasaki, H., Chiorino, M. A., & Roccati, R. (2004). Non-destructive testing of the Sanctuary of Vicoforte. *Proc., 13th Int. Brick and Block Masonry Conf.*, *Vol. 4*, 1109–1118. https://citeseerx.ist.psu.edu/viewdoc/download?doi=10.1.1.568.7309&rep=rep1&type=pdf

Aoki, T., Yuasa, N., Hamasaki, H., Nakano, Y., Takahashi, N., & Tanigawa, Y. (2011). Safety assessment of the Sanctuary of Vicoforte, Italy. In *Int. J. Materials and Structural Integrity* (Vol. 5, Issue 3).

Arangio, S., Calò, F., Di Mauro, M., Bonano, M., Marsella, M., & Manunta, M. (2014). An application of the SBAS-DInSAR technique for the assessment of structural damage in the city of Rome. *Structure and Infrastructure Engineering*, *10*(11), 1469–1483. https://doi.org/10.1080/15732479.2013.833949

Arpa Piemonte. (2000). *ARPA*. Http://Www.Arpa.Piemonte.It.

Arpa Piemonte. (2017). *Rapporto tecnico sulla qualità dell'aria e sulle attività dell'agenzia a supporto dell'emergenza per gli incendi boschivi in Piemonte nel mese di ottobre 2017*.

Ashraf, S., Fuh-Gwo Yuan, S., Ashraf Zargar, S., Chen, Q., Wang, S., & Yuan, F.-G. (2020). Machine learning for structural health monitoring: challenges and opportunities. *Spiedigitallibrary.Org*, *11379*(23), 1137903–1137904. https://doi.org/10.1117/12.2561610

Bal, İ. E., Dais, D., Smyrou, E., & Sarhosis, V. (2021). Monitoring of a historical masonry structure in case of induced seismicity. *International Journal of Architectural Heritage*, *15*(1), 187–204. https://doi.org/10.1080/15583058.2020.1719230

Balageas, D., Fritzen, C. P., & Güemes, A. (2010). Structural Health Monitoring. In *Structural Health Monitoring*. Wiley-ISTE. https://doi.org/10.1002/9780470612071

Barsocchi, P., Bartoli, G., Betti, M., Girardi, M., Mammolito, S., Pellegrini, D., & Zini, G. (2020). Wireless sensor networks for continuous structural health monitoring of historic masonry towers. *Taylor & Francis*, *15*(1), 22–44. https://doi.org/10.1080/15583058.2020.1719229

Bartoli, G., Chiarugi, A., & Gusella, V. (1996). Monitoring Systems on Historic Buildings: The Brunelleschi Dome. *Journal of Structural Engineering*, *122*(6), 663–673. https://doi.org/10.1061/(ASCE)0733-9445(1996)122:6(663)

Bassoli, E., Bovo, M., Mazzotti, C., Vincenzi, L., & Forghieri, M. (2017). The role of environmental effects in the structural health monitoring: the case study of the Ficarolo Tower in Rovigo, Italy. *Anidis 2017 Pistoia*.

Bauer-Marschallinger, B., & Paulik, C. (2019a). *Copernicus Global Land Operations "Vegetation and Energy". Validation Report (QAR). SWI1km-V1_I1.11*.

Bauer-Marschallinger, B., & Paulik, C. (2019b). *Copernicus Global Land Operations "Vegetation and Energy". Product Usera Manual (PUM). Soil Surface Moisture 1 km, version 1, Issue l1.30*.

Bauer-Marschallinger, B., Paulik, C., Hochstöger, S., Mistelbauer, T., Modanesi, S., Ciabatta, L., Massari, C., Brocca, L., & Wagner, W. (2018). Soil moisture from fusion of scatterometer and SAR: Closing the scale gap with temporal filtering. *Remote Sensing*, *10*(7), 1–26. https://doi.org/10.3390/rs10071030

Bauer-Marschallinger, B., Paulik, C., & Jacobs, T. (2019). *Product Users Manual (PUM). SWI1km, version 1.0. Issue I1.10*.

Bauer-Marschallinger, B., Paulik, C., & Jacobs, T. (2020). Product Users Manual (PUM). SWI1km, version 1.0. Issue I1.20. In *Copernicus Global Land Operations*.

Bauer-Marschallinger, B., & Stachi, T. (2019). *Scientific Quality Evaluation (SQE) 2018. SWI V3_I1.00*.

Beckmann, P., & Bowles, R. (2004). *Structural aspects of building conservation*.

Elsevier Butterworth-Heinemann.

Bishop, C. M. (2006). Pattern Recognition and Machine Learning. In 128(9) (Ed.), *Religion und Konflikt*. https://doi.org/10.13109/9783666604409.185

Boller, C. (2009). Encyclopedia of Structural Health Monitoring. In *Encyclopedia of Structural Health Monitoring*. https://doi.org/10.1002/9780470061626

Bonano, M., Manunta, M., Pepe, A., Paglia, L., & Lanari, R. (2013). From previous C-band to new X-band SAR systems: Assessment of the DInSAR mapping improvement for deformation time-series retrieval in urban areas. *IEEE Transactions on Geoscience and Remote Sensing*, *51*(4), 1973–1984. https://doi.org/10.1109/TGRS.2012.2232933

Borri, A., & Corradi, M. (2019). Architectural heritage: A discussion on conservation and safety. *Heritage*, *2*(1), 631–647. https://doi.org/10.3390/heritage2010041

Boscato, G., Dal Cin, A., Russo, S., & Sciarretta, F. (2014). SHM of Historic Damaged Churches. *Advanced Materials Research*, *838–841*, 2071–2078. https://doi.org/10.4028/WWW.SCIENTIFIC.NET/AMR.838-841.2071

Boscato, G., Rocchi, D., & Russo, S. (2012). Anime Sante church's dome after 2009 L'Aquila earthquake, monitoring and strengthening approaches. *Advanced Materials Research*, *446–449*, 3467–3485. https://doi.org/10.4028/www.scientific.net/AMR.446-449.3467

Boser, B. E., Guyon, I. M., & Vapnik, V. N. (1992). Training algorithm for optimal margin classifiers. *Proceedings of the Fifth Annual ACM Workshop on Computational Learning Theory*, 144–152. https://doi.org/10.1145/130385.130401

Box, G. E., Jenkins, G. M., Reinsel, G. C., & Ljung, G. M. (2015). *Time Series Analysis: Forecasting and Control* (5th editio).

Bozzano, F., Esposito, C., Mazzanti, P., Patti, M., & Scancella, S. (2018). Imaging multi-age construction settlement behaviour by advanced SAR interferometry. *Remote Sensing*, *10*(7). https://doi.org/10.3390/rs10071137

Brincker, R., & Andersen, P. (2006). Understanding Stochastic Subspace Identification. *Conference Proceedings of the Society for Experimental Mechanics Series*.

Brownjohn, J. M. W., Lee, J., & Cheong, B. (1999). Dynamic performance of a curved cable-stayed bridge. *Engineering Structures*, *21*(11), 1015–1027. https://doi.org/10.1016/S0141-0296(98)00046-7

Bukkapatnam Tirumala, A. (2008). *Experimental Investigation of Unsaturated Soil Stiffness.* LSU Master's Theses. 3551.

Bull, L. A., Gardner, P. A., Gosliga, J., Rogers, T. J., Dervilis, N., Cross, E.,

Papatheou, E., Maguire, A. E., Campos, C., & Worden, K. (2021). Foundations of population-based SHM, Part I: Homogeneous populations and forms. *Mechanical Systems and Signal Processing*, *148*, 107141. https://doi.org/10.1016/j.ymssp.2020.107141

Cabboi, A., Gentile, C., & Saisi, A. (2017). From continuous vibration monitoring to FEM-based damage assessment: Application on a stone-masonry tower. *Construction and Building Materials*, *156*, 252–265. https://doi.org/10.1016/j.conbuildmat.2017.08.160

Calderini, C., Chiorino, M. A., Lagomarsino, S., & Spadafora, A. (2006). Non linear modelling of the elliptical dome of Vicoforte. *Structural Analysis of Historical Constructions, New Dehli, 2*(3), 1177–1186.

Cappello, C., Zonta, D., & Glisic, B. (2016). Expected utility theory for monitoring-based decision-making. *Proceedings of the IEEE*, *104*(8), 1647–1661. https://doi.org/10.1109/JPROC.2015.2511540

Catbas, F. N., Susoy, M., & Frangopol, D. M. (2008). Structural health monitoring and reliability estimation: Long span truss bridge application with environmental monitoring data. *Engineering Structures*, *30*(9), 2347–2359. https://doi.org/10.1016/j.engstruct.2008.01.013

Cavalagli, N., Botticelli, L., Gioffrè, M., Gusella, V., & Ubertini, F. (2017). Dynamic monitoring and nonlinear analysis of the dome of the basilica of S.Maria degli Angeli in Assisi. *COMPDYN 2017 - Proceedings of the 6th International Conference on Computational Methods in Structural Dynamics and Earthquake Engineering*, *1*(January), 2542–2553. https://doi.org/10.7712/120117.5587.18117

Cavalagli, N., Kita, A., Falco, S., Trillo, F., Costantini, M., & Ubertini, F. (2019). Satellite radar interferometry and in-situ measurements for static monitoring of historical monuments: The case of Gubbio, Italy. *Remote Sensing of Environment*, *235*(November). https://doi.org/10.1016/j.rse.2019.111453

Ceravolo, R., Coletta, G., Lenticchia, E., Minervini, D., & Quattrone, A. (2020). Dynamic investigations on the health state and seismic vulnerability of morandi's pavilion v of turin exhibition center. *IABSE Symposium, Wroclaw 2020: Synergy of Culture and Civil Engineering - History and Challenges, Report*, 741–748. https://doi.org/10.2749/WROCLAW.2020.0224

Ceravolo, R., Coletta, G., Miraglia, G., & Palma, F. (2021). Statistical correlation between environmental time series and data from long-term monitoring of buildings. *Mechanical Systems and Signal Processing*, *152*, 107460. https://doi.org/10.1016/j.ymssp.2020.107460

Ceravolo, R., De Lucia, G., Miraglia, G., & Pecorelli, M. L. (2020). Thermoelastic finite element model updating with application to monumental buildings. *Computer-Aided Civil and Infrastructure Engineering*, *35*(6), 628–642.

https://doi.org/10.1111/mice.12516

Ceravolo, R., De Lucia, G., Pecorelli, M. L., & Zanotti Fragonara, L. (2015). Monitoring of historical buildings: Project of a dynamic monitoring system for the world's largest elliptical dome. *2015 IEEE Workshop on Environmental, Energy, and Structural Monitoring Systems, EESMS 2015 - Proceedings*, 113–118. https://doi.org/10.1109/EESMS.2015.7175862

Ceravolo, R., De Marinis, A., Pecorelli, M. L., & Zanotti Fragonara, L. (2017). Monitoring of masonry historical constructions: 10 years of static monitoring of the world's largest oval dome. *Structural Control and Health Monitoring*, *24*(10). https://doi.org/10.1002/STC.1988

Ceravolo, R., Pistone, G., Fragonara, L. Z., Massetto, S., & Abbiati, G. (2016). Vibration-based monitoring and diagnosis of cultural heritage: A methodological discussion in three examples. *International Journal of Architectural Heritage*, *10*(4), 375–395. https://doi.org/10.1080/15583058.2013.850554

CGLS. (2013). *Copernicus Global Land Service. Providing bio-geophysical products of global land surface - Soil Water Index*.

CGLS. (2014a). *VITO Earth Observation*.

CGLS. (2014b). *VITO Earth Observation - Soil Water Index*.

Chakraborty, D., Kovvali, N., Chakraborty, B., Papandreou-Suppappola, A., & Chattopadhyay, A. (2011). Structural damage detection with insufficient data using transfer learning techniques. *Sensors and Smart Structures Technologies for Civil, Mechanical, and Aerospace Systems 2011*, *7981*, 1175–1183. https://doi.org/10.1117/12.882025

Chang, F. K., Prosser, W. H., & Schulz, M. J. (2002). Editorial: Letter of Introduction from the Editors of Structural Health Monitoring. *Structural Health Monitoring*, *1*(1), 3–4. https://doi.org/10.1177/147592170200100101

Chiorino, M. A., Calderini, C., Spadafora, A., & Spadavecchia, R. (2008). Structural assessment, testing, rehabilitation and monitoring strategies for the world's largest elliptical dome and Sanctuary at Vicoforte. *RILEM Symposium on On Site Assessment of Concrete, Masonry and Timber Structures - SACoMaTiS 2008*, 529–538.

Chiorino, M. A., Ceravolo, R., Lai, C. G., & Casalegno, C. (2012). Survey, seismic input and structural modeling of the "Regina Montis Regalis" Basilica and large elliptical dome at Vicoforte, Italy. *Structural Analysis of Historical Constructions*, 1432–1440.

Chiorino, M. A., Ceravolo, R., Spadafora, A., Zanotti Fragonara, L., & Abbiati, G. (2011). Dynamic characterization of complex masonry structures: The sanctuary of vicoforte. *International Journal of Architectural Heritage*, *5*(3),

296–314. https://doi.org/10.1080/15583050903582516

Chiorino, M. A., Spadafora, A., Calderini, C., & Lagomarsino, S. (2008). Modeling strategies for the world's largest elliptical dome at vicoforte. *International Journal of Architectural Heritage*, *2*(3), 274–303. https://doi.org/10.1080/15583050802063618

Chu, F., Yuan, S., & Peng, Z. (2008). Machine Learning Techniques. *Encyclopedia of Structural Health Monitoring*. https://doi.org/10.1002/9780470061626.SHM184

Chuvieco, E. (2009). *Fundamentals of satellite remote sensing. An Environmental Approach* (2nd ed.). https://doi.org/10.1201/b18954

Cigna, F., Lasaponara, R., Masini, N., Milillo, P., & Tapete, D. (2014). Persistent scatterer interferometry processing of COSMO-skymed stripmap HIMAGE time series to depict deformation of the historic centre of Rome, Italy. *Remote Sensing*, *6*(12), 12593–12618. https://doi.org/10.3390/rs61212593

Clemente, P., & Buffarini, G. (2008). Dynamic Response of Buildings of the Cultural Heritage. *Encyclopedia of Structural Health Monitoring*. https://doi.org/10.1002/9780470061626.SHM173

Clementi, F., Formisano, A., Milani, G., & Ubertini, F. (2021). Structural Health Monitoring of Architectural Heritage: From the past to the Future Advances. *International Journal of Architectural Heritage*, *15*(1), 1–4. https://doi.org/10.1080/15583058.2021.1879499

CloudFerro. (2019). *CREODIAS*.

Coccimiglio, S., Coletta, G., Dabdoub, M., Miraglia, G., Lenticchia, E., & Ceravolo, R. (2021). Use of Copernicus Satellite Data to Investigate the Soil-Structure Interaction and Its Contribution to the Dynamics of A Monitored Monumental Building. *Lecture Notes in Civil Engineering*, *200 LNCE*, 1171–1179. https://doi.org/10.1007/978-3-030-91877-4_133

Coccimiglio, S., Coletta, G., Lenticchia, E., Miraglia, G., & Ceravolo, R. (2022). Combining satellite geophysical data with continuous on-site measurements for monitoring the dynamic parameters of civil structures. *Scientific Reports*, *12*(1), 2275. https://doi.org/10.1038/s41598-022-06284-7

Coletta, G., Miraglia, G., Gardner, P., Ceravolo, R., Surace, C., & Worden, K. (2020). A Transfer Learning Application to FEM and Monitoring Data for Supporting the Classification of Structural Condition States. *European Workshop on Structural Health Monitoring*, 947–957.

Coletta, G., Miraglia, G., Pecorelli, M. L., Ceravolo, R., Cross, E., Surace, C., & Worden, K. (2019a). Use of the cointegration strategies to remove environmental effects from data acquired on historical buildings. *Engineering Structures*, *183*(May 2018), 1014–1026.

https://doi.org/10.1016/j.engstruct.2018.12.044

Coletta, G., Miraglia, G., Pecorelli, M. L., Ceravolo, R., Cross, E., Surace, C., & Worden, K. (2019b). Use of the cointegration strategies to remove environmental effects from data acquired on historical buildings. *Engineering Structures*, *183*, 1014–1026. https://doi.org/10.1016/j.engstruct.2018.12.044

Cozzo, P. (2002). *Regina Montis Regalis. Il santuario di Mondovì da devozione locale a tempio sabaudo*.

Cozzo, P., Lucia, G. D. E., & Longhi, A. (2017). Un Miracolo "Sfortunato"? Valori E Ambizioni Di Un Luogo "Miracolato": Il Santuario Di Vicoforte (Mondovì). In Olimpia Niglio (Ed.), *Conoscere, Conservare, Valorizzare il Patrimonio Culturale Religioso* (pp. 73–61). Canterano, Arcacne Editrice.

Cross, E. (2012). *On Structural Health Monitoring in Changing Environmental and Operational Conditions*. Doctoral dissertation, University of Sheffield.

Cross, E., & Worden, K. (2012). Cointegration and why it works for SHM. *Journal of Physics: Conference Series*, *382*(1). https://doi.org/10.1088/1742-6596/382/1/012046

Cross, E., Worden, K., & Chen, Q. (2011). Cointegration: a novel approach for the removal of environmental trends in structural health monitoring data. *Proceedings of the Royal Society A: Mathematical, Physical and Engineering Sciences*, *467*(2133), 2712–2732. https://doi.org/10.1098/RSPA.2011.0023

D'alessandro, A., Costanzo, A., Ladina, C., Buongiorno, F., Cattaneo, M., Falcone, S., La Piana, C., Marzorati, S., Scudero, S., Vitale, G., Stramondo, S., & Doglioni, C. (2019). Urban Seismic Networks, Structural Health and Cultural Heritage Monitoring: The National Earthquakes Observatory (INGV, Italy) Experience. *Frontiers in Built Environment*, *5*, 127. https://doi.org/10.3389/fbuil.2019.00127

Dabdoub, M. (2021). *Damage Thresholds for Historical Structures. MSc Thesis, Politecnico di Torino*. Politecnico di Torino.

De Stefano, A., & Ceravolo, R. (2007). Assessing the health state of ancient structures: The role of vibrational tests. *Journal of Intelligent Material Systems and Structures*, *18*(8), 793–807. https://doi.org/10.1177/1045389X06074610

Deraemaeker, A., Reynders, E., De Roeck, G., & Kullaa, J. (2008). Vibration-based structural health monitoring using output-only measurements under changing environment. *Mechanical Systems and Signal Processing*, *22*(1), 34–56. https://doi.org/10.1016/j.ymssp.2007.07.004

Doebling, S., Farrar, C. R., Prime, M., & Shevitz, D. (1996). *Damage identification and health monitoring of structural and mechanical systems from changes in their vibration characteristics: a literature review*. https://www.osti.gov/biblio/249299

Dong, Y., & Lu, N. (2016). Dependencies of Shear Wave Velocity and Shear Modulus of Soil on Saturation. *Journal of Engineering Mechanics*, *142*(11). https://doi.org/10.1061/(asce)em.1943-7889.0001147

Dorafshan, S., Thomas, R. J., & Maguire, M. (2018). *Comparison of deep convolutional neural networks and edge detectors for image-based crack detection in concrete*. https://doi.org/10.1016/j.conbuildmat.2018.08.011

Drucker, H., Burgers, C. J., Kaufman, L., Smola, A., & Vapnik, V. (1996). Support vector regression machines. *Advances in Neural Information Processing Systems*, *9*.

Engle, R., & Granger, C. (1987). Co-integration and error correction: representation, estimation, and testing. *Econometrica: Journal of the Econometric Society*, 251–276.

Erazo, K., Sen, D., Nagarajaiah, S., & Sun, L. (2019). Vibration-based structural health monitoring under changing environmental conditions using Kalman filtering. *Mechanical Systems and Signal Processing*, *117*, 1–15. https://doi.org/10.1016/j.ymssp.2018.07.041

ESA. (2013a). *LST processing*.

ESA. (2013b). *The European Space Agency. Sentinel Online. Land Surface Temperature*.

EU-India Economic Cross Cultural Programme. (2006). Guidelines for the Conservation of Historical Masonry Structures in Seismic Area. *Improving The Seismic Resistance Of Cultural Heritage Buildings*.

EUMETSAT. (2017). *Product User Manual (PUM) Metop ASCAT Soil Moisture CDR and offline products*.

Ezekiel, M. (1930). *Methods of correlation analysis.* Wiley.

Fan, W., & Qiao, P. (2011). Vibration-based damage identification methods: A review and comparative study. In *Structural Health Monitoring* (Vol. 10, Issue 1, pp. 83–111). https://doi.org/10.1177/1475921710365419

Farrar, C. R., Doebling, S. W., & Nix, D. A. (2001). Vibration-based structural damage identification. In *Philosophical Transactions of the Royal Society A: Mathematical, Physical and Engineering Sciences* (Vol. 359, Issue 1778, pp. 131–149). Royal Society. https://doi.org/10.1098/rsta.2000.0717

Farrar, C. R., & Worden, K. (2012). Structural Health Monitoring: A Machine Learning Perspective. In *Structural Health Monitoring: A Machine Learning Perspective*. https://doi.org/10.1002/9781118443118

Ferrato Lisa-jen. (2012). Multispectral vs. hyperspectral. In *Comparing hyperspectral and multispectral imagery for land classification of the lower Don river, Toronto* (p. 14). Lisa-jen Ferrato A.

Figueiredo, E., Park, G., Farrar, C. R., Worden, K., & Figueiras, J. (2011). Machine learning algorithms for damage detection under operational and environmental variability. *Structural Health Monitoring*, *10*(6), 559–572. https://doi.org/10.1177/1475921710388971

Flah, M., Nunez, I., Ben Chaabene, W., & Nehdi, M. L. (2020). Machine Learning Algorithms in Civil Structural Health Monitoring: A Systematic Review. *Archives of Computational Methods in Engineering*, *0123456789*. https://doi.org/10.1007/s11831-020-09471-9

Florides, G., & Kalogirou, S. (2004). Measurements of ground temperature at various depths. *Proceedings of the 3rd International Conference on Sustainable Energy Technologies, Nottingham, UK*, 28–30.

Forgács, T., Sarhosis, V., & Bagi, K. (2018). Influence of construction method on the load bearing capacity of skew masonry arches. *Engineering Structures*, *168*, 612–627. https://doi.org/10.1016/j.engstruct.2018.05.005

Frangopol, D. M., & Messervey, T. B. (2008). Maintenance Principles for Civil Structures. In *Encyclopedia of Structural Health Monitoring*. https://doi.org/10.1002/9780470061626.shm108

Friswell, M. I. (2007). Damage identification using inverse methods. *Philosophical Transactions of the Royal Society A: Mathematical, Physical and Engineering Sciences*, *365*(1851), 393–410. https://doi.org/10.1098/rsta.2006.1930

Fuller, W. (2009). *Introduction to statistical time series* (John Wiley & Sons. (ed.); Vol. 428).

Gao, Y., & Mosalam, K. M. (2018). Deep Transfer Learning for Image-Based Structural Damage Recognition. *Computer-Aided Civil and Infrastructure Engineering*, *33*(9), 748–768. https://doi.org/10.1111/MICE.12363

García-Macías, E., & Ubertini, F. (2020). MOVA/MOSS: Two integrated software solutions for comprehensive Structural Health Monitoring of structures. *Mechanical Systems and Signal Processing*, *143*. https://doi.org/10.1016/j.ymssp.2020.106830

Gardner, P., Liu, X., & Worden, K. (2020). On the application of domain adaptation in structural health monitoring. *Mechanical Systems and Signal Processing*, *138*, 106550. https://doi.org/10.1016/j.ymssp.2019.106550

Garro, M. (1962). *Opere di consolidamento e restauro. Relazione riassuntiva, dattiloscritto, Santuario Basilica di Mondovì.*

Gentile, C., Guidobaldi, M., & Saisi, A. (2016). One-year dynamic monitoring of a historic tower: damage detection under changing environment. *Meccanica*, *51*(11), 2873–2889. https://doi.org/10.1007/s11012-016-0482-3

Gentile, C., Ruccolo, A., & Canali, F. (2019a). Long-term monitoring for the condition-based structural maintenance of the Milan Cathedral. *Construction*

and Building Materials, *228*, 117101. https://doi.org/10.1016/j.conbuildmat.2019.117101

Gentile, C., Ruccolo, A., & Canali, F. (2019b). Continuous monitoring of the Milan Cathedral: dynamic characteristics and vibration-based SHM. *Journal of Civil Structural Health Monitoring*, *9*(5), 671–688. https://doi.org/10.1007/S13349-019-00361-8

Gentile, C., Ruccolo, A., & Saisi, A. (2019). Continuous Dynamic Monitoring to Enhance the Knowledge of a Historic Bell-Tower. *International Journal of Architectural Heritage*, *13*(7), 992–1004. https://doi.org/10.1080/15583058.2019.1605552

Higgins, S. (1895). *Inspection of steel-tired wheels*. *Proceeding*, 988–989.

Hulley, G. C., Ghent, D., Göttsche, F. M., Guillevic, P. C., Mildrexler, D. J., & Coll, C. (2019). Land Surface Temperature. In G. Hulley & D. Ghent (Eds.), *Taking the Temperature of the Earth* (1st ed., pp. 57–127). Elsevier Inc. https://doi.org/10.1016/b978-0-12-814458-9.00003-4

ICOMOS. (1964). *International Charter On The Conservation And Restoration Of Monuments And Sites (Venice Charter 1964)*.

ICOMOS. (2003). *Icomos Charter- Principles For The Analysis, Conservation And Structural Restoration Of Architectural Heritage (2003)*.

Jang, K., Kim, N., & An, Y. K. (2019). Deep learning–based autonomous concrete crack evaluation through hybrid image scanning: *Https://Doi.Org/10.1177/1475921718821719*, *18*(5–6), 1722–1737. https://doi.org/10.1177/1475921718821719

Jolliffe, I. T. (2002). *Principal Component Analysis*. https://doi.org/10.1007/B98835

Kasimzade, A. A., Şafak, E., Ventura, C. E., Naeim, F., & Mukai, Y. (2018). Seismic isolation, structural health monitoring, and performance based seismic design in earthquake engineering: Recent developments. In *Seismic Isolation, Structural Health Monitoring, and Performance Based Seismic Design in Earthquake Engineering: Recent Developments*. https://doi.org/10.1007/978-3-319-93157-9

Kita, A., Cavalagli, N., & Ubertini, F. (2019). Temperature effects on static and dynamic behavior of Consoli Palace in Gubbio, Italy. *Mechanical Systems and Signal Processing*, *120*, 180–202. https://doi.org/10.1016/j.ymssp.2018.10.021

Lagomarsino, S., Cattari, S., & Calderini, C. (2012). DELIVERABLE D41 European Guidelines for the seismic preservation of cultural heritage assets. *PERPETUATE PERformance-Based APproach to Earthquake ProTection of CUlturAl HeriTage in European and Mediterranean Countries*.

Lagomarsino, S., Modaressi, H., Pitilakis, K., Bosiljkov, V., Calderini, C., D'ayala, D., Benouar, D., & Cattari, S. (2010). PERPETUATE Project: The proposal of a performance-based approach to earthquake protection of cultural heritage. *Advanced Materials Research*, *133*, 1119–1124. https://doi.org/10.4028/www.scientific.net/AMR.133-134.1119

Lai, C. G., Corigliano, M., Scandella, L., & Lizárraga, H. S. (2009). *Definition of seismic input at the "Regina Montis Regalis" Basilica of Vicoforte, Northern Italy*.

Lazecky, M., Perissin, D., Bakon, M., De Sousa, J. M., Hlavacova, I., & Real, N. (2015). Potential of satellite InSAR techniques for monitoring of bridge deformations. *2015 Joint Urban Remote Sensing Event, JURSE 2015*, *June*. https://doi.org/10.1109/JURSE.2015.7120506

Lenticchia, E., Miraglia, G., & Ceravolo, R. (2021). Exploring Problems and Prospective of Satellite Interferometric Data for the Seismic Structural Health Monitoring of Existing Buildings and Architectural Heritage. *10th International Conference on Structural Health Monitoring of Intelligent Infrastructure*.

Limongelli, M. P., Turksezer, Z. I., & Giordano, P. F. (2019). Structural health monitoring for cultural heritage constructions: A resilience perspective. *IABSE Symposium, Guimaraes 2019: Towards a Resilient Built Environment Risk and Asset Management - Report*, 1552–1559. https://doi.org/10.2749/guimaraes.2019.1552

Lorenzoni, F., Casarin, F., Modena, C., Caldon, M., Islami, K., & da Porto, F. (2013). Structural health monitoring of the Roman Arena of Verona, Italy. *Journal of Civil Structural Health Monitoring*, *3*(4), 227–246. https://doi.org/10.1007/S13349-013-0065-0

Lou, M., Wang, H., Chen, X., & Zhai, Y. (2011). Structure-soil-structure interaction: Literature review. *Soil Dynamics and Earthquake Engineering*, *31*(12), 1724–1731. https://doi.org/10.1016/j.soildyn.2011.07.008

Maria D'Altri, A., Sarhosis, V., Milani, G., Rots, J., Cattari, S., Lagomarsino, S., Sacco, E., Tralli, A., Castellazzi, G., & De Miranda, S. (2020). Modeling strategies for the computational analysis of unreinforced masonry structures: review and classification. *Springer*, *27*, 1153–1185. https://doi.org/10.1007/s11831-019-09351-x

Masciotta, M. G., Ramos, L. F., & Lourenço, P. B. (2017). The importance of structural monitoring as a diagnosis and control tool in the restoration process of heritage structures: A case study in Portugal. *Journal of Cultural Heritage*, *27*, 36–47. https://doi.org/10.1016/j.culher.2017.04.003

Masciotta, M. G., Roque, J. C. A., Ramos, L. F., & Lourenço, P. B. (2016). A multidisciplinary approach to assess the health state of heritage structures: The

case study of the Church of Monastery of Jerónimos in Lisbon. *Construction and Building Materials*, *116*, 169–187. https://doi.org/10.1016/j.conbuildmat.2016.04.146

McDonald, M., Engineering, S. Ž.-J. of S., & 2017, undefined. (2017). Measuring ground reaction force and quantifying variability in jumping and bobbing actions. *Ascelibrary.Org*, *143*(2), 04016161. https://doi.org/10.1061/(ASCE)ST.1943-541X.0001649

Meng, X., Roberts, G. W., Dodson, A. H., Cosser, E., Barnes, J., & Rizos, C. (2004). Impact of GPS satellite and pseudolite geometry on structural deformation monitoring: Analytical and empirical studies. *Journal of Geodesy*, *77*(12), 809–822. https://doi.org/10.1007/s00190-003-0357-y

Milillo, P., Giardina, G., DeJong, M., Perissin, D., & Milillo, G. (2018). Multi-Temporal InSAR Structural Damage Assessment: The London Crossrail Case Study. *Remote Sensing*, *10*(2), 287. https://doi.org/10.3390/rs10020287

Ministero dei beni cultural e ambientali. (1986). *Interventi sul patrimonio monumentale a tipologia specialistica in zone sismiche: raccomandazioni*.

Ministero delle Infrastrutture e dei Trasporti. (2008). "Norme tecniche per le costruzioni" (in Italian). *DECRETO 14 Gennaio 2008. Approvazione Delle Nuove Norme Tecniche per Le Costruzioni.*

Ministero delle Infrastrutture e dei Trasporti. (2018). "Norme tecniche per le costruzioni" (in Italian). *DECRETO 17 Gennaio 2018. Aggiornamento Delle «Norme Tecniche per Le Costruzioni».*

Ministero delle Infrastrutture e dei Trasporti. (2019). Istruzioni per l'applicazione dell'«Aggiornamento delle "Norme tecniche per le costruzioni"». *CIRCOLARE 21 Gennaio 2019, n. 7 C.S.LL.PP. Istruzioni per l'applicazione Dell'«Aggiornamento Delle "Norme Tecniche per Le Costruzioni"» Di Cui Al Decreto Ministeriale 17 Gennaio 2018.*

Miraglia, G. (2019). *Hybrid simulation techniques in the structural analysis and testing of architectural heritage*. Doctoral dissertation, Politecnico di Torino.

Mitchell, T. M. (2000). *Machine Learning* (McGraw-Hill Science (ed.)). McGraw-Hill Science/Engineering/Math.

Montgomery, D. (1996). Introduction to Statistical Quality Control. In John Wiley & Sons (Ed.), *Technometrics* (Issue 3). https://doi.org/10.1080/00401706.1997.10485124

Moser, P., & Moaveni, B. (2011). Environmental effects on the identified natural frequencies of the Dowling Hall Footbridge. *Mechanical Systems and Signal Processing*, *25*(7), 2336–2357. https://doi.org/10.1016/j.ymssp.2011.03.005

Nayci, N., Abruzzese, D., Güler, C., Tağa, H., Cammarano, P., Vuth, S. M., & Türkoğlu, H. G. (2020). Multidisciplinary Researches in Cultural Heritage

Studies: An Approach on Akkale Cistern in Erdemli, Mersin. *Cultural Heritage and Science*, *1*(1), 15–22.

Ni, Y. Q., Hua, X. G., Fan, K. Q., & Ko, J. M. (2005). Correlating modal properties with temperature using long-term monitoring data and support vector machine technique. *Engineering Structures*, *27*(12 SPEC. ISS.), 1762–1773. https://doi.org/10.1016/j.engstruct.2005.02.020

Novello, G., & Piumatti, P. (2012a). La Geometria come filo di Arianna: note di approfondimento sul rapporto ideazione-costruzione della più grande cupola di forma ovata del mondo. Geometrical analysis of the largest oval dome in the world. *DISEGNARECON*, 167–176.

Novello, G., & Piumatti, P. (2012b). Geometrical analysis of the largest oval dome in the world. *DISEGNARECON*, 167–176. https://doi.org/10.6092/ISSN.1828-5961/3165

Ottoni, F., & Blasi, C. (2015). Results of a 60-year monitoring system for Santa Maria del Fiore Dome in Florence. *International Journal of Architectural Heritage*, *9*(1), 7–24. https://doi.org/10.1080/15583058.2013.815291

Overschee, P. Van, & De Moor, B. (1996). *Subspace Identification for Linear Systems*. Kluwer Academic Publishers.

Oyler, J. W., Mildrexler, D. J., Comiso, J. C., & Hulley, G. C. (2019). Surface Temperature Interrelationships. In G. Hulley & D. Ghent (Eds.), *Taking the Temperature of the Earth* (1st ed., pp. 185–202). Elsevier Inc. https://doi.org/10.1016/b978-0-12-814458-9.00006-x

Pan, S. J., Tsang, I. W., Kwok, J. T., & Yang, Q. (2011). Domain adaptation via transfer component analysis. *IEEE Transactions on Neural Networks*, *22*(2), 199–210. https://doi.org/10.1109/TNN.2010.2091281

Pan, S. J., & Yang, Q. (2010). A survey on transfer learning. In *IEEE Transactions on Knowledge and Data Engineering* (Vol. 22, Issue 10, pp. 1345–1359). https://doi.org/10.1109/TKDE.2009.191

Pau, A., & Vestroni, F. (2008). Vibration analysis and dynamic characterization of the Colosseum. *Struct. Control Health Monit.*, *15*(8), 1105–1121. https://doi.org/10.1002/stc.253

Paulik, C., Naeimi, V., Dorigo, W., Wagner, W., & Kidd, R. (2012). A global validation of the ASCAT Soil Water Index (SWI) with in situ data from the International Soil Moisture Network. *International Journal of Applied Earth Observation and Geoinformation*, *30*, 10189.

Pecorelli, M. L., Ceravolo, R., De Lucia, G., & Epicoco, R. (2017). A vibration-based health monitoring program for a large and seismically vulnerable masonry dome. *Journal of Physics: Conference Series*, *842*(1). https://doi.org/10.1088/1742-6596/842/1/012009

Pecorelli, M. L., Ceravolo, R., & Epicoco, R. (2020). An Automatic Modal Identification Procedure for the Permanent Dynamic Monitoring of the Sanctuary of Vicoforte. *International Journal of Architectural Heritage*, *14*(4), 630–644. https://doi.org/10.1080/15583058.2018.1554725

Peeters, B., & De Roeck, G. (2001). One-year monitoring of the Z24-Bridge: environmental effects versus damage events. *Earthquake Engineering and Structural Dynamics*, *30*(2), 149–171. https://doi.org/https://doi.org/10.1002/1096-9845(200102)30:2<149::AID-EQE1>3.0.CO;2-Z

Peeters, B., Maeck, J., & De Roeck, G. (2004). Vibration-based damage detection in civil engineering: Excitation sources and temperature effects. *Noise and Vibration Worldwide*, *35*(6), 33.

Pernica, G. (1990). Dynamic Load Factors for Pedestrian Movements and Rhythmic Exercises. *Canadian Acoustics*, *18*(2), 3–18.

Pham, T., Dan, L., Fatahi, B., & Khabbaz, H. (2017). A review on the influence of degree of saturation on small strain shear modulus of unsaturated soils. *19th International Conference on Soil Mechanics and Geotechnical Engineering*, 1225–1228.

Ponzo, F. C., & Ditommaso, R. (2020). Structural Health Monitoring of existing structures and infrastructures combining on-site and satellite data. *EGU General Assembly 2020, Online, 4–8 May 2020.*, EGU2020-13600. https://doi.org/10.5194/egusphere-egu2020-13600, 2020

Rainer, J. H., Pernica, G., & Allen, D. E. (1988). Dynamic Loading and Response of Footbridges. *Canadian Journal of Civil Engineering*, *15*(1), 66–71. https://doi.org/10.1139/l88-007

Ramos, L. F., Aguilar, R., Lourenço, P. B., & Moreira, S. (2013). Dynamic structural health monitoring of Saint Torcato church. *Mechanical Systems and Signal Processing*, *35*(1–2), 1–15. https://doi.org/10.1016/j.ymssp.2012.09.007

Ramos, L. F., Marques, L., Lourenço, P. B., De Roeck, G., Campos-Costa, A., & Roque, J. (2010). Monitoring historical masonry structures with operational modal analysis: two case studies. *Mechanical Systems & Signal Processing*, *24*(5), 1291–1305. https://doi.org/10.1016/j.ymssp.2010.01.011

Recommendations PCM. (2008). *Directive of the President of the Council of Ministers for the assessment and reduction of the seismic risk of cultural heritage with reference to technical standards for construction. 29/01/2008. G.U. no. 25, 29/01/2008 (suppl. ord. no. 24) (in Italian)*.

Recommendations PCM. (2011). *Assessment and mitigation of seismic risk of cultural heritage with reference to the Italian Building Code (NTC2008).*

Directive of the Prime Minister, 9/02/2011. G.U. no. 47, 26/02/2011 (suppl. ord. no. 54) (in Italian).

Remedios, J. (2012). *Land Surface Temperature - Sentinel-3 Optical Product and Algorith Definition*.

Roach, D. (2008). Use of Leave-in-Place Sensors and SHM Methods to Improve Assessments of Aging Structures. *Encyclopedia of Structural Health Monitoring*. https://doi.org/10.1002/9780470061626.SHM197

Russo, S. (2013). On the monitoring of historic Anime Sante church damaged by earthquake in L'Aquila. *Structural Control and Health Monitoring*, *20(9)*, 1226–1239.

Rytter, A. (1993). *Vibrational based inspection of civil engineering structures*. Doctoral dissertation, Aalborg University.

Saisi, A., & Gentile, C. (2015). Post-earthquake diagnostic investigation of a historic masonry tower. *Journal of Cultural Heritage*, *16*(4), 602–609.

Saisi, A., Gentile, C., & Ruccolo, A. (2017). Static and dynamic monitoring of a Cultural Heritage bell-tower in Monza, Italy. *Procedia Engineering*, *199*, 3356–3361. https://doi.org/10.1016/J.PROENG.2017.09.563

Saisi, A., Gentile, C., & Ruccolo, A. (2018). Continuous monitoring of a challenging heritage tower in Monza, Italy. *Journal of Civil Structural Health Monitoring*, *8*(1), 77–90. https://doi.org/10.1007/S13349-017-0260-5

Salawu, O. S. (1997). Detection of structural damage through changes in frequency: A review. *Engineering Structures*, *19*(9), 718–723. https://doi.org/10.1016/S0141-0296(96)00149-6

Saloustros, S., Pelà, L., Contrafatto, F. R., Roca, P., & Petromichelakis, I. (2019). Analytical derivation of seismic fragility curves for historical masonry structures based on stochastic analysis of uncertain material parameters. *Taylor & Francis*, *13*(7), 1142–1164. https://doi.org/10.1080/15583058.2019.1638992

Sandrolini, F., Franzoni, E., Sassoni, E., & Diotallevi, P. P. (2011). The contribution of urban-scale environmental monitoring to materials diagnostics: A study on the Cathedral of Modena (Italy). *Journal of Cultural Heritage*, *12*(4), 441–450. https://doi.org/10.1016/j.culher.2011.04.005

Santuario di Vicoforte (Magnificat) - Kalatà! (2022). https://kalata.it/esperienza/santuario-di-vicoforte-magnificat-cupola-ellittica/

Shi, H., Worden, K., & Cross, E. (2016). A nonlinear cointegration approach with applications to structural health monitoring. *Journal of Physics: Conference Series*, *744*(1). https://doi.org/10.1088/1742-6596/744/1/012025

Sim, J., Blakeborough, A., & Williams, M. (2005). Dynamic loads due to rhythmic

human jumping and bobbing. *Structural Dynamics: EURODYN 2005, Paris.*, 467–472.

Smarsly, K., Dragos, K. ., & Wiggenbrock, J. (2016). Machine learning techniques for structural health monitoring. *Proceedings of the 8th European Workshop on Structural Health Monitoring (EWSHM 2016), Bilbao, Spain*, 5–8.

Sohn, H. (2007). Effects of environmental and operational variability on structural health monitoring. *Philosophical Transactions of the Royal Society A: Mathematical, Physical and Engineering Sciences*, *365*(1851), 539–560. https://doi.org/10.1098/rsta.2006.1935

Sohn, H., Dzwonczyk, M., Straser, E. G., Kiremidjian, A. S., Law, K. H., & Meng, T. (1999). An experimental study of temperature effect on modal parameters of the Alamosa Canyon bridge. *Earthquake Engineering and Structural Dynamics Dyn*, *28*(8), 879–897. https://doi.org/https://doi.org/10.1002/(SICI)1096-9845(199908)28:8<879::AID-EQE845>3.0.CO;2-V

Sohn, H., Farrar, C. R., Hemez, F., & Czarnecki, J. (1996). A Review of Structural Health Monitoring Literature 1996 – 2001. *Los Alamos National Laboratory, USA, 1*.

Sohn, H., Worden, K., & Farrar, C. R. (2002). Statistical damage classification under changing environmental and operational conditions. *Journal of Intelligent Material Systems and Structures*, *13*(9), 561–574. https://doi.org/10.1106/104538902030904

Sonda, D., Cossu, M., & Miyamoto, H. K. (2015). Methodology for Seismic Improvement of Ancient Heritage Monuments in India. *The Masterbuilder*, *February*.

Stanley, R. K. (1995). Nondestructive Testing Handbook 9: Special Nondestructive Testing Methods. *American Society of Nondestructive Testing.*

Taylor, J. (1997). *Introduction to error analysis, the study of uncertainties in physical measurements* (2nd ed.). University Science Books.

Tipping, M. (2001). Sparse Bayesian learning and the relevance vector machine. *Journal of Machine Learning Research*, *1*(jun), 211-244.

Tronci, E. M., Beigi, H., Feng, M. Q., & Betti, R. (2022). Transfer Learning from Audio Domains a Valuable Tool for Structural Health Monitoring. *Conference Proceedings of the Society for Experimental Mechanics Series*, 99–107. https://doi.org/10.1007/978-3-030-77143-0_11

Tronci, E. M., De Angelis, M., Betti, R., & Altomare, V. (2020). Vibration-based structural health monitoring of a RC-masonry tower equipped with non-conventional TMD. *Engineering Structures*, *224*, 111212. https://doi.org/10.1016/J.ENGSTRUCT.2020.111212

Ubertini, F., Cavalagli, N., Kita, A., & Comanducci, G. (2018). Assessment of a monumental masonry bell-tower after 2016 Central Italy seismic sequence by long-term SHM. *Bulletin of Earthquake Engineering*, *16*(2), 775–801. https://doi.org/10.1007/s10518-017-0222-7

Ubertini, F., Comanducci, G., Cavalagli, N., Pisello, A. L., Materazzi, A. L., & Cotana, F. (2017). Environmental effects on natural frequencies of the San Pietro bell tower in Perugia, Italy, and their removal for structural performance assessment. *Mechanical Systems and Signal Processing*, *82*, 307–322. https://doi.org/10.1016/j.ymssp.2016.05.025

UNI CEN ISO/TR 7250-2:2011. (2011). In *Misurazioni di base del corpo umano per la progettazione tecnologica - Parte 2: Rilevazioni statistiche relative a misurazioni del corpo umano corporee provenienti da singole popolazioni ISO*.

UNI EN ISO 7250-1:2010. (2010). In *Misurazioni di base del corpo umano per la progettazione tecnologica - Parte 1: Definizioni delle misurazioni del corpo umano e luoghi*.

VDI. (2000). *VDI 4640/1, Thermal use of the underground - Fundamentals, approvals, environmental aspects, VDI – 4640, Part 1. Verein Deutscher Ingenieure*.

Wong Hung Leung. (1975). *Dynamic soil-structure interaction*. California Institute of Technology.

Worden, K., Cheung, L. Y., & Rongong, J. A. (2001). Damage detection in an aircraft component model. *Proc. 19th Int. Modal Analysis Conf., Orlando, Florida*, 1234–1239.

Worden, K., & Manson, G. (2006). The application of machine learning to structural health monitoring. *Philosophical Transactions of the Royal Society A: Mathematical, Physical and Engineering Sciences*, *365*(1851), 515–537. https://doi.org/10.1098/RSTA.2006.1938

Xia, Y., Chen, B., Weng, S., Ni, Y. Q., & Xu, Y. L. (2012). Temperature effect on vibration properties of civil structures: A literature review and case studies. *Journal of Civil Structural Health Monitoring*, *2*(1), 29–46. https://doi.org/10.1007/s13349-011-0015-7

Zanotti Fragonara, L. (2012). *Dynamic models for ancient heritage structures*. Doctoral dissertation, Politecnico di Torino.

Zhang, Q. W., Chang, T. Y. P., & Chang, C. C. (2001). Finite-Element Model Updating for the Kap Shui Mun Cable-Stayed Bridge. *Journal of Bridge Engineering*, *6*(4), 285–293. https://doi.org/10.1061/(ASCE)1084-0702(2001)6:4(285)

Zhu, M., Wan, X., Fei, B., Qiao, Z., Ge, C., Minati, F., Vecchioli, F., Li, J., &

Costantini, M. (2018). Detection of building and infrastructure instabilities by automatic spatiotemporal analysis of satellite SAR interferometry measurements. *Remote Sensing*, *10*(11). https://doi.org/10.3390/rs10111816

Zonta, D., Glisic, B., & Adriaenssens, S. (2014). Value of information: Impact of monitoring on decision-making. *Structural Control and Health Monitoring*, *21*(7), 1043–1056. https://doi.org/10.1002/STC.1631

Zuchtriegel, G., Petti, L., Greco, D., & Manzo, A. (2020). Giganti fragili : il progetto di monitoraggio del tempio di Nettuno a Paestum. In *Monitoraggio e manutenzione delle aree archeologiche : cambiamenti climatici, dissesto idrogeologico, degrado chimico-ambientale : atti del Convegno internazionale di studi, Roma, Curia Iulia, 20-21 marzo 2019. - (Bibliotheca archaeologica) 2240-8347 ; 6*. "L'Erma" di Bretschneider.

I would like to express my gratitude to my supervisor, Prof. Rosario Ceravolo, who patiently guided me scientifically and humanly in these last years.

My deep gratitude goes to Prof. Cecilia Surace and Prof. Keith Worden for placing their confidence in me from the beginning and for the invaluable research advices.

Gaetano and Giovanni, words aren't able to express my gratitude for you. You have been my pillars of strength in this path. You, with your enthusiasm, made me love research. Having met you has deeply enriched me as a person.

I would like to say thank you to Simona, Valerio, Stefania, Erica and Linda for the laughs, the good times, the encouragement, the support and the help: these years would not have been so beautiful without you.

I want to express my thanks to Annapaola, Ale and Vittoria, my lifelong friends. No matter if we are physically distant, we will be linked forever.

And finally, I would like to thank with all my heart my mother, my sister and Francesco for always being with me. You are the points of reference in my life. Thanks also to Pollo, who always makes me happy.